

DEVELOPMENT OF G-QUADRUPLEX STABILIZERS AS ANTICANCER DRUG
THERAPY AND SELECTIVE AGONISTS OF THE HUMAN OXYTOCIN
RECEPTOR AS A THERAPEUTIC TOOL FOR NEUROPSYCHIATRIC
DISORDERS

MARIA FLORENCIA SASSANO

A dissertation submitted to the faculty of the University of North Carolina at Chapel Hill in partial fulfillment of the requirements for the degree of Doctor of Philosophy in the School of Pharmacy (Medicinal Chemistry and Natural Products).

Chapel Hill
2009

Approved by:

Dr. Michael B. Jarstfer, Chair

Dr. Kenneth F. Bastow

Dr. Cort A. Pedersen

Dr. Bryan L. Roth

Dr. Qisheng Zhang

©2009
Maria Florencia Sassano
ALL RIGHTS RESERVED

ABSTRACT

MARIA FLORENCIA SASSANO: Development of g-quadruplex stabilizers as anticancer drug therapy and selective agonists of the human oxytocin receptor as a therapeutic tool for neuropsychiatric disorders
(Under the direction of Dr. Michael B. Jarstfer)

The principal aim of pharmacology in drug discovery is the characterization of drug activity by system-independent scales that allow prediction of drug activity in all cellular systems. This thesis concentrated in two drug targets: telomeres and GPCRs. Telomere biology is a validated anticancer drug target. G-protein-coupled receptors (GPCRs) recognize external ligands and transmit signals to cellular G-proteins (guanine-nucleotide-binding proteins) to elicit a response. These receptors are tractable for drug discovery because they are on the cell surface therefore drugs do not need to penetrate the cell to produce an effect [1]. In 2000, nearly half of all prescription drugs in the US were targeted towards GPCRs [2].

The projects in this dissertation will describe two different approaches to the successful identification of small-molecules that interact with their validated targets. The first project focused on the identification of new G-quadruplex stabilizers and their ability to inhibit human telomerase as an anticancer drug modality. The second project focused on the efforts made towards the identification of novel small-molecules that selectively activate the human oxytocin receptor to regulate complex behaviors in animal models with therapeutic implications in various neuropsychiatric disorders.

ACKNOWLEDGEMENTS

I would like to thank all the people that were involved in this dissertation work and had provided guidance to my graduate career. In particular, I would like to thank my advisor, Dr. Michael Jarstfer, who has shown me the way to become a better scientist. I have and will always consider him and his family my friends. Dr. Cort Pedersen has trained me and introduced me to the fascinating world of behavioral pharmacology. Dr. Sheryl Moy spent her time mentoring me and striving for my success. Together with Randy Nonneman, they showed me the intricate world of mouse behavior. Dr. Bryan L. Roth provided his invaluable opinion to this project since the beginning and I am honored to have been (and be) part of his team. Also, I would like to thank Dr. Bill Janzen from the CICBDD center for allowing me to collaborate with them in the DiscoverRX project.

Quiero darle las gracias a mi familia que siempre estuvo presente a lo Campanelli: Mamá y Horacio, Papá y Marta, mis abuelos, Abu y Tito, y mis nohermas, Pato y Ale. Los quiero profundamente con todo el corazón. A Blanca, gracias por la buena onda. Finalmente, quiero dedicarle este trabajo a Gustavo Garagorry Machado, que me incentivó y me apoyó, desde aquella conversación en la cocina de Céspedes hasta hoy (9 años después), en esta locura de proyecto que muchas veces pensé que era irrealizable. Mirá a donde llegamos...

A Gusti,

Por un millón de proyectos más...

TABLE OF CONTENTS

LIST OF TABLES.....	ix
LIST OF FIGURES.....	xi
Chapter	
I. INTRODUCTION.....	1
Overview of Drug Discovery Processes.....	1
Background and significance.....	10
Novel G-quadruplex stabilizers.....	10
Novel non-peptide human oxytocin receptor agonists and positive allosteric modulators.....	13
Oxytocin.....	14
Oxytocin receptor.....	23
OT peripheral functions.....	32
Evidence that OT controls complex behavior.....	34
OT deficiencies in human disease.....	46
OT as a potential treatment for neuropsychiatric disorders.....	51
Current development of OTR agonists.....	52
Development of small-molecule positive allosteric modulators for OTR and therapeutic advantages.....	54

	Potential for significant contribution to the development of biotechnology or for commercial products derived from biotechnology.....	57
	Brief outline of this research work.....	58
II.	IDENTIFICATION OF NEW G-QUADRUPLEX STABILIZERS AND THEIR ABILITY TO INHIBIT HUMAN TELOMERASE.....	60
	Introduction.....	60
	Methods and materials.....	64
	Results and discussion.....	71
	FRET analysis for the identification of telomerase inhibitors.....	71
	Identification of Telomerase inhibitors.....	71
	G-quadruplex ligand specificity is revealed by polymerase stop assay.....	74
	Evaluation of G-quadruplex stabilization by circular dichroism.....	81
	Future plans.....	87
III.	VALIDATION AND OPTIMIZATION OF MEDIUM TO HIGH-THROUGHPUT CELL- BASED FLUORESCENT ASSAYS.....	89
	Introduction.....	89
	Methods and materials.....	99
	Results and discussion.....	116
	Validation of fluorescence-based intracellular calcium mobilization assay for the identification of hOTR agonists and allosteric modulators in a 96 well-plate format.....	116
	Optimization of fluorescence-based intracellular calcium mobilization assay for the identification of hOTR agonists and allosteric modulators for a 384 well-plate format.....	117
	Execution of medium-throughput screen for the identification of hOTR agonists and allosteric modulators for a 384 well-plate format.....	123

	Implementation of Fluo-8 No Wash Calcium Assay Kit for the fluorescence-based intracellular calcium mobilization assay for the identification of hOTR agonists and allosteric modulators for a 384 well-plate format.....	127
	Comparison between a chemiluminescent assay and the FLIPR ^{TETRA} [®] system fluorescence cell-based assay for identification of hOTR agonists and positive allosteric modulators.....	134
	Future plans.....	139
IV.	VALIDATION OF ACTIVES.....	141
	Introduction.....	141
	Methods and materials.....	145
	Results and discussion.....	154
	Efficacy screen.....	154
	Counter screens.....	156
	Confirmation of actives by IP ₃ release assay.....	162
	Cytotoxicity evaluation of actives.....	167
	Future plans.....	174
V.	MOUSE MODELS OF COMPLEX BEHAVIOR AFFECTED BY THE OXYTOCIN PATHWAY.....	175
	Introduction.....	175
	Methods and materials.....	178
	Results and discussion.....	192
	Toxicity test.....	192
	Self-grooming behavior test.....	193
	Hot plate nociception (HPN) test	197
	Elevated plus maze (EPM) test	199

Elevated zero maze (EZM) test.....	204
Social memory duration test	206
Acoustic Startle Response (ASR) and prepulse inhibition (PPI) test	209
Open field locomotion test	218
Future plans.....	242
VI. FUTURE PLANS.....	245
REFERENCES.....	256

LIST OF TABLES

Table

2.1. IC ₅₀ for telomerase inhibition in a direct telomerase assay.....	76
2.2. IC ₅₀ calculated for the inhibition of DNA synthesis in the polymerase stop reaction.....	80
3.1. Comparison of volumes and concentrations dispensed of drugs and controls for the different formats of the screen.....	110
3.2. Confirmed hits that showed agonistic behavior for the human OTR.....	125
3.3. Confirmed hits that showed positive allosteric modulator behavior for the human OTR.....	126
3.4. Assay statistics for the Screen Quest™ Fluo-8 No Wash Calcium Assay Kit for a homogeneous assay.....	130
3.5. EC ₅₀ values for OT, AVP, carbetocin, and compound 39.....	133
3.6. Representative plate-based statistical data for controls.....	133
3.7. Statistical data for the comparison of the PathHunter™ β-arrestin Detection kit and the FLIPR ^{TETRA} ® system.....	136
3.8. Potencies and efficacies of OTR agonists in FLIPR ^{TETRA} ® and DiscoverRx systems.....	137
4.1. EC ₅₀ of the natural ligands for the human OT / AVP receptors.....	144

4.2. EC ₅₀ calculated for the actives from pure compounds.....	160
4.3. Similarity among the OTR in human, mouse, and rat.....	173
4.4. Similarity between the human, the mouse, and rat OTR protein sequences.....	173
5.1. Statistical data obtained for OT, saline, and MK-801 intraperitoneal effect in a 3 hs open field test for non-cannulated male mice.....	225
5.2. Statistical data obtained for OT dose dependent effect in the open field locomotion test (2 h) for non-cannulated male mice.....	227
5.3. Statistical data obtained for cmpd39 dose dependent effect in the open field locomotion test (2 h) for non-cannulated male mice..	238
5.4. Statistical data obtained for cmpd39 dose dependent effect in the open field locomotion test (2 h) for non-cannulated male mice in the first interval investigated (75-110).....	241

LIST OF FIGURES

Figures

1.1. Schematic diagram of the drug discovery process.	4
1.2. The flow of materials and data from assay to reported results in HTS.....	9
1.3. The stages of new drug development, starting with preclinical testing and ending with activities monitoring a marketed drug product.....	9
1.4. Ligands of the oxytocin receptor.....	15
1.5. Organization of the oxytocin (OT) and vasopressin (VP) gene structure including schematic depiction of the putative cell-specific enhancers.....	18
1.6. Schematic structure of the human OT receptor with amino acid residues shown in one-letter code.	24
1.7. Schematic model of the human oxytocin receptor indicating amino acid residues which are putatively involved in ligand-binding, cholesterol-binding, and associated signal transduction events.....	25
1.8. Schematic model of the structure of the (OT) receptor and its interaction with OT.....	27
1.9. Primary sequence alignments of the human OT receptor (OTR), the human vasopressin 2 receptor (V ₂ R), the human vasopressin	

1a receptor ($V_{1a}R$), and the human vasopressin 1b receptor ($V_{1b}R$).....	29
1.10. Cmpd39 is the most potent and selective OTR agonist reported up-to-date.....	55
2.1. Structures of initial hits identified as G-quadruplex stabilizers in the fluorescent based screen of the NCI diversity set.....	72
2.2. Concentration dependence of telomerase inhibition in a direct telomerase assay.....	73
2.3. Representative gel from NSC 35489 used to obtain a dose response curve of the telomerase inhibitors in a direct telomerase assay.....	75
2.4. Representative concentration dependent profile for compound NSC 354961 in a direct telomerase assay.....	76
2.5. Selectivity test of hits for G-quadruplex stabilization by polymerase stop assay.....	78
2.6. Concentration dependent inhibition of DNA synthesis by NSC 176327 containing the human telomeric sequence [TTAGGG] ₄	79
2.7. Concentration dependent inhibition of DNA synthesis by NSC 176327 containing the human telomeric sequence [TTAGGG] ₄	80
2.8. Characteristic pattern of peaks for Na and K solutions	

and their respective G-quadruplex shapes.....	82
2.9. CD spectra and stoichiometry analysis of NSC 176327.....	84
2.10. CD spectra and stoichiometry analysis of NSC 305831.....	85
3.1. GPCR signaling pathways of interest for HTS, including the regulatory pathway signaled by β -arrestins.....	92
3.2. Graphic representation of the FLIPR Calcium 4 Assay Kit.....	95
3.3. β -galactosidase enzyme fragment complementation.....	98
3.4. OT dose response curve map for 96 well plate format.....	102
3.5. OT dose response curve map for 384 well plate format.....	103
3.6. Plate map for 96 well plate format low throughput screen.....	107
3.7. Standard Operating Procedure for High Throughput Screen Assay.....	107
3.8. Plate map for 384 well plate format for high throughput screen.....	110
3.9. Map plate for validation of Fluo-8 NW dye for 1536 well-plate format.....	112
3.10. Map plate for validation of PathHunter Detection Technology.....	115
3.11. Screen of NCI Diversity Set revealed agonists and positive allosteric modulators.....	118

3.12. Dose response curve for activation of the hOTR in a 96 well plate format.....	118
3.13. Optimization of cell conservation and plate treatment for a 384 well plate format.....	120
3.14. Dose response curves for OT and L 371,257, a selective OT antagonist in the 384 well-plate format.....	122
3.15. Multi-well graph from agonists and positive allosteric modulators screen displaying controls location and kinetic profiles.....	124
3.16. DMSO Tolerance for a 384 well plate format using a Screen Quest™ Fluo-8 No Wash Calcium Assay Kit for a homogeneous assay.....	131
3.17. Representative dose response curves for OT, AVP, carbetocin, and compound 39 in the CHO-hOTR (A) and CHO-hV _{1a} R assays (B).....	132
3.18. Dose response curves for OT, AVP, carbetocin, and compound 39 in the FLIPR and DiscoverX platforms.....	138
4.1. Dose response curves of agonists.....	157
4.2. Dose response curves of positive allosteric modulators.....	159
4.3. Dose response curves for the fluorescence-based intracellular calcium mobilization assay using wild type CHO cells for the identification of compounds that release Ca ²⁺ non-specifically.....	161

4.4. Dose response curves for the fluorescence-based intracellular calcium mobilization assay for compound 39 against hOTR and the VR family.....	163
4.5. PLC- Catalyzed Hydrolysis of [³ H] PIP ₂ caused by receptor activation.....	165
4.6. Monitoring of IP ₃ release to confirm activation of the hOTR.....	166
4.7. Cell toxicity assessment of compound 39 in a SRB assay using HEK-293 cells.....	169
4.8. Pipeline flowchart.....	170
4.9. Primary sequence alignments of the OTR for human (h), mouse (m), and rat (r).....	172
5.1. Apparatus used for animal neurophysiological and behavioral testing.....	190
5.2. OT self-grooming effect.....	195
5.3. Compound 39 self-grooming effect via intraperitoneal administration.....	196
5.4. OT effects on latency to respond to the hot plate nociception test.....	198
5.5. Comparison between untreated C57BL/6J mice and literature data.....	201

5.6. Isoflurane effect as an anesthetic to be used in the elevated plus maze with ICV cannulated C57BL/6J mice.....	201
5.7. OT anxiolytic effects in the elevated plus maze in ICV cannulated mice.....	202
5.8. Anxiolytic-like effects of OT in Balb/C mouse strain in EPM.	203
5.9. Anxiolytic-like effects of OT in C57BL6/J and Balb/C male mouse strains in EZM.	205
5.10. Social memory duration of male C57BL/J mice after exposure to different female strangers.....	208
5.11. Dose-dependent effect of subcutaneous MK-801 on acoustic startle response and prepulse inhibition in male C57BL/6J mice.....	211
5.12. Dose-dependent effect of ICV OT on acoustic startle response and PPI in mice treated with MK-801 (1 mg/kg) subcutaneously.....	212
5.13. Dose-dependent effects of i.p. OT on acoustic startle response in mice treated with s.c. injections of MK-801.....	215
5.14. Dose-dependent effects of i.p. OT on prepulse inhibition in mice treated with s.c. injections of MK-801.....	216
5.15. Dose-dependent effects of i.p. cmpd39 on prepulse inhibition in mice treated with s.c. injections of MK-801.....	219
5.16. Dose-dependent effects of i.p. cmpd39 on acoustic startle response in mice treated with s.c. injections of MK-80.....	220

5.17. OT effect in the open field test for ICV cannulated male mice (15 min).....	223
5.18. OT and MK-801 intraperitoneal effect in a 3 hs open field test for non-cannulated male mice.....	224
5.19. OT and MK-801 intraperitoneal effect in an open field test: 75-105 and 135-255 min intervals.....	226
5.20. OT dose dependent effect in the horizontal and total distance traveled for the open field locomotion test (2 hs).....	228
5.21. OT dose dependent effect in time spent and distance traveled in the center region for the open field locomotion test (2 hs).....	230
5.22. OT dose dependent effect in repetitive fine movements and upright rearing movements of the open field locomotion test (2 h).....	231
5.23. Cmpd39 dose dependent effect in the horizontal and total distance traveled for the open field locomotion test (2 h).....	235
5.24. Cmpd39 dose dependent effect in time spent and distance traveled in the center region for the open field locomotion test (2 h).....	236
5.25. Cmpd39 dose dependent effect in repetitive fine movements and upright rearing movements of the open field locomotion test (2 h).....	237

5.26. Cmpd39 and MK-801 effect in an open field test (TOTDIST, HACT, and CTRDIST): 75-110 and 115-145min intervals.....	239
5.27. Cmpd39 and MK-801 effect in an open field test (STRCNT, RMOVNO, and CTRTIME): 75-110 and 115-145 min intervals.....	240
6.1. A simple cycle of life illustrates numerous points at which OT may affect behaviors and physiology to facilitate the propagation of the species.....	246

ABBREVIATIONS

ACTH	Adrenocorticotrophic hormone, corticotropin
ADME	Absorption, distribution, metabolism, and excretion
ANOVA	Analysis of variance
ASR	Acoustic startle response
ASD	Autism spectrum disorders
AVP	Vasopressin
BBB	Blood-brain barrier
CNS	Central nervous system
CRH	Corticotropin-releasing hormone
CSF	Cerebrospinal fluid
CTRDIST	Center distance
CTRTIME	Center time
DMPK	Drug metabolism and pharmacokinetics
EC _x	x maximal effective concentration
EPM	Elevated plus maze
ERE	Estrogen response element
EZM	Elevated zero maze
GnRH	Gonadotropin-releasing hormone
GPCR	G-protein coupled receptor
GTP	Guanosine-5'-triphosphate
HACT	horizontal activity
hOTR	Human oxytocin receptor
HPA	Hypothalamic-pituitary-adrenal axis
HPN	Hot plate nociception
hs	Hours
HTS	High-throughput screen
ICV	Intra-cerebroventricular
IC _x	x maximal inhibitory concentration

i.p.	Intraperitoneal
IP3	Inositol triphosphate or inositol 1, 4, 5- triphosphate
ITI	Inter-trial intervals
K _d	Dissociation constant
K _i	Dissociation constant (binding affinity)
LH	Luteinizing hormone
min	Minutes
mOTR	Mouse oxytocin receptor
NIH	National Institute of health
NMDA	N-methyl-D-aspartic acid receptor
NO	Nitric oxide
OCD	Obsessive-compulsive disorder
OT	Oxytocin
OT KO	Oxytocin knockout
OTR	Oxytocin receptor
PCP	Phencyclidine
PIP2	Phosphatidyl inositol 4, 5-bisphosphate or Ptd Ins (4, 5) P ₂
PLC	Phospholipase C
PPI	Prepulse inhibition
PVN	Paraventricular nucleus
RLU	Relative light units
RMOVNO	Upright rearing movement numbers
RT	Room temperature
s.c.	Subcutaneous
SEM	Standard error of the mean
SNPs	Single-nucleotide polymorphism
SON	Supraoptic nucleus
SOP	Standard Operating Procedure
STRCNT	Stereotypy counts
TC	Tissue culture
TOTDIST	Total distance traveled

UNC-CH	University of North Carolina at Chapel Hill
VR	Vasopressin receptor
WT	Wild type

CHAPTER 1

INTRODUCTION

The principal aim of pharmacology in drug discovery is the characterization of drug activity by system-independent scales that allow prediction of drug activity in all cellular systems. This thesis concentrated in two drug targets: telomeres and GPCRs. Telomere biology is a validated anticancer drug target. G-protein-coupled receptors (GPCRs) are a very relevant class of biological targets because they recognize external ligands and transmit signals to cellular G-proteins (guanine-nucleotide-binding proteins) to elicit a response. These receptors are tractable for drug discovery because they are on the cell surface therefore drugs do not need to penetrate the cell to produce an effect [1]. In 2000, nearly half of all prescription drugs in the US were targeted towards GPCRs [2]. This thesis will explore screening and characterization of telomere and GPCR targeted agents in two separate projects.

Overview of Drug Discovery Processes

Once a target has been validated, the drug discovery process can be broadly divided into two phases: the discovery phase, involving high-throughput screening

(HTS) in which large sections of chemical space are sampled for biological activity, and the lead optimization phase, during which chemically tractable and validated hits obtained from HTS are subject to methodological synthetic modification in order to optimize activity (Fig. 1.1.). Lead optimization assays characteristically use recombinant proteins from appropriate sources, for example human receptors for drugs designed to target human pathways, to allow superior prediction of the therapeutic activity of the molecules [1].

Identification of targets

The first step in any drug discovery campaign is to understand the molecular biology of a disease or illness and to identify target proteins that play pivotal roles in the disease state. These efforts concentrate in identifying the targets that show a relationship with protein function and the symptoms of a disease. The sequence and three-dimensional structure of the target protein does not necessarily need to be known as direct or indirect rational design approaches for drug discovery can be taken [3].

High-throughput screening (HTS)

Once a target has been validated, the drug discovery process continues into the discovery phase, involving high-throughput screening in which large sections of chemical space are sampled for biological activity. HTS of chemical compounds to identify probes used in chemical biology and modulators of molecular targets is a mainstay of pharmaceutical development. The flexibility and diversity associated

with HTS including assay formats, chemical library diversities, reagent and sample delivery methods, detection methods, the level of automation, and the data analysis algorithms, has allowed numerous areas of biology to interface with an equally

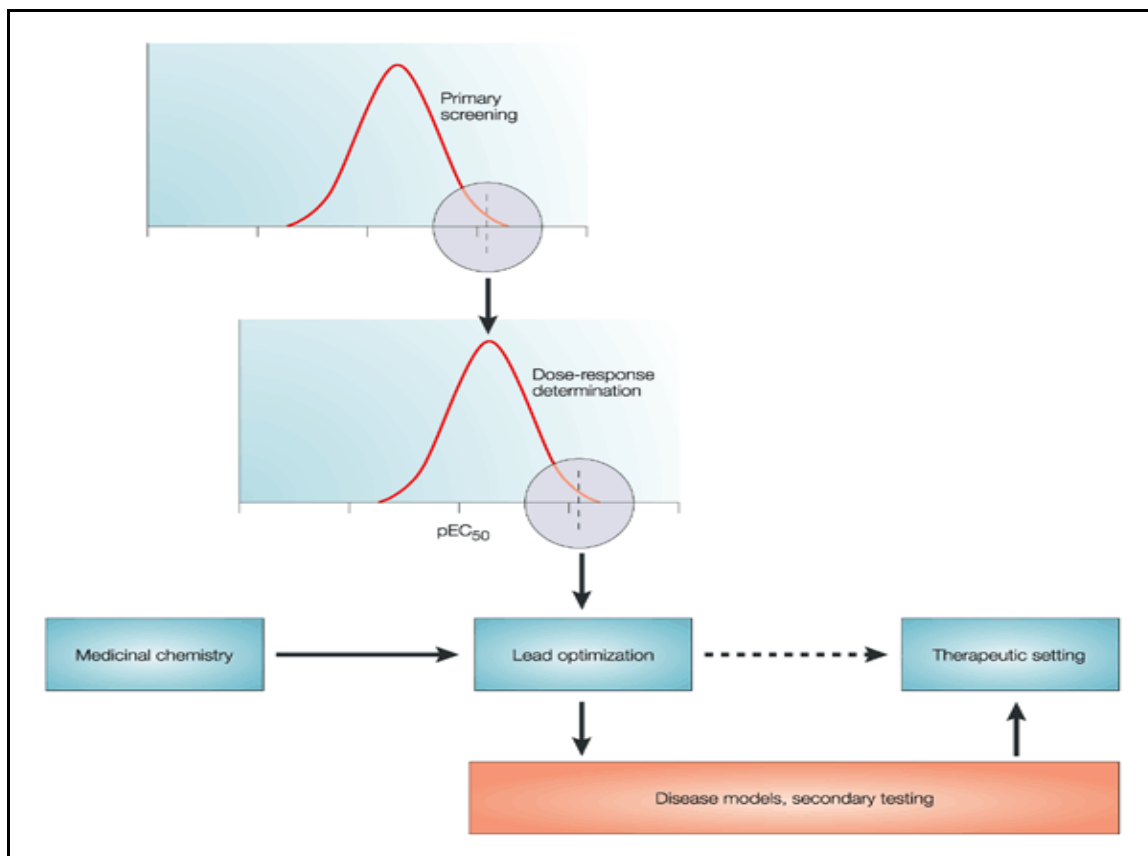


Fig 1.1. Schematic diagram of the drug discovery process. The discovery phase of drug discovery consists of HTS testing of as many compounds as possible at a single concentration. The Gaussian distribution shows the responses for a library of compounds; a predetermined criterion for activity is used to select compounds for testing in a dose-response mode. Under these circumstances, the compounds producing the greatest response at a single concentration (values furthest right on the Gaussian curve) are subjected to a dose-response analysis. The resulting dose-response curves yield potencies quantified as EC_{50} values; the Gaussian distribution for these data show that a small percentage of the compounds show high potency. These compounds are promoted to the lead optimization stage during which the activity of original lead molecule is optimized through chemical modification. If the lead optimization assay is well matched to the required therapeutic profile, then compounds of sufficient activity (and drug-like properties with sufficient safety profile) go on to clinical testing. Picture borrowed from [1].

diverse palate of chemistry. Increasingly, HTS is being used to identify chemical probes of genes, pathways, and cell functions, with the ultimate goal of comprehensively delineating relationships between chemical structures and biological activities [4, 5]. Achieving this goal requires methodologies that efficiently generate pharmacological data from the primary screen and reliably profile the range of biological activities associated with large chemical libraries. In the early 1990s, the advent of combinatorial chemistry and commercial consolidation of small molecule collections resulted in a tremendous increase in compound numbers, requiring the development of high-throughput screening (HTS) to effectively assay the chemical diversity. In addition, sensitive *in vitro* assays became readily available with the advancement of techniques to produce recombinant proteins and engineered cell lines [4, 6].

Important aspects of a small-molecule screen can be divided into five categories: the assay, the library, the HTS process, the post-HTS analysis of data and compound structures, and the screen results (Fig. 1.2.). Assays fall into three general types: isolated molecular target assays, cell-free multicomponent assays, and cell- or organism-based assays. Cellular assays can be subdivided into reporter gene-type assays and phenotypic assays that measure outputs resulting from intact cellular processes. The library should include quality control procedures. The HTS process should contain assay controls, including inter-plate controls to assess systematic variations of the response, and intra-plate controls to establish the assay window and to analyze the uniformity of the biological response. During the post-HTS analysis verification of chemical structure of active compounds should take

place. Finally, ranking of primary screening actives should allow description of the outcome of the HTS [5].

Validation of hits

Secondary screens test many fewer compounds (e.g., the 1% most active compounds from the primary screen) and typically use at least duplicate measurements. Paradoxically, compounds with the highest measured activity levels on a primary screen will on average be less extreme on a secondary screen because of a statistical artifact known as 'regression toward the mean'. Accordingly, marginal hits on the first run may fail to validate on the second run merely because of random measurement error, although the size of the statistical artifact can be minimized by improving measurement precision (e.g., by obtaining replicate measurements). Confirmed hits with an established biological activity according to a structure-activity relationship (SAR) series and medicinal chemistry are termed 'leads' that can develop into drug candidates for clinical testing [6].

Most drugs on the market were not discovered in their final form but went through a process of experimentation and modification to make the best possible therapeutic agent. The starting point of modern drug discovery is identification of a lead compound. The lead compound serves as an initial prototype that is modified to retain or enhance the desired activity and to eliminate or minimize unwanted properties. A lead compound may present high toxicity, low selectivity, problems with ADME (absorption, distribution, metabolism, and excretion) processes, or complex or expensive manufacturing processes. The lead has to be transformed into a drug

to impart suitable drug-like properties such as low toxicity and the ability to reach the site of action in appropriate concentrations, as well as acceptable cost of synthesis. The optimized compounds should be screened for efficacy in a suitable animal model [3].

Drug discovery pipeline

The drug research and development process is complex, lengthy, and expensive. For every 10,000 compounds synthesized or isolated as potential drugs, only one on average will successfully complete all the requirements to make it to the market. Currently, the estimated cost of bringing a new drug to the market is \$800 million, and the average length of time from discovery to patient is 10 to 15 years [3]. Figure 1.3. shows a scheme of the stages necessary for a new drug to reach the market.

The projects in this dissertation will describe two different approaches to the successful identification of small-molecules that interact with their respective identified targets. Both of these projects involved the discovery and design stages of drug discovery. The first project focused on the identification of new G-quadruplex stabilizers and their ability to inhibit human telomerase as an anticancer drug modality. The second project focused on the identification of novel small-molecules that selectively activate the human oxytocin receptor to regulate complex behaviors in animal models with therapeutic implications in various neuropsychiatric disorders. The second section includes validation and optimization of high-throughput assays

to identify actives, their validation against the receptor target and the effects of the active molecules in specific animal models that are clinically relevant.

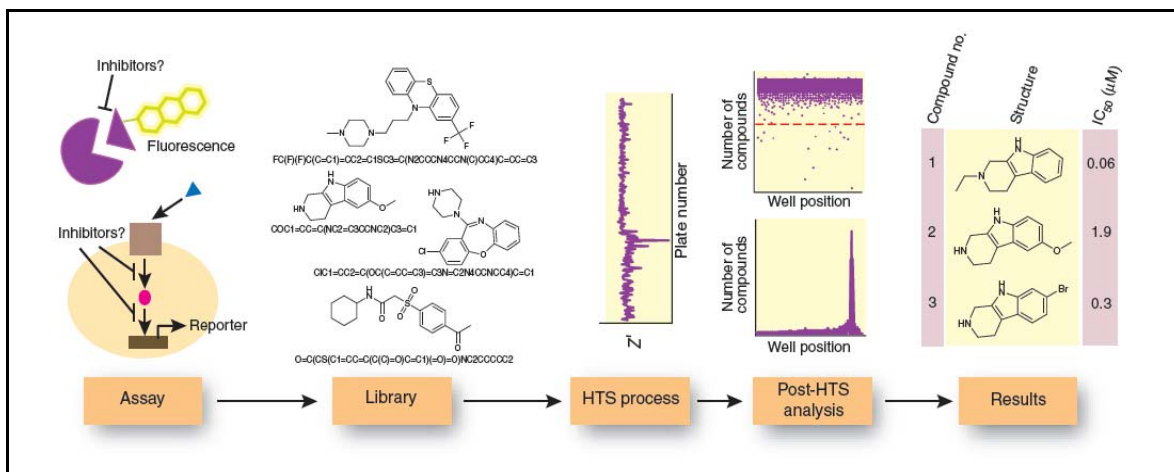


Fig. 1.2. The flow of materials and data from assay to reported results in HTS. Picture borrowed from [5].

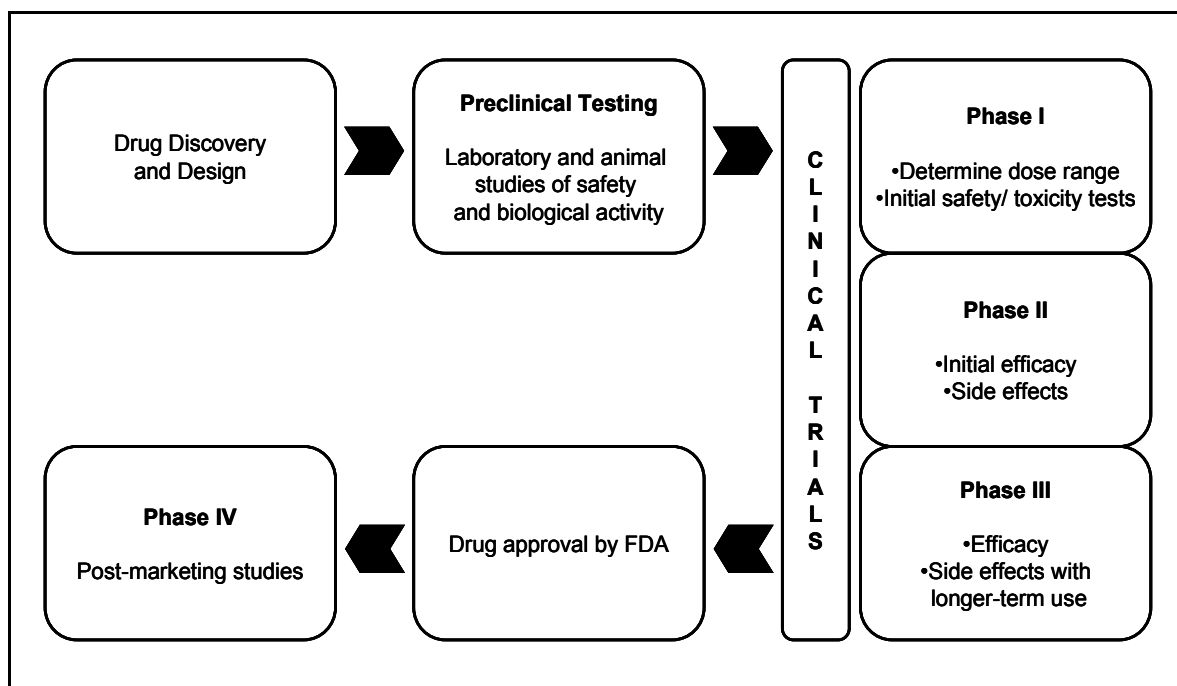


Fig. 1.3. The stages of new drug development, starting with preclinical testing and ending with activities monitoring a marketed drug product. Borrowed from [3].

BACKGROUND AND SIGNIFICANCE

Novel G-quadruplex stabilizers

Human chromosomes terminate with telomeres, which contain double-stranded G-rich, repetitive DNA followed by a single-stranded overhang of the G-rich sequence. Single-stranded oligonucleotides containing G-rich telomeric repeats have been observed in vitro to fold into a variety of G-quadruplex topologies depending on the solution conditions. G-quadruplex structures are notable in part because G-quadruplex ligands inhibit both the enzyme telomerase and other telomere-binding proteins. Because telomerase is required for growth by the majority of cancers, G-quadruplex-stabilizing ligands have become an attractive platform for anticancer drug discovery [7]. Intense interest exists in the identification, design, and synthesis of small molecules that might selectively bind to defined sites in DNA or RNA [8].

Telomeres

Telomeres are the DNA–protein complexes that define the ends of eukaryotic chromosomes and function as a cap to protect chromosome ends from unwanted cellular activities such as DNA recombination and degradation [9]. Human telomeric DNA is typically comprised of 5–12 kb of a repetitive, double-stranded DNA (5'-TTAGGG-3'/3'-AATCCC-5') followed by a 150- to 300-nucleotide, guanosine-rich, single-stranded overhang. In normal somatic cells, telomeric DNA shortens by approximately 50–200 bases during each cell cycle due to inefficient replication of

linear chromosomes by the normal DNA replication machinery and apparent degradation [10]. This routine loss of telomeric DNA, which eventually results in chromosomal instability, is offset in proliferating cells including the majority of cancer cells by the action of telomerase and is a major factor in immortalization and tumorigenesis [11, 12]

Telomerase

Telomerase is a ribonucleoprotein with reverse transcriptase activity that specifically extends the G-rich strand of telomeric DNA. Telomerase activity is over-expressed in 85% of cancer cell types, but is not detected in normal somatic cells. This enzyme's ability to catalyze the synthesis of telomeric DNA repeats is responsible for telomere-length homeostasis [12]. As a result, cancer cells increase their replicative lifespan indefinitely by extending and maintaining the length of their telomeres [9]. Inhibition of telomerase induces cell senescence and cell death in cancer cells [12]. Because telomere maintenance is required for continuous cellular proliferation, and because telomerase is differentially expressed in cancer cells when compared to normal cells, selective telomerase inhibitors have been sought as an anticancer drug approach. One approach to telomerase inhibition involves sequestering its substrate, single-stranded telomeric DNA, by inducing it to form G-quadruplex structures [12, 13]. Although DNA exists predominantly in a right-handed duplex form in the genome, specific regions of the genome can exist in single-stranded form, or can adopt multistranded structures such as triplexes or tetraplexes, for example telomeric DNA can form a G-quadruplex [8, 14].

G-quadruplexes

Single-stranded, G-rich telomeric DNA is capable of folding into four-stranded intramolecular quadruplex structures containing a tetrad of G–G base pairs [15]. Several conformations of G-quadruplexes formed by the human telomeric DNA sequence have been observed. An antiparallel G-quadruplex topology has been determined for the solution structure of a human telomeric sequence in the presence of Na^+ . The crystal structure of a K^+ -stabilized quadruplex formed by human telomeric DNA was found to be in a parallel propeller-like arrangement. However, the solution structure of a K^+ -stabilized human telomeric DNA was reported independently by two separate groups to exhibit a mixed type structure with three of the strands parallel to each other and one strand antiparallel. It is necessary for the RNA template of telomerase to associate with the G-rich single strand of the telomere to effectively catalyze DNA repeat addition. Telomerase from several species cannot utilize intramolecular G-quadruplex structures as a primer for DNA synthesis and telomerase activity is perturbed by G-quadruplex formation. In addition, it has been shown that the G-quadruplex-binding ligands can displace telomere-associated proteins such as hPOT1 and telomerase from the telomere in treated cells [8]. This unmasking of the 3'-overhang invokes a rapid DNA damage response, which rapidly leads to selective cell death and anti-tumor activity in vivo [12].

G-quadruplex binding ligands

Small-molecule G-quadruplex-binding ligands have been explored as an approach towards telomerase inhibition. By inducing or stabilizing G-quadruplexes, G-quadruplex-binding ligands have the potential to affect human biology by several mechanisms. One of the greatest challenges in this field is the production of ligands with significant selectivity for specific G-quadruplex DNA structures as compared to canonical dsDNA [7]. Compounds that selectively stabilize quadruplex DNA within telomeres might effectively block telomerase activity by locking the nucleic acid substrate into an unfavorable conformation for its replication. Such small molecules may be potentially valuable as therapeutic agents [8, 14] and chemical tools to study the biological relevance of G-quadruplexes. Small-molecule ligands that induce the formation of G-quadruplex structures have been reported, although none as yet have reached the clinic [12, 16]. In Chapter 2, a HTS for G-quadruplex binders was developed and the actives resulting from it were validated.

Novel non-peptide human oxytocin receptor agonists and positive allosteric modulators

Human behavior is complex and poorly understood. Understanding the pharmacological basis for complex behavior would allow the development of tools to regulate behavioral disorders, which would be of great benefit in certain disease states. There is a substantial amount of evidence that oxytocin (OT) and activation of the oxytocin receptor (OTR) at the central nervous system (CNS) level modify complex behaviors.

There is a pressing need for selective small molecules that selectively activate the OT system within the CNS. Such small molecules could serve as new chemical tools to elucidate the complex roles for oxytocin in complex behaviors and provide leads for a drug discovery campaign focused on specific neuropsychiatric disorders. The work presented in Chapter 3-5 was focused on both the identification of agonists and positive allosteric modulators of the OTR through a HTS campaign and the confirmation that small-molecules can influence complex behaviors through the OT pathway. Potential leads were validated with secondary and counter screens for OTR-efficacy and specificity. A previously reported synthetic agonist was then tested with well established animal models for anxiety, analgesia, and deficits in social memory and prepulse inhibition.

Oxytocin

All neurohypophysial hormones are nonapeptides with a disulfide bridge between Cys residues 1 and 6. This results in a peptide constituted of a six-amino acid cyclic part and a COOH-terminal α -amidated three-residue tail. OT and vasopressin (AVP) differ from each other in terms of two amino acids (Ile vs. Phe at position 3 and Leu vs. Arg at position 8, respectively (Figure 1.4.), which enables AVP and OT peptides to selectively bind their respective receptors [17, 18]. OT and AVP have been found only in mammals and probably have developed in parallel with typical mammalian behaviors, such as uterine contraction during labor and milk ejection essential for lactation.

OT gene structure

In all species, OT and vasopressin genes are on the same chromosomal locus but are transcribed in opposite directions (Fig. 1.5.). The human gene for OT-neurophysin I encoding the OT prepropeptide is mapped to chromosome 20p13 and consists of three exons: the first exon encodes a translocator signal, the nonapeptide hormone, the tripeptide processing signal (GKR), and the first nine residues of neurophysin; the second exon encodes the central part of neurophysin (residues 10–76); and the third exon encodes the COOH-terminal region of neurophysin (residues 77– 93/95) [17].

The main function of neurophysin, a small (93–95 residue) disulfide-rich protein, appears to be related to the proper targeting, packaging, and storage of OT within the granula before release into the bloodstream. OT is found in high concentrations (0.1 M) in the neurosecretory granules of the posterior pituitary complexed in a 1:1 ratio with neurophysin. In such complexes, OT-neurophysin dimers are the basic functional units [20]. The protonated α -amino group (Cys-1) in OT forms an essential contact site to neurophysin via electrostatic and multiple hydrogen bonding interactions. Due to its dependence on amino group protonation (pK_a ; 6.4), the binding strength between OT and neurophysin is much higher in an acidic compartment like the neurosecretory granules (pH: 5.5). Conversely, the dissociation of the complex is facilitated as the complex is released from the neurosecretory granules and enters the plasma (pH 7.4) [17] .

Analysis of various gene constructs in transgenic mice led to the proposal that cell-specific enhancers for OT and vasopressin gene expression are not located on

the 5'-upstream regions of these genes, but is present in the intergenic region 0.5–3 kb downstream of the vasopressin gene (see fig. 1.5.). The human and rat OT promoters could be stimulated by the ligand-activated estrogen receptors ER α and ER β , the thyroid hormone receptor THR α , and the retinoic acid receptors RAR α and RAR β in a variety of cells [21, 22]. The estrogen-induced rise in uterine OT mRNA is probably mediated via the common hormone response element in the OT gene promoter [17].

OT synthesis and localization

OT and AVP are mainly synthesized in the magnocellular neurons of the SON (supraoptic nucleus) and PVN (paraventricular nucleus) in the hypothalamus; they are the most important nuclei of the hypothalamic-neurohypophysial system. OT and AVP are assembled on ribosomes at the level of the soma of the neurons as precursors which are subsequently processed in the neurosecretory vesicles. During the intravesicular post-translational processing, OT precursor undergoes sequential proteolytic cleavage and other enzymatic modifications, such as glycosylation, phosphorylation, acetylation, and amidation that lead to the three final products: OT, neurophysin and a carboxy-terminal glycoprotein. The OT prepropeptide is subject to cleavage and other modifications as it is transported down the axon to terminals located in the posterior pituitary [23]. The mature peptide products, OT and its carrier molecule neurophysin, are stored in the axon terminals until neural inputs elicit their release [17]. Action potentials in the neurosecretory magnocellular neurons in the PVN and SON trigger the release of OT from their axon terminals in the

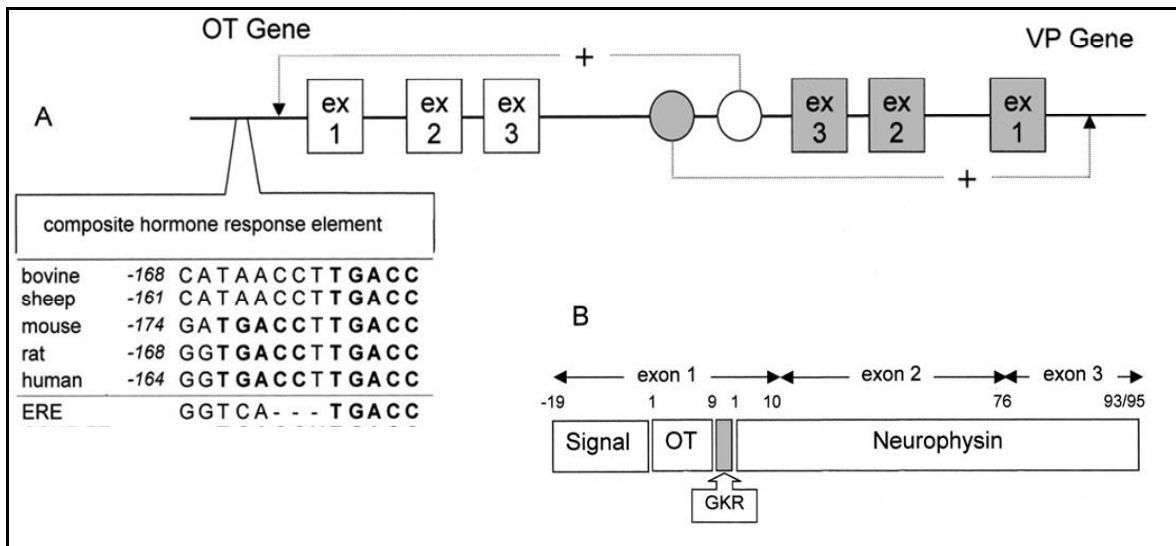


Fig. 1.5. Organization of the oxytocin (OT) and vasopressin (VP) gene structure including schematic depiction of the putative cell-specific enhancers (open circle, enhancer of OT gene; shaded circle, enhancer of VP gene). A. Details of the approximately 2160-bp region (composite hormone response element) of the upstream OT gene promoter conserved across five species including the sequence of the response elements estrogen response element (ERE). **B.** D domain organization of preprooxytocin including the processing sites. The precursor is split into the indicated fragments by enzymatic cleavages, one involving a glycylylarginine (GKR) sequence and leaving a carboxamide group at the COOH-terminal end of OT. Signal: signal peptide. Picture from [17].

neurohypophysis [24].

OT release in the hypothalamus-neurohypophysis axis

Within the neurohypophysis each axon produces several nerve terminals that constitute about 50% of the total volume of the neural lobe. Once activated, magnocellular neurons release OT into the blood stream where it is transported to distant target organs, such as mammary gland and kidney. Several other biologically active substances, including neuropeptide Y, tyrosine hydroxylase, dynorphin, thyrotropin-releasing hormone, atrial natriuretic factor, galanin and nitric oxide (NO) synthase, are co-released with OT and AVP from magnocellular neurons, however, the reciprocal effects between them and OT are still unknown [25].

Oxytocinergic magnocellular axons do not reach only the posterior pituitary, but also terminate in the arcuate nucleus, the lateral septum, the medial amygdaloid nucleus, and the median eminence [26]. In the magnocellular SON and PVN nuclei, OT is also locally released from dendrites acting as a self-neuromodulator: this intranuclear release is fundamental for the synchronization of the depolarization of OT neurons during lactation and for the positive feed-back of OT dendritic release in the SON during parturition [27]. In fact, the somatodendritic release occurs in response to a variety of stimuli, including suckling, parturition, dehydration, hemorrhage, fever, physical restraint, pain, mating and territorial marking behaviors, administration of hypertonic solutions or pharmacological challenges.

OT neurons are also localized in the dorsal-caudal part of the PVN. The axons of these parvicellular cells are part of the descending tract directed to the

sympathetic centers of the spinal cord and to the parasympathetic caudal autonomic centers, including the dorsal motor nucleus of the nervus vagus and the nucleus of tractus solitarii [28]. The peripheral synthesis of OT has also been demonstrated in placenta, uterus, corpus luteum, amnion, testis, and heart [25].

Hypothalamic OT can reach the anterior pituitary through the hypothalamic-pituitary portal vascular system. In rats, OT is released into the portal vessels and specific OTR are present in the adenohypophysis. OT seems to be involved in the regulation of the release of different adenohypophysial hormones, in particular prolactin, adrenocorticotrophic hormone (ACTH) and gonadotropins. Pituitary OTR gene expression is restricted to lactotrophs and increases at the end of gestation [29]. However, it is unclear whether OT, released during lactation, is responsible for the concomitant secretion of prolactin from the adenohypophysis.

The endocrine response to stress is mediated by the activation of the hypothalamic-pituitary-adrenal axis; in particular, corticotropin-releasing hormone (CRH) and AVP stimulate ACTH secretion from the anterior pituitary. In rats, OT has been demonstrated to potentiate the release of ACTH induced by CRH: in fact, if CRH is responsible for the immediate secretion of ACTH following an acute stress, when CRH levels begin to decrease during prolonged stress, the persistent level of OT in the median eminence seems to be related to the delayed ACTH response and the generation of ACTH pulsatile secretory bursts [30]. On the contrary, in humans, OT infusion inhibited the plasma ACTH responses to CRH, and suckling and breast stimulation increased and decreased, respectively, plasma OT and ACTH levels. These observations indicate an inhibitory influence of OT on ACTH secretion.

Luteinizing hormone (LH) secretion from the adenohypophysis is primarily regulated by the gonadotropin-releasing hormone (GnRH). OT has been demonstrated to stimulate LH release. For example, its administration to proestrous rats can advance the LH surge with an earlier ovulation. Moreover, OT seems to sensitize the pituitary before full GnRH stimulation and in women, pre-ovulatory OT administration leads to the onset of the mid-cycle LH surge [31].

The magnocellular neurons also release OT and VP from their perikarya, dendrites, and/or axon collaterals [32]. Although the amount of release is small compared with the amount released from the neurohypophysis, the concentration of OT and AVP in the extracellular fluid of the SON resulting from this somatodendritic release has been calculated to be 100- to 1,000-fold higher than the basal plasma concentration, i.e., more than 1–10 nM. High-frequency electrical discharges of OT neurons as they occur, e.g., during the milk ejection reflex, might release even higher local OT concentrations [33].

Plasma OT does not readily cross the blood-brain barrier, and there is no relationship between the release of OT into the blood by the neurohypophysis and the variations in OT concentrations in the cerebrospinal fluid (CSF). Peripheral stimulations such as suckling or vaginal dilation that elicit large increases in plasma OT may or may not change the concentration of OT in the CSF. As shown in rats, electrical stimulation of the neurohypophysis only evokes the release of OT into the blood, whereas stimulation of the PVN elicits a release of OT into the blood and into the CSF [17, 34].

OT in the CSF probably derives from neurons that extend to the third ventricle, the limbic system, the brain stem, and the spinal cord. In the CSF, OT is normally present at concentrations of 10–50 pM, and its half-life is much longer (28 min) than in plasma (1–2 min) [35]. In humans and in monkeys, OT concentrations in the CSF follows a circadian rhythm in the with peak values at midday. No such circadian rhythms have been observed in the CSF of rats, cats, guinea pigs, or goats. Circadian rhythms in plasma OT concentrations have not been reported [36]. Moreover, OT fragments such as OT-(1--6) or OT-(7--9) could cross the blood-brain barrier more easily and possibly exert their effects exclusively on the brain, e.g., to influence learning and memory processes [17, 37].

Intranuclear release of these peptides occurs in response to a wide variety of stimuli, including suckling; parturition; hemorrhage; certain kinds of stress such as fever, physical restraint, and pain; mating and territorial marking behaviors; dehydration; administration of hypertonic solutions; and a range of pharmacological stimuli. During parturition and suckling, OT is released within the SON and apparently excites via a short positive-feedback loop the same cells by which it is produced and secreted. This autoexcitatory mechanism leads to further amplification of local and/or neurohypophysial OT release and ensures synchronous firing of oxytocinergic neurons [17, 27, 38, 39] .

Oxytocin receptor (OTR)

OTR Structure

The OT receptor is a typical member of the rhodopsin-type (class I) GPCR family (fig.1.6.) [40]. The high homology of the nonapeptides of the evolutionary line isotocin-mesotocin-OT is also reflected in the high homology of the corresponding receptors. Sequence homologies with the vasopressin V₁ (nearly 50%) and V₂ receptors (40%) are significantly lower. About 100 amino acids (25%) are invariant among the 370–420 amino acids in the human receptors for vasopressin V₂, V_{1a}, V_{1b}, and OT including key amino acid residues that are involved in receptor function (fig.1.7) , [17, 41].

The combined evidence from studies involving site-directed mutagenesis, photoaffinity labeling and molecular modeling indicate that the cyclic part of the OT molecule is lodged in the upper one-third of the receptor binding pocket and interacts with transmembrane domains 3, 4 and 6, whereas the linear C-terminal part of the OT molecule remains closer to the surface and interacts with transmembrane domains 2 and 3, in addition to the first extracellular loop (see fig. 1.8.) [41].

OTR gene structure

The encoded OTR receptor is a 389- amino acid polypeptide with 7 transmembrane domains. As discussed above, the OTR/VR subfamily shows a high sequence homology (see fig. 1.9. for primary gene sequence alignment). To date,

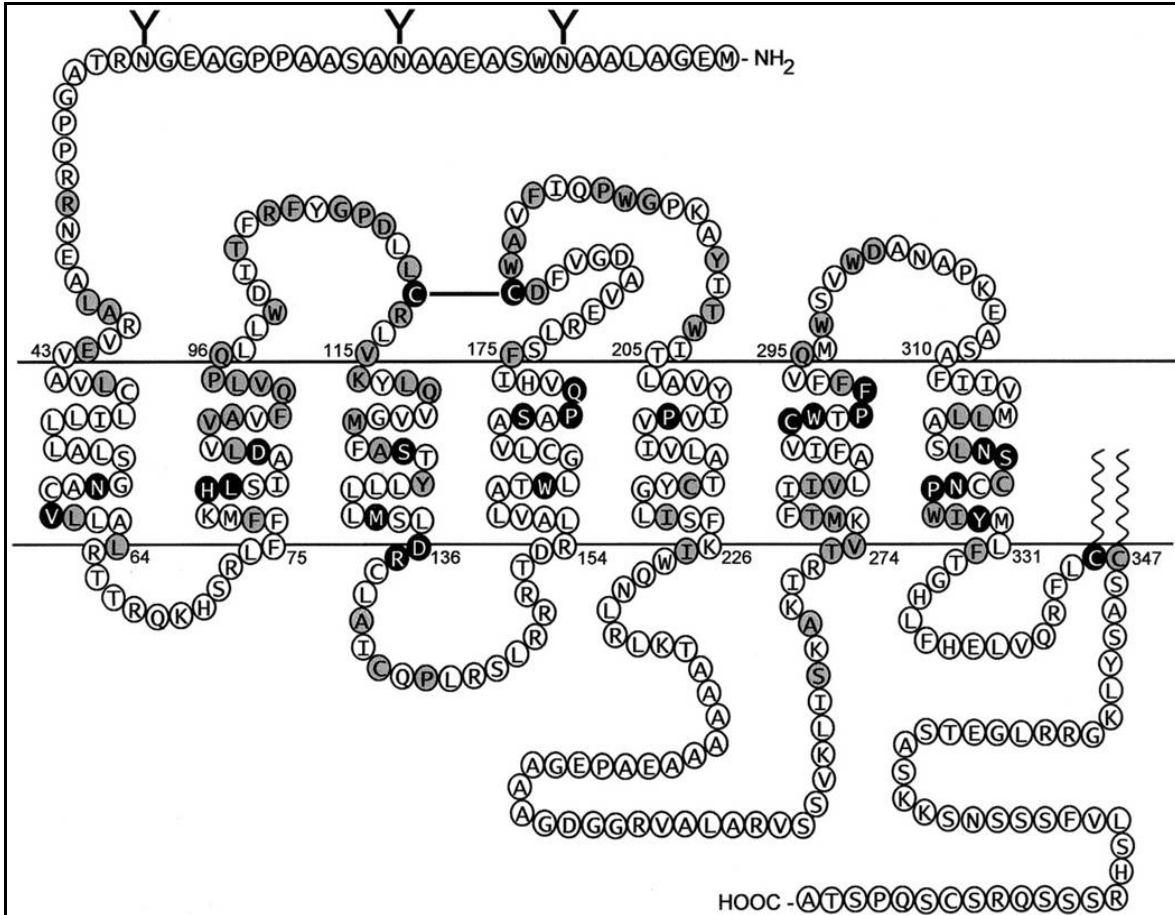


Fig. 1.6. Schematic structure of the human OT receptor with amino acid residues shown in one-letter code. Residues conservative within the OT/vasopressin receptor subfamily are outlined in gray, and residues conservative for the whole G protein-coupled receptor superfamily are outlined in black. The putative *N*-glycosylation ("Y") and palmitoylation (at C346/C347) sites are marked. Picture borrowed from [17].

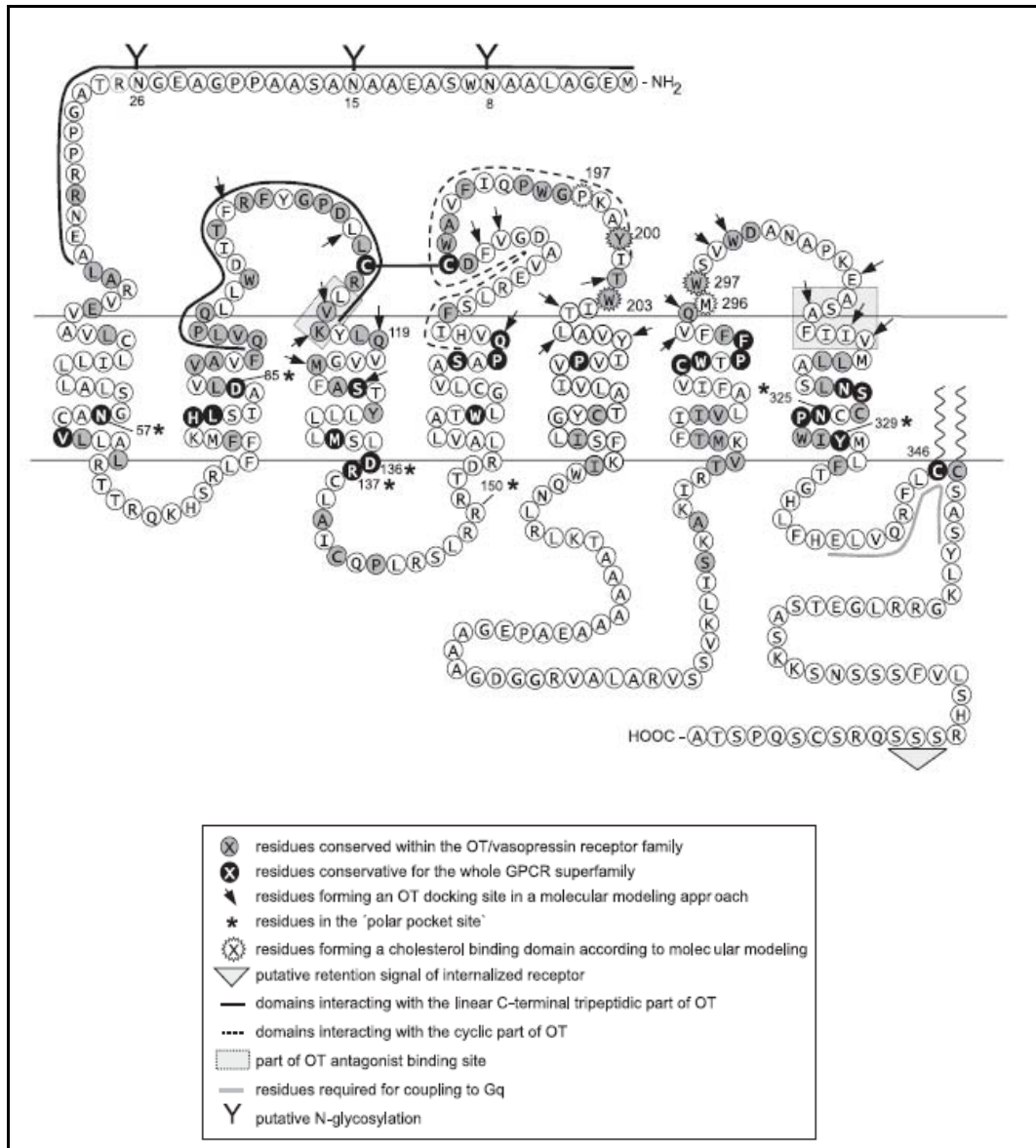


Fig. 1.7. Schematic model of the human oxytocin receptor indicating amino acid residues which are putatively involved in ligand-binding, cholesterol-binding, and associated signal transduction events. The glutamine and lysine residues highly conserved within the vasopressin/oxytocin receptor family may partly define an agonist-binding pocket which is common to all the different subtypes of this receptor family. An oxytocin docking site has been proposed by a molecular modeling approach (marked by arrows). In the inactive receptor conformation, the highly conserved arginine (R137) may be constrained in a pocket which is formed by

polar residues (indicated by asterisks). Following agonist binding this arginine side chain may be shifted out of the 'polar pocket' thereby unmasking a G protein binding site. Receptor domains putatively interacting with oxytocin, peptide oxytocin antagonists and $G_q\alpha$ are marked by lines and dashed boxes as indicated. The amino acid residues marked by a circle with asterisk edge have been predicted to form a cholesterol docking domain according to molecular modeling. Picture borrowed from [42].

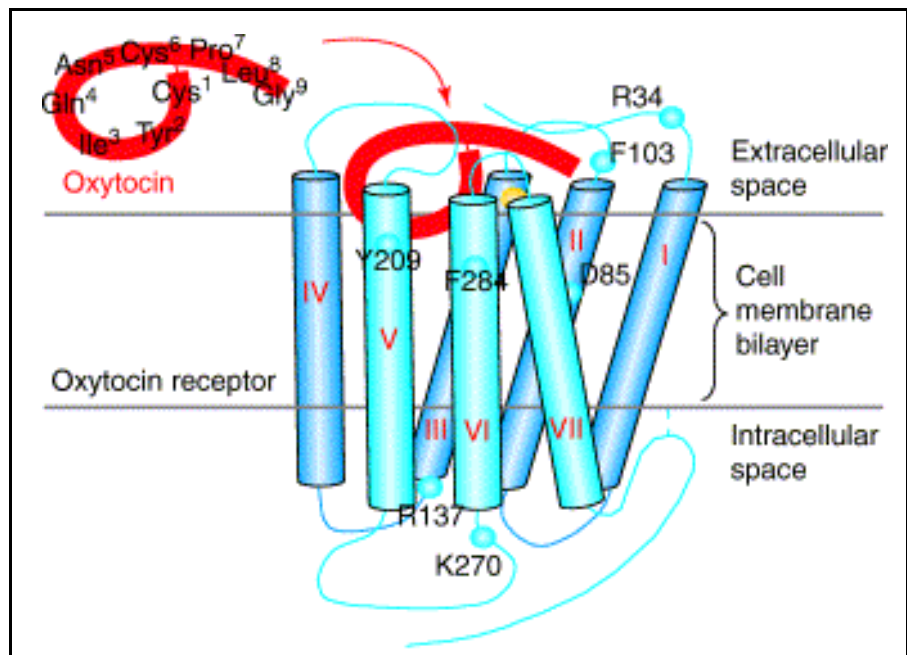


Fig. 1.8. Schematic model of the structure of the (OT) receptor and its interaction with OT. The endogenous ligand, the nonapeptide OT, is shown at the top left with residues numbered 1–9. The OT receptor (shown in blue) is depicted in its proposed interaction with the ligand (shown in red). The seven putative transmembrane domains are indicated by Roman numerals. Picture from [41].

the OT receptor encoding sequences from pig, rat, sheep, bovine, mouse, and rhesus monkey have also been identified.

The OT receptor gene is present in a single copy in the human genome and was mapped to the gene locus 3p25–3p26.2. The gene spans 17 kb and contains 3 introns and 4 exons. Exons 1 and 2 correspond to the 5'-prime noncoding region. Exons 3 and 4 encode the amino acids of the OT receptor. Intron 3, which is the largest at 12 kb, separates the coding region immediately after the putative transmembrane domain 6. Exon 4 contains the sequence encoding the seventh transmembrane domain, the COOH terminus, and the entire 3'-noncoding region, including the polyadenylation signals [17].

Signal transduction, G Protein coupling, and receptor regulation

OTR are functionally coupled to $G_{q/11\alpha}$ GTP binding proteins that stimulate, together with the $G\beta\gamma$ heteroduplex, the activity of phospholipase C- β isoforms. Phospholipase C- β generates inositol trisphosphate and 1, 2-diacylglycerol. Inositol trisphosphate triggers Ca^{2+} release from intracellular stores, whereas diacylglycerol stimulates protein kinase C, which phosphorylates unidentified target proteins.

OTR require at least two essential components for high affinity OT binding: divalent cations such as Mn^{2+} or Mg^{2+} and cholesterol. Divalent metal ions like Mg^{2+} have long been known to increase the response of target cells to OT and to shift the dose-response curve to the left. Thus addition of Mg^{2+} was found to increase both the OT binding capacity and the affinity state of the OT receptor. This is

OTR	MEGALAANWSAEANASAAPPGAEGNRTAGPPRRNEALARVEVAVLC	47
V2R	MLMASTTSAVPGHPSLPSLPSNSSQERPLDTRDPLLARAEALALLS	45
V1aR	MRLSAGPDA GPSGNSSPWPLATGAGNTSREAEALGEGNGPPRDV RNEELAKLEIAVLA	59
V1bR	MDSGPLWDANPTPRGTLSAPNATTPWLGRDEELAKVEIGVLA	42

OTR	LILLLALSNGNACVLLAL RTTRQKHSRLFFFMKHLSTADLVVAVFQVLPQLLWDITFRFY	106
V2R	IVFVAVALSNGLVLAALARRGRGRHWAPIHVEFIGHLCLADLAVALFQVLPQLAWKATDRFR	106
V1aR	VTFAVAVLGNSSVLLALHRTPR KTSRMHLEFIRHLSLADLAVAFFQVLPQMCWDITYRFR	118
V1bR	TVLVLATGGNLAVLLTLGQLGR KRSRMHLEFVHLALTDLAVALFQVLPQLLWDITYRFQ	101
	***** TM 1 *****	***** TM 2 *****
OTR	GPDLLCRLVKYLQVVGMFASYLLLLMSIDRCLAICQPLRSLR RRTDRLAVLATWLG	164
V2R	GPDALCRAVKYLQVVGMYASSYMLAMTDHRRAICRPLAYRHGSGAHWNRPVLVAFS	167
V1aR	GPDWLCRVVKKHLQVFGMFASAYMLVVMTADRYIAVCHP LKTLQQPARRSRLMIAAAWVLS	178
V1bR	GPDLLCRAVKYLQVLSMFASYMLLAMTDRYLAVCHP LRSLQQPGQSTYLLIAAPWLLA	161
	***** TM 3 *****	*****
OTR	LVASAPQVHIFSLRE VADGVFDCWAVEFIQPWGPKAYITWITLAVYIVPVIVLATCYG	221
V2R	LLLSLPQLFIF AQRNVEGGSGVTDWCACFAEPWGRRTYVTWIALMVFVAPTGLIAACQV	226
V1aR	FVLSTPOYFVFS MIEVNNVTKARDCWATFIQPWGSRAYVTWMTGGIFVAPVVILGT	237
V1bR	AIFSLPQVFIFSL REVIQSGVLDCAWDFGFPWGPRAYLTTWTTLAFVLEVTMLTACYS	220
	** TM 4 *****	***** TM 5 *****
OTR	LISFKIWQNLRLKTA AAAAAEPEGAAAGDGRVALARVSSVKLISAKIRTVK	275
V2R	LIFREIHASLVPGP SERPGRRRGRRTGSPGEGAHVSAAVAKTVR	271
V1aR	FICYNIWCNVRGKTASRQSK GAEQAGVAFQKGFLAPCVSSVKSISRAKIRTVK	291
V1bR	LICHEICKNLKVKTQAWRVGGGGWRTWDRPSPSTLAATTRGLPSRVSSINTISR	281
	*** *****	
OTR	MTFIIIVLAFIVCWTPPEFFVQMWVWDAN APKEASAFIIVMLLASLNSCONPWIIYMLFT	333
V2R	MTLVIVVVVYVLCWAPPEFLVQLWAARD PEAPLEGAPFVLLMLLASLNSCTNPWIYASFS	329
V1aR	MTFVIVTAYIVCWAPPEFIIQMWVWDPMVSWTESENPTITITALLGSLNSCONPWIIYMF	352
V1bR	MTFVIVLAYIACWAPPEFSVQMWVWDKNAPDEDSTNVAFITISMLLGNLNSCONPWIIYMGFN	342
	***** TM 6 *****	***** TM 7 *****
OTR	GHLFHELVRFLCCSASYLKGRRLGETSASKKSNSSSFVLSHRSSSQRSCSQPSTA	389
V2R	SSVSSELRSLL CCARGRTPPSLGPQDESCCTASSSLAKDTSS	371
V1aR	GHLLQDCVQSFPCQNMKEKFNKEDTDSMSRRQTFYSNNRSPNTSTGMWKDSPKSSKSIKF	413
V1bR	SHLLPRPLRHLCGGPQPRMRRRLSDGSLSSRHTLLTRSSCPATLSLSLSLTLSGRPRP	403
V1aR	IPVST	418
V1bR	EESPRDLELADGEGTAETIIF	424

Fig. 1.9. Primary sequence alignments of the human OT receptor (OTR), the human vasopressin 2 receptor (V₂R), the human vasopressin 1a receptor (V_{1a}R), and the human vasopressin 1b receptor (V_{1b}R). The putative transmembrane helices 1-7 are underlined (asterisks). The residues conservative within the subfamily (~25% of the whole sequence) are outlined in gray, while those conservative for the whole G protein-coupled receptor superfamily are outlined in black. Picture borrowed from [17].

similar to cholesterol's effect on OTR. In addition, Mg^{2+} has been proposed to display its effect on the OT receptor interaction by influencing positive cooperativity [43]. It appears that cholesterol and Mg^{2+} are essential allosteric modulators of the OT receptor and may be involved in the regulation of OT-mediated signaling functions. Cholesterol can modulate receptor function by both changes of the membrane fluidity and direct binding effects, e.g., in case of the OTR [44]. Plasma membranes with lowered cholesterol content showed a decreased capacity (B_{max}) of binding sites and/or a decreased affinity (K_d) of ligand-receptor binding [17].

Progesterone is considered to be essential to maintain the uterine quiescence. Progesterone specifically binds to the rat OTR with high affinity ($K_d = 20$ nM) and thereby inhibits the receptor function [45]. In case of the human OTR, a direct inhibitory interaction [inhibitory constant (K_i) = 30 nM] with a progesterone metabolite, 5- β -pregnane- 3, 20-dione, has been reported. Progesterone could act as a negative modulator of the OT receptor and thus offered a plausible mechanism of how progesterone could contribute to uterine quiescence.

OTR distribution in the CNS

The brain distribution of OT receptors shows a wide interspecies variability. In the rat, they are present in the olfactory system, basal ganglia, thalamus, limbic system (bed nucleus of the stria terminalis, central amygdaloid nucleus, and ventral subiculum), hypothalamus (ventromedial nucleus), brain stem, and spinal cord with age-related changes in their density. In humans, OT binding sites have been mainly found in the pars compacta of substantia nigra and globus pallidus, as well as in the

paracrine manner from their dendrites of the SON to synchronize bursts of OT release [47]. Each burst leads to massive release of OT into the bloodstream to the lactating breasts. There it causes contraction of the myoepithelial cells in the walls of the lactiferous ducts, sinuses, and breast tissue alveoli. In humans, within 30 s to 1 min after a baby begins to suckle the breast, milk begins to flow. Probably, other important factors, such as the sight, smell, and sound of the baby, facilitate this process [48]. This process is called milk ejection or milk let-down reflex and continues to function until weaning [17]. Electrophysiological studies indicated a positive feedback mechanism during birth similar to that occurring during suckling [49].

Male reproductive system

In several species, a pulse of systemic OT, presumably of hypothalamic origin, appears to be associated with ejaculation. OT could act peripherally by stimulating smooth muscle cells of the male reproductive tract, but could also have central effects in the brain by modulating sexual behavior. In the human, the complete OT system appears to be present in testis, epididymis, and prostate. OT is present in the prostate at concentrations higher than in the plasma and can increase the resting tone of prostatic tissue from guinea pig, rat, dog, and human (58, 182, 265). OT also stimulates contractile activity of mammalian prostates in vitro (58). This evidence suggests that OT is involved in the contraction of the prostate and the resulting expulsion of prostatic secretions at ejaculation (413).

anterior cingulate and medial insula, but not in the hippocampus, amygdala, entorhinal cortex and olfactory bulb [25].

OT peripheral functions

Female reproductive system

Circulating oxytocin is mostly known for its ability to elicit the contraction of uterine smooth muscle at term and that of myoepithelial cells that surround the alveoli of the mammary gland during lactation. The pregnant uterus is one of the traditional targets of OT. OT is one of the most potent uterotonic agents and is clinically used to induce labor. Accordingly, the development of highly specific OT antagonists may be of therapeutic value for the prevention of preterm labor and the regulation of dysmenorrhea [18]. In several species, the ovary has been shown to contain OT and may be a site of local OT production [46].

The other classical role assigned to OT is milk ejection from the mammary gland. The secretion of the mammary glands is triggered when the infant begins to suck on the nipple. The stimulation of tactile receptors at that site generates sensory impulses that are transmitted from the nipples to the spinal cord and then to the secretory oxytocinergic neurons in the hypothalamus. These neurons display a synchronized high-frequency bursting activity, consisting of a brief (3–4 s) high-frequency discharge of action potentials recurring every 5–15 min. During this activity, a dual mode of OT secretion has been identified. OT neurons secrete a large amount of neuropeptide into the blood and, in parallel; they secrete it in a

Kidney

The kidney controls hydromineral excretion, which is regulated in part by neurohypophysial hormones OT and AVP. Neurons are activated by hypovolemia or hyperosmolarity. When plasma sodium concentration exceeds 130 mM, the levels of both OT and AVP increase as an exponential function of plasma sodium concentration. OT is a non-hypertensive natriuretic agent involved in normal osmolar regulation [50].

Cardiovascular system and thymus

Peripherally injected OT decreases mean arterial pressure and reduce heart rate in rats. It appears that the complete OT system is present in rat vasculature. Thus OT might play a direct role in volume and pressure regulation in a paracrine/autocrine manner. The neurohypophysial peptides have been shown to trigger thymocyte proliferation and could induce immune tolerance of this conserved neuroendocrine family [17].

Adenohypophysis

It has been suggested that some hypothalamic OT reaches the anterior pituitary lobe via the hypothalamo-pituitary portal vasculature. OT might thus be able to influence anterior pituitary hormones as a hypothalamic regulating factor. OT is present in nerve terminals in the median eminence. It was found to be released into the portal vessels, and specific OT receptors are present in the rat adenohypophysis. Another pathway for OT delivery to the adenohypophysis might

be the short portal vessels connecting the posterior and anterior lobes. OT may participate in the physiological regulation of the adenohipophysial hormones prolactin, ACTH, and the gonadotrophins [17].

Evidence that OT controls complex behavior

Social behavior, cognition, and memory

A substantial amount of evidence demonstrates that OT modifies behavior in mammals, especially in rodents. During the past decade, a new field of research, social neuroscience, has emerged to investigate social behavior and social cognition in the organization of a 'social brain". Social behavior is essential for reproduction and includes recognition of key social interactions. The olfactory system has evolved to allow intraspecies communication pertaining to the gender, reproductive state, and location of possible mates as well as territory, and social status. From the sensed social information a mammal can learn about individual identity. By imprinting, which is permanently storing social information, animals recognize parents, siblings (filial) and appropriate sexual partners (sexual). This learning is critical for survival and reproduction. In rodents, recognizing conspecifics is a short-lived processed. In the field, rodents live in colonies with a common pheromonal signature spread via grooming [51].

Initial studies on the role of OT in social memory showed an attenuation of social recognition when OT was administered peripherally in high doses in male rats. This attenuation was blocked with administration of OT antagonists [52, 53]. Later

studies with more physiological levels of OT demonstrated that peripheral administration of OT at low doses, in fact, facilitated social recognition in male rats [54]. These findings suggest that the effects of OT on social recognition follow an inverted U-shaped dose response curve where moderate doses facilitate, and high doses attenuate social recognition. The same dose response curve has been found in OT administered centrally (ICV) in male rats. OT antagonist administered centrally blocked the facilitating effects of low dose OT but did not disrupt social recognition per se. This antagonist also blocked the attenuation effects of high doses of OT [55]. The ability of OT agonists to facilitate social recognition in males and not females, and the ability of OT antagonists to interfere with normal social recognition in females but not males suggested the possibility of a sexual dimorphism with respect to the roles of OT in social recognition in the rat [56]. The deficit in social interactions caused by chronic phencyclidine administration is used as a valid animal model of schizophrenia. OT was able to reverse this deficit in rats. This report suggests that deficits in the central oxytocinergic system may underlie the social impairment exhibited in this animal model [57].

The evidence for OT in social recognition in mice, both female and male, is more straight-forward than that in rats. Investigations of an OT knockout (OT-KO) mouse revealed a total deficit in social recognition. Male OT-KO mice, which completely lack the OT peptide, never displayed the typical reduction in olfactory investigation upon repeated exposures to the same stimulus female. This deficit was not due to a more general deficit in olfaction suggesting that OT is critical to the

processing of specific social cues. The deficit in social recognition was reversible with both ICV and site-specific injections of OT. Furthermore, normal social recognition was blocked in wild type (WT) mice with a single ICV injection of OT antagonist before the initial encounter [58]. The ability to rescue social recognition in OT-KO mice with a single injection of OT clearly demonstrates the importance of this peptide in the processing of social cues and subsequent social recognition in the male mouse. The social recognition deficits of the OT-KO mice are not limited to male mice. The female OT-KO mice also show a significant deficit in social recognition that was not attributable to other behavioral changes. In addition, OT-KO females are unable to distinguish healthy from parasite infected males during mate selection [59, 60]. The essential role of OT in social memory in female mice has also been demonstrated by the effects of OT-KO on the Bruce effect. OT-KO females failed to remain pregnant if re-exposed to either their mate or a novel male. Only females that were allowed to remain with their mate maintained pregnancy [61]. This inability to distinguish between the mate and novel male in the OT-KO females demonstrates the importance of OT in long-term social memory as well as short-term social recognition [56]. Mice with a null mutation of OT (OT-KO) show no decrease in investigation of another mouse after repeated encounters as opposed to wild-type mice that decrease 50% investigation time when reintroduced to the same stranger. These mutant mice do not show deficits on several tests of nonsocial memory nor do they differ in tests of olfactory function. Thus, the social memory deficits present in mice appear to be specific to the social domain [51, 56, 58, 62-64].

Trust

In humans, social behavior is key for survival; it includes communication, recognition, and expectation. Human interactions are partly driven by feelings of trust. Many reports address the biological basis of trust. Intranasal administration of OT to healthy human subjects substantially increased trust among them in a trust game with real monetary stakes. The effects of OT on trust were not due to general increase in readiness to take risks, but to a person's willingness to accept social risks arising through interpersonal interactions [65]. OT treatment did not alter the trusting behavior even after they have learned that their trust had been breached several times [66]. OT also increased generosity in healthy subjects that had to split a sum of money with a stranger. The test dissociated generosity from altruism and showed a connection of OT with emotional identification with another person [67].

Infer mental state of others

In another study, OT improved the ability to infer the affective mental state of others by interpreting subtle social cues in the "reading the mind in the eyes" test. The ability of mind-reading is pervasive in human social interactions. The capability of OT treatment to aid in the ability to infer the affective mental state of others might reduce ambiguity in social situations and encourage social approach and affiliation [68]. OT also showed a role in the regulation of gazing to the eye region of human faces to, maybe, enhance facial processing, emotion recognition, interpersonal communication, and social approach behavior in humans [69, 70].

Maternal behavior

Social attachment, social affiliation, sex behavior, and parental care are among the most highly motivated social behaviors. The onset of maternal care, switching from avoidance to intense interest, is of particular interest in the study of the OTR system [51]. Oxytocin may be critical for linking pup signals to surging motivated maternal behaviors. Blockade of OT neurotransmission results in a significant inhibition of the onset of maternal behavior but fails to affect maternal behavior once it has been established [71]. Central OT given to estrogen-primed, ovariectomized, virgin female rats induced a rapid onset of full maternal behavior in a dose dependent manner [72, 73]. In addition, OT improves long-lasting spatial memory during motherhood [74, 75]. OTR knockout (OTR-KO) female mice showed defects in maternal nurturing, OTR-KO males were more aggressive in a social setting, and OTR- KO infants emitted fewer vocalizations than wild-type littermates in response to social isolation [76]. Intravenous administration of a non-peptide OT antagonist disrupted parental-like behavior in monkeys [77].

These OT-mediated affects may be manifest in humans. Early parental separation (EPS) increases the risk for emotional disorders in adulthood, and studies have shown that administration of intranasal OT to EPS subjects attenuated cortisol release when compared with control subjects. An altered central sensitivity to OT after EPS could explain some of the underline biological reasons for emotional distress [78].

Greater evidence implicates OT in human maternal care. OT levels are very stable throughout all trimesters of pregnancy, and are positively associated with

maternal–fetal attachment as measured by the maternal–fetal attachment scale (self-reported feelings regarding the mothers' views of their fetus [79]. OT levels in the first trimester and early postpartum period have been positively correlated with certain maternal bonding behaviors, such as gaze with infant, vocalizations to infant, and affectionate touch [80]. Viewing images of their children activates dopaminergic pathways in the mothers' brains associated with reward that also contain high levels of OT and AVP receptors [81]. Mothers with variants of the serotonin transporter and the OTR genes (the 5-HTT SLC6A4 and OTR rs53576 polymorphisms, respectively) show lower levels of sensitive responsiveness to their toddlers (rated by observers on the aid given by the mothers to their children on cognitively difficult tasks [82], implicating these systems in production and bonding of OT in maternal responsiveness. The effect of the rs53576 polymorphism on OTR pharmacology is not known. It is possible that that OT may promote parental care and subsequent feelings of attachment in both the parent and the offspring; however, more study is needed.

Pair bonding

Pair bonding in monogamous species is another example of social motivation that is regulated in part by OT. Prairie voles treated with OT present a partner preference formation, and conversely, antagonists reduce partner preference formation without reducing mating behavior [83-85]. Species-specific OTR expression in the brain appear to be associated with a monogamous versus a non-monogamous social structure [86]. This pattern of expression and its involvement in

reward pathways of the prairie vole brain could be a potential cellular basis for these effects [87].

In humans, OT significantly increased positive communication behavior in relation to negative behavior during a couple's conflict discussion and it reduced salivary cortisol levels after the conflict [88]. OT further strengthens the anxiolytic effect of social support (presence of a friend) during the Trier Social Stress Test (public speaking and arithmetic in front of an audience), as measured by decreased corticosterone in men [89]. In women, OT is positively correlated with higher self-reported feelings of attachment (tendency to express and share emotions) on the Temperament and Character Inventory [90]. Women viewing pictures of loved ones have high brain activity in dopaminergic pathways associated with reward, which also contain high levels of OT receptors [81], as do people self-describing as being "intensely in love" [91, 92]. However, no study has conclusively shown that being in a relationship, or "in love," is associated with high levels of OT [93]. These findings support the role of OT in facilitating approach and pair bonding behavior.

Sexual behavior

Oxytocin is also involved in initiating and maintaining female sexual behavior in rats. Central administration of OT facilitates receptive and proceptive components of female sexual behavior and decreases male-directed agonistic behavior in estradiol-primed female rats. These effects are abrogated with the use of an OT antagonist [94, 95]. In another study, i.v. administration of a non-peptide OT antagonist decreased female monkey's sexual behavior [77].

In men, OTR can be found in the corpus cavernosum and epididymis of the penis. OT binding to the OTR in this region may affect contractility [96, 97] and subsequent ejaculation [98]. Plasma OT levels increase during sexual arousal and orgasm significantly raise OT levels in men [99]. In men, intranasal inhalation of OT significantly increases plasma OT and epinephrine levels for at least 1 h, and increases self-perception of arousal during masturbation [100]. Additionally, a recent case study indicates that intranasal OT administered during coitus may treat anorgasmia in men in cases where medical conditions, drug abuse, and psychological issues have been ruled out [101, 102].

In women, the primary medical use of OT treatment is to bring about labor, as it quickly advances uterine contractions [103]. OT has also been used to facilitate breast-feeding, as it aids in milk let-down, but its efficacy is uncertain [104]. One case study reports that intranasal inhalation of OT to stimulate breast-feeding increases vaginal lubrication and feelings of arousal [105]. Furthermore, plasma OT levels significantly correlate with higher levels of arousal and lubrication as measured by the Female Sexual Function Index [106]. Plasma OT levels increase in women during sexual arousal and are elevated further by orgasm [99, 102, 107].

Anxiety, fear, and stress response

OT is also involved in anxiety and stress response. Female OT-KO mice displayed more anxiety-related behavior and released more corticosterone after psychogenic stressors than WT animals. Male WT mice presented anxiolytic-like behavior when administered central OT, and this effect was blocked by

administration of an OTR antagonist. These findings support the hypothesis that central OT has anxiolytic properties and attenuates the stress response to psychogenic provocation [108-110]. In healthy humans, the combination of social support and OT decreased cortisol levels and increased calmness concomitant with decreased anxiety in response to stress during the Trier Social Stress Test [89]. Intranasal (IN) OT given to healthy men showed anxiolytic effects by depressing amygdala activation in socially relevant stimuli and reducing coupling to brainstem regions implicated in fear. OT also seems to impact fear conditioning and extinction through modulation of the amygdala function in humans [111].

Aggression

Little is known about the role of OT in human aggression. Higher levels of auto-antibodies reactive for OT are found in males with conduct disorder than in controls [112]. OT administration has been shown to reduce amygdalar activity in response to fear-inducing visual stimuli [111], and anxiety levels appear to be linked to aggression in several animal models [113-115]. In humans, OT may act to decrease anxiety by increasing recognition [116] and feelings of affiliation [65].

Learning and memory

Recent animal studies suggest that OT is implicated in the CNS control of learning and memory [117-121]. Similar to rodent studies, the available data in humans indicate that OT is generally amnesic in both men and women. In humans, OT selectively influences memory performance depending on the kind of memory

test and the psychobiological relevance of stimuli [122]. For example, during face portrait recognition tests, OT improved identity recognition. Similarly, in men treated with intranasal OT, word recall is significantly impaired in comparison to both placebo controls and subjects administered Lys8-vasopressin [123]. In conclusion, oxytocin has distinct effects on memory performance for facial identity and may contribute to the modulation of social behavior [116].

Healthy males given OT show deficits in learning processes [119]. Initial word storage (correctly remembered words after first presentation) and rate of storage (number of trials to recall words at least once) are significantly impaired, with no differences between groups treated with OT, AVP, or placebo in measures of attention or arousal [119, 121]. These amnesic effects of OT are consistent with direct actions of OT on memory processes, but access to the brain remains problematical [102]. OT has also been shown to modulate learning about socially relevant stimuli. This suggests that OT within the amygdala plays a role in processing negative information about negative stimuli, but OT is particularly important for more socially relevant (gaze directed) stimuli.

Self-grooming

Self-grooming behavior is used as a marker of central nervous system OTR activation in mice (or is it all rodents all mammals?); central OT administration induces this behavior whereas selective OTR antagonists inhibit it [124]. These findings were corroborated by eliciting exaggerated grooming in OT-KO mice with OT treatment [125].

Pain

Central administration of OT elevates pain threshold in rats and mice. Specifically, OT increases latency to remove the tail from heat, while an OT antagonist inhibits the antinociceptive properties of OT [126-129]. In addition, OT-KO mice have significantly increased nociception following stress compared to WT mice [102, 130]. OT seems to attenuate nociception by connections from OT neurons in the PVN to the dorsal horn of the spinal cord by acting specifically upon a subpopulation of lamina II glutamatergic interneurons [130]. This generally elevates inhibition at the level of the spinal cord [131]. Furthermore, pain stimulation decreases OT concentration throughout the brain, particularly in hypothalamic regions, although notably not in the PVN [126, 127]. Interestingly, a recent study reports that OT may underlie ethnic differences in pain perception. African American women demonstrated significantly lower pain tolerance across tasks and also exhibited lower plasma OT levels compared to non-hispanic white women when given three types of pain-testing procedures [132]. OT levels are also correlated with other measures of pain perception and tolerance, such as norepinephrine and beta-endorphin levels [102, 132].

Addiction

OT has also been reported to play a role in drug addiction. It attenuated the development of rapid and chronic morphine tolerance in mice as well as various signs of the naloxone-precipitated withdrawal reaction [133]. It also reduced the self-injected heroin dose in rats [134]. Tolerance or sensitization developed by chronic

cocaine administration was inhibited by pretreatment with OT [135]. Central and peripheral administration of OT blocked the development of rapid tolerance to ethanol, which supports the theory that OT acts on CNS mechanisms to influence adaptive responses to drugs [136]. OT likely interferes with the development of physical dependence [137].

Sensorimotor gating

Disruption of the OT gene (OTKO) made mice more susceptible to the psychosis-related effects produced by psychotomimetic drugs. Animals lacking OT showed large deficits in the prepulse inhibition of the acoustic startle reflex, which is a measure of sensorimotor gating deficits [138]. In addition, peripheral administration of OT was able to block amphetamine- and MK-801-induced disruption of PPI in rats, suggesting that oxytocin may play an important role in the modulation of dopaminergic and glutamatergic regulation of PPI [139]. Restoration of psychotomimetic-disrupted PPI is strongly associated with antipsychotic drugs and is considered a predictive marker for antipsychotic activity [140]. Members of both the typical and atypical antipsychotic families (haloperidol, raclopride, and risperidone) consistently restore PPI disrupted by dopamine agonists [140, 141]. In contrast, the ability to restore MK-801-disrupted PPI is more selectively associated with members of the 'atypical' antipsychotic family (risperidone) [141-143]. Based upon its ability to restore amphetamine- and dizocilpine-reduced PPI, oxytocin demonstrates a potent "atypical"-like antipsychotic profile [139, 141].

OT deficiencies in human disease

The demonstrable roles of OT in complex social behavior highlighted above suggest that deficits in the OT pathway could contribute to social deficits in humans. Indeed, strong evidence shows that disruption of the OT system contributes to deficits in reciprocal social interactions, such as pair, parental, and infant attachment, characterizing autism spectrum disorders (ASD), schizophrenia, and depression [144-146]. Various reports also suggest a link between OT and neuropsychiatric disorders, in particular obsessive-compulsive disorder, addiction, post-traumatic stress disorder, and anxiety. Importantly, several studies provide direct preliminary support for the use of OT in humans for the treatment of some of these disorders.

Autism and autism spectrum disorders (ASD)

One of the key pieces of evidence suggesting a tie between OT and autism is the lower plasma levels of OT observed in autistic children and the increase of OT with age in normal but not autistic children [147]. ASD children also show alterations in the endocrine OT system; OT is synthesized as a prohormone that is sequentially processed to peptides. These peptides are the bioactive amidated form (OT) and the C-terminal extended peptides, OT-Gly, OT-Gly-Lys and OT-Gly-Lys-Arg, which are designated together as OT-X. Autistic children show a significant decrease in plasma OT and an increase in the precursor OT-X level (the immature C-terminal extended OT form) [148].

Several studies indicate that single nucleotide polymorphisms (SNPs) in the OT [149] and OTR genes [150-152] are linked with ASD. Specifically, it has been reported that common single nucleotide polymorphisms (SNPs) in the 3p24-26 region containing the OTR gene could confer risks for ASD. There is a significant association of two specific SNPs of the OTR, rs2254298, and rs53576 with autism, as they have been discovered in a significantly higher rate in autistic subjects in the Chinese population. The association has also been observed in a Caucasian sample of the United States, but only for the rs2254298 polymorphism [150, 153, 154].

Current pharmaceutical therapies used with ASD are palliative, focusing on antipsychotics, antidepressants, anxiolytics, and mood stabilizers [155-157]. Intravenous OT administration to individuals diagnosed with autism or Asperger's syndrome showed improvements in affective speech comprehension and reduction of repetitive behaviors, two of the abnormal core behaviors present in ASD. These studies provide preliminary support for the use of OT in humans for the treatment of these disorders [158, 159].

Schizophrenia

The involvement of OT in this disease is supported by studies that showed that CSF OT levels were increased in schizophrenic patients, particularly in those taking neuroleptics and that, in drug-free patients; they were significantly higher after three weeks of treatment. Drug-induced increase of oxytocin concentrations may be of significance in the clinically observed amnesic syndromes and debilitation in schizophrenics treated with neuroleptics [160]. Diminished plasma OT levels were

also found in schizophrenic patients with neuroendocrine dysfunction and emotional deficits. In addition, OT levels predicted schizophrenic patients' ability to correctly identify facial emotions [161]. Variations of immunoreactivity towards the OT precursor neurophysin in different CNS regions have been observed for certain brain areas in untreated schizophrenia, consistent with altered OT function [162]. Social perception in primates is largely visual. Face perception has been the primary focus for much of human social neuroscience. Deficits in face recognition (prosopagnosia) have been reported in patients with schizophrenia and autism [51, 163].

Depression

Some symptoms of depression, in particular, social withdrawal, cognitive impairment, appetite modification, and stress reactivity have been related to OT [164, 165]. OT neurons were activated in the PVN in patients with major depression or bipolar disorder and an increased density of OT-expressing neurons was detected in the PVN postmortem of patients with major depression [166]. These findings may be associated with activation of the hypothalamic-pituitary-adrenal axis in these patients. Recently, a significantly negative correlation was found between plasma OT and scored symptoms of depression and anxiety in patients affected by major depression [167, 168]. A recent study of depressed women reveals increased pulsatile variability and total OT release during an affiliation-focused image task [169].

Lower plasma OT levels have been linked to higher levels of psychological distress and less parental attachment [170]. Increased OT levels postpartum have

been associated with elevated mood and decreased anxiety. In humans, breast-feeding similarly decreases cortisol levels while increasing OT levels and is associated with a decrease in negative feelings [171]. Compared with non-lactating women, postpartum mothers (2 days after birth) who have received OT during labor, just after birth, or were not medicated, have significantly lower scores on the anxiety and aggression scales, and higher on the socialization scale, of the Karolinska Scales of Personality [172]. This data suggests that both exogenous and endogenous OT maintain lower anxiety levels and promote sociability in women through the early postpartum period.

Obsessive-compulsive disorder (OCD)

OT influences physiological activities, including memory, grooming, maternal, and sexual behaviors that may be related to some OCD features. OT receptors have been identified in areas of the brain implicated in the patho-physiology of OCD [173]. The increase of grooming behavior elicited by OT in rodents is considered a model of compulsions, as cleaning behaviors are prototypical symptoms in OCD patients [174]. The most consistent data derive mainly from the evidence that pregnancy and the postpartum period show an increased risk for the onset of a subtype of OCD, which is characterized by contamination obsessions [175, 176]. It was suggested that women are vulnerable to the induction of exacerbation of OCD after exposure to elevated levels of OT, such as those occurring during pregnancy. Increased levels of OT in CSF of adults with OCD were also reported [25, 177]. Conflicting results came from the attempts to administer OT to OCD patients to improve avoidance

behaviors, such as a patient developing psychotic symptoms and reported subjective feelings not reflected in the self-rating questionnaires, [178, 179].

Addiction

Cocaine abuse during pregnancy seems to be associated with lower levels of OT, depression, and hostility [180]. Ethanol tolerance has been demonstrated in mice, but human studies are needed to test the hypothesis that OT is involved in alcohol tolerance and cognitive dysfunctions observed in alcoholics [25, 181, 182].

Post-traumatic stress disorder (PTSD)

OT attenuates memory consolidation and retrieval, facilitates the extinction of an activated avoidance response and decreases avoidance behavior [183]. OT administration showed reduced memory retrieval and conditioned response in patients with PTSD. It seems that alterations of the OT system following severe early stress and abuse experiences may interfere with the brain development and increase the subsequent risk of developing PTSD and, more in general, psychiatric disorders. The serum activity of the prolyl endopeptidase (PEP), an enzyme that cleavages many active behaviorally active neuropeptides including OT, was found to be increased in PTSD patients and particularly in those with a concomitant major depression: it was, therefore, hypothesized that increased PEP activity might play a role in the pathophysiology of behavioral and affective symptoms of PTSD through an increased degradation of different neuropeptides [25, 184].

Anxiety disorders

OT levels are positively related to sociality, calmness, and tolerance in mothers and negatively to stress and anxiety [25]. OT seems to be an important regulator of anxiety and fear response, mainly with an anxiolytic effect. Recently, downregulation of OTR has been related to the pathophysiology of social anxiety disorder [25, 111].

OT as a potential treatment for neuropsychiatric disorders

Prepulse inhibition (PPI) of the startle reflex is a form of sensorimotor gating displayed across a variety of species in which the reflexive reaction to a sudden, intense sensory stimulus is reduced by a preceding, weaker sensory stimulus. This gating process is an attentional mechanism that filters potentially distracting stimuli so that attention can be focused on relevant information. Deficits in sensorimotor gating are a feature of many psychiatric and neurological disorders including schizophrenia and autism spectrum disorders [185-192]. Use of antipsychotics such as amperozide (serotonin antagonist) and clozapine (dopamine and partial serotonin agonist) significantly increases plasma OT levels, indicating that OT may act as a natural antipsychotic [193]. Preliminary results support the hypothesis that OT has therapeutic effects on symptoms of schizophrenia and that intranasal oxytocin may be an effective method of augmenting established antipsychotic medication [194, 195].

Disadvantages of OT as a therapeutic tool

The evidence shown above points to OT as key for the treatment of several neuropsychiatry disorders. Unfortunately, there are several reasons to believe that OT will not be a successful drug candidate. OT has a half-life of only 4-10 min [196], is rapidly degraded in the blood, and it does not cross the blood-brain barrier efficiently when administered systemically (due to absence of a specific transport system for OT and degradation by brain endothelial enzymes) [197]. It also shows cross-reactivity with the vasopressin receptor which is involved in regulation of blood pressure and volemia [32]. It is likely that OT would present systemic side effects, as its best understood functions in physiology involve stimulation of uterine smooth muscle contraction during parturition and milk ejection during lactation, control of the estrous cycle length, follicle luteinization, and ovarian steroidogenesis in females, sexual arousal and penile erection in males, osmoregulation through excretion of water and salts in the kidney, and reduction of heart rate and arterial pressure [17]. Given these limitations, the search for small molecule OTR agonists has recently been initiated.

Current development of OTR agonists

Because of the role of OT in uterine contractions, the majority of reports regarding the OTR as a drug target are focused on preventing or stimulating uterine contractions and controlling postpartum hemorrhaging [198-201]. OT is the most common clinically used OTR agonist and is used to induce labor, control postpartum hemorrhage, and facilitate milk letdown. The use of OT for neuropharmacological purposes suffers from two major drawbacks. First, OT has a short ($2-5 \text{ min}^{-1}$) half

life, and second, CNS penetration of the hydrophilic peptide cannot be achieved by traditional drug delivery including intravascular or oral administration.

Both peptide- and small molecule-based OTR agonists have been developed [202-205]. Peptide-based OTR agonists are OT analogs that exhibit longer half-lives and higher metabolic stability. The best representative molecule of this group is carbetocin (see fig.1.4. for structure). It has a lower binding affinity to the OTR ($K_d=2\text{nM}$) than OT ($EC_{50}=0.18\text{nM}$) and significant affinity for the V_{1a} and V_2 receptors ($K_d=7.3\text{nM}$ and 61 nM , respectively). Carbetocin has been approved in Canada and the United Kingdom for the treatment of postpartum hemorrhage after birth. While peptide analogs may achieve longer half-lives, the issue of CNS penetration cannot be overcome by this approach. These two issues highlight a pressing need for non-peptide small molecule, selective OT agonists.

There are only two published reports of small-molecule OT agonists [204, 206]. Pitt et al. screened a vasopressin-targeted library for OT activity and identified two hits. The structural features of these were combined and optimized to generate compound 39 (cmpd39), with an $EC_{50} = 33\text{ nM}$ and >25 fold selectivity over human V_2 receptor and no reported activity at the V_{1a} or V_{1b} receptors (see figure 1.10.). A recent patent application by these same authors reported this and some other pyrazole-fused benzodiazepines as OT agonists making this scaffold the only reported structural class of small molecules with OT activity (US patent # US 200710117794 A1). Ring et al. at Wyeth Pharmaceuticals have reported anxiolytic efficacy of one of these non-peptide OT agonist, but they have provided no structural information, no doubt for proprietary reasons, as well as very limited pharmacology

information. The limited number of OTR agonists highlights a need to develop new small molecules OT agonists that can cross the BBB and are more selective against the vasopressin receptors. [196].

Development of small-molecule positive allosteric modulators for OTR and therapeutic advantages

To overcome the cross-reactivity of OT with the vasopressin receptors and the consequent side effects, highly selective OTR agonists are required [207, 208]. A novel approach to address selectivity is to find molecules that activate OTR without binding the OT binding site. It is known that some G-protein-coupled receptors (GPCRs) families display high sequence conservation within the orthosteric binding site across receptor subtypes, increasing the challenge in identifying selective agonists. Recently, allosteric modulators of GPCRs have been identified and the approach presents an alternative to agonists, promising new tools for the discovery of molecules that can modify receptor activity [208-211]. Allosteric modulators mediate receptor activation by interacting with distinct recognition sites on the receptor that typically are less conserved, but are conformationally linked to the ligand binding site [212]. It is more likely that molecules interacting with allosteric sites will be more selective because the ligand binding site is not targeted. This selectivity can be achieved through manipulation of the affinity to the sub-type receptor or cooperativity between orthosteric and allosteric binding sites.

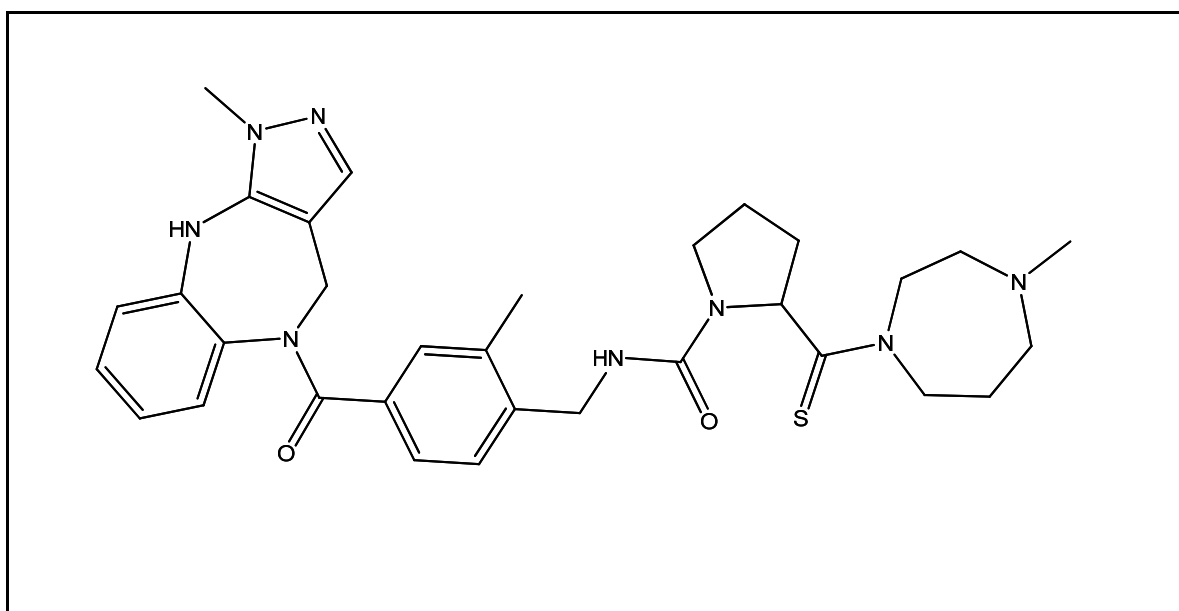


Fig. 1.10. Cmpd39 is the most potent and selective OTR agonist reported up-to-date.

Occupation of allosteric binding sites alters the receptor conformation thereby potentiating or inhibiting binding of the primary ligand with subsequent effects on intracellular signaling. There are several reports demonstrating the successful application of high-throughput screening for the identification of GPCRs allosteric modulators. Most of these studies have focused on receptors for classical neurotransmitters but some peptide receptors have been studied (CRF1, neurokinin NK₁, opioid μ , δ). Successes include mGluR2 [213], mGluR4 [214], mGluR5 [215-218], M₄ mAChR [219], M1 mAChR [220], and α 7 nAChR [221]. There have been no reports of positive allosteric modulators that can modulate OT activity.

In addition to the expected increase in selectivity, allosteric modulators offer other significant advantages of agonist that bind the orthosteric site. Allosteric modulator drugs only alter activity of receptors when the endogenous ligand is present. Indiscriminant activation of all receptors that bind the primary ligand does not occur, markedly diminishing the side effect profile of these drugs. This is known as the “ceiling level” to the allosteric effect as the allosteric modulators do not have any effect in the absence of orthosteric ligand; they can selectively “tune up” the effects of the endogenous ligand while maintaining the normal spatial and temporal profile associated with physiological ligands. More over, these modulators do not cause receptor desensitization. Although modulators significantly alter the efficacy of primary ligands, their maximum effects are constrained within a relatively narrow range which in turn diminishes their potential toxicity. Because of these advantages, we designed an HTS to identify positive allosteric modulators and agonists of the OTR. There seems to be a considerable overlap of the binding sites of structurally

diverse allosteric modulators. In addition, we expect a successful outcome of this HTS campaign because most of the allosteric modulators predominantly coordinate to amino acid residues in TM3, TM5, TM6 and TM7, the same transmembrane regions forming the orthosteric site in the biogenic amine family A GPCR, which includes the oxytocin receptor [222].

Potential for significant contribution to the development of biotechnology or for commercial products derived from biotechnology

As is pointed out above, pharmaceutical companies have focused almost exclusively on synthesis of OT antagonists for the purpose of blocking premature labor. Development of drugs that activate central OTRs is in its early infancy. No reports of OTR allosteric modulators have been published. Therefore, it appears that development of CNS-penetrating drugs that increase OTR activity is a nearly unexplored pharmacotherapeutic frontier.

The lack of progress in developing this class of drugs is surprising given the broad range of clinically-relevant central effects of OT. The large number of potential clinical applications of OT agonists or OTR allosteric modulators suggests that they could be enormously successful commercially. These applications include treating anxiety, depressive, psychotic and pain disorders with efficacy comparable to currently marketed drugs. In addition oxytocinergic drugs may be effective in treating social motivation and cognition deficits in schizophrenia, autism spectrum disorders and many personality disorders as well as sexual motivation and arousal disorders for which there are no currently available pharmacotherapeutic agents. OT-like

drugs could also be more effective in treating alcohol and drug craving than currently available drugs. OT drugs may circumvent complications of anxiolytic, analgesic, and antipsychotic drugs in current use. Based on animal studies, OT-like drugs would not create the dependence that often occurs with chronic administration of sedative/hypnotics or opiates. Also, OT drug treatment of withdrawal would not perpetuate sedative/hypnotic or opiate dependence as do many current detoxification treatment regimens. Oxytocinergic drugs would be unlikely to produce the extrapyramidal and metabolic side effects of typical and atypical antipsychotics.

The development of OT agonist or allosteric modulator drugs that penetrate the brain also would be a boon to the study of the roles of central OT in normal animal and human behavior, emotion and other brain functions as well as CNS disorders. In addition to testing the effects of administration of these drugs in animals and human subjects, some of these drugs could be suitable for use as PET ligands which may permit *in vivo* localization and quantification of OTRs in the developing and adult human brain.

Brief outline of this research work

The work reported in this thesis focused on the discovery and initial characterization of small molecules with potentially useful biological activity. Medium- and high-throughput assays were used to identify prospective hits and promising compounds underwent further validation. Chapter 2 reports the small-molecules validated as new G-quadruplex stabilizers and their ability to inhibit human telomerase as a prospective approach to treat cancer. Chapters 3 through 5

document the identification of novel non-peptide human oxytocin receptor agonists and positive allosteric modulators. This research is described in three discrete stages. Chapter 3 includes the HTS assay development, validation, and HTS campaign. Chapter 4 includes secondary and counter screens, as well as cytotoxicity tests. Chapter 5 shows the phenotypic assays performed with the actives found in previous instances. Finally, Chapter 6 focuses on the possible therapeutic uses that OTR agonists and allosteric modulators could have in the treatment of many diseases that the OTR system is involved. The many disorders that this system is involved are used in this chapter to delineate the many benefits of pharmacological therapy of an OT-like molecule.

CHAPTER 2

IDENTIFICATION OF NEW G-QUADRUPLEX STABILIZERS AND THEIR ABILITY TO INHIBIT HUMAN TELOMERASE

INTRODUCTION

The telomere is a nucleoprotein complex located at the ends of eukaryotic chromosomes. It is essential for maintaining the integrity of the genome. For much of the cell cycle, telomeric DNA is maintained in a loop structure, which serves to protect the vulnerable ends of chromosomes. Many of the key proteins in the telomere have been identified, although their interplay is still imperfectly understood and structural data are only available for a few. One strand of telomeric DNA comprises simple guanine-rich repeats for most of its length, culminating in a short overhang of single-stranded sequence at the extreme 3' end that consists of tandem repeats of short guanine-rich sequences, such as 5'-dTTAGGG in mammals. This can, at least in vitro, fold into a wide variety of four-stranded quadruplex structures [223]. Replication of eukaryotic chromosomes by DNA polymerase cannot fully copy the ends of telomeric DNA [224], as the polymerase is unable to fully replicate the extreme 3' end of a DNA sequence; this is known as the "end-replication problem". Consequently, each replicative cycle of the cell results in the erosion of the parental

guanine-rich 3' end and telomeric DNA progressively shortens in the absence of any compensating mechanism. The shortening, by approximately 50–100 bases per round of cell division in human cells, leads to a DNA damage response at the telomere resulting in cell cycle arrest or cell death [225].

It is vital that the noncoding telomeric DNA at chromosome ends be replenished to prevent cell cycle arrest or loss of genetic information upon continued shortening. In particular, germ-line cells are immortal and have full telomerase activity; stem cells are mortal and have some telomerase activity, but not enough to replenish all telomeres lost from telomere erosion [226]. This telomere stabilization is accomplished by the activation of the reverse transcriptase telomerase, a unique DNA polymerase that binds to the guanine-rich 3' end of telomeric DNA and synthesizes the addition of further hexanucleotide repeats onto the end using its own endogenous RNA template.

In contrast to somatic cells, the telomeres of tumor cells do not shorten as a result of DNA replication but instead have short yet stable telomeres. In most cases, this stabilization is also accomplished by telomerase, which is expressed in over 80–85% of human tumors even though it is absent in neighboring normal somatic tissue. Telomerase thus plays a key role in maintaining the malignant phenotype by stabilizing telomere length and integrity. This constitutes one of the key hallmarks of cellular immortalization and cancer [227]. The roles of telomerase in ensuring cellular immortality and its differential expression in cancer cells compared to normal cells has made telomerase an important research focus. This in turn has led to

increasing interest in the study of telomeres as potential therapeutic targets in oncology [228, 229].

G-quadruplexes are higher-order DNA and RNA structures formed from G-rich sequences that are built around tetrads of hydrogen-bonded guanine bases. Potential quadruplex sequences have been identified in G-rich eukaryotic telomeres and more recently in non-telomeric genomic DNA, e.g. in nuclease-hypersensitive promoter regions. The natural role and biological validation of these structures is starting to be explored, and there is particular interest in them as targets for therapeutic intervention [15]. The *in vivo* importance of G-quadruplex-DNA has been speculated for quite some time [230]. A growing body of evidence for the biological relevance of G-quadruplex-DNA has emerged from recent literature: putative G-quadruplex forming sequences are thoroughly distributed along the human genome (37,000 sequences) [231]. These sequences are particularly found at telomeric regions and gene promoters [232]. The putative quadruplex formation correlates with gene expression level; and an array of proteins with various functions has been shown to interact specifically with G-quadruplexes [233].

G-quadruplexes are implicated in several biological dysfunctions [234]. In particular, the formation of G-quadruplex-DNA at the end of telomeres has been reported to obstruct telomerase association and inhibit its activity [235]. Additionally, G-quadruplex formation at the telomere may increase genomic instability by hampering normal recognition of the telomere by telomere-associated proteins [230]. G-quadruplexes could serve as regulators towards cancer cell growth, opening the possibility of building novel anti-cancer therapeutic strategies. There is a general

consensus that G-quadruplex ligands that stabilize the G-quadruplex structure could lead to the discovery of novel anti-cancer agents.

METHODS AND MATERIALS

Amplification of hTERT and hTR plasmids

The hTERT- and hTR- expressing plasmids were a gift from Dr. Joaquim Lingner (pVan107 and pBS-U1-hTR) [236]. Both plasmids were amplified following the MAX Efficiency[®] DH5 α [™] Competent cells protocol (Invitrogen, cat# 18258-012). The amplified plasmids were purified using a plasmid purification kit (Qiagen, Plasmid Maxi kit). The hTERT and hTR expressing plasmids were purified by using the high-copy and low-copy plasmid procedures, respectively). After ethanol precipitating the plasmids, an agarose gel was run to assess purity of plasmids. UV-spectroscopy measurements at 260nm were used to quantify the plasmid concentrations (Nanodrop information). A restriction endonuclease map was used to confirm the identity of the plasmids. The restriction enzymes EcoRI, MluI, and HindIII were used for hTERT (New England Biolabs). The hTERT plasmid (1ug) was incubated with 1X restriction enzyme buffer (specific for each restriction enzyme), and 20 units of EcoRI, 10 units of MluI, or 20 units of HindIII in a total volume of 50 μ l for each reaction. The hTR plasmid (2.4ug) was incubated with 1X restriction enzyme buffer (specific for each restriction enzyme), and 20 units of EcoRI, 10 units of MluI, or 20 units of EcoRI combined with 10 units of MluI total volume of 50 μ l for each reaction. The reactions were incubated at 37°C for 1 hour, followed by five minutes incubation at 95°C to inactivate the enzymes. Comparison of the fragments obtained by electrophoresis from the restriction enzyme digestions with the

fragments expected from the sequence software allowed for a positive identification of the amplified plasmids.

Super-telomerase extract preparation

Super-telomerase cell extracts were prepared as reported by Cristofari et al [236]. Essentially, HEK 293T/17 ($2-6 \times 10^5$ cells per well in a 6-well plate) were transfected with 4 μg of total plasmid DNA using Lipofectamine 2000 (Invitrogen) following manufacturer's protocol. The mass ratio of hTERT- and hTR- expressing plasmids is 1:5 (0.75 μg pVan107 and 3.38 μg pBS-U1-hTR). One day after transfection, cells were trypsinized, transferred to a 25 cm^2 flask, and grown one more day. Two days after transfection, cells ($3-4 \times 10^6$) were detached using trypsin, washed once in PBS and lysed in 400 μl of Chaps lysis buffer (10mM Tris-HCl pH 7.5, 1mM MgCl_2 , 1mM EGTA, 0.5% CHAPS, 10% glycerol, supplemented before use with protease inhibitor cocktail (Roche) and 5mM β -mercaptoethanol). After incubation at 4°C for 30 min on a rotator, cell debris was removed by centrifuging extracts at 4°C for 10 min at 13,000 $\times g$. The protein content of the supernatant, assessed with the Coomassie Plus Assay kit (Pierce), was 1.6 mg/ml. The supernatant was aliquoted in portions of 4 μl , quick frozen on dry ice and stored without loss of activity for several months at -80°C.

FRET analysis for the identification of Telomerase inhibitors

Potential G-quadruplex stabilizers were previously identified in our lab using a fluorescence based assay. When the dual- labeled telomeric repeat Fam-21hT-Tam

(IDT) folds into a G-quadruplex structure, it brings the ends of the DNA closer together, leading to a FRET effect between the donor (fluorescein) and the acceptor (tetramethylrhodamine) that are covalently attached to both ends of the telomeric repeat. The extent of G-quadruplex formation can be evaluated by measuring the emission of light at a specific wavelength. Our lab screened the NCI diversity set using this technology and identified twenty-nine compounds, which showed the greatest signal quenching at 550nm, as potential hits.

Several compounds, NSC 12155, 17600, 35489, 95609, 130813, 176327, 305831, 354961, 357777, and 638432, were obtained from the NCI repository for further testing (see figure 2.1 for structures). Compounds were obtained as powders, dissolved in DMSO, and diluted to 1.25mM in DMSO for use in subsequent assays.

Telomerase Assay

Telomerase activity was measured using a modification of a previously described direct assay [235]. Each 25 μ l reaction contained 50 mM Tris-HCl, pH 8.0, 50 mM KCl, 1 mM MgCl₂, 5 mM β -mercaptoethanol, 1 mM spermidine, 1 μ M human telomere primer (5'-TTAGGGTTAGGGTTAGGG), 0.5 mM dATP, 0.5 mM dTTP, 2.9 μ M dGTP, 0.17 μ M [α -³²P]-dGTP (3000 Ci/mmol, 10 uCi/uL; Perkin-Elmer), and 4 μ l of the super-telomerase cell extract (1.6 mg/ml). Primer extension was carried out at 30 °C for 90 min. The telomerase inhibitor UR61 was used as a negative control for enzymatic activity. After the addition of a ³²P-labeled loading control (15 or 115 nucleotide, 5'-end labeled DNA oligonucleotide, 1000 cpm per reaction), the primer extension products were extracted with phenol/chloroform/isoamyl alcohol and

ethanol precipitated in the presence of 0.6 M NH₄OAc and 35 ng/μl glycogen. Products were precipitated at -80 °C in 2.5 vol of absolute ethanol for 30 min followed by centrifugation at 22,000xg at 4 °C for 25 min and washing with 2 vol of 70% ethanol. The final pellets were dissolved in a formamide loading buffer containing 40% formamide, 10 mM Tris-HCl, pH 8.0, 10 mM EDTA, 0.05% xylene cyanol, and 0.05% bromophenol blue. The products were heated at 95 °C for 5 min and resolved on a prewarmed, 0.4 mm thick, 20 x 20 cm, 10% polyacrylamide/7 M urea/1x TBE gel. The gel was run at 800 V for 45 min in 1x TBE. After drying the gel and exposing it to a phosphorimager screen (Molecular Dynamics) overnight, telomerase activity was imaged using a phosphorimager (Molecular Dynamics Storm 860) and quantified with Image Quant (version 5.2). The intensities of each band in each sample were summed and normalized to the loading control.

IC₅₀ for the most potent compounds were determined by direct telomerase assay with five point dose response curves for each compound (50 μM, 5 μM, 0.5 μM, 50 nM, and 5 nM). Each reaction was run in triplicate per experiment and repeated twice. Assay controls included buffer (positive) and 200 nM UR61 (negative). Each kinetic trace was normalized to the loading control signal to correct for loading of the extracts. Data was analyzed using Graph Pad Prism 5 for Windows to obtain dose response curves and the IC₅₀ values.

Polymerase stop assay

The specificity of G-quadruplex binders was characterized using a modification of a previously reported polymerase stop assay [7]. Primer 5'- AATACGACTCAC

TATAG-3', DNA templates Temp [TTAGGG]₄: 5'TCCAACCTATGTATAC [TTAGGG]₄ TTAGCCACGCAATTGCTATAGTGAGTCGTATTA-3' and Temp [TTAGAG]₄: 5'-TCCAACCTATGTATAC[TTAGAG]₄TTAGCCACGCAATTGCTATAGTGAGTCGTTA-3', and all other DNAs were purchased from IDT (San Diego, CA). Single-stranded oligonucleotides were 5'-end labeled using T4 polynucleotide kinase and [γ -³²P] ATP at 37°C. The kinase activity was inactivated by heating at 70°C for 8 min and the labeled primer was purified on a Microspin G-25 column (GE Healthcare). Labeled DNA primer (15 nM) and template (10 nM) were annealed in GoTaq buffer (1x) with 0.1 mM dNTP by heating at 95°C for 5 min and were slowly cooled to room temperature. Ligands were added at various concentrations (ranging from 50 to 0.1 μ M) and incubated at room temperature for 30 min. Taq DNA polymerase (2.5 U) was added and the mixtures were incubated at 55°C for 20 min. The controls used were Temp [TTAGGG]₄, Temp [TTAGAG]₄, 1 μ M BRACO-19 (a selective G-quadruplex-binding compound), and primer [237]. Data are reported as the average of triplicate experiments. The polymerase extension reactions were stopped by adding 2x stop buffer (10 mM EDTA, 10 mM NaOH, 0.1% xylene cyanol, and 0.1% bromophenol blue in formamide solution). Samples were heated at 95°C for 5 min and were loaded onto a 10% denaturing polyacrylamide gel. The gel was run at 800 V for 1 h. After drying the gel and exposing it to a phosphorimager screen (Molecular Dynamics) overnight, polymerase activity was imaged using a phosphorimager and quantified with Image Quant.

Circular dichroism spectroscopy

CD spectra were recorded on a P-star 180 spectropolarimeter using a quartz cell of 1-mm optical path length and scanned at 25°C using a wavelength of 220-320nm, a measuring step of 0.5 nm, and a band width of 2.0 nm. The time per point was set to 0.25s and the sample period to 25.5 us. The human telomeric oligonucleotide d [G₃ (T₂AG₃)₃] was purchased from IDT. The DNA was desalted using G-25 Microspin columns following manufacturer's instructions (GE Healthcare). The DNA was dissolved in TE (10 mM Tris-HCl, pH 7.5, and 1 mM EDTA) at a final concentration of 15 µM in a final volume of 400ul. The TE buffer included 10 mM LiCl to prevent precipitation of the DNA from the solution. DNA samples were prepared by heating at 95°C for 5 min and cooling to room temperature. DNA samples were titrated with 0.5 mol equivalents of each compound. After each addition of ligand, the reactions were allowed to equilibrate for at least 15 min to collect the CD spectra. Controls for G-quadruplex formation included 50 mM solutions of Na⁺ or K⁺. The compound / DNA ratio varied as follows: 0:1, 0.5:1, 1:1, 1.5:1, 2:1, 2.5:1, 3:1, and 3.5:1.

Specificity assay

Inhibition of T7 polymerase by selected compounds was used to test the specificity of the compounds. A modified version of the manufacturer's protocol was used (Ampliscribe T7 Kit, Epicentre). A linearized template DNA with the appropriate promoter (50ng/ul) was incubated with 1x T7 reaction buffer, 7.5mM ATP, CTP, GTP, and UTP at 95°C for 5 min and cool down to RT. DTT was then added at 10

mM. Then, the test compounds were incorporated at 5 and 50 μ M together with the Ampliscribe T7 enzyme solution (2 μ l). The reaction was incubated at 37°C for 2 hs. DNase (1u) was later added to remove the template DNA for 30 min at 37°C. The products were heated at 95 °C for 5 min and resolved on a prewarmed, 0.4 mm thick, 10 x 10 cm, 3.5% polyacrylamide/7 M urea/1x TBE gel. The gel was run at 120 V for 45 min in 1x TBE. The gel was imaged using a phosphorimager (Molecular Dynamics Storm 860) and quantified using ImageQuant.

RESULTS AND DISCUSSION

FRET analysis for the identification of telomerase inhibitors

Potential G-quadruplex stabilizers were previously identified in our lab using a fluorescence based assay to screen the NCI diversity set. When the telomeric repeat Fam-21hT-Tam (IDT) was stabilized into a G-quadruplex structure, the ends of the DNA came closer together, leading to a FRET effect between the donor (fluorescein) and the acceptor (tetramethylrhodamine) that were covalently attached to both ends of the telomeric repeat. The extent of G-quadruplex formation was evaluated by measuring the emission of light at a specific wavelength. Several compounds, NSC 12155, 17600, 35489, 95609, 130813, 176327, 305831, 354961, 357777, and 638432, were obtained from the NCI repository for further testing. Figure 2.1 shows the structures for these compounds.

Identification of Telomerase inhibitors

A direct telomerase assay was used to evaluate the effect of compounds identified from the G-quadruplex stabilizer screen on telomerase activity. The following compounds were initially tested: NSC 12155, 17600, 35489, 95609, 130813, 176327, 305831, 354961, 357777, and 638432 (structures shown in figure 2.1). Figure 2.2. shows the percent inactivation of telomerase for each compound calculated by normalizing the signals to the loading controls and comparing the areas between the samples and the positive control. The 2'-O-Me oligomer UR61 (CAGUUAGGGUUAG) was used as a positive control for telomerase inhibition [238].

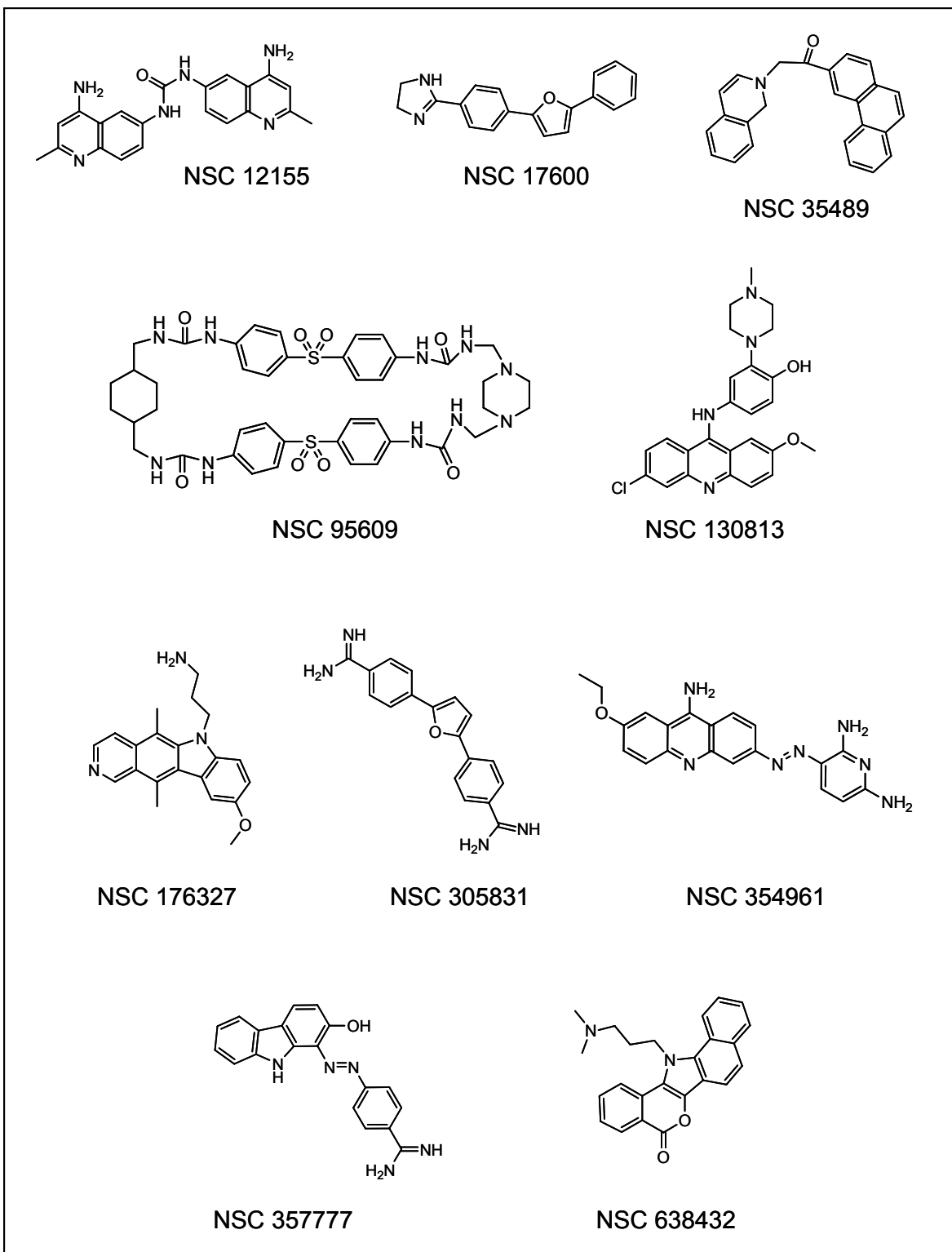


Fig. 2.1. Structures of initial hits identified as G-quadruplex stabilizers in the fluorescent based screen of the NCI diversity set.

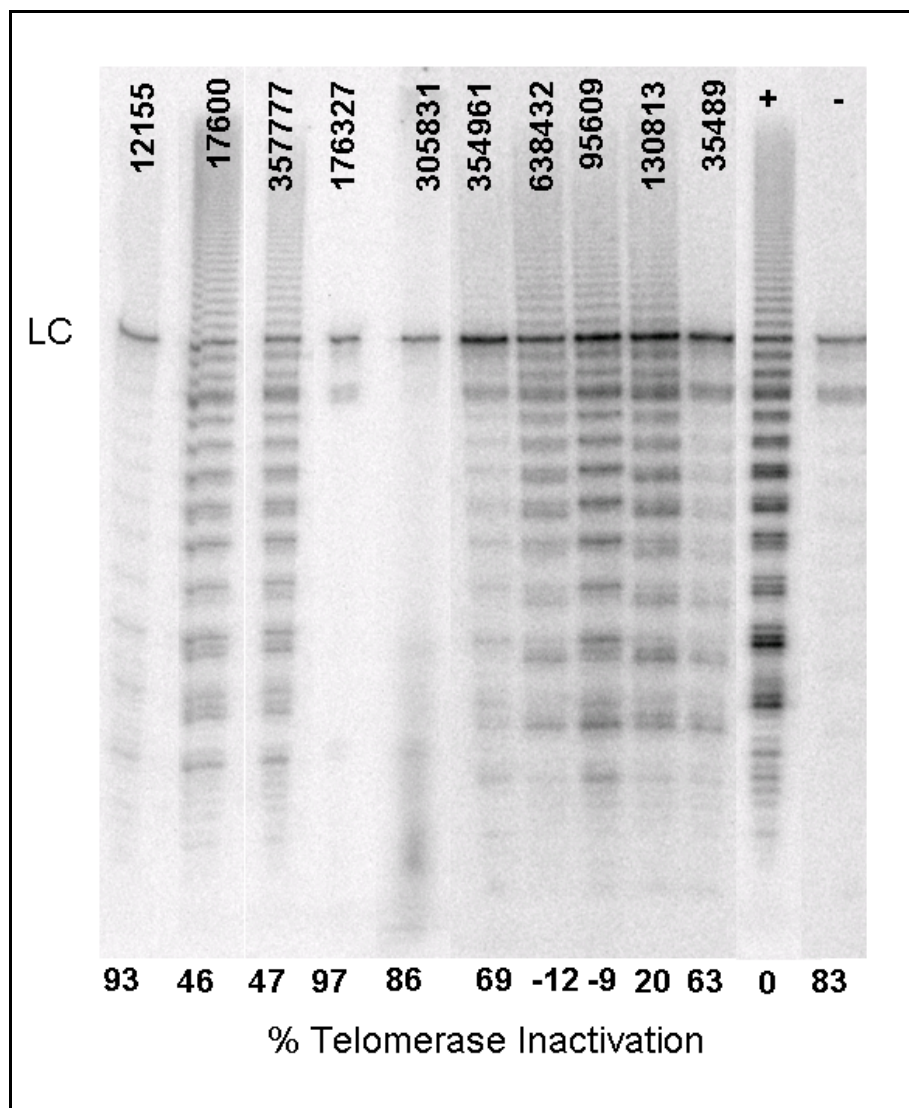


Fig 2.2. Concentration dependence of telomerase inhibition in a direct telomerase assay. Compounds were incubated with a telomerase extract and percent telomerase activity was calculated. Compounds were added at 10 μ M. Percent telomerase activity inhibition is reported. (+) Positive control of telomerase activity: no inhibitors added. (-) Negative control of telomerase activity: UR61 at 200nM. LC: 32 P-labeled loading control (115 nucleotides; 5'-end labeled DNA oligonucleotide).

From these compounds, only the compounds that showed 60% inhibition of telomerase activity or above were chosen to continue with IC₅₀ studies. These compounds were: NSC 12155, 176327, 305831, 354961, and 35489. They demonstrated telomerase inhibition of 93, 97, 86, 69, and 63 %, respectively. Figure 2.3. shows a representative gel that was run to obtain a dose response curve of the inhibitors. Signals were normalized to the loading controls (LC) and the areas were plotted versus concentration to generate the IC₅₀ values shown in Table 2.1. The curve for compound 354961 is shown in figure 2.4. as a representative dose response profile.

G-quadruplex ligand specificity is revealed by polymerase stop assay

Compounds that bind to and stabilize G-quadruplex DNA commonly exhibit non specific DNA-binding properties. To test the selective action of the compounds found to inhibit telomerase with the human telomeric sequence, a Taq polymerase stop assay was used. A primer extension assay was used to measure the drug-induced stability of the telomeric G-quadruplex formed in the template strand. Two types of templates were used: one that can form a G-quadruplex and one that cannot as a control. In a typical experiment, the polymerase stop product at the G-quadruplex-forming site occurs first at the lower drug concentrations in the G-quadruplex-forming template. At higher concentrations product accumulates at the primer site, either due to drug binding to the primer/template duplex or another unrevealed mechanism of inhibition, preventing polymerase extension [239]. Two different concentrations of the compounds found to inhibit telomerase activity were

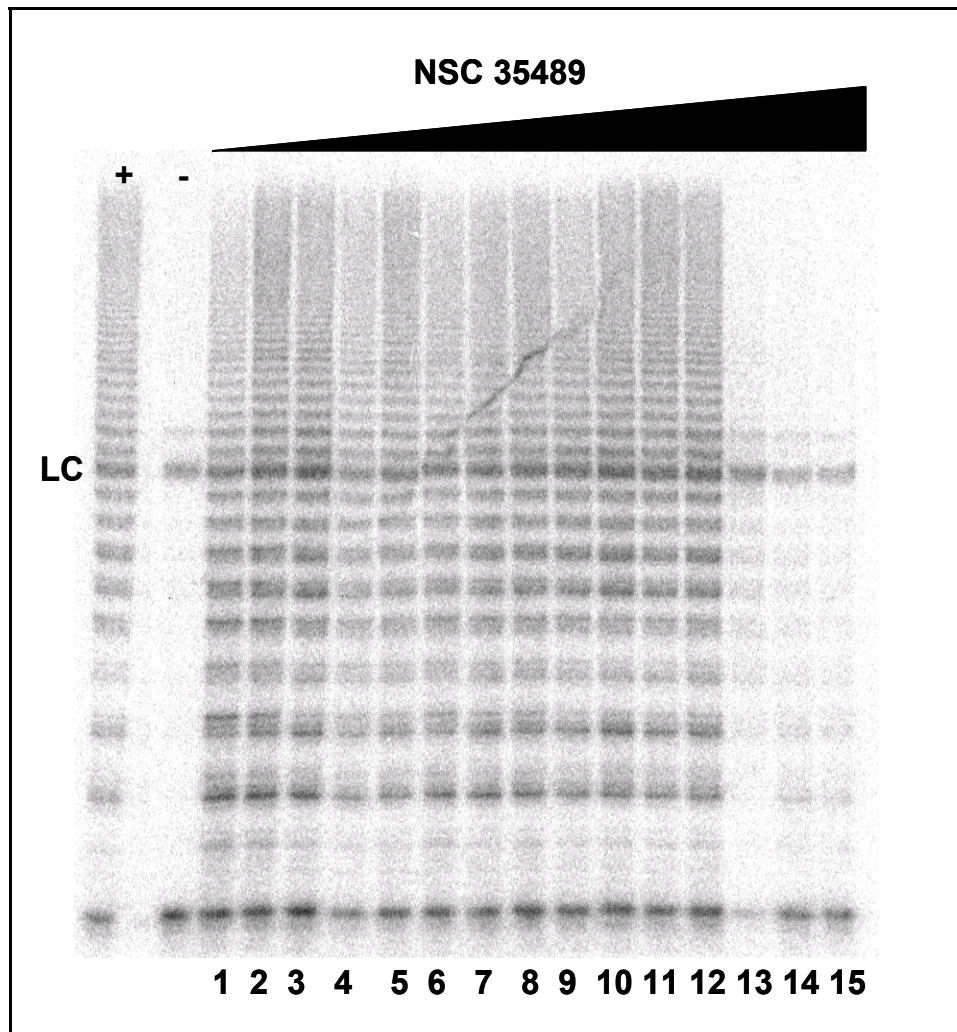


Figure 2.3. Representative gel from NSC 35489 used to obtain a dose response curve of the telomerase inhibitors in a direct telomerase assay. Lanes 1-3, 5nM; lanes 4-6, 50nM; lanes 7-9, 500nM; lanes 10-12, 5uM; and lanes 13-15, 50uM. (+) Positive control of telomerase activity: no inhibitors added. (-) Negative control of telomerase activity: UR61 at 200nM. LC: ^{32}P -labeled loading control (115 nucleotide; 5'-end labeled DNA oligonucleotide).

Compound ID	IC ₅₀ (uM)
12155	36
176327	1.5
305831	7.5
354961	18
35489	65

Table 2.1. IC₅₀ for telomerase inhibition in a direct telomerase assay. Only the compounds that showed 60% inhibition of telomerase activity or above were chosen to continue with these studies.

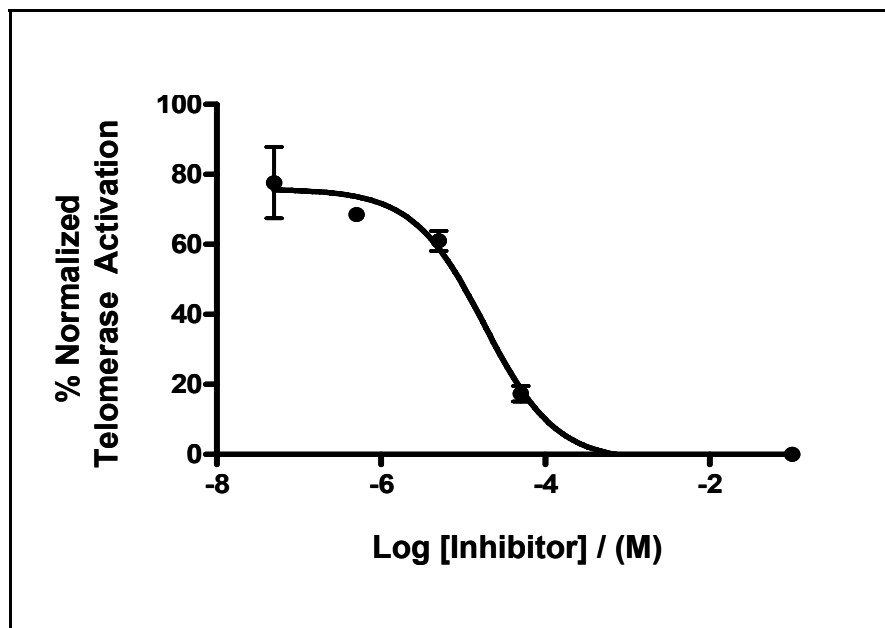


Figure 2.4. Representative concentration dependent profile for compound NSC 354961 in a direct telomerase assay. Points on curve were run in triplicates. The IC₅₀ calculated was 18 ± 2 μM.

tested initially in a Taq polymerase stop assay to evaluate their specificity towards stabilization of G-quadruplexes. Figure 2.5. shows the results of Taq DNA polymerase primer extension on DNA templates containing four repeats of the human telomeric sequence, Temp [TTAGGG]₄ [240]. Another DNA template, Temp [TTAGAG]₄, contained four repeats of a non-G-quadruplex-forming sequence and it was used as a control for selectivity. BRACO-19, a G-quadruplex stabilizing ligand, was used as a control. NSC 176327, NSC 12155, NSC 354961, and NSC 305831 showed polymerase stop products at the G-quadruplex forming site, therefore, these compounds were tested further to evaluate if they stabilize G-quadruplexes in a dose-response manner. We found that only NSC 176327 and NSC 305831 showed specific G-quadruplex stop site products, proving that these compounds inhibited the DNA synthesis of Temp [TTAGGG]₄ by Taq polymerase selectively. The calculated IC₅₀ for the inhibition of DNA synthesis by these compounds is 8 μM and 39 μM, respectively. The primer extension reaction using the non-G-quadruplex-forming Temp [TTAGAG]₄ revealed no G-quadruplex stop products for these two compounds. The remainder of the compounds showed stop products revealing non-specific DNA binding (data not shown). Fig 2.6. and 2.7. show a representative gel and the dose response curve obtained for NSC 176327, respectively; data for 305831 is not shown (this experiment was repeated three times for reproducibility). Both, NSC 176327 and NSC 305831 show selectivity for G-quadruplex forming templates (see Table 2.2.). These results made it imperative that we investigated whether these compounds stabilized G-quadruplex structures.

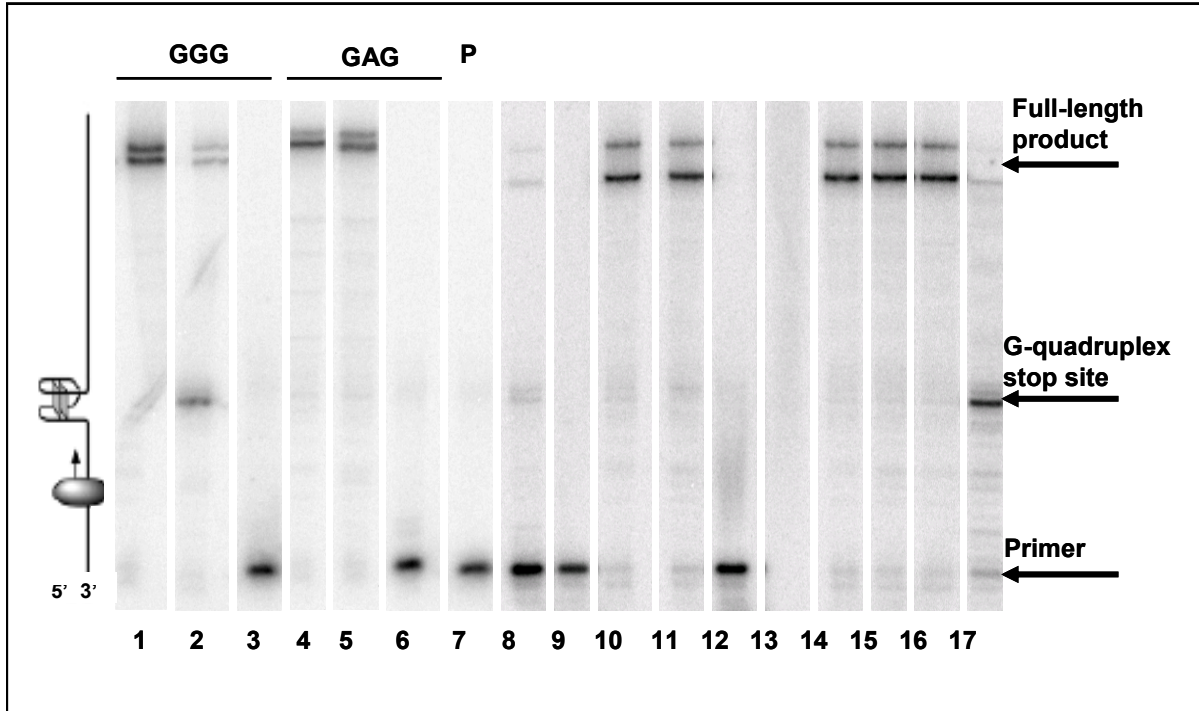


Fig 2.5. Selectivity test of hits for G-quadruplex stabilization by polymerase stop assay. Two different concentrations of the compounds were tested initially in a Taq polymerase stop assay to evaluate their specificity towards stabilization of G-quadruplexes. Lane 1: Temp [TTAGGG]₄, G-quadruplex forming template as control. Lane 2: Temp [TTAGGG]₄ with 1 μM BRACO-19. Lane 3: Temp [TTAGGG]₄ with 50 μM BRACO-19. Lane 4: Temp [TTAGAG]₄, non G-quadruplex forming template as control. Lane 5: Temp [TTAGAG]₄ with 1 μM BRACO-19. Lane 6: Temp [TTAGAG]₄ with 50 μM BRACO-19. Lane 7: Labeled primer (P) at 15 nM. Lanes 8-9: NSC 354961 at 5 and 50 μM. Lanes 10-11: NSC 305831 at 0.5 and 5 μM. Lanes 12-13: NSC 12155 at 5 and 50 μM. Lanes 14-15: NSC 35489 at 5 and 50 μM. Lanes 16-17: NSC 176327 at 0.5 and 5 μM.

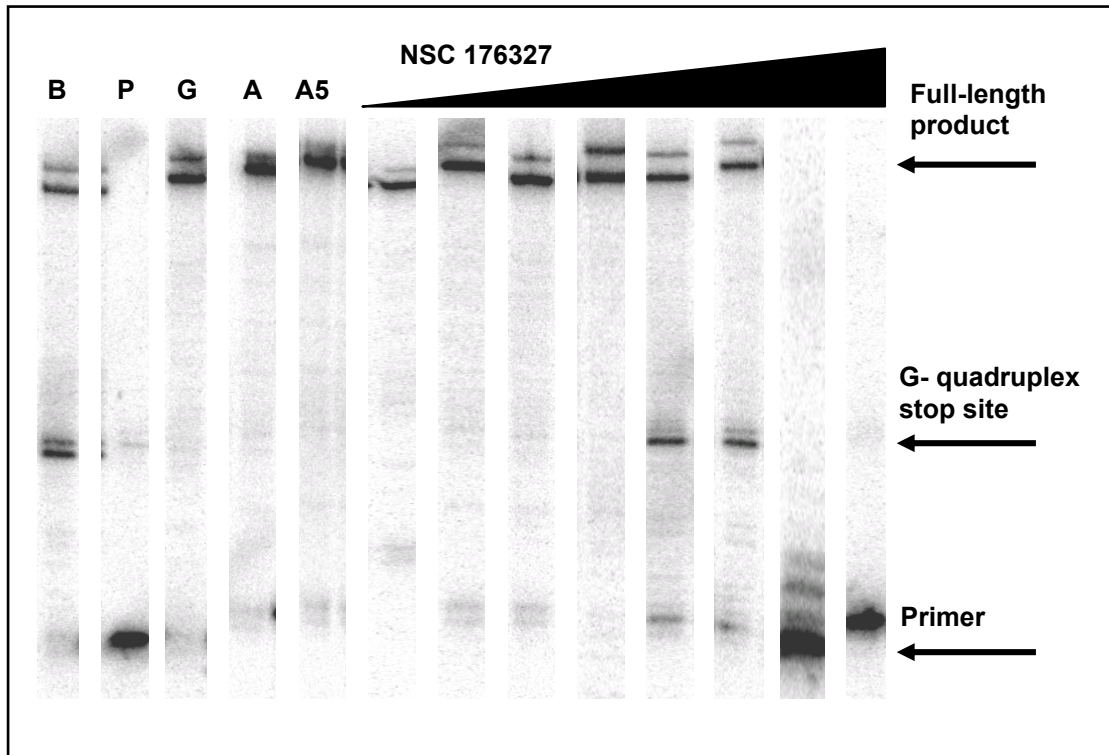


Fig 2.6. Concentration dependent inhibition of DNA synthesis by NSC 176327 containing the human telomeric sequence [TTAGGG]₄. Polymerase stop reaction dose response curve. B: Temp [TTAGGG]₄ with 1 μM BRACO-19. Labeled primer (P) at 15 nM. G: Temp [TTAGGG]₄. A: Temp [TTAGAG]₄. A5: Temp [TTAGGG]₄ with NSC 176327 at 5 μM. NSC 176327 concentrations are: 0.1, 0.25, 0.5, 2.5, 5, 10, 25, and 50 uM, respectively.

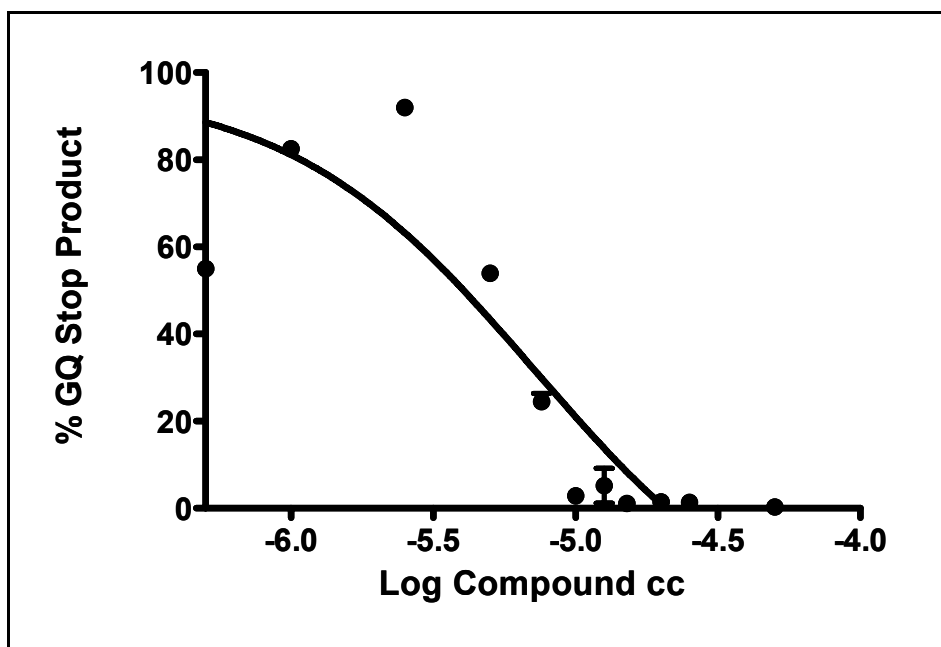


Fig 2.7. Concentration dependent inhibition of DNA synthesis by NSC 176327 containing the human telomeric sequence [TTAGGG]₄. Dose response curve of NSC 176327: the IC₅₀ reported is 8 μM for the inhibition of DNA synthesis in the polymerase stop assay.

Compound ID	Temp [TTAGGG] ₄	Temp [TTAGAG] ₄
	G-quadruplex-forming	non-G-quadruplex-forming
176327	8	---
305831	39	---

Table 2.2. IC₅₀ calculated for the inhibition of DNA synthesis in the polymerase stop reaction. The primer extension reaction using the non-G-quadruplex-forming Temp [TTAGAG]₄ revealed no G-quadruplex stop products. The results are expressed in μM.

Evaluation of G-quadruplex stabilization by circular dichroism

Circular dichroism is used to determine binding mode and affinity of ligand-DNA interactions. It is a more accessible technique that serves as a low-resolution complement to NMR and X-ray diffraction methods. Ligand-DNA interactions can be studied by virtue of the interpretation of induced ligand CD signals resulting from the coupling of electric transition moments of the ligand and DNA bases within the asymmetric DNA environment [241, 242].

The observation of an ligand-induced change in CD spectrum of a DNA sample is indicative of a ligand-DNA interaction [242]. In addition, CD can assist in determining the presence of G-quadruplexes and can help diagnose the type of G-quadruplex structure present [243]. CD measures the difference in absorbance of circularly polarized light by a chromophore in an asymmetric environment and can be used to examine the structure of DNA in solution. For example, parallel and antiparallel G-quadruplexes display characteristic patterns of peaks in the 240-320 nm wavelength range, which are not present in linear DNA [244]. This technique can be used to confirm the presence of G-quadruplexes in DNA and discriminate between parallel and anti-parallel strand orientation [245]. The presence of the Na^+ cation generally promotes the formation of an anti-parallel G-quadruplex in human telomeric DNA, while the K^+ cation favors the parallel propeller and hybrid structures (figure 2.8) [246].

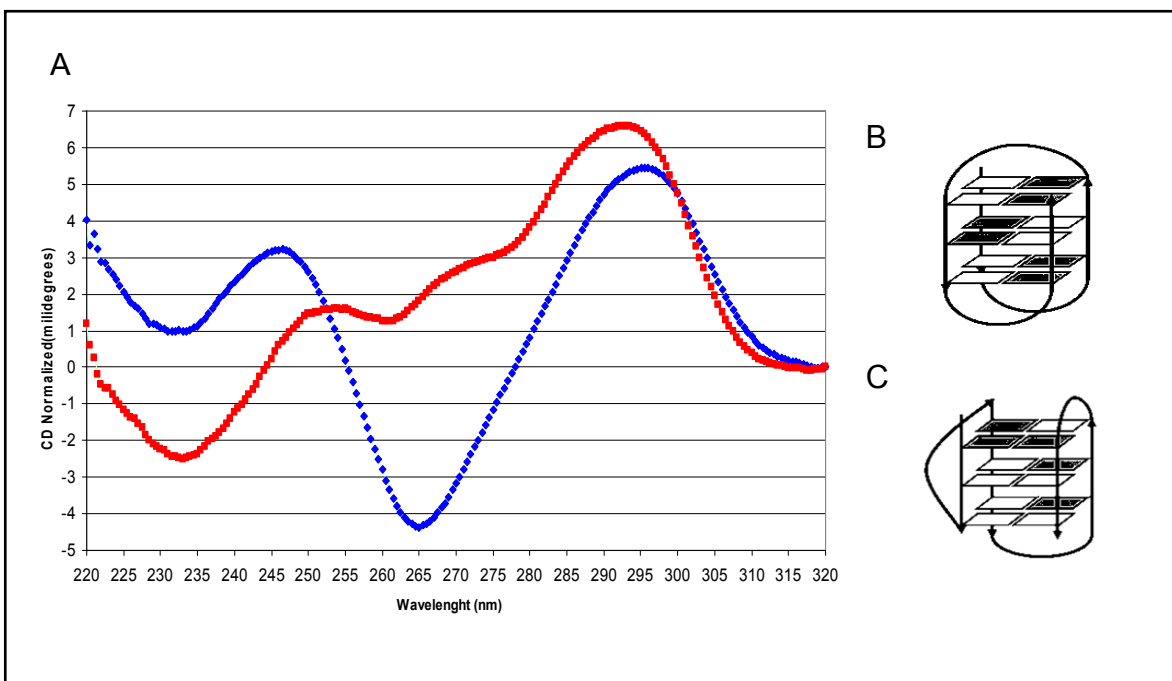


Fig 2.8. Characteristic pattern of peaks for Na and K solutions and their respective G-quadruplex shapes. The CD spectra were obtained as explained in the Methods section. A. A 50mM Na⁺ solution (blue) shows characteristic positive peaks at 295 and 245 nm and a negative peak at 265nm. A 50mm K⁺ solution (red) shows positive peaks at 293 and 253nm. B. Antiparallel folding of the G-quadruplex, typical of a Na⁺ solution (basket-type structure). C. Parallel folding seen in K⁺ solutions (hybrid: 3 + 1, propeller-type structure).

Compounds NSC 176327 and 305831 were the only two compounds that showed selective formation of G-quadruplex products in the polymerase stop assay (Figure 2.1.). Therefore, the interactions of these compounds with repeats of human telomeric DNA were monitored using CD spectroscopy. The human telomeric oligonucleotide d[5'-G₃(T₂AG₃)₃-3'] alone showed a major positive band at 250 nm, and a minor band at 295 nm (Fig 2.8.A. and 2.9.A.) [7]. To determine the stoichiometry of the binding of both compounds to human telomeric G-quadruplexes, titrations of these ligands into a fixed concentration of human telomeric DNA were tested.

The titration of increasing amounts of NSC 176327 (0.5 to 6 mol equivalents) with a fixed concentration of human telomeric DNA revealed a major negative peak at 253 nm and the disappearance of the positive peak at 295nm present before (Fig 2.9.A.). This suggests the ligand-induced formation a new structure, presumably a G-quadruplex, although it is not clear what conformation is favored. This steep decrease of the 253 nm band stopped when a 4:1 ratio of NSC 176327 to DNA was reached (fig 2.9.B.).

Addition of 0.5 to 4 mol equivalents of compound 305831 resulted in a new spectrum with a significant increase in the 293 nm peak and a small positive peak at 283 nm. This profile is similar to the one seen in a K⁺ solution (fig 2.8), suggesting the formation of a propeller-type structure. This positive band increased until a 1.5:1 ratio of NSC 305831 to DNA was reached (fig 2.10.A. and B.).

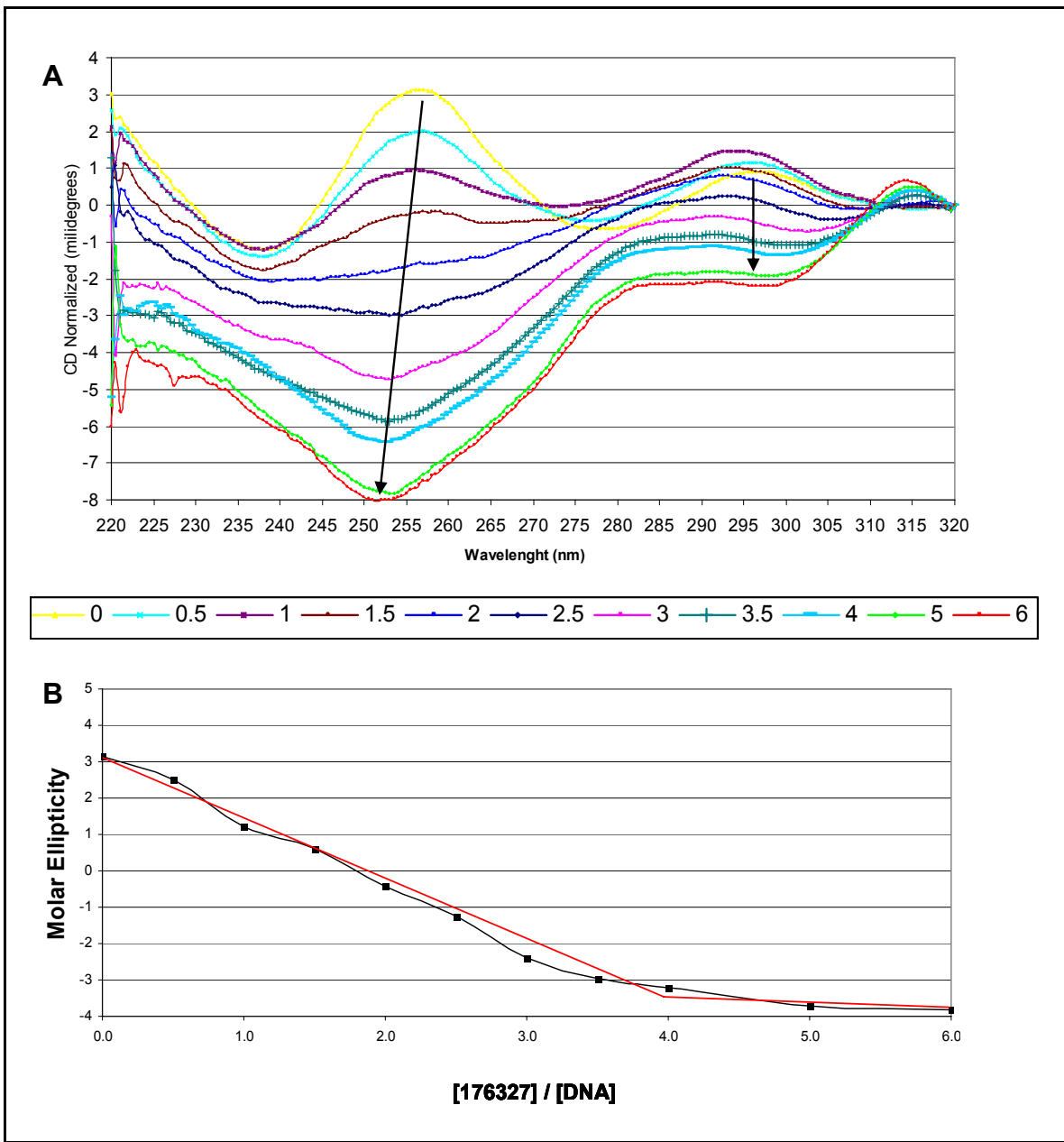


Fig 2.9. CD spectra and stoichiometry analysis of NSC 176327. A. Titration of NSC 176327 with human telomeric DNA shows a major negative peak at 253nm and the disappearance of the positive peak at 295nm present before. B. Stoichiometry analysis of the titration shows that the spectrum equilibrates at a ratio of 4:1.

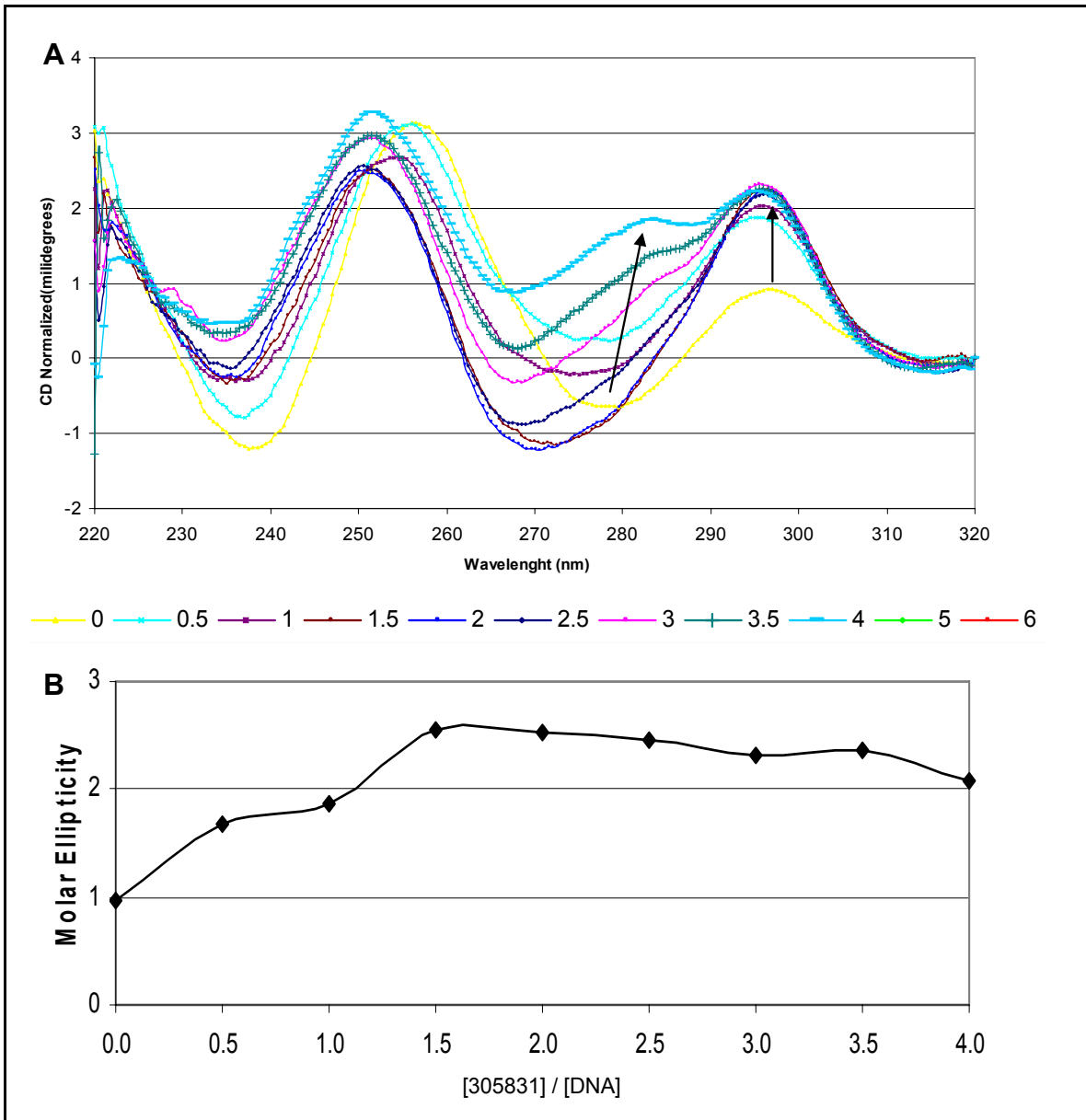


Fig 2.10. CD spectra and stoichiometry analysis of NSC 305831. A. Titration of NSC 305831 with human telomeric DNA presents an increase in the 293 nm peak and a small positive peak at 283 nm. C. The ratio for spectrum equilibrium is 1.5:1 for this compound.

The data in this chapter demonstrates that a G-quadruplex formation assay can accurately identify G-quadruplex binding compounds that inhibit telomerase. Specifically, the work confirmed that NSC 176327 and NC 305831 are selective G-quadruplex stabilizers of the human telomeric sequence. Our CD data shows that NSC 305831 favors the formation of a propeller-type structure in a molar ratio of 1.5:1. NSC 176327 seems to produce a mix of G-quadruplex formations, and the ratio was 4:1. Investigation of the literature confirms our findings as analogs of NSC 305831 have been reported as stabilizers of G-quadruplex structures [241]. For NSC 176327, we found that the structure belongs to the natural plant product ellipticine. This compound is reported to bind to DNA with high affinity (10^6 M^{-1}). The literature delineates an interaction between ellipticine and telomerase, suggesting that this takes place through DNA binding. We have strengthened this hypothesis by showing strong data that confirms that this small molecule interacts directly with telomeric DNA and stabilizes the G-quadruplexes structures [247].

Targeting G-quadruplex-DNA represents a challenge since its particular DNA arrangement is polymorphic in nature and is not abundant as compared to duplex-DNA. The advances made in the design and the synthesis of G-quadruplex ligands convinces us that the development of compounds able to discriminate not only G-quadruplex from duplex-DNA, but between the various structures of G-quadruplexes is imminent [236].

FUTURE PLANS

We have confirmed that a HTS for molecules that can induce G-quadruplex formation can identify new telomerase inhibitors. There are several directions this research can be directed in the future. One tract would be to investigate ellipticine and its analogs in an effort to demonstrate the role of telomere biology in ellipticine pharmacology and to optimize ellipticine for selective anti-cancer effects. Also, it would be worth to screen larger, more diverse libraries of compounds to enrich the known chemical space of G-quadruplex interacting structures.

A number of toxic effects have been shown for ellipticine, but because this compound shows amenability for structural modification, it is possible to apply rational drug design to improve its anti-cancer quality, or at least, reduce its side effects. A number of successful ellipticine analogs have been designed and synthesized with improved toxicities and anticancer activities. In addition, the identification of NSC 305831 as a compound that selectively targets quadruplex structures will allow this molecule to be used as a tool to unravel the roll of telomerase in cancer [241]. Considerable research efforts have been directed towards gaining a greater understanding of the mechanism of action of these compounds and their analogs that will aid further in the optimization of drug design [247]. The use of G-quadruplex ligands as tools to evaluate the therapeutic potential of telomeres and to help elucidate the complex interrelations with the telomeric-interacting proteins such as telomerase and capping proteins, will facilitate the

understanding of the roll of these ligands on cancer cells and how they induce specific responses, such as telomere instability and focused DNA damage [236].

CHAPTER 3

VALIDATION AND OPTIMIZATION OF MEDIUM TO HIGH-THROUGHPUT CELL- BASED FLUORESCENT ASSAYS

INTRODUCTION

High-throughput screening of GPCRs

GPCRs transduce extracellular stimuli to intracellular responses via the coordinated action of a variety of proteins and intracellular messenger pathways. Many, if not all, of these pathways can be used in a variety of high-throughput assays [248]. Truly high-throughput assays have been developed to carry out the assays on a miniaturized scale. Assays like cAMP and calcium mobilization have been successfully scaled down to a 1536-well format [249, 250]. In the academic setting, 96-well and 384-well formats are used, with a corresponding decrease in throughput.

This throughput is still much higher than conventional radioligand binding assays. It affords the opportunity to distinguish agonists, partial agonists, inverse agonists, allosteric modulators, and antagonists, and it does not present the

disadvantages of using radioactivity. For example, in calcium mobilization assays, agonists can be distinguished from antagonists and allosteric modulators in 'dual-addition' experiments, in which test compounds are added first, and known agonists are added in a second addition. In such experiments, test compounds that are agonists activate a calcium response after the first addition, compounds that are antagonists inhibit the agonist response after the second addition, and compounds that are positive allosteric modulators enhance the agonist response after the second addition [249].

Functional assays to screen GPCRs

In contrast to radioligand-binding assays, functional assays produce ligand profiles that reveal how ligands modulate GPCR signal transduction (i.e. agonist versus partial agonist). Functional GPCR screening relies on the detection of second messengers, which are produced as a result of receptor specific signal transduction pathways. Typically, Ca^{2+} is measured using fluorometric dyes and analyzed using automated fluorescent plate readers [251]. Although the activation of many GPCRs will not induce a Ca^{2+} signal, the use of chimeric and/or promiscuous G proteins enables most GPCRs to couple to Ca^{2+} [252, 253]. Multiple downstream signaling events can occur following receptor activation, even among members of a single receptor family, consequently it is difficult to predict which of the signaling events is relevant physiologically and therefore useful as a readout. This is particularly problematic when searching for agonists and partial agonists because chemically

distinct agonists frequently elicit functionally distinct readouts (a phenomenon referred to as 'functional selectivity' or 'agonist-directed trafficking') [254-256].

One ubiquitous feature of signaling through GPCRs and other cell surface receptors is the short-term and long-term loss of cellular sensitivity following presentation of stimulus, a phenomenon referred to as desensitization [257]. Some of the effector proteins that are activated by many GPCRs, including GRKs and second messenger-activated protein kinases, take part in feedback regulation of GPCR signaling. Typically, activation of a GPCR leads to activation and inhibition of specific signaling pathways in the cell, short-term desensitization mediated by phosphorylation of GPCRs by GRKs followed by β -arrestin binding to GPCRs that uncouple the receptor at the plasma membrane from the G-protein, and endocytosis of the receptor followed by post-endocytic sorting of the receptor either back to the plasma membrane (receptor recycling) or to lysosomes for degradation. Short-term desensitization may also involve phosphorylation of GPCRs by second messenger-dependent protein kinases; this uncouples GPCRs at the plasma membrane from G proteins. Long-term desensitization may include one or more of the following processes: down-regulation of receptors and/or downstream components in the signaling pathway (e.g., G-proteins and effector proteins) by proteolytic protein degradation in lysosomes or at the plasma membrane, decreased synthesis of receptor protein and/or downstream proteins, and enhanced mRNA degradation. The extent to which each of these processes is responsible for desensitization is cell type and receptor specific [257]. Fig 3.1. shows the GPCR signaling pathways that can be used to screen, including the regulation of GPCRs by β -arrestins.

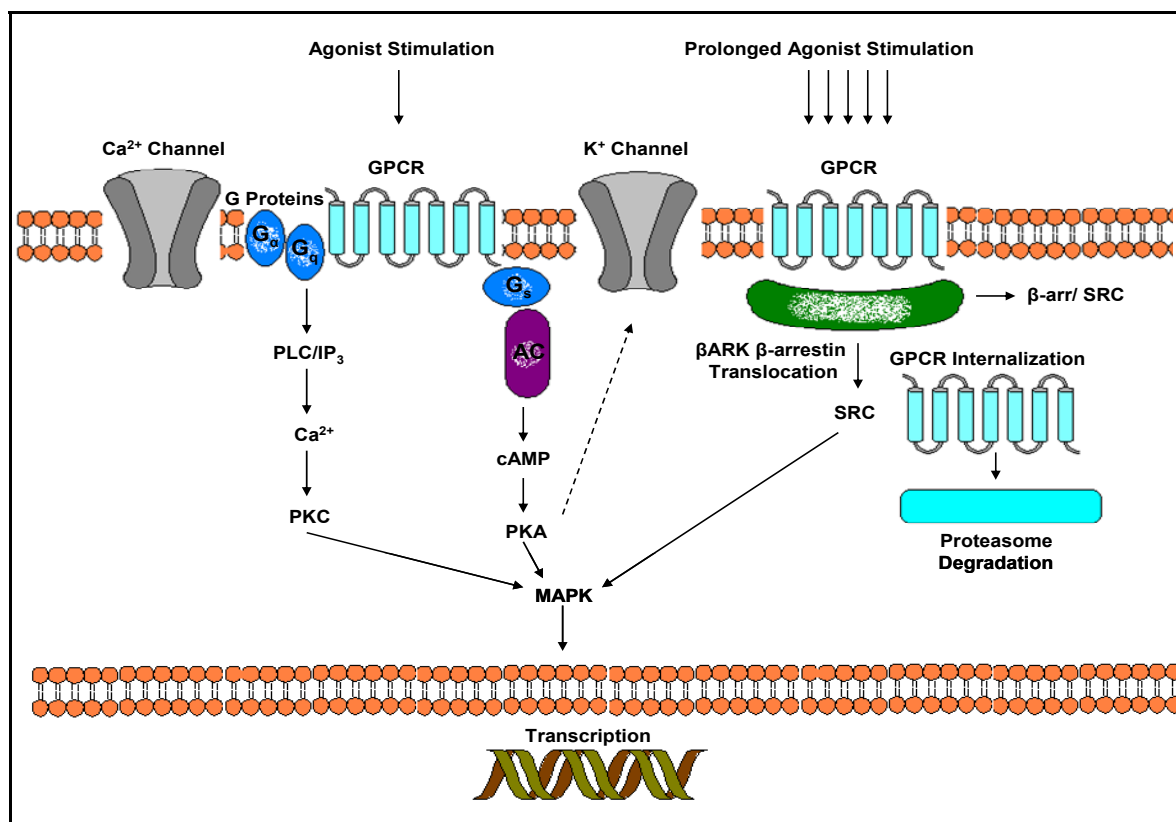


Fig 3.1. GPCR signaling pathways of interest for HTS, including the regulatory pathway signaled by β -arrestins. Agonist stimulation. Stimulation of GPCRs by agonists leads to activation of multiple signaling pathways, including those involving second messengers such as cAMP, IP₃, and Ca²⁺. GPCRs in the plasma membrane couple to these pathways via G proteins that link the receptors to enzymes such as adenylyl cyclase (AC) and phospholipase C (PLC) or ionic conductance channels including the Ca²⁺ and K⁺ channels. PKA, protein kinase A; PKC, protein kinase C. **Prolonged agonist stimulation.** Prolonged stimulation of the receptor leads to recruitment to the cell membrane of β -arrestin. This leads to uncoupling of the GPCR from G proteins and the second messenger pathways and leads to three subsequent and parallel processes. β -arrestin couples the GPCR to SRC, which can link the receptor to MAPK. This creates alternative signaling via the GPCR, in contrast to its G protein-mediated functions. β -arrestin also serves as an adaptor linking the receptor to clathrin-coated vesicles, which internalize the receptor. This **Identification of lead candidates** can lead to targeting the receptor to degradation in the proteasome. Picture adapted from [258].

Due to the limited availability of structural data on GPCRs, the design of ligands for this family still heavily depends on ligand based design techniques. For many GPCRs, the natural ligand can provide a good starting point in the lead identification. Especially for peptide binding GPCRs, screening of diverse or focused compound libraries still remains a successful lead identification, which has yielded the discovery of several potent GPCR ligands. Such compounds have been classified frequently as functional mimetics, as they elicit agonist or antagonist activity but are not necessarily structural homologues. Nonpeptide receptor agonists are now becoming known in peptide classes where initially only nonpeptide antagonists were identified [257].

Quantification of second messengers for the identification of hits

Improving hit specificity and sensitivity in automated or semi-automated processes is key to identify candidate hits rapidly and accurately [6]. Diverse technologies have been developed for this purpose, including Ca^{2+} , inositol phosphate, and β -arrestin readouts. Our efforts mainly focused on the Ca^{2+} mobilization technology to take advantage of this second messenger that is intrinsic to OTR activation. β -arrestin quantifying tools provide information that is independent of the type of G-protein bound, hence this technology is generic to virtually all GPCRs. Several dyes have been implemented to increase signal-to-background ratio, and reduce false positives for the fluorescence-based intracellular calcium mobilization assays used in the FLIPR^{TETRA®} system. In this chapter, the

validation of three different dyes used for different stages of the screening campaign is described.

The FLIPR Calcium 4 Assay Kit from Molecular Devices (Sunnyvale, CA) is a no-wash, mix-and-read, calcium mobilization assay that utilizes a novel masking dye technology that significantly lowers background fluorescence and improves signal-to-noise without washing the cells. This kit has a greater light extinction in the extracellular solution due to the novel masking dye (fig 3.2.). One source of potential fluorescence outside the cells is extrusion of the indicator out of the cell by organic anion transporters. To reduce this artifact, probenecid is used to inhibit this transport and reduce the baseline signal.

For the optimization step of the screening campaign, the Fluo-4 NW Calcium assay kit from Invitrogen (Carlsbad, CA) was utilized. Fluo-4 is a fluorescent Ca^{2+} indicator available as a cell-permeant ester. This kit requires neither a wash step nor a quencher dye. The elimination of the wash step results in lower variability and higher Z' values and the possibility of testing activity in non-adherent cell lines. The fluo-4 NW indicator is nonfluorescent and stable in pH 7–7.5 buffer for several hours, so spontaneous conversion to the Ca^{2+} -sensitive form is not a significant source of background fluorescence. Contributions to baseline fluorescence by the growth medium (e.g., esterase activity, or proteins interacting with receptors of interest) are eliminated by removing the medium prior to adding the indicator dye to the wells. A water-soluble form of probenecid that is easy to dissolve in buffer and safer to use than the free acid that requires 1M NaOH to dissolve, is provided with the kit [259].

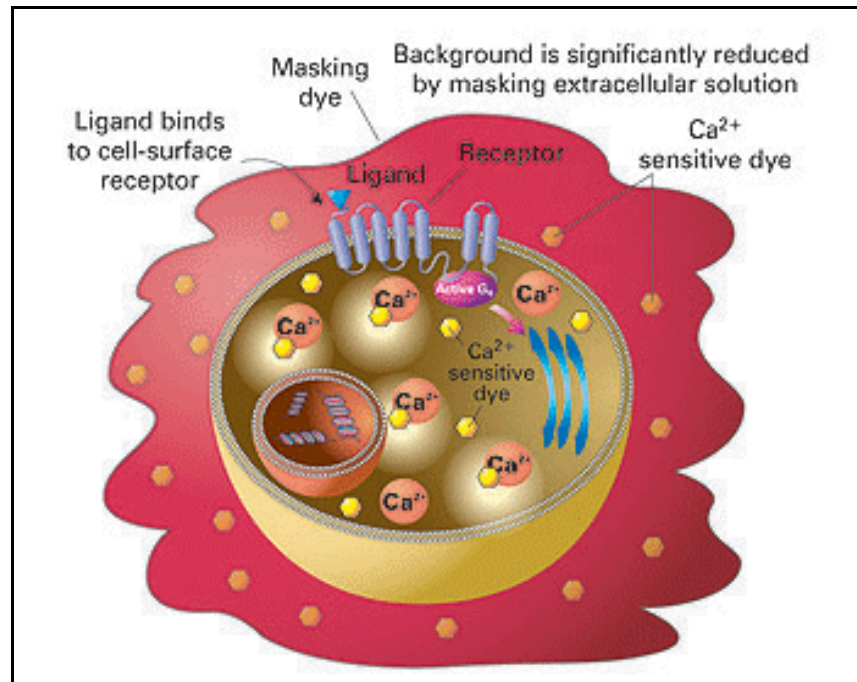


Fig 3.2. Graphic representation of the FLIPR Calcium 4 Assay Kit. Increase in cytosolic Ca²⁺ can be detected by FLIPR microplate readers using the calcium-sensitive dye indicator. Scheme borrowed from [260].

In order to proceed with the HTS in a 1536 well plate format, a homogeneous assay needed to be validated. Screen Quest™ Fluo-8 NW Calcium Assay Kit provided a fluorescence-based assay for detecting the intracellular calcium mobilization without the removal of the cell media prior to the dye loading step. Once inside the cell, the lipophylic blocking groups of Fluo-8 AM are cleaved by non-specific cell esterases, resulting in a negatively charged fluorescent dye that stays inside cells [261].

Another technology was also explored to assess its robustness in GPCR screening. The direct analysis of GPCR activation via β -arrestin recruitment could provide a simple assay protocol to identify multiple pharmacologies (agonists, antagonists, allosteric modulators, etc.). The β -arrestin signaling pathway is generic to virtually all GPCRs. GPCR mediated β -arrestin recruitment occurs independent of G-protein coupling status. Agonist stimulated G protein-coupled receptors (GPCRs) initiate cell responses by modulating the activity of effector molecules via activation of specific G proteins. Following this signaling event, activated GPCRs undergo phosphorylation by specific GPCR kinases (GRKs). This phosphorylation promotes the binding of arrestin molecules to the GPCR, which in turn uncouples the receptor from the G-protein leading to receptor desensitization, a temporary state during which the system becomes refractory to further stimulation [262]. The DiscoverX PathHunter technology offers a generic assay to investigate interactions between β -arrestins and activated GPCRs. The direct measure of GPCR activation by detection of β -arrestin binding to the GPCR of interest and can be used with any G_i -, G_q -, or

Gs-coupled receptor. This assay takes advantage of the β -galactosidase enzyme fragment complementation depicted in fig 3.3.

There is a pressing need for small molecules that selectively activate the OT system within the CNS. These small molecules will serve as new chemical tools to elucidate the complex roles for oxytocin in social behavior, and they will provide new potential leads for a drug discovery campaign in the treatment of specific neuropsychiatric disorders. This stage of the project was focused on both the identification of agonists and positive allosteric modulators of the OTR through a HTS campaign.

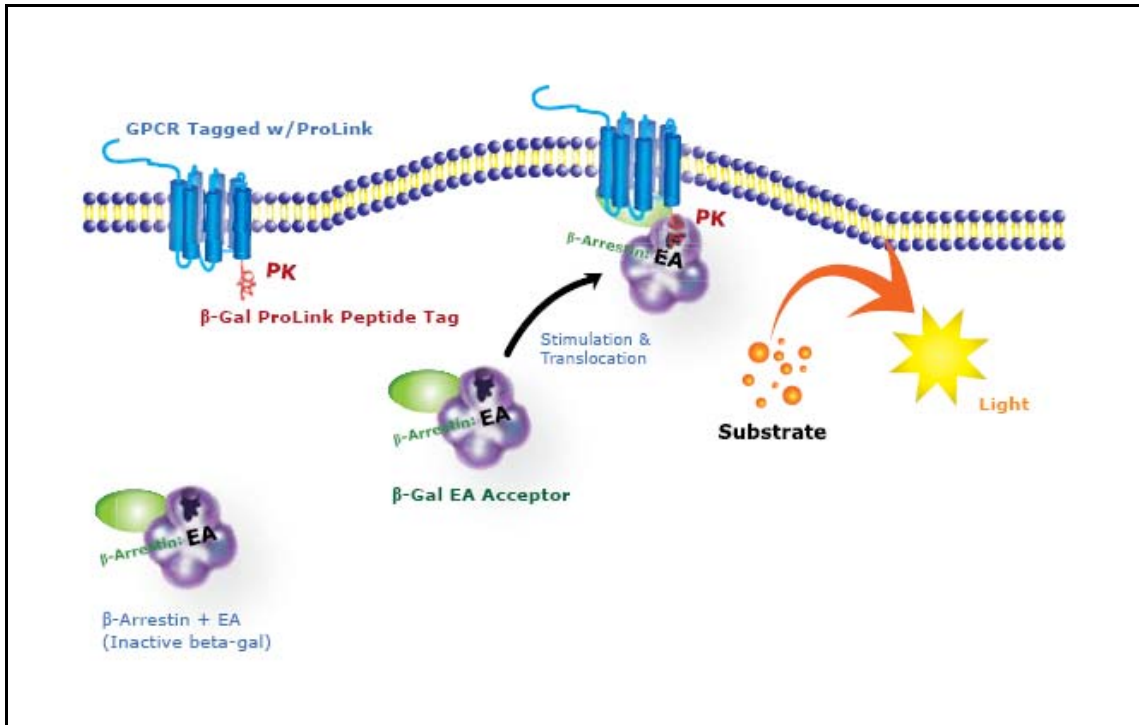


Fig 3.3. β -galactosidase enzyme fragment complementation. β -arrestin is fused to an large N-terminal deletion mutant fragment of β -gal, the enzyme acceptor (EA). The GPCR of interest is fused to a small weakly complementing fragment of β -gal, termed ProLink™ (PK). In cells that stably express these fusion proteins, ligand stimulation results in the interaction of β -arrestin and the ProLink-tagged GPCR, forcing the complementation of the two β -gal fragments and resulting in the formation of a functional enzyme that converts substrate to a detectable chemiluminescent signal. Picture borrowed from [263].

METHODS AND MATERIALS

Materials. All reagents were ACS reagent grade and used without further purification unless otherwise noted. Oxytocin, vasopressin (Sigma), and carbetocin (Bachem) were purchased in the powder form. Compound 39 was synthesized by the Center for Integrative Chemical Biology and Drug Discovery at UNC-CH. Several dyes for calcium mobilization assays were obtained from commercial sources: FLIPR Calcium 4 Assay Kit (Molecular Devices), Fluo-4 NW Calcium Assay Kit (Invitrogen, Carlsbad, CA), and the Screen Quest™ Fluo-8 No Wash Calcium Assay Kit (ABD Bioquest, Sunnyvale, CA).

The NCI Diversity set was obtained from the Developmental Therapeutics Program of the NCI/NIH's repository; it consisted of 1,900 structurally diverse small molecules that were provided in 100% DMSO at 10mM. Aliquots of the library were taken and these were diluted to a final concentration of 20 μ M (2x) using assay buffer. The final DMSO concentration was at 1%.

The Prestwick and a portion of the Asinex Gold Libraries were provided by the Biomanufacturing Research Institute and Technology Enterprise (BRITE Center at NCCU). The Prestwick Library consisted of 1,100 compounds that are mostly FDA-approved drugs. Aliquots of the library were taken and these were diluted to a final concentration of 20 μ M (2x) using assay buffer. The final DMSO concentration was below 1%. A portion of the Asinex Gold library was screen in the medium-throughput screen. It consisted of 29,000 structurally diverse compounds.

The stably transfected CHO-hOTR, CHO-V_{1a}, CHO-V_{1b}, CHO-V₂, and CHO wild type cells were kindly provided by the NIMH Psychoactive Drug Screening Program at UNC-CH. Reagents used for cell culture were purchased from Gibco-Invitrogen. The PathHunter™ CHO-K1 OTR β-Arrestin Cell Line, PathHunter™ Detection Kit, and the PathHunter™ eXpress β-Arrestin GPCR Assays were obtained from DiscoverRx (Fremont, CA).

Cell culture. Stably transfected CHO-hOTR and CHO-V_{1a} cells were grown in OT/V_{1a} media that consists of: Hams F-12, 400 µg/ml geneticin sulfate (G-418), 10% calf serum, 15mM HEPES, and 50 U of penicillin/ 50 µg of streptomycin. The CHO-V_{1b} /V₂ media was made with Hams F-12, 150 µg/ml zeocine, 10% calf serum, 15 mM HEPES, and 50 U of penicillin/ 50 µg of streptomycin. CHO wild type cells were grown in DMEM, 10% fetal bovine or calf serum and 50 U of penicillin/ 50 µg of streptomycin. All the cell lines were incubated at 37°C and 5% CO₂ in 75cm² flasks until 80% confluency was reached. At that point, they were either passaged to new flasks to allow expansion of growing cells or they were plated to be used in the assays. Cells were incubated with 0.05% Trypsin –EDTA at 37°C for 5 minutes for dissociation. The stably transfected cell lines were used in the assays until they have reached a passage number of 20, after which they were discarded as they started to show a decrease in response maybe due to receptor expression inefficiency. In this case, a new batch of fresh cells from stocks stored in liquid nitrogen was grown.

Cell plating for screen. Stably transfected cells were plated on uncoated 96 or 384 well tissue culture polystyrene plates (Greiner Bio-one, Monroe, NC). The plating densities were 40,000 cells/well in 100 μ l of media for the 96 well plates, or 15,000 cells/well in 20 μ l of media for the 384 well plates. Cells were at 37°C and 5% CO₂ for 18-24 hours before starting the assay to allow cells to adhere. This cell growth protocol was optimized to ensure similar cell conditions and health throughout the screening campaign.

OT dose response curve preparation. OT powder was dissolved in DMSO to a final concentration of 1mM. This stock solution is stable at -20°C for several months. Each day, an OT dose response curve was determined prior to initiating the screen to determine EC₂₀ concentrations and to compare inter-day results.

For the 96 well-plate format, a 16 point curve was prepared as 10x serial dilutions of the stock with initial concentrations starting at 10 μ M and 3 μ M, plating each concentration by triplicate as shown in Fig 3.4. Only half of the plate was used for the curve. For the 384 well-plate format, a 16 point curve was prepared as explained above. Each concentration was plated six times as shown in Fig 3.5.

	1	2	3	4	5	6
A	10^{-12}	10^{-12}	10^{-12}	3×10^{-12}	3×10^{-12}	3×10^{-12}
B	10^{-11}	10^{-11}	10^{-11}	3×10^{-11}	3×10^{-11}	3×10^{-11}
C	10^{-10}	10^{-10}	10^{-10}	3×10^{-10}	3×10^{-10}	3×10^{-10}
D	10^{-9}	10^{-9}	10^{-9}	3×10^{-9}	3×10^{-9}	3×10^{-9}
E	10^{-8}	10^{-8}	10^{-8}	3×10^{-8}	3×10^{-8}	3×10^{-8}
F	10^{-7}	10^{-7}	10^{-7}	3×10^{-7}	3×10^{-7}	3×10^{-7}
G	10^{-6}	10^{-6}	10^{-6}	3×10^{-6}	3×10^{-6}	3×10^{-6}
H	10^{-5}	10^{-5}	10^{-5}	3×10^{-5}	3×10^{-5}	3×10^{-5}

Fig 3.4. OT dose response curve map for 96 well plate format. Final concentrations are expressed in M. Only half of a plate is used for this step.

	1	2	3	4	5	6
A	10^{-12}	10^{-12}	10^{-12}	10^{-12}	10^{-12}	10^{-12}
B	3×10^{-12}					
C	10^{-11}	10^{-11}	10^{-11}	10^{-11}	10^{-11}	10^{-11}
D	3×10^{-11}					
E	10^{-10}	10^{-10}	10^{-10}	10^{-10}	10^{-10}	10^{-10}
F	3×10^{-10}					
G	10^{-9}	10^{-9}	10^{-9}	10^{-9}	10^{-9}	10^{-9}
H	3×10^{-9}					
I	10^{-8}	10^{-8}	10^{-8}	10^{-8}	10^{-8}	10^{-8}
J	3×10^{-8}					
K	10^{-7}	10^{-7}	10^{-7}	10^{-7}	10^{-7}	10^{-7}
L	3×10^{-7}					
M	10^{-6}	10^{-6}	10^{-6}	10^{-6}	10^{-6}	10^{-6}
N	3×10^{-6}					
O	10^{-5}	10^{-5}	10^{-5}	10^{-5}	10^{-5}	10^{-5}
P	3×10^{-5}					

Fig 3.5. OT dose response curve map for 384 well-plate format. Final concentrations are expressed in M. OT concentration in original plate was 2x for the Fluo4-NW dye and 5x for the Fluo-8 NW dye. Only one quarter of a plate is used for this step.

Sample compounds and control dilutions preparation. Dilutions of drugs and controls (OT at maximum concentration) for first addition of protocol were made in assay buffer as 2x stocks. The final DMSO content was below 1%. Oxytocin dilutions (OT at maximum concentration and EC₂₀) for second addition of protocol were made in assay buffer as 4x stocks. The negative (min) control was the assay buffer. The positive controls are the EC₂₀ control, which was prepared according to the values obtained daily from the dose response curve, and the maximum concentration of OT that was 10 µM. All sample compounds were tested initially at a final concentration of 10 µM.

Data collection and analysis. Data was collected using ScreenWorks™ 2.0.0.22 software (Molecular Devices) and analyzed using Graph Pad Prism 5 for Windows. Each kinetic trace was normalized to the initial fluorescence intensity to correct for loading of the cells, and it was reported as % normalized activation. This parameter was calculated as (sample value – min control value) / (max control value – min control value). For agonist calculations (first dispense), the no OT control was used as the minimum control. For the positive allosteric modulator calculations, the minimum control was the value obtained for OT at EC₂₀. The maximum control was OT at maximum concentration for both calculations.

Definition and selection of initial hits. Compounds from the primary screen were considered actives and were selected to undergo further testing according to the following criteria: 50% or more normalized % activation compared to the average

normalized % activation for agonists and for positive allosteric modulator. Actives were briefly examined to discard false positives based on fluorescence readout, reactivity, promiscuity of compounds found in PubChem, and compounds that presented adverse effects reported in the literature. A large number of actives could provide a substantial amount of data that is challenging to handle. In this case, we chose those actives that fell above average normalized % activation + 1 sd calculated from all the actives.

Validation of fluorescence-based intracellular calcium mobilization assay for the identification of hOTR agonists and allosteric modulators in a 96 well-plate format.

Dye preparation. To validate an OTR assay for HTS, the FLIPR Calcium 4 Assay Kit (Molecular Devices) was first used. The preparation of the dye (component A) was conducted according to the manufacturer's instructions. In short, component A was dissolved in 10 ml of 1x Hanks' Balanced Salt Solution and 20 mM HEPES, pH 7.4. This stock solution can be stored at -20°C for several months. The working solution of the dye has to be prepared daily by dissolving 1 ml of the stock solution in 30 ml of assay buffer made as follows: 1x HBSS (138 mM NaCl, 5.3 mM KCl, 1.3 mM CaCl₂, 0.49 mM MgCl₂, 0.41 mM MgSO₄, 0.44 mM KH₂PO₄, and 0.34 mM Na₂HPO₄), 20 mM HEPES, 2.5 mM Probenecid, corrected to pH 7.4 with NaOH 10 N. The dye working solution was kept in the dark at room temperature or 37 °C throughout the day.

Cell preparation. Media from plated cells was aspirated and replaced with 30 μ l of fresh dye working solution. Cells were incubated with the dye for 45 min at 37 °C and then at RT in the dark for another 15 min.

OT dose response curve, sample compound, and OT control dilutions

preparation. The dilutions were made as explained before. These dilutions were plated in a 96 well plate according to plate map in Fig 3.6.

Fluorescence-based intracellular calcium mobilization assay: 96-well plate

format. A FLIPR^{TETRA}® system (Molecular Devices, Sunnyvale, CA) was used to read fluorescence (excitation wavelength: 470-495nm, emission wavelength: 515-575nm) in each well every 1 s for 30 sec, to establish a baseline reading. After this period, the FLIPR^{TETRA}® transferred 30 μ l of the 2X compound solution from the compound plate to the cell plate (first addition). Readings were made every 1s for 5min to identify possible hOTR agonists. A second dispense transferred 20 μ l of 4x OT at the EC₂₀ obtained from that day's dose response curve from the OT plate to the cell plate, and readings were made every 1 s for 3 min (see Table 3.1.). This portion of the assay was designed to identify possible hOTR positive allosteric modulators. The SOP for this assay is represented in Figure 3.7. Each plate was run twice; the compounds tested belonged to the same drug plate. Data collection and analysis was performed as explained above.

	1	2	3	4	5	6	7	8	9	10	11	12
A	Min											Max
B	Min											Max
C	EC ₂₀											EC ₂₀
D	EC ₂₀	Test compounds at 2x (20 µM)										EC ₂₀
E	EC ₂₀											EC ₂₀
F	EC ₂₀											EC ₂₀
G	Max											Min
H	Max											Min

Fig 3.6. Plate map for 96 well plate format low throughput screen. Max, Oxytocin at 10 µM. Min, assay buffer. EC₂₀, Oxytocin at 20% according to daily dose response curve.

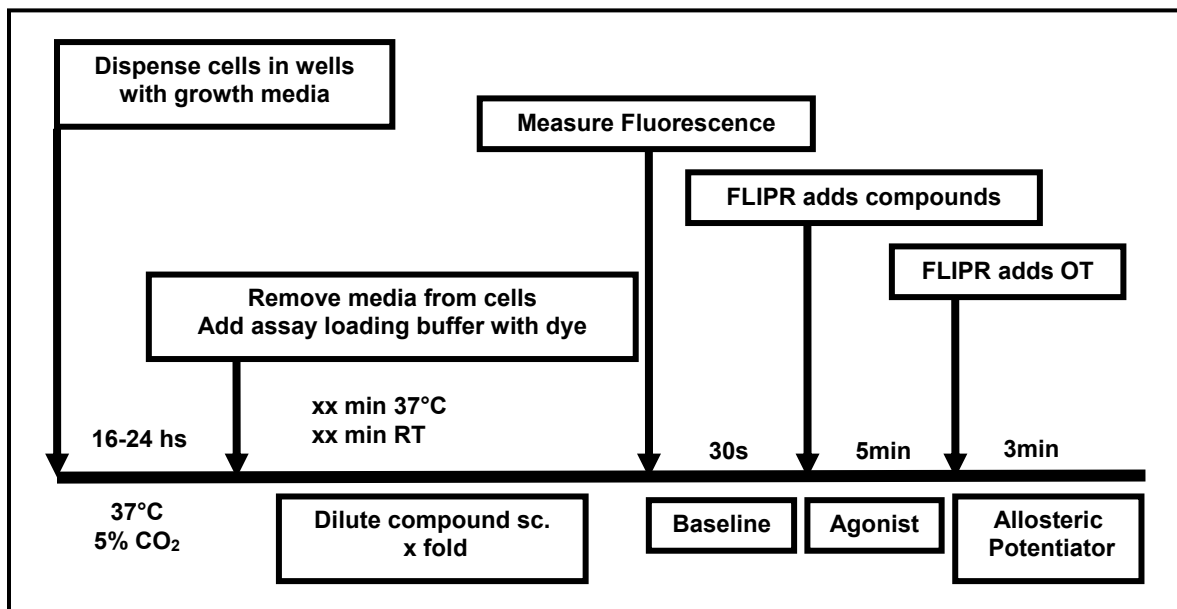


Figure 3.7. Standard Operating Procedure for High Throughput Screen Assay.

Optimization and execution of fluorescence-based intracellular calcium mobilization assay for the identification of hOTR agonists and allosteric modulators for a 384 well-plate format. This stage of the screening campaign was performed at the BRITE center at NCCU.

Dye preparation. The dye recommended by the screening center was Fluo-4 NW Calcium Assay Kit (Invitrogen, Carlsbad, CA). The preparation of the Fluo4-NW dye mix (component A) was done according to instructions from the manufacturer. The assay buffer consisted of 1X HBSS, 20 mM HEPES. A 250mM stock solution of probenecid was made by adding 1 ml of assay buffer to one vial of water soluble probenecid (Component B). This solution could be stored at $\leq -20^{\circ}\text{C}$ for up to 6 months. To make the dye mix, 100ml of assay buffer and 1ml of the probenecid stock solution were added to one bottle of Component A. This 1X dye loading solution was sufficient for ten microplates, and the final probenecid concentration was 2.5 mM. The dye working solution was kept in the dark at room temperature throughout the day and then discarded.

Cell preparation. Media from plated cells was discarded and replaced with 20 μl of fresh dye working solution. Cells were incubated with the dye for 45 min at 37 $^{\circ}\text{C}$ and then at RT in the dark for another 15 min.

OT dose response curve, sample compound, and OT control dilutions preparation. The dilutions were made as explained before. These dilutions were plated in a 384 well-plate according to plate map in Fig 3.8.

Fluorescence-based intracellular calcium mobilization assay: 384-well plate format. A FLIPR^{TETRA}® system (Molecular Devices, Sunnyvale, CA) was used to read fluorescence as described above with minor changes. In this 384-well plate assay, the dispensing volumes were 20 µl of the 20 µM (2x) compound solutions and 10 µl of OT at 5x EC₂₀ (see Table 3.1.). The SOP for this assay is represented in Figure 3.7. Data was collected and analyzed in the same manner as for the 96-well plate format.

Implementation of Fluo-8 No Wash Calcium Assay Kit for the fluorescence-based intracellular calcium mobilization assay for the identification of hOTR agonists and allosteric modulators for a 384 well-plate format. The validation of this dye was required by the Scripps Research Institute Molecular Screening Center previous to start the high throughput screen at their premises. This kit allows for a homogenous assay without removal of cell media prior to dye addition. This step is crucial to scale up the assay to a 1536 well plate format to allow screening of more than 200,000 compounds at the Screening Center.

Dye preparation. Screen QuestTM Fluo-8 No Wash Calcium Assay Kit (ABD Bioquest, Sunnyvale, CA) was recommended by the Screening Center. Fluo8-NW dye-loading solution was prepared according to the manufacturer; instructions. The Fluo-8 NW stock solution was made by adding 200 µl DMSO into component A (Fluo-8NW) and mixing well. The 1x assay buffer consisted of 10ml of 10x Pluronic

	1	2	3	4	5	6	7	8	9	10	11	12	13	14	15	16	17	18	19	20	21	22	23	24							
A	M	E	S	S	S	S	S	S	S	S	S	S	S	S	S	S	S	S	S	S	S	S	X	X							
B	M	E	S	S	S	S	S	S	S	S	S	S	S	S	S	S	S	S	S	S	S	S	X	X							
C	M	E	S	S	S	S	S	S	S	S	S	S	S	S	S	S	S	S	S	S	S	S	X	X							
D	M	E	S	S	S	S	S	S	S	S	S	S	S	S	S	S	S	S	S	S	S	S	X	X							
E	M	E	S	S	S	S	S	S	S	S	S	S	S	S	S	S	S	S	S	S	S	S	X	X							
F	M	E	S	S	S	S	S	S	S	S	S	S	S	S	S	S	S	S	S	S	S	S	X	X							
G	M	E	S	S	S	S	Test compounds at 2x (20 µM)											S	S	S	S	X	X								
H	M	E	S	S	S	S												S	S	S	S	S	S	S	S	S	S	S	S	X	X
I	M	E	S	S	S	S												S	S	S	S	S	S	S	S	S	S	S	X	X	
J	M	E	S	S	S	S												S	S	S	S	S	S	S	S	S	S	S	X	X	
K	M	E	S	S	S	S	S	S	S	S	S	S	S	S	S	S	S	S	S	S	S	X	X								
L	M	E	S	S	S	S	S	S	S	S	S	S	S	S	S	S	S	S	S	S	S	X	X								
M	M	E	S	S	S	S	S	S	S	S	S	S	S	S	S	S	S	S	S	S	S	X	X								
N	M	E	S	S	S	S	S	S	S	S	S	S	S	S	S	S	S	S	S	S	S	X	X								
O	M	E	S	S	S	S	S	S	S	S	S	S	S	S	S	S	S	S	S	S	S	X	X								
P	M	E	S	S	S	S	S	S	S	S	S	S	S	S	S	S	S	S	S	S	S	X	X								

Fig 3.8. Plate map for 384 well plate format for high throughput screen. Column 1 represents the Min (M) and column 2 represents the EC₂₀ (E) controls (both light blue). Columns 23 and 24 represent the Max (X) control (pink). Columns 3 to 22 contain sample compounds (S) at 10 µM (final concentration).

	Media	Dye	First dispense		Second dispense	
Format	Volume (µl)	Volume (µl)	Volume (µl)	Conc.	Volume (µl)	Conc.
96 wells	100 (discard)	30	30	2x	20	4x
384 Fluo4-NW	20 (discard)	20	20	2x	10	5x
384 Fluo8	20 (do not discard)	20	10	5x	10	6x

Table 3.1. Comparison of volumes and concentrations dispensed of drugs and controls for the different formats of the screen. First dispense concentrations correspond to controls and drug plates. Second dispense concentrations correspond to EC₁₀ OT.

F127 Plus (component B), 90ml of 1X HBSS and 1ml of Tryptan red dye. Both solutions could be aliquoted and stored at ≤ -20 °C in the dark for at least a month if repeated freeze-thaw cycles were prevented. The Fluo-8 NW dye-loading solution for one cell plate was made by adding 20 μ l of DMSO reconstituted Fluo-8 NW stock solution into 10ml of 1x assay buffer, mixing them well. This work solution was stable for at least 2 hours at RT avoiding light. The remainder of the dye working solution could be aliquoted and frozen at ≤ -20 °C in the dark indefinitely.

Cell preparation. Media from plated cells (see cell plating section) was kept in the wells and 20 μ l of dye working solution was added. Cells were incubated with the dye for 1 h at 37 °C and then for 30 min at RT in the dark.

Dose response curves and controls preparation. Dose response curves were generated for OT, AVP, carbetocin, and compound 39. The 16-point curves were prepared as 10x serial dilutions for each compound with initial concentrations starting at 10 μ M and 3 μ M. Each point was plated four times, plating as shown in Fig 3.9. The working concentrations to make the plate were 5x.

Fluorescence-based intracellular calcium mobilization assay using the Fluo-8 dye. Assays were conducted as described above with the following minor modifications: 10 μ l for the 5x compound solutions (first dispense) and 10 μ l for the OT at 6x of EC₂₀ (second dispensed) (see Table 3.1.). The SOP for this assay is represented in Figure 3.6. Data was collected and analyzed in the same manner as for the 96 and 384 well plate format.

	Controls	OT	AVP	Carbetocin	Compound 39	Controls
Row	1-2	3-6	7-10	11-14	15-18	23- 24
A	Max	0.0003nM	0.0003nM	0.0003nM	0.0003nM	Min
B	Max	0.001nM	0.001nM	0.001nM	0.001nM	Min
C	Max	0.003nM	0.003nM	0.003nM	0.003nM	Min
D	Max	0.01nM	0.01nM	0.01nM	0.01nM	Min
E	Min	0.03nM	0.03nM	0.03nM	0.03nM	B
F	Min	0.1nM	0.1nM	0.1nM	0.1nM	B
G	Min	0.3nM	0.3nM	0.3nM	0.3nM	B
H	Min	1nM	1nM	1nM	1nM	B
I	B	3nM	3nM	3nM	3nM	Min
J	B	10nM	10nM	10nM	10nM	Min
K	B	30nM	30nM	30nM	30nM	Min
L	B	100nM	100nM	100nM	100nM	Min
M	Max	300nM	300nM	300nM	300nM	Max
N	Max	1 μ M	1 μ M	1 μ M	1 μ M	Max
O	Max	3 μ M	3 μ M	3 μ M	3 μ M	Max
P	Max	10 μ M	10 μ M	10 μ M	10 μ M	Max

Fig 3.9. Map plate for validation of Fluo-8 NW dye for 1536 well plate format.

The concentrations of all compounds are expressed as final; they were all prepared as 5x in the dispensing plate. Columns 1, 2, 23, and 24 are reserved for controls that will be run during the HTS.

Comparison between a chemiluminescent assay and the FLIPR^{TETRA}[®] system fluorescence cell-based assay for identification of hOTR agonists and positive allosteric modulators. The PathHunter[™] CHO-K1 OTR β -Arrestin Cell Line was used with the PathHunter Detection Kit. This technology was tested in a 96 well plate format in collaboration with the Center for Integrative Chemical Biology and Drug Discovery at UNC.

PathHunter[™] cell line culture. The PathHunter CHO-K1 OTR β -Arrestin cell line was obtained from the manufacturer. They were grown in media that consists of Hams F-12, 300 μ g/ml hygromycin, 800 μ g/ml geneticin sulfate (G418), 10% fetal bovine serum, and 1x penicillin/streptomycin/glutamine, following the manufacturer's instructions. The cell line was incubated at 37°C and 5% CO₂ in 75cm² flasks until 70% confluency was reached. At that point, they were either passaged to new flasks to allow expansion of growing cells or they were plated to be used in the assays. Cells were incubated with 0.05% Trypsin –EDTA at 37°C for 5 minutes for dissociation.

Cell plating. Cells were seeded at 20,000 cells/ well in 90 μ l of complete medium in white-walled with clear bottom, 96-well plates and incubated overnight @ 37°C and 5% CO₂ to allow adherence to plate.

Drug plate preparation. OT, vasopressin, carbetocin, compound 39, and NSC 42414 were dissolved in DMSO to a concentration of 1mM. A dose response curve

of 12 points was run for each compound. Each concentration was prepared as a 10x solution of the desired final concentration. DMSO concentration did not exceed 1% in the final reaction volume. The dilution scheme for the curve was 2x and 10x intercalated dilutions, starting with 500 μ M, as shown in fig. 3.10. The OT EC₁₀ concentration was 0.05nM. All the dilutions were made in HBSS.

Dye preparation. The detection reagent was prepared from the kit components as specified by the manufacturer. In short, 1 part of Gal substrate was added to 5 parts of the Emerald solution and 19 parts of HBSS. This mix was kept at RT in dark for the day of analysis. The remainder of the dye was aliquoted and stored at -20°C to be used later.

Chemiluminesce-based intracellular enzyme fragment complementation assay.

Cells were incubated with 10 μ l per well of the compounds' dilutions for 90 minutes at 37°C. The positive allosteric modulator was added 10 min prior to adding OT at EC₁₀. Detection reagent (50 μ l) was added to each well to incubate at RT for 60 minutes. Cell plates were read on an Envision standard luminescence plate reader (PerkinElmer, Boston, MA). Each plate (see layout in fig 3.10.) was prepared and read by duplicate.

	1	2	3	4	5	6	7	8	9	10	11	12
Cc. (μM)	50	10	5	1	0.5	0.1	0.05	0.01	0.005	0.001	0.0005	0.0001
A-B	Oxytocin											
C	Vasopressin											
D	Carbetocin											
E	Compound 39											
F	Allosteric potentiator											
G	OT EC ₁₀						Max. OT					
H	Buffer						OT EC ₁₀					

Fig 3.10. Map plate for validation of PathHunter Detection Technology. All compounds were tested at the same concentrations (expressed here in μM). These are expressed as final, but they were all prepared as 10x. Rows G and H were used for controls: OT EC₁₀, 0.05nM and Max OT at 50 μM .

RESULTS AND DISCUSSION

The impact that the OT system is currently having in the involvement in neuropsychiatric diseases and the potential that OT is presenting as a therapeutic tool, poses an vital need to obtain analogs of this hormone that will present more advantages than this natural ligand (see chapter 1). The validation and optimization of a HTS protocol will provide a robust tool for the identification of agonists and positive allosteric modulators of this receptor. The current literature does not report any effort to screen for modulators of the OTR; hence our work will provide new molecules as well as new tools for the development of this field.

Validation of fluorescence-based intracellular calcium mobilization assay for the identification of hOTR agonists and allosteric modulators in a 96 well-plate format.

The NIMH Psychoactive Drug Screening Program, directed by Dr. Bryan Roth at UNC, has established a fluorescence-based assay in a 96 well plate format that reports Ca^{2+} release after stimulation of the hOTR. The assay utilizes CHO cells stably transfected with the human OT receptor. A typical assay with this cell line generated a Z' factor of 0.6, with a CV% below 10, a S:B ratio above 5 and a significantly low plate-to-plate and day-to-day variability. In the past, the assay has been used to evaluate OT receptor antagonists primarily for counter screening purposes.

Our efforts focused on further validating the assay for high throughput screening to identify positive allosteric modulators and agonists of the human OTR. In a pilot assay, we screened the NCI Diversity Set, 1990 compounds, and identified 25 compounds (1.25% success rate) that show a 50% or more increase of normalized % activation in duplicate assays. We found that 15 compounds acted as agonists and 10 as positive allosteric modulators. Tables 3.2. and 3.3. show a complete list of confirmed active agonists and positive allosteric modulator. Ergosterol was identified as a hit serving as a *de facto* positive internal control as cholesterol and its analogs have been demonstrated to be positive allosteric modulators of the hOTR [42, 44, 50, 264, 265]. Figure 3.11 shows a representative plate map for this 96 well plate format (3.11.A.) and the scatter plot for the complete library screen (3.11.B.). Figure 3.12. shows the dose response curve for OT that we have reproduced from the literature with a similar EC_{50} of 0.4nM [17]. This data shows that the screen can be implemented for the identification of agonists and positive allosteric modulators of the hOTR in a low-throughput format as 96 wells per plate.

Optimization of fluorescence-based intracellular calcium mobilization assay for the identification of hOTR agonists and allosteric modulators for a 384 well-plate format.

In order to be able to screen larger, more diverse libraries, we shifted our efforts in optimizing the OTR assay in a 384 well plate format. This format affords an assay compatible with libraries of more than 20,000 compounds. To successfully

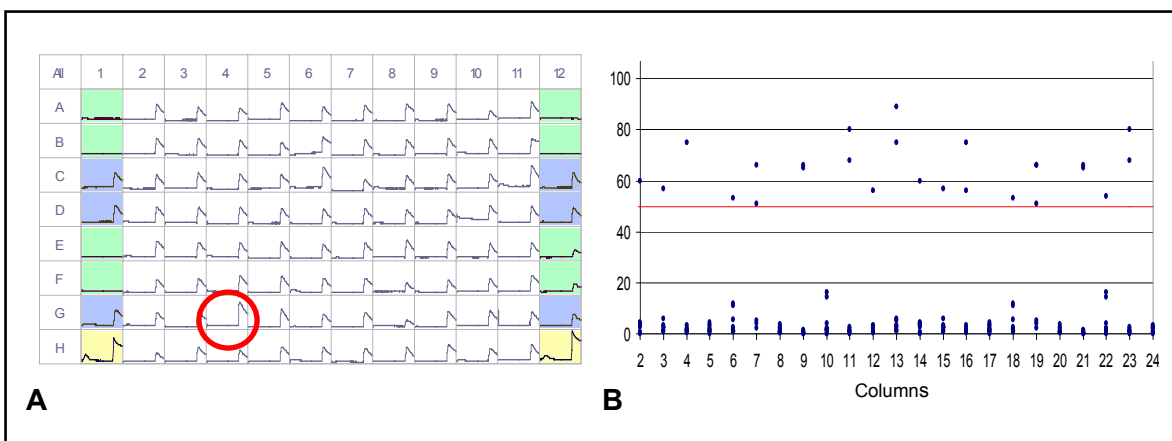


Figure 3.11. Screen of NCI Diversity Set revealed agonists and positive allosteric modulators. A. Representative plate from screen in a 96 well plate format. Plate controls were loaded in columns 1 and 12. Max control (yellow) is OT at 100nM. Min control (green) is no OT. EC₄₀ control (blue) is OT at 0.1nM. A prospective positive allosteric modulator that has a 67% signal increase is shown (red circle). **B.** Scatter plot of entire 1990 compound library screen.

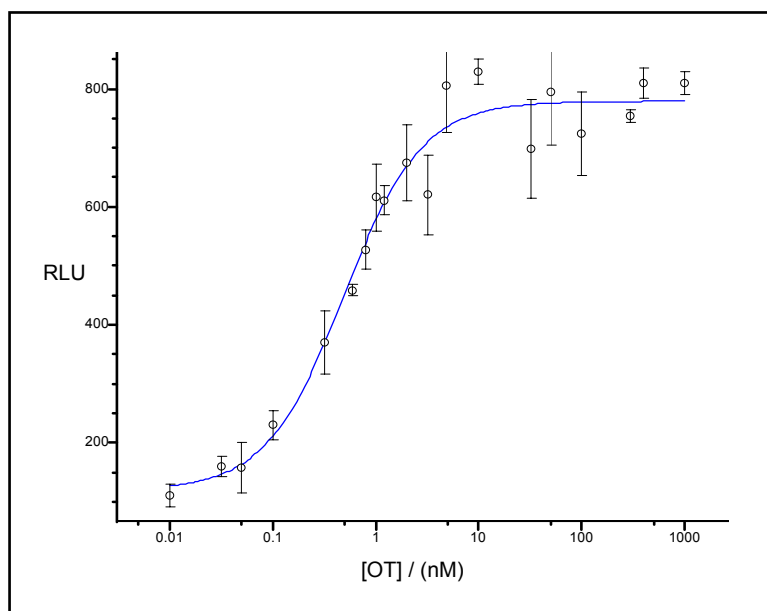


Figure 3.12. Dose response curve for activation of the hOTR in a 96 well plate format. The EC₅₀ for OT is 0.4 nM.

scale up the assay, we optimized cell culture and density, DMSO tolerance, readout variability, reagent volumes and the standard operating protocol. The BRITE Center provided the Prestwick chemical library that contains 1120 small molecules, 90% being marketed drugs and 10% bioactive alkaloids or related substances, and thus it presents the greatest possible degree of drug-likeness.

Our first efforts concentrated in optimizing cell culture and plating. We compared keeping our cells frozen immediately before plating vs. passing them throughout the screening process. We also determined optimal plating conditions. We found out that cells that have been kept in liquid nitrogen, thawed and plated the day before the screen, did not respond consistently; therefore a passage-plate scheme was developed to ensure optimal cell condition and number for every day of the screen. Cell plate treatment was also investigated to ensure that pretreatment of the plates (poly-D-Lys or gelatin) did not interfere with the health and/or attachment of the cells. Fig 3.13.A, C, and D summarizes our findings. We found that cells needed to be grown continuously at 37°C and plated in tissue culture (TC) treated plates without any further treatment. Frozen cells do not attach evenly to the bottom of the wells. Also, the use of poly-D-Lys treated plates prevented the cells from attaching to the wells (data not shown). Fig 3.13.A. also shows the optimal cell density per well for a 384 well plate format. We chose to plate between 12,500 and 15,000 cells per well. Tolerance to DMSO was also investigated to assess the maximum final concentration allowed for the screen. Fig 3.13.B. shows that DMSO final concentration should not exceed 1.25 %.

Dose response curves for OT and a small molecule oxytocin antagonist, L-

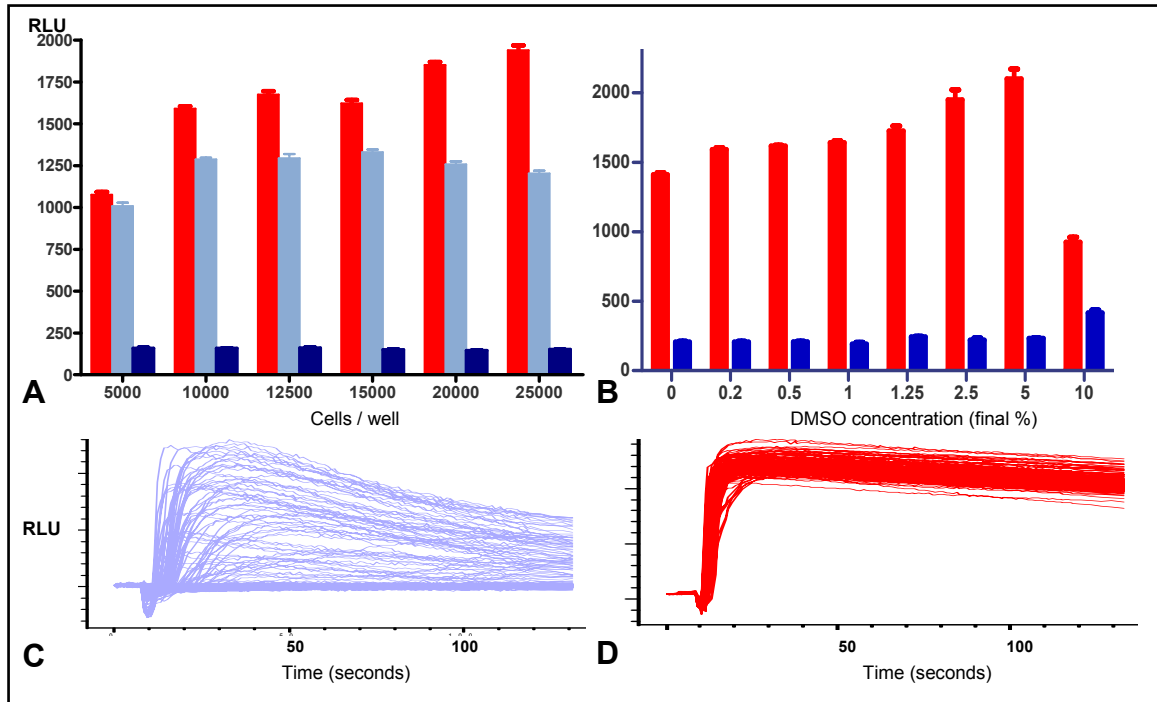


Fig 3.13. Optimization of cell conservation and plate treatment for a 384 well plate format. **A.** Maximum signal of frozen cells (red) vs. cells grown at 37°C (light blue signal= max., blue= min.). Incubated cells show a maximum and stable signal at 1250 RLU. Frozen cells show an increasing signal even at 25000 cells per well, when cells are over grown. Max signal: [OT] =100nM. **B.** Max signal of OT (red) and min signal (blue) in increasing DMSO concentrations **C.** Cells plated in poly-D-Lys plates (light blue) show a CV of 90%. **D.** Cells plated in TC plates (red) have a CV of 12% at maximum response OT concentration. Max. response OT concentration = 100nM.

371,257 (Tocris Bioscience, Ellisville, MO) were used to further validate the assay. The EC_{50} obtained for OT was 0.19nM and the IC_{50} calculated for the antagonist was 7.9nM, both values are in concordance with the literature [17, 266] (Fig 3.14.). We screened the Prestwick chemical library to assess reproducibility of the assay. All plates were run in duplicates. Compounds were considered active if the average of both readings exceeded 50% normalized activation. From a pool of 1,100 compounds, we found 12 compounds that showed activation of the hOTR (3 agonists and 9 positive allosteric modulators). The hit rate for this case was 1.09% and the Z' score was 0.71 [267]. Tables 3.2. and 3.3. show a complete list of active agonists and positive allosteric modulator confirmed hits. From this data we concluded that the assay is optimized for screening in a 384 well plate format.

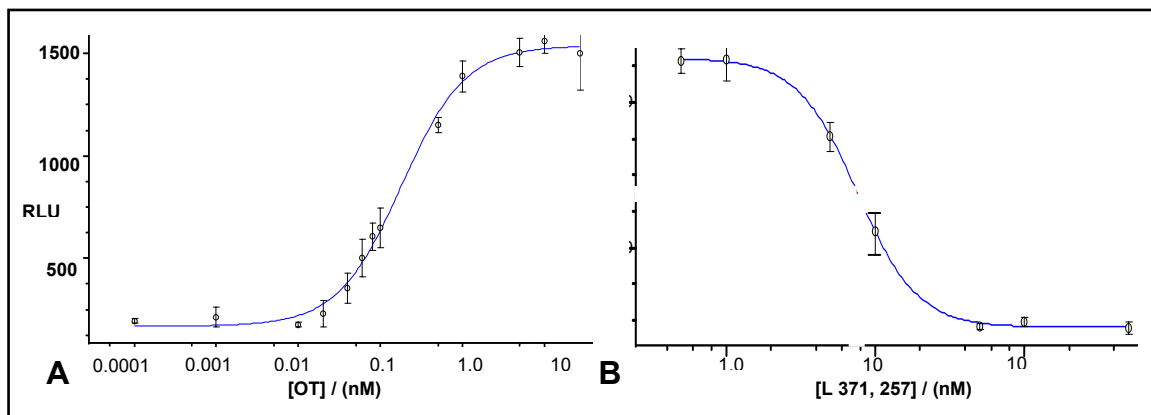


Fig 3.14. Dose response curves for OT and L 371,257, a selective OT antagonist in the 384 well-plate format. A. The EC_{50} for OT was 0.19 nM (data point in triplicate). **B.** The IC_{50} for the antagonist was 7.9 nM (data points in quadruplicate). [OT] = 100 nM.

Execution of medium-throughput screen for the identification of hOTR agonists and allosteric modulators for a 384 well-plate format.

The Asinex Gold library was screen in 384 well plates. On every plate, we included positive (OT maximum concentration and OT at EC₂₀) and negative (no OT) controls to allow Z' calculations as well as normalized % activation of the compounds screened (see methods section). Fig 3.15. shows raw data from the screen, as well as individual profiles of the controls, hOTR agonists, and positive allosteric modulators.

For this first instance of the screen, 132 compounds showed an increase in direct normalized activation of $\geq 50\%$ (agonists), and 18 were identified as potential positive allosteric modulators. The hit rate was 0.52% and the Z' was 0.69. To confirm these hits, a duplicate was run for the 132 compounds. The normalized activation was reproduced only for 6 compounds, decreasing the hit rate to 0.02%. Tables 3.2. and 3.3. show a complete list of active agonists and positive allosteric modulator confirmed hits.

Hits obtained from the three libraries were investigated to assess if they presented any inconvenient to allow validation. We searched the literature available, mainly through PubChem and ChemFinder, to obtain any information on these compounds. The criteria to discard hits included toxicity, high molecular weight, fluorescence (giving false positives), druglikeness, Lipinski's rule of five evaluation, known biological activity, derivation feasibility, etc. The hits that passed these selection criteria were then validated for the hOTR (see chapter 4).

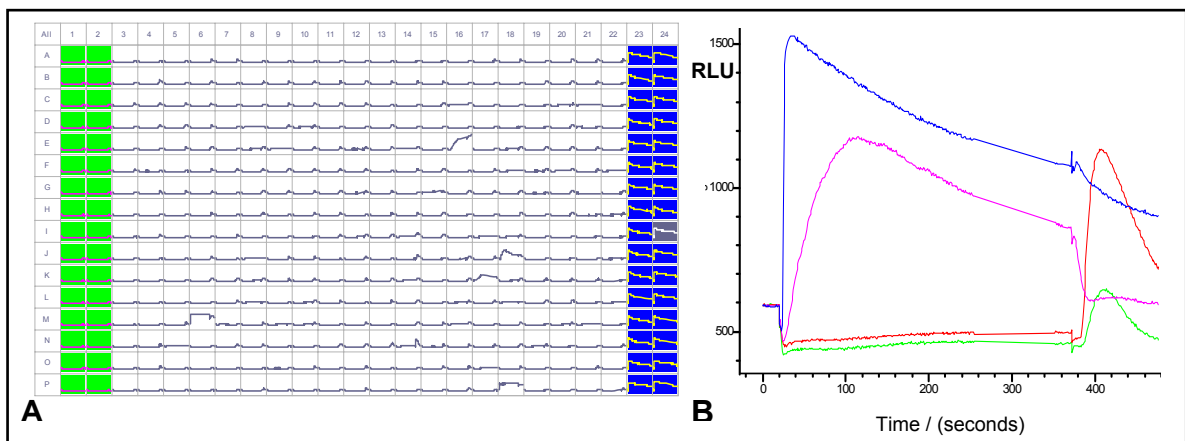


Figure 3.15. Multi-well graph from agonists and positive allosteric modulators screen displaying controls location and kinetic profiles. A. The green wells represent the negative and EC₂₀ (OT at 0.20nM) controls and the blue wells represent OT at maximum response (100nM). CV= 8%. B. Kinetic profile for controls, agonists, and positive allosteric modulators of hOTR. Positive controls are shown: OT at maximum response (100nM) (blue) and OT at EC₂₀ (0.25nM) (green). The magenta line represents the profile for an agonist and the red line shows a profile for a positive allosteric modulator of the hOTR. Normalized % hOTR activation is 65%, and 56% respectively.

Library	Compound ID	Normalized % Activation	
NCI Diversity Set	NSC 13768	137	
	NSC105550	138	
	NSC 108944	152	
	NSC 112675	137	
	NSC 40016	140	
	NSC 305743	145	
	NSC 204936	164	
	NSC 347512	135	
	NSC 54278	146	
	NSC 62594	146	
	NSC 201430	157	
	NSC 88947	139	
	NSC 62791	162	
	NSC 69573	144	
	NSC 371876	163	
	NSC 63875	158	
	Prestwick	PWK432932 (Oxethazaine)	61
		PWK433161 (Spiperone)	109
PWK433795 (Thonzonium bromide)		65	
Asinex	BAS 02532822:831592	61	
	BAS 02331893:830669	61	
	BAS 03008198:831063	70	
	ASN 03368019:834900	70	
	BAS 00411435:826486	96	

Table 3.2. Confirmed hits that showed agonistic behavior for the human OTR.

Library	Compound ID	Normalized % Activation
NCI Diversity Set	NSC 42414	166
	NSC 14343	139
	NSC 626629	148
	NSC 166395	150
	NSC 195952	155
	NSC 191411	145
	NSC 13970	143
	NSC 103779	131
	NSC 67690	149
	Prestwick	PWK-433179 clemastine fumarate
PWK-433335 metrizamide		51
PWK-433411 thiocolchicoside		52
PWK-433557 lycorine hydrochloride		55
PWK-433379 quercetine dihydrate		82
PWK-433558 karakoline		56
PWK-433751 niacin		56
PWK-433796 Idazoxan hydrochloride		50
PWK-433604 Metoprolol tartrate		54
Asinex	ASN 05588520:820716	65

Table 3.3. Confirmed hits that showed positive allosteric modulator behavior for the human OTR.

Implementation of Fluo-8 No Wash Calcium Assay Kit for the fluorescence-based intracellular calcium mobilization assay for the identification of hOTR agonists and allosteric modulators for a 384 well-plate format.

The validated and optimized fluorescence-based assay let us plan for a high-throughput screen campaign. Our resources, including available libraries and robotic hardware, did not allow us to perform the screen at a larger scale, i.e. screen 100,000's compounds. In order to fulfill our needs to screen a structurally more diverse array of compounds, we recruited the services of the Molecular Libraries Probe Centers Network (MLPCN). This center is a part of the NIH's Molecular Libraries Initiative (MLI). It comprises 5 specialty centers that are part of the NIH's strategic funding plan, the Roadmap Initiative. The Scripps Research Molecular Screening Center (SRMSC) is dedicated to the discovery of new molecular probes. This center accepted our assay to identify agonists and positive allosteric modulators of the oxytocin system (application number: 1 R03 MH 085678-01A1). The assay was transferred to the SRMSC to be recapitulated and miniaturized to 1536-well format.

Transferring the screen to the SRMSC required several steps towards optimizing the screen; mainly performing the screen without the need to remove the cell culture media before dye addition (homogeneous assay). According to the manufacture's instructions, the dyes that we have used in the past required removal of cell culture media before addition of it to the cells. We validated the use of a homogeneous assay following the NCGC Assay Guidance Manual [268]. We also

validated the Vasopressin (V_{1a}) receptor counterscreen and provided control compounds to be implemented in their screening campaign.

Our developed SOP was retested using the Screen Quest™ Fluo-8 No Wash Calcium Assay Kit to validate a homogeneous primary hOTR assay. Table 3.4. contains the assay statistics for this no-wash assay that is amenable for HTS. Plate-to-plate and day-to-day variability was within accepted values as OT EC_{50} values did not shift more than 2-fold between plates or between any given days. The same variability was found for AVP in the counterscreen. The DMSO tolerance for this assay was up to 1.25% final DMSO concentration for the CHO-hOTR assay. The tolerance for the CHO-h V_{1a} assay was up to 1% as shown in Fig. 3.16. The EC_{50} values for the agonists OT and AVP were also reported.

To facilitate the HTS, an appropriate agonist concentration needed to be validated for the primary screen of positive allosteric modulators. In addition, control compounds had to be provided to determine the adequate HTS assay controls. Four compounds were chosen to be tested: OT; AVP; carbetocin, a commercially available peptide-based OTR agonist; and compound 39, one of the two reported small molecule OTR selective agonists [204]. Figure 3.17. shows representative dose response curve for these control compounds for hOTR (3.17.A.) and h V_{1a} R (3.17.B.). Representative plate-based statistics for these compound controls were also provided (Tables 3.5. and 3.6.).

The statistical analysis obtained for the implementation of the Screen Quest™ Fluo-8 No Wash Calcium Assay Kit provided the robust data required by the SRIMSC in order to initiate the miniaturization process to a 1536 well format. At this

point in time, the assay transfer has been completed and the assay implementation is waiting in their pipeline. Updates will be provided as soon as they become available. The screening center anticipated that this screen will be completed within 6 months.

	CHO-hOTR		CHO-hV _{1a}	
	Agonist	Potentiator	Agonist	Potentiator
Z'	0.90 ± 0.09	0.85 ± 0.08	0.8 ± 0.1	0.88 ± 0.09
S:B ratio	14 ± 7	10 ± 2	17 ± 5	10 ± 4
CV%				
Max	3 ± 2	idem	5 ± 2	idem
EC ₅₀	5 ± 1	idem	4.3 ± 0.4	idem
EC ₂₀	6.2 ± 0.5	idem	7 ± 1	idem
EC ₁₀	7 ± 1	Idem	5.8 ± 0.3	idem

Table 3.4. Assay statistics for the Screen Quest™ Fluo-8 No Wash Calcium Assay Kit for a homogeneous assay. CHO-hOTR cell line is used for the primary screen. CHO-V1a cell line is used for the counterscreen.

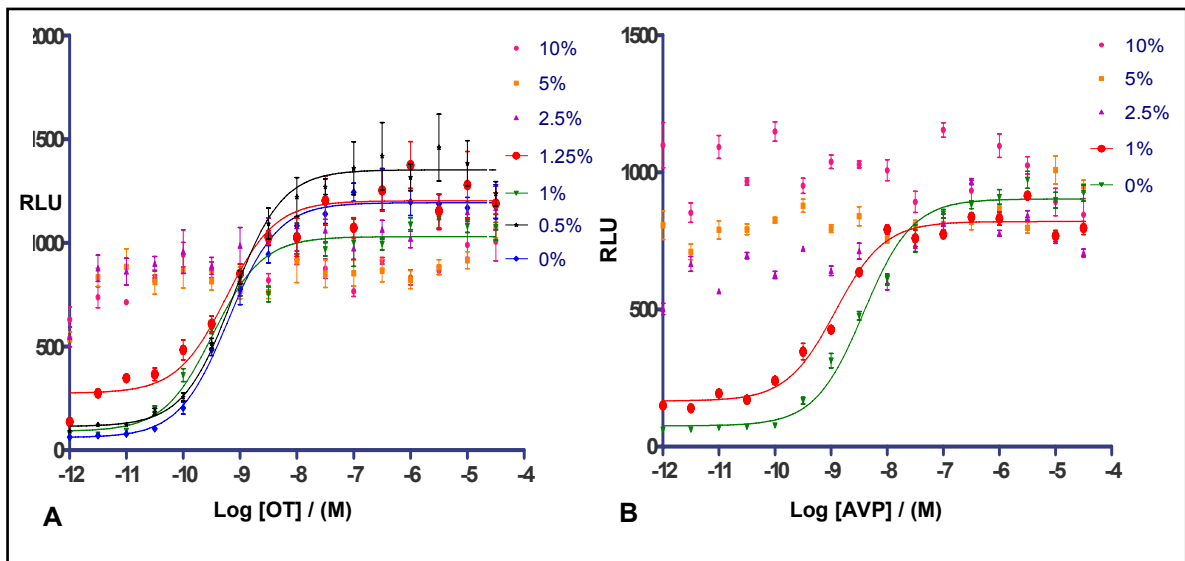


Figure 3.16. DMSO Tolerance for a 384 well plate format using a Screen Quest™ Fluo-8 No Wash Calcium Assay Kit for a homogeneous assay. A. Dose response curves of OT diluted in increasing amounts of DMSO for CHO-hOTR. The EC_{50} values for the different DMSO % in parenthesis were: 0.62 (0%), 0.74 (0.5%), 0.33 (1%), and 0.57 (1.25%); all expressed in nM. Higher DMSO % did not a dose-dependent signal. **B.** Dose response curve of AVP diluted in increasing amounts of DMSO for CHO-V1aR. The EC_{50} values for the different DMSO % in parenthesis were: 3.8 (0%) and 1.2 (1%); all expressed in nM. Higher DMSO % did not a dose-dependent signal.

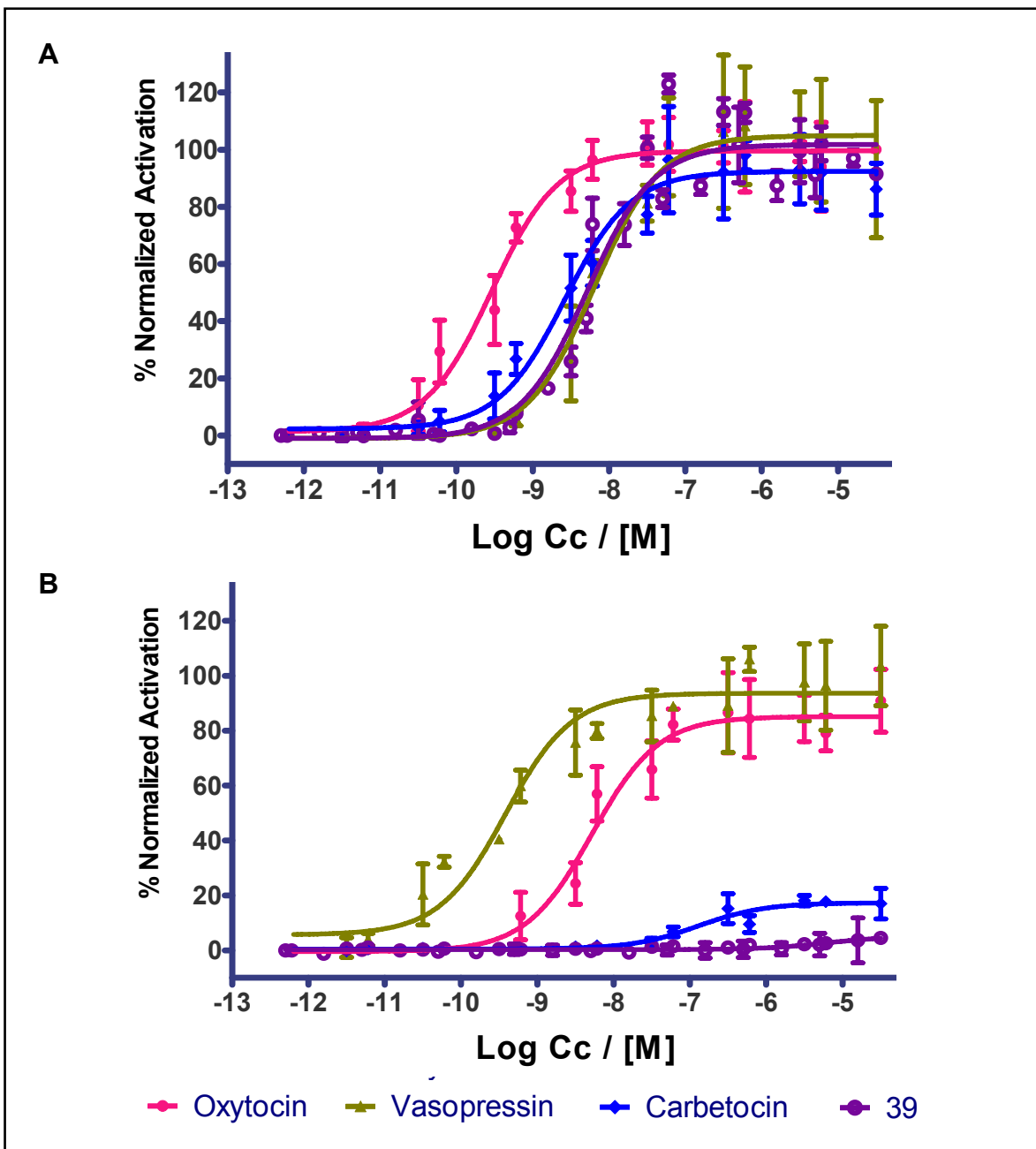


Fig. 3.17. Representative dose response curves for OT, AVP, carbetocin, and compound 39 in the CHO-hOTR (A) and CHO-hV_{1a}R assays using the Screen Quest™ Fluo-8 No Wash Calcium Assay Kit (B). Carbetocin and compound 39 do not activate the V1aR receptor significantly as these compounds are selective for the OTR (B).

EC₅₀ (nM)	hOTR	hV_{1aR}
OT	0.30 ± 0.09	5 ± 2
AVP	5 ± 2	0.3 ± 0.2
Carbetocin	3 ± 1	170 ± 60
Compound 39	5 ± 1	10170 ± 6000

Table 3.5. EC₅₀ values for OT, AVP, carbetocin, and compound 39.

	Oxytocin	Vasopressin	Carbetocin	Compound 39
S:B	17 ± 3	18 ± 4	17 ± 3	18 ± 4
CV%	6 ± 2	8 ± 5	11 ± 3	11 ± 5
Z	0.8 ± 0.1	0.7 ± 0.2	0.6 ± 0.1	0.6 ± 0.2

Table 3.6. Representative plate-based statistical data for controls.

Comparison between a chemiluminescent assay and the FLIPR^{TETRA®} system fluorescence cell-based assay for identification of hOTR agonists and positive allosteric modulators.

GPCR activation can be measured using a vast number of methods. Most of the drug discovery industry is focused on quantifying this activation through the use of the well implemented fluorescence cell-based assay FLIPR^{TETRA®} system. The data that we have collected with the FLIPR^{TETRA®} system was compared to a novel *in vivo* application of the established Enzyme Fragment Complementation technology pioneered by DiscoverRx (Fremont, CA). This technology is based in the direct analysis of GPCR activation via β -arrestin recruitment in a chemoluminescent assay. Attention is focused towards expanding OTR screening repertoire to be able to identify those compounds that escape the detection limits of the well know technologies that are currently being used. DiscoverRx's claim is that the β -arrestin signaling pathway is generic to virtually all GPCRs, and that this signaling occurs irrespective of the G-protein coupling mechanism. Therefore, they have developed the PathHunter[™] Detection kit that is used in conjunction with PathHunter cell lines and ProLabel[™] /ProLink[™] expression vectors inside whole cells. This novel *in vivo* application of the enzyme fragment complementation (EFC) technology promises the detection of transient interactions and improvement of screening throughput. It can be used with any Gi-, Gq-, or Gs-coupled receptor.

A data analysis comparison was done to assess if the PathHunter[™] β -arrestin detection kit provided data as robust as the FLIPR^{TETRA®} system. An assay

validation was performed first to evaluate the reproducibility of the assay. The results are shown in Table 3.7.

To complete the validation of this assay, dose response curves were analyzed for OT, AVP, carbetocin, and compound 39. These OTR analogs' curves were compared to curves obtained on a FLIPR^{TETRA}[®] system (Fig. 3.18.). Table 3.8. shows the potencies and efficacies obtained for these molecules. The dose response curves showed significant differences among the OTR agonists. The efficacies obtained with the DiscoverRx platform, with both cell lines, were considerably reduced when compared to the natural ligand curve. The differences in the maximal responses for the agonists could be explained by functional selectivity (see future plans).

Overall, the comparison between technologies demonstrates that the DiscoverRx platform is compatible with screening the hOTR. Maybe, this technology identifies active compounds that the FLIPR technology does not. On the other hand, the FLIPR technology measures a second messenger downstream from the activated GPCR, allowing for amplification of the quantified signal, therefore leading to more false positive results. This artifact might be eliminated by quantifying the direct recruitment of β -arrestin to the activated receptor. It is important to have in mind that the fused fragments that the protein and the receptor have could modify their native responses, giving another array of false positives.

	FLIPR ^{TETRA} ®	DiscoverX	DiscoverX Express
Z'	0.90 ± 0.09	0.88 ± 0.08	0.86
S:B	14 ± 7	45 ± 8	6.2
CV%			
Max [OT]= 500nM	3 ± 2	12 ± 3	9.0
Min [OT]= 0.005nM	6.2 ± 0.5	25 ± 6	---
Buffer	7 ± 1	8 ± 4	5.3

Table 3.7. Statistical data for the comparison of the PathHunterTM β-arrestin Detection kit and the FLIPR^{TETRA}® system. The DiscoverX column shows the data for the PathHunterTM Cell Lines. The DiscoverX Express refers to the PathHunterTM eXpress β-Arrestin GPCR Kits using the assay-ready, frozen PathHunterTM eXpress cells.

	FLIPR ^{TETRA} [®]	DiscoverX	DiscoverX Express
EC ₅₀ (nM)			
OT	0.30 ± 0.09	23 ± 22	44.7
AVP	5 ± 2	1600 ± 900	2680
Carbetocin	3 ± 1	5 ± 2	5.3
Compound 39	5 ± 1	310 ± 260	480
Efficacy (%)			
OT	---	---	---
AVP	105	41 ± 6	38
Carbetocin	92	32 ± 5	32
Compound 39	102	51 ± 6	48

Table 3.8. Potencies and efficacies of OTR agonists in FLIPR^{TETRA}[®] and DiscoverX systems. Potencies and efficacies of the DiscoverX Express cell lines were run as single points only. Efficacies were calculated considering the OT response as 100%.

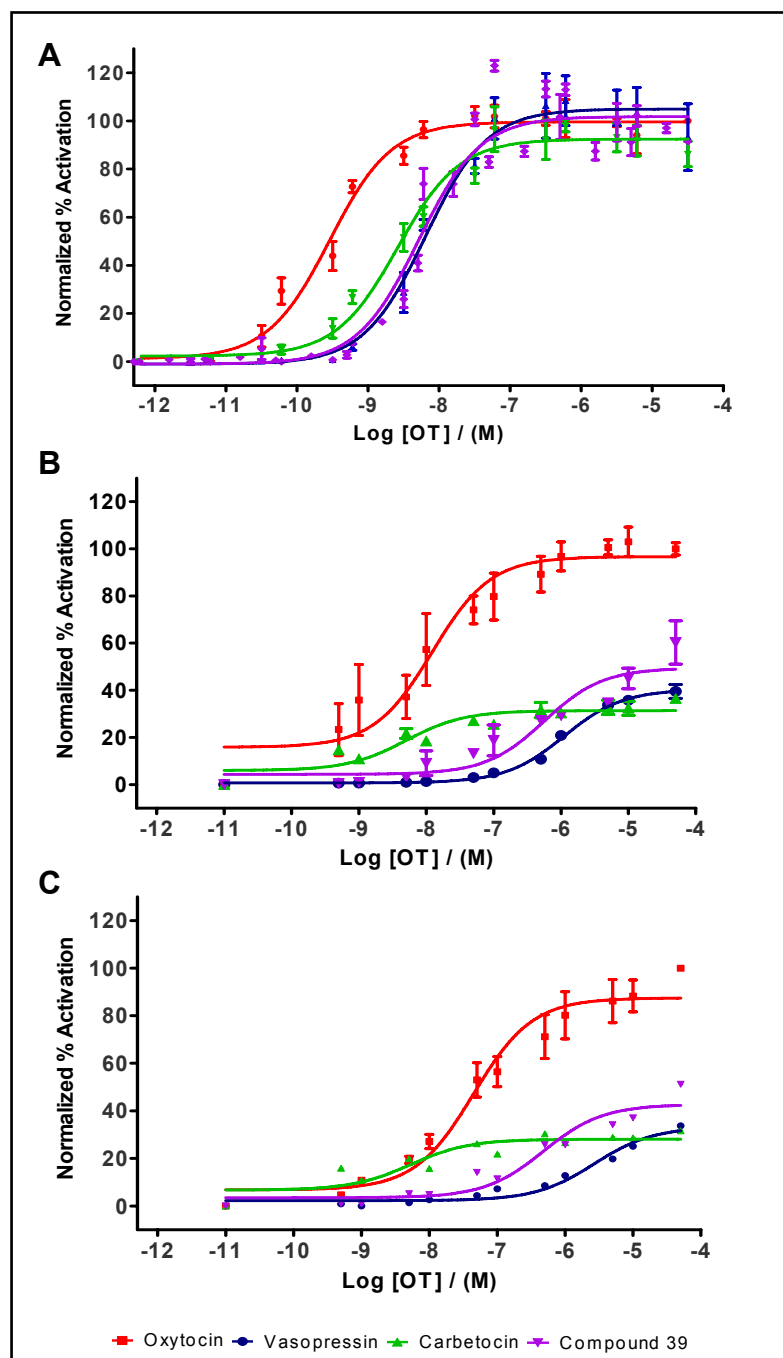


Fig 3.18. Dose response curves for OT, AVP, carbetocin, and compound 39 in the FLIPR and DiscoverRx platforms. A. FLIPR^{TETRA} platform. **B.** PathHunterTM eXpress β -Arrestin GPCR Kit using the PathHunterTM OTR Cell Line **C.** PathHunterTM eXpress β -Arrestin GPCR Kit using the frozen PathHunterTM OTR eXpress cell line.

more accurately the effects of the compounds being tested. Also, our results could be hinting the presence of functional selectivity [271, 272]. In order to validate this hypothesis, direct arrestin translocation with a native receptor will need to be investigated.

FUTURE PLANS

The compounds found to activate the hOTR needed to be validated to discard false positives and non-selective active hits. These procedures will be addressed in chapter 4.

The implementation of the Screen Quest™ Fluo-8 No Wash Calcium Assay Kit for the 384 well plate format was completed successfully. The assay was transferred to the MLPCN and it is in queue for assay implementation, which includes assay recapitulation, miniaturization to a 1536 well plate format, and pilot screening. The primary uHTS campaign will begin immediately following the completion of the assay implementation. According to the center's guidelines, these processes require 6 months for completion. The secondary and tertiary assays (i.e. 'hit confirmation") will be completed within 12 months from assay transfer.

The technology comparison between the FLIPR^{TETRA}® platform and the PathHunter™ β-Arrestin GPCR Kit from DiscoverX brought up interesting questions. Given the independence of this technology with specific G-protein recruitment, our data could suggest that the OTR could signal through multiple G proteins and not be limited only to G_q. There is already some evidence of this promiscuity; therefore further investigation needs to be addressed in the future [269, 270].

The fragment complementation technology signal could be somewhat artificial as the modified β-arrestin recruitment over the 90 minute period could lead to non-specific complementation due to transient translocation. The activation of the receptor in its native form should be investigated. An option would be to follow tagged arrestin as it is recruited to the membrane after receptor activation to assess

CHAPTER 4

VALIDATION OF ACTIVES

INTRODUCTION

A high-throughput screening campaign is a useful first step towards successful target-based drug and chemical tool discovery. This process allows the identification of hundreds of compounds with a specific biochemical or biological activity that is selected for by the type of assay. False positives are inherent to any high throughput screen, so a major task required after identifying initial hit compounds from a screen is to distinguish real “hits” from the false positive artifacts identified by the assay.

In Chapter 3, I identified small molecules that activated the OTR in a fluorescent-based cell assay. The chosen technology measured intracellular Ca^{2+} release as a result of ligand binding to OTR stably expressed in CHO cells. Its concomitant receptor activation, and coupling to the G_q subunit causes a Ca^{2+} release downstream effect. Ca^{2+} release could be non-specific if the compounds tested activate endogenous receptors of the cell line chosen for the assay.

Another common source for false positives is from fluorescent compounds. These molecules present a signal by themselves when dispensed into the wells. Yellow colored compounds show a considerable increase in signal when tested.

Therefore, there is a need to distinguish between true actives that affect OTR and those that generate an irrelevant signal. To overcome this obstacle, dose response curves were tested to discard those compounds that did not show a concentration dependent signal.

The OTR receptor belongs to the vasopressin / oxytocin receptor subfamily of GPCR receptors (see chapter 1) and they display a high degree of sequence identity [17, 18] (see Chapter 1, figures 1.6. and 1.9. for conserved residues and sequences alignment). The endogenous ligands for these receptors (OT and vasopressin (AVP) in humans and rodents) are also highly related peptides [202, 273]. Given this conservation in both peptides and receptors, it is expected that OT and AVP cross react with their receptors. Table 4.1. shows the EC₅₀ of the natural ligands OT and AVP for this subfamily of human receptors.

The objective of this research plan was to identify selective and potent small molecule agonists and positive allosteric modulators of the hOTR. To prevail over the selectivity issue present with the VR family, selectivity counter screens were conducted with the three vasopressin receptors subtypes mentioned above. Dose response curves of the active compounds were assayed against V_{1a}, V_{1b}, or V₂ receptors stably transfected CHO cells to assess efficacy and potency against these receptors in comparison with the OTR.

Quantification of IP₃ species correlates with receptor activation and Gq coupling. To confirm specific activation of the OTR, quantification of the IP₃ species were tested as a response of dose dependent concentrations of the active compounds.

Toxicity assessment is crucial when deciding if a molecule will continue the pipeline of the drug discovery process or it will be discarded. Initial cellular toxicity testing gives some insight into the response the tested molecules will have in the animal testing stage.

The rationale of validating the potential leads that arise from the HTS is supported by a pressing need for small molecules that selectively activate the OT system within the CNS. These small molecules will serve as new chemical tools to elucidate the complex roles for oxytocin in complex behavior, and they will provide new potential leads for a drug discovery campaign in the treatment of specific neuropsychiatric disorders.

	OTR	V_{1a}R	V_{1b}R	V₂R
OT	0.2-0.4	15-20	20	>1000
AVP	5-7	0.2	0.1	180

Table 4.1. EC₅₀ of the natural ligands for the human OT / AVP receptors. The EC₅₀ values are given in nM and have been obtained with fluorescent-based cell assays using the FLIPR[®] Tetra system.

METHODS AND MATERIALS

Materials. All reagents were ACS reagent grade and used without further purification unless otherwise noted. Oxytocin, vasopressin (Sigma), carbetocin (Bachem), and the oxytocin antagonist L-371,251 (Tocris) were purchased in the powder form. Compound 39 was synthesized by the Center for Integrative Chemical Biology and Drug Discovery at UNC-CH. The FLIPR Calcium 4 Assay Kit (Molecular Devices) was used for the fluorometric assays. The NCI Diversity set was obtained from the Developmental Therapeutics Program of the NCI/NIH's repository. The Prestwick and the Asinex Gold Libraries were provided by the Biomanufacturing Research Institute and Technology Enterprise (BRITE Center at NCCU). The stably transfected CHO-hOTR, CHO-V_{1a}, CHO-V_{1b}, CHO-V₂, and CHO wild type cells were kindly provided by the NIMH Psychoactive Drug Screening Program at UNC-CH. the HEK 293 cell line was purchase from the UNC Tissue Culture Facility. The reagents used for cell culture were purchased from Gibco-Invitrogen.

Efficacy and counter screens

Cell culture. For the efficacy assay, stably transfected CHO-hOTR cells were grown in OT/V_{1a} media that consists of: Hams F-12, 400 ug/ml geneticin sulfate (G-418), 10% calf serum, 15 mM HEPES, and 50 U of penicillin/ 50 µg of streptomycin. For the counter screens, stably transfected CHO-h V_{1a}R cells were grown in OT/V_{1a} media that consists of: Hams F-12, 400 µg/ml geneticin sulfate (G-418), 10% calf serum, 15mM HEPES, and 50 U of penicillin/ 50µg of streptomycin. Stably

transfected CHO-h V_{1b}R and CHO-h V₂R cells were grown in V_{1b}/ V₂ media that consists of: Hams F-12, 150µg/ml zeocine, 10% calf serum, 15mM HEPES, and 50 U of penicillin/ 50 µg of streptomycin. Wild-type CHO cells were grown in COS/HEK media that consists of: DMEM, 10% fetal bovine or calf serum, and 50 U of penicillin/ 50 µg of streptomycin. Cell lines were incubated at 37°C and 5% CO₂ in 75 cm² flasks until 80% confluency was reached. At that point, cells were either passaged to new flasks to allow expansion of growing cells or were plated for assays. Cells were incubated with 0.05% Trypsin –EDTA at 37°C for 5 minutes for dissociation. The stably transfected CHO-hOTR cell line was used in the assays until they have reached a passage number of 20, after which they were discarded as they started to show a decrease in response, maybe due to receptor expression inefficiency. In this case, a new badge of fresh cells was grown from cells stored in liquid nitrogen.

Cell plating for efficacy assay. Stably transfected cells were plated on uncoated 96 well tissue culture polystyrene plates (Greiner Bio-one, Monroe, NC). The plating densities were 40,000 cells/well in 100 µl of media. Cells were incubated at 37°C and 5% CO₂ for 18-24 hours before assays to allow cells to adhere.

Dye preparation. The FLIPR Calcium 4 Assay Kit (Molecular Devices) was used for secondary screens. The dye (component A) was prepared according to the manufacturer instructions. Component A was dissolved in 10 ml of 1x Hanks' Balanced Salt Solution and 20 mM HEPES, pH 7.4. This stock solution is stable at - 20 °C for several months. The working solution of the dye was prepared daily by

dissolving 1ml of the stock solution in 30 ml of assay buffer made as follows: 1x HBSS (138 mM NaCl, 5.3 mM KCl, 1.3 mM CaCl₂, 0.49 mM MgCl₂, 0.41 mM MgSO₄, 0.44 mM KH₂PO₄, and 0.34 mM Na₂HPO₄), 20mM HEPES, 2.5 mM Probenecid, corrected to pH 7.4 with NaOH 10 N. The dye working solution was kept in the dark at room temperature or 37 °C throughout the day.

Cell preparation. Media from plated cells was aspirated and replaced with 30ul of fresh dye working solution. Cells were incubated with the dye for 45 min at 37 °C and then at RT in the dark for another 15 min.

Controls and active compounds' dose response curve preparation. OT, AVP, compound 39 and all the actives found during the screening campaign were obtained in powder form from their respective sources. The powders were dissolved in DMSO to generate a 1mM solution. Dilutions of prospective agonists and controls for the first addition of the protocol were made in assay buffer as 2x stocks. The final DMSO content was below 1%. Dilutions of prospective modulators and controls for the second addition of the protocol (including OT at EC₂₀) were made in assay buffer as 4x stocks. Controls were added to each plate; they included OT (efficacy) or AVP (counter) at maximum response and at EC₂₀, and the assay buffer as a negative. Eight point dose response curves were done for each compound confirmed in the HTS to obtain EC₅₀ values. Ten-fold serial dilutions of a 50µM stock solution were prepared and each concentration was plated by triplicate.

Fluorescence-based intracellular calcium mobilization assay. A FLIPR^{TETRA}® system (Molecular Devices, Sunnyvale, CA) was used to read fluorescence (excitation wavelength: 470-495 nm, emission wavelength: 515-575 nm) in each well every 1 s for 30 sec, to establish a baseline reading. After this period, the FLIPR^{TETRA}® transferred 30 µl of the 2X compound solution from the compound plate to the cell plate (first addition). These readings were made every 1s for 5 min to validate hOTR agonists. A second dispense transferred 20 µL of 4x OT (or AVP for the counter screens) at the EC₂₀ from the OT (AVP) plate to the cell plate, and readings were made every 1 s for 3 min. This portion of the assay was designed to validate hOTR positive allosteric modulators. The SOP for this assay is represented in Figure 3.7. Each dose response curve was obtained from duplicate data points.

Data collection, analysis, and interpretation. Data was collected using ScreenWorksTM 2.0.0.22 software (Molecular Devices) and analyzed using Graph Pad Prism 5 for Windows. Each kinetic trace was normalized to the initial fluorescence intensity to correct for loading of the cells and was reported as percent normalized activation. Percent normalized activation was calculated as (sample value – min control value) / (max control value – min control value) * 100. For agonist calculations (first dispense), the no OT (AVP) control was used as the minimum control. For the positive allosteric modulator calculations, the minimum control was the value obtained for OT (AVP for counter screen) at EC₂₀. The maximum control was OT (or AVP) at maximum concentration for both calculations. The equation to fit the data was $Y=100/(1+10^{((\text{LogEC}_{50}-X)*\text{Hill Slope}))}$ (obtained

from Graph Pad Prism 5 for Windows). Only compounds that presented EC₅₀ in the low µM range were tested further. Any compound that showed significant % normalized activation in wild-type CHO cells were discarded as the calcium response measured was not specific to the activation of the receptors studied.

SPA PIP₂ Hydrolysis assay

Cell culture for the SPA assay. Stably transfected CHO-hOTR cells were grown in media that consists of: DMEM supplemented with 5% dialyzed FBS and 50 U of penicillin/ 50 µg of streptomycin. Culture of this cell line was done as explained in the previous subsection.

Cell plating. Stably transfected cells were plated on uncoated 96 well tissue culture polystyrene plates (Greiner Bio-one, Monroe, NC). The plating density was 30,000 cells/well in 100 µl of media. Cells will be incubated at 37°C and 5% CO₂ for an additional 24 hours before starting the assay (day 1).

SPA assay. [³H] inositol phosphates accumulation was detected using a scintillation proximity assay.

Day 2. Growth media was replaced by 100 µl of inositol-free BME (supplemented with 5% dialyzed FBS and 50 U of penicillin/ 50 µg of streptomycin) and incubated again for 1.5 hours at 37°C. Medium was removed and 100 µl of inositol-free BME

containing 5% dialyzed FBS and 0.01 $\mu\text{Ci}/\mu\text{l}$ [^3H] myo-inositol was added. The cells were incubated for an additional 18 hours at 37°C.

Day 3. Working buffer preparation; 1x Hank's balanced salt solution, 11 mM d-glucose (dextrose), 35 mM LiCl, and 0.2% sodium bicarbonate. This buffer was incubated at 37°C for 30 to 60 minutes. Assay: the inositol-free BME was aspirated from the cells and replaced with 100 μl of compounds to be incubated for 1 hour at 37°C. Antagonist dilutions were added 10 min prior to adding the OT dilutions. Assay were terminated by aspiration of the drug solutions from the cells and addition of 30 μl of 50 mM formic acid stop solution followed by incubation for 1 hr at room temperature.

While the cells were lysing, the RNA binding YSi SPA beads (Amersham, CA) were aliquoted by diluting to 2.67 mg/ml in cold H_2O . A volume of 75 μl of the bead slurry was added to each of the 96 wells on the plate and kept on ice. To each of these wells, 30 μl of formic acid supernatant was applied and the plate was then agitated at 4°C for 30 min. The beads were allowed to settle at 4°C for 4 hours and then counted in a Wallac Micro Beta Trilux scintillation counter (Perkin Elmer, Waltham, MA).

Controls and active compounds dose response curve preparation. Eight point dose response curves were done for each compound confirmed in the efficacy assay. Ten-fold serial dilutions of a 100 μM stock solution were prepared and each concentration was plated by triplicate. Controls were added to each plate; they

included OT at maximum response and the assay buffer. All dilutions were made using the working buffer prepared on day 3.

Data collection, analysis, and interpretation. Data was collected using Excel and analyzed using Graph Pad Prism 5 for Windows. Each trace was normalized to the initial count per minute intensity to correct for loading of the cells, and it was reported as % normalized activation. This parameter was calculated as $(\text{sample value} - \text{min control value}) / (\text{max control value} - \text{min control value}) * 100$. The equation to fit the data was shown above. Only compounds that present EC_{50} in the low μM range and complete dose response curves will be tested further.

Cytotoxicity

Cell culture. Human embryonic cells (HEK 293) were grown in DMEM supplemented with 10% FBS and 50 U of penicillin/ 50 μg of streptomycin. These cells were incubated at 37°C and 5% CO_2 in 75 cm^2 flasks until 80% confluency was reached. At that point, they were either passaged to new flasks to allow expansion of growing cells or they were plated to be used in the assays. Cells were incubated with 0.05% Trypsin –EDTA at 37°C for 5 minutes for dissociation.

Cell exposure to test compounds. Cells were plated on uncoated 96 well clear flat-bottom polystyrene tissue-culture plates (Corning). The plating density was 5,000 cells per well in 190 μl of media. The plates were incubated at 37°C in an

incubator with 5% CO₂ for 72 hs. A plate containing only cells was set aside for a no-growth control (day 0). This control plate was incubated at 37°C with 5% CO₂ until cells attached (2-3 hs.). These control cells were immediately fixed as explained below. Two columns in the plate were reserved for the negative control.

Cell fixation. Without removing the cell culture supernatant, 100 µl of cold 10% (wt/vol) trichloroacetic acid was added to each well. The plates were further incubated at 4°C for 1 h. The plates were washed four times with slow-running tap water and excess water was removed. The plates were dried using a blow dryer. At this point the plates could be stored indefinitely at RT.

Cell staining. A sulforhodamine B solution (Sigma) was prepared at 0.057% (wt/v). Each well was dispensed 100 µl of this staining solution. The plates were incubated at RT for 30 min and then quickly rinsed four times with 1% acetic acid to remove unbound dye. The plates were dried using a blow dryer. Stained and dried plates could be stored indefinitely at RT.

OD measurement. To solubilize the protein-bound dye, 200 µl of a 10 mM Tris base solution (pH 10.5) was added to each well. The plates were shaken on a gyratory shaker for 5 min. The OD was measured at 510 nm in a microplate reader.

Controls and active compounds' dose response curve preparation. Ellipticine, compound 39, and all the actives found during the screening campaign were

obtained in powder from their respective sources. The powders were dissolved in DMSO to 1mM. Dilutions of prospective agonists and controls were made in distilled water as 20x stocks. Eight point dose response curves were done for each compound confirmed. Two-fold serial dilutions of a 2 mM stock solution were prepared for each compound and each concentration was plated by triplicate. Ellipticine was used as a positive control and two-fold serial dilutions of a 16 µM stock solution were prepared. Each concentration was plated by triplicate.

Data collection, analysis, and interpretation. Data was collected using Excel (Microsoft) and analyzed using Graph Pad Prism 5 for Windows. The cell-growth control % was calculated as $(\text{sample OD} - \text{day 0 OD}) / (\text{negative control OD} - \text{day 0 OD}) * 100$. From these results, the growth inhibition % was calculated as $100 - \text{cell-growth control \%}$. The equation to fit the data was $Y = \text{Bottom} + (\text{Top} - \text{Bottom}) / (1 + 10^{-(X - \text{LogIC}_{50})})$ (obtained from Graph Pad Prism 5 for Windows). IC₅₀ values were derived from the dose response curves. Compounds that presented a 50% cell-growth inhibition or above were considered toxic and they were discarded for future investigation.

RESULTS AND DISCUSSION

In chapter 3, several compounds were identified in an HTS. Here, we validated their activity. Compound 39 was used as an external control; this is one of only two reported small molecule selective agonists for the hOTR [204]. The pharmacological data available for this molecule is much reduced, so we decided to consider it as an active that has been obtained during the HTS. It underwent all the testing as every active we found. The data for this compound served as controls for the different stages of hit validation and also, we provided a more detailed pharmacological profile of it.

Purified actives were validated in secondary assays including fluorescence-based secondary screens for efficacy and inositol triphosphate release to confirm activation of the hOTR. The next step was to confirm that these compounds did not cause a non-specific calcium release through activation of endogenous receptors present in wild type CHO cells. Next, the remaining actives were tested against $V_{1a}R$, $V_{1b}R$, and V_2R stably transfected CHO cell lines to assess selectivity for the OTR.

Efficacy screen

Dose response curves were done for each compound confirmed in the HTS to obtain EC_{50} and maximum efficacy. Only compounds that presented EC_{50} in the low μM range were tested further. A dose response curve of every hit confirmed during the HTS stage was evaluated. There were 17 agonist-like molecules and 14

positive allosteric modulators that were investigated (see Tables 3.2. and 3.3. in Chapter 3). Figures 4.1. and 4.2. show dose-dependent curves for the available active compounds from the HTS. The compounds BAS 00411435:826486, BAS 02331893:830669, and Lycorine hydrochloride were not available in the purified powder form for purchase therefore they were not tested. For the investigation of positive allosteric modulators, OT was used at the EC₂₀ concentration. The data obtained during the HTS could not be reproduced with the purified form of the following compounds: NSC 42414, karakoline, clemastine fumarate salt, thiocolchicoside, nicotinic acid, idaxozan hydrochloride, and metoprolol. Table 4.2. shows the EC₅₀ values calculated for each compound.

Evaluation of the dose response curves, maximum responses, and EC₅₀ values of the remainder of the compounds rendered 9 agonists that showed satisfactory results to be tested in the next step of the validation pipeline. Some of the agonistic compounds evaluated were discarded because their structures showed possible toxicity (contained As or Ag). Thonzonium bromide was discarded because it acted as a detergent.

Unfortunately, none of the prospective allosteric modulators showed a consistent response in this stage of validation, therefore they were discarded for further investigation. ASN 05588520:820716, NSC 167452, and NSC 120877 showed efficacies of 30% or lower at 10 µM in the dose response curves. Quercetin did not show a dose dependent response; the values at 50 µM were lower than at 10 µM, and all the other points in the curve did not show a response. Because metrizamide showed a very significant variability, it was not considered a true active

and it was discarded. NSC 92893 was discarded as a potential modulator as it had a positive signal when tested for agonistic activity as well.

The OTR / VR system belongs to the GPCR Class I subfamily which is considered to be more challenging when investigating for the identification of allosteric modulators (Dr. Arthur Christopoulos, personal communication). In order to identify positive allosteric modulators for the OTR and VR family, a larger compound library that was more structurally diverse needed to be screened in order to obtain successful hits. We have submitted our screen to the Scripps Research Institute Molecular Screening Center as explained in Chapter 3.

Counter screens

Non-specific Ca²⁺ release in fluorescence-based intracellular calcium mobilization assay. The next step was to confirm that the compounds selected from the efficacy assays did not cause a non-specific calcium release through activation of endogenous receptors present in wild type CHO cells. Figure 4.3 shows the dose response curves obtained for the agonistic-like molecules. Actives that caused a significant Ca²⁺ release in the wild type CHO cell line counter screen were discarded as they did not activate the OTR specifically. NSC 48458 showed a 1.8-fold activation for the CHO-OTR cell line, therefore the signal read was considered to be caused by non-specific calcium release. Only compound 39 showed specific activation of hOTR. More over, this molecule did not produce any Ca²⁺ release, even at 100 μ M. This compound was the only candidate that

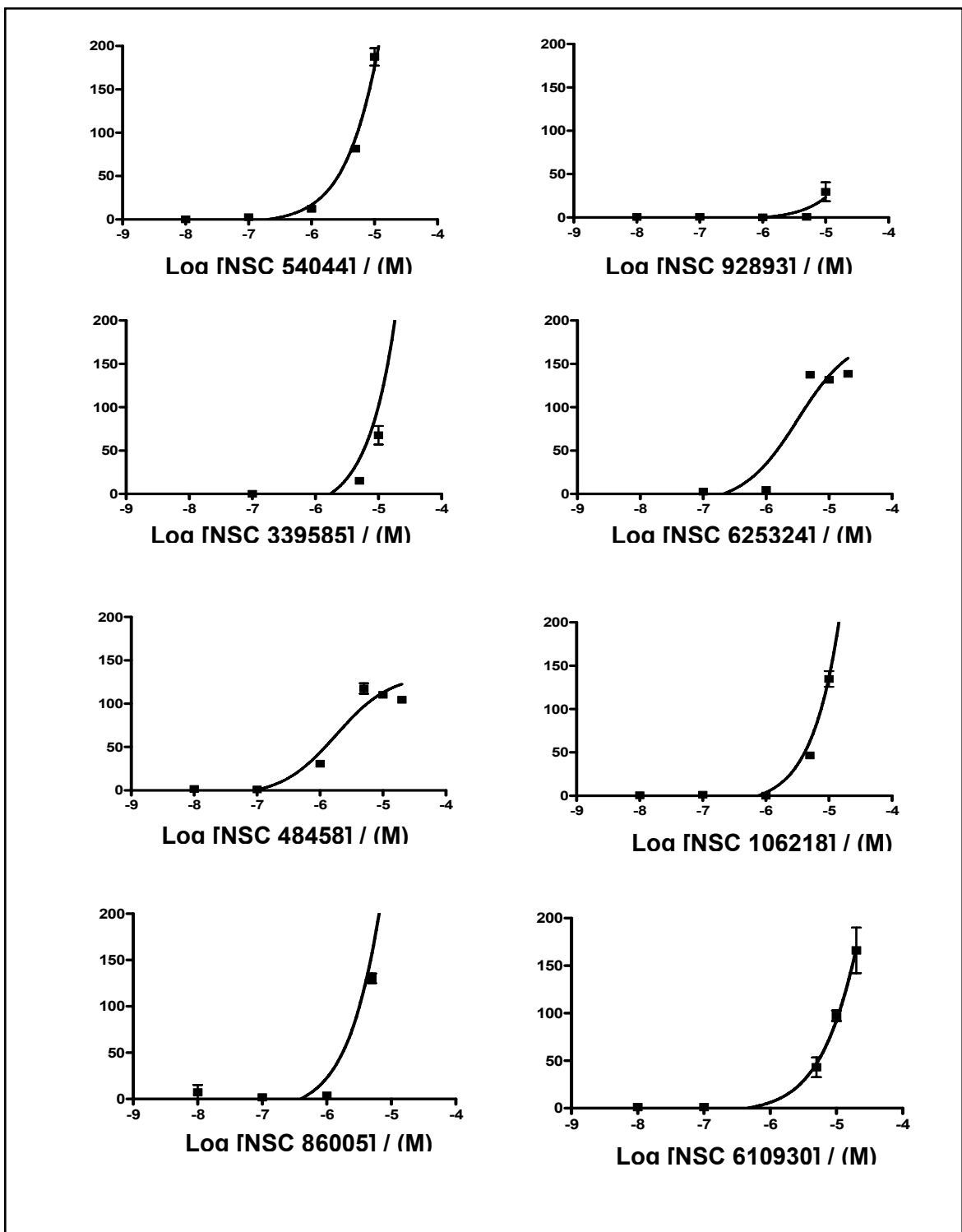


Fig 4.1. Dose response curves of agonists. Fluorescence-based intracellular calcium mobilization assay with stably transfected CHO-hOTR cells. The results are expressed as normalized % activation.

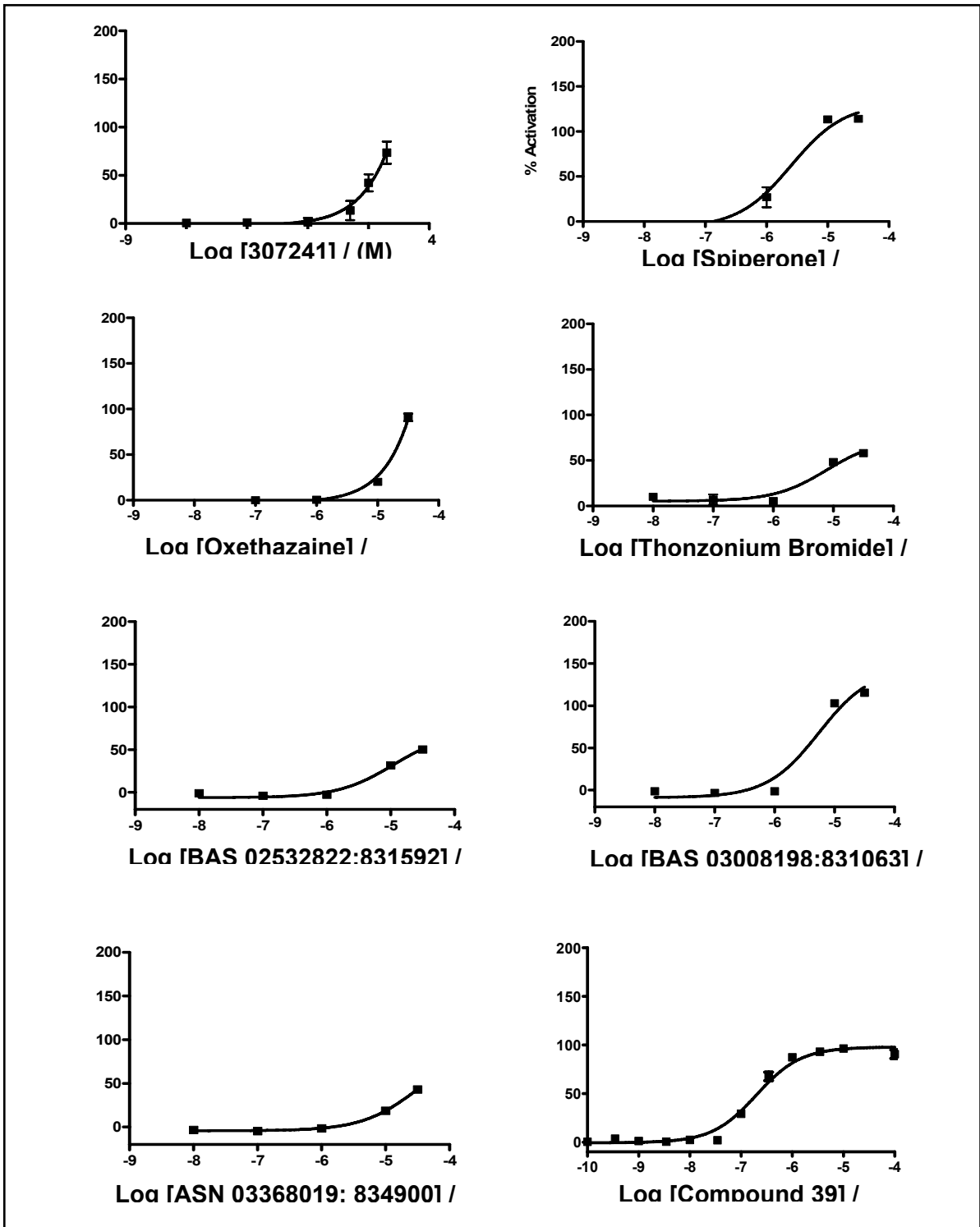


Fig 4.1. (continued). Dose response curves of agonists. Fluorescence-based intracellular calcium mobilization assay with stably transfected CHO-hOTR cells. The results are expressed as normalized % activation.

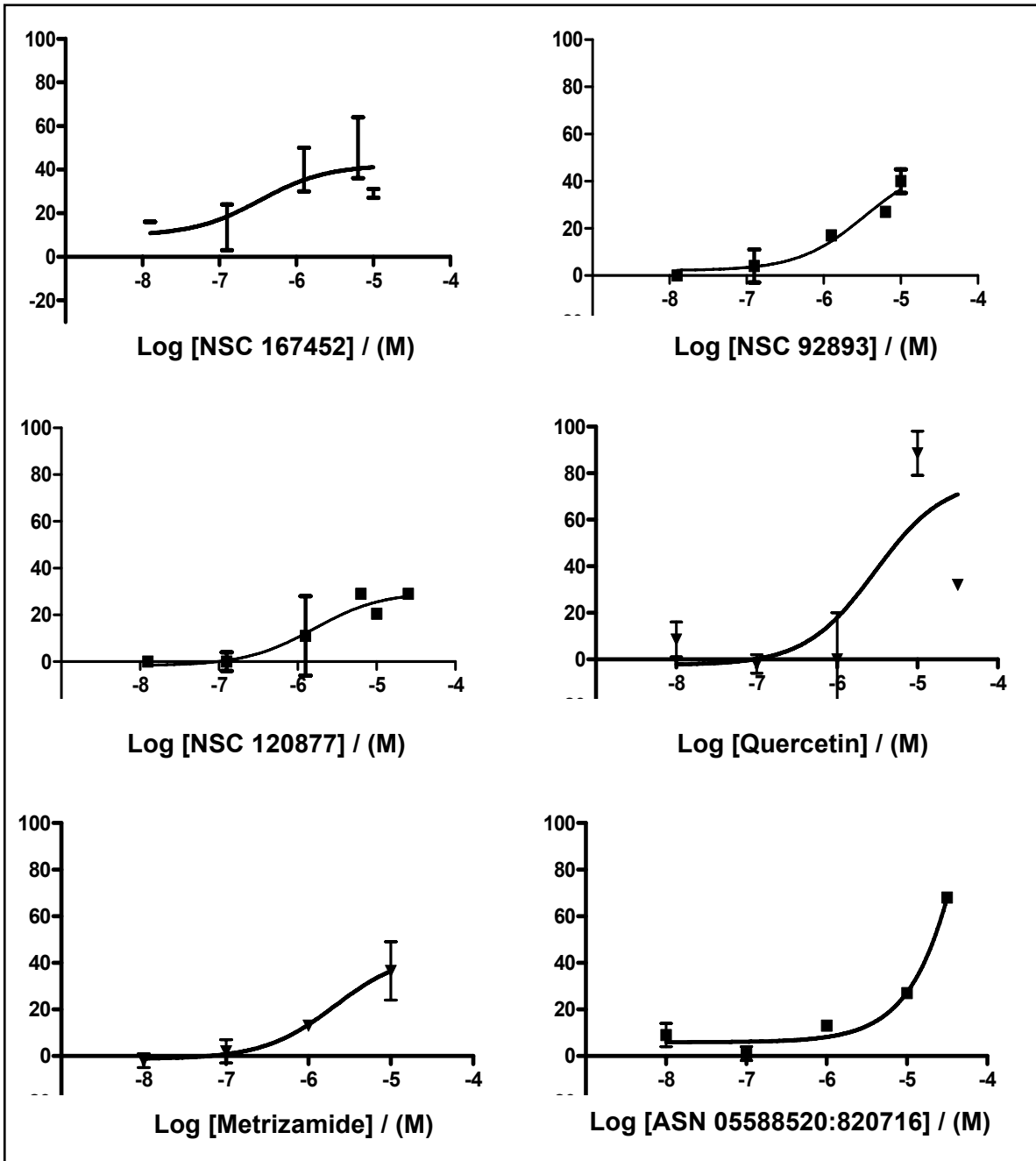


Fig 4.2. Dose response curves of positive allosteric modulators. Fluorescence-based intracellular calcium mobilization assay with stably transfected CHO-hOTR cells. The results are expressed as normalized % activation.

Type	Library	Compound ID	EC ₅₀ / (μM)
Agonist	NCI	NSC 54044	52
		NSC 92893	1400
		NSC 339585	4700
		NSC 625324	3.2
		NSC 48458	1.8
		NSC 106218	6200
		NSC 86005	39.7
		NSC 610930	74
		NSC 307241	175
			Prestwick
Oxethazaine	12000		
Thonzonium Bromide	7.7		
	Asinex	BAS 02532822:831592	11
		BAS 03008198:831063	5.5
		Compound 39	0.2
Modulator	NCI	NSC 167452	0.33
		NSC 92893	2.5
		NSC 120877	1.6
	Prestwick	Quercetin	3.0
		Metrizamide	2.8
	Asinex	ASN 05588520:820716	230

Table 4.2. EC₅₀ calculated for the actives from pure compounds. Fluorescence-based intracellular calcium mobilization assay with stably transfected CHO-hOTR cells. The results are expressed as normalized % activation. See efficacy section for an explanation of how compounds were discarded for further validation.

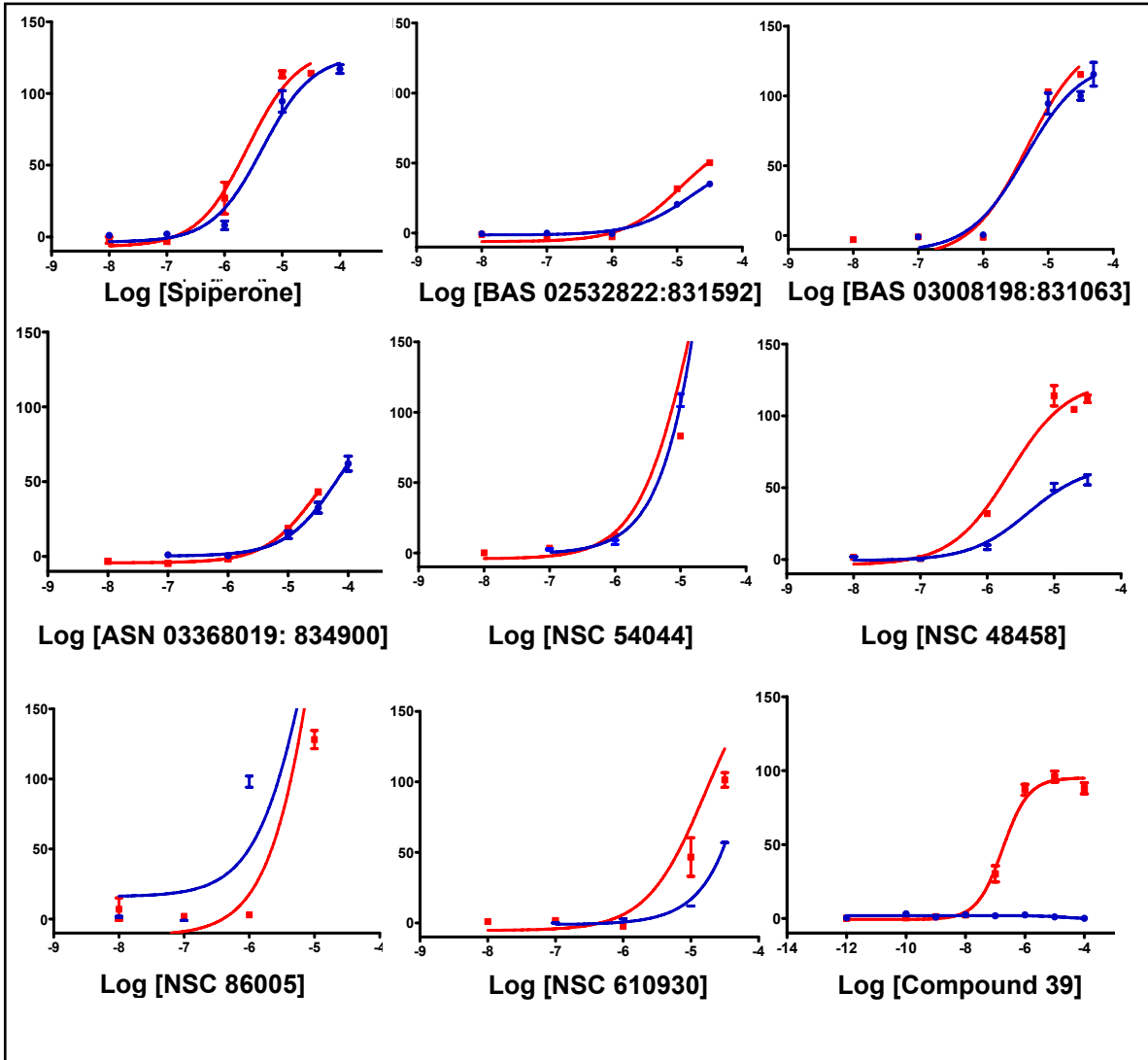


Fig 4.3. Dose response curves for the fluorescence-based intracellular calcium mobilization assay using wild type CHO cells for the identification of compounds that release Ca^{2+} non-specifically. The log [compound] is expressed in M. The results are expressed as normalized % activation. The signals observed for the wild type CHO cell line (blue) are compared to the signals obtained in the same assay with CHO-hOTR (red). Note that only compound 39 showed specific activation of hOTR. NSC 48458 showed a 1.8-fold activation for the CHO-OTR cell line, therefore it was not considered selective for this receptor.

underwent the next step of hit validation.

Selective activation of the hOTR. Compound 39 underwent further testing to assess how selective this compound was for the hOTR when compared to the VR family. In the future, new compounds that show agonistic-like and allosteric modulation behavior will be tested as well against the VR family of receptors.

Compound 39 was reported previously as a selective agonist of the OTR, but its published pharmacological profile was limited to the comparison of the selectivity for the OTR against the V₂R [204]. In this section, the pharmacological profile was extended to the complete VR family. The EC₅₀ calculated for the hOTR and the hV_{1b}R were 183 nM and 4.3 μM, respectively, showing a selectivity of 23x for the hOTR. The normalized % activation for V_{1a}R and V₂ was less than 20% even at 100 μM (fig. 4.4.). The EC₅₀ reported in the literature for a hOTR reporter gene assay was 33 nM, with a 25-fold selectivity compared to the V₂R and no agonist activity for the V_{1a} or V_{1b} receptors [204].

Confirmation of actives by IP₃ release assay

Ligand induced modulation of the OTR receptor causes coupling of the G_q subunit and consequent activation of phospholipase-C which hydrolyzes membrane bound PIP₂ into diacylglycerol and free IP₃ (the first effector molecule of the signaling cascade) as shown in figure 4.5. This IP₃ release is directly related to GPCR activation, therefore, quantification of IP₃ species correlates with receptor activation and G_q coupling. To confirm specific activation of the OTR, quantification of the IP₃

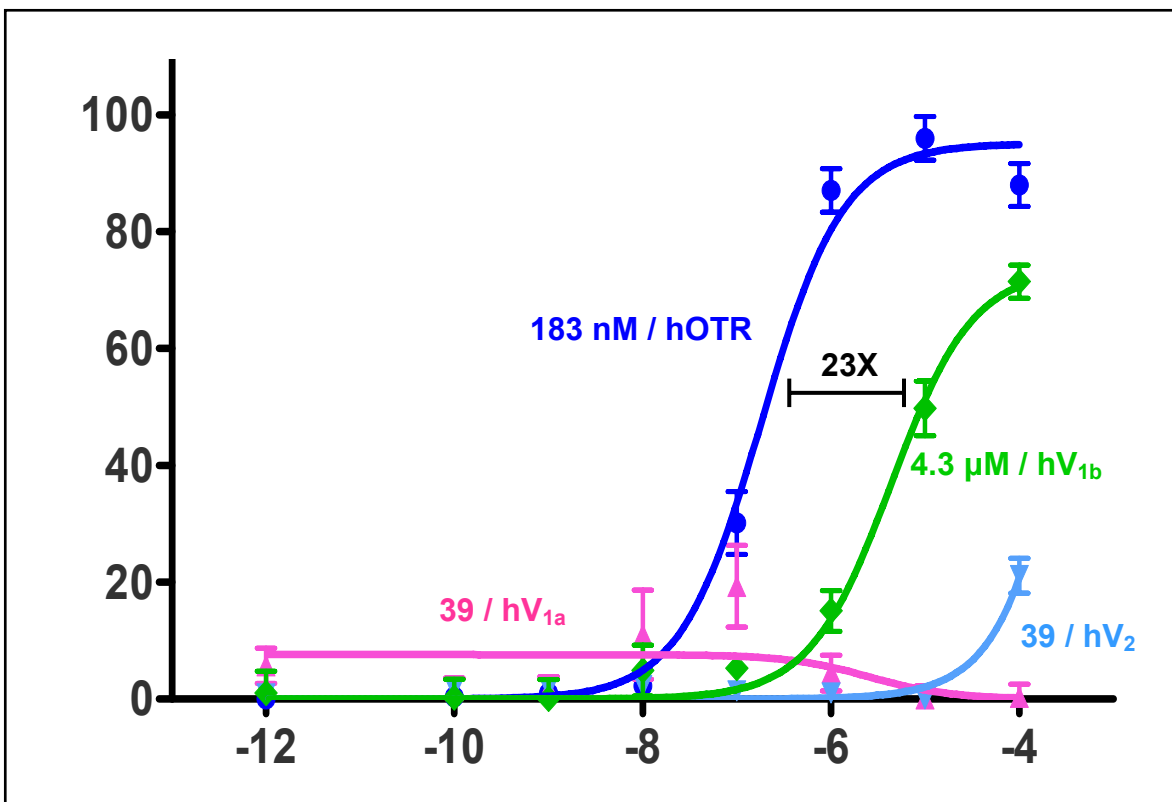


Fig 4.4. Dose response curves for the fluorescence-based intracellular calcium mobilization assay for compound 39 against hOTR and the VR family. Results are reported as normalized % activation. Each data point is mean \pm SD (n=4).

species were tested as a response of dose dependent concentrations of the active compounds.

A scintillation proximity assay (SPA) was used to monitor IP₃ release to confirm activation of the hOTR [274]. Phospholipase C (PLC) catalyzes the hydrolysis of PtdIns(4,5)P₂, which results in both formation of the second messengers Ins(1,4,5)P₃ and diacylglycerol and alteration in the membrane association and/or activity of PtdIns(4,5)P₂-binding proteins. This method for quantification of intracellular inositol phosphate production applied a commercially available yttrium silicate RNA binding resin that binds tritiated IP₃ but not PIP₂ [274]. LiCl was used to inhibit inositol phosphate phosphatases, allowing quantification of [³H] inositol phosphates accumulated as a result of PLC-catalyzed hydrolysis of [³H]PtdIns(4,5)P₂ caused by receptor activation (fig 4.5.). This test was used to validate selective activation of the hOTR as PIP₂ is directly hydrolyzed as a result of G_q coupling caused by receptor activation.

A dose response curve of IP₃ release in OT-treated cell extracts was performed to standardize the signal. Background was determined using cells treated with buffer only and did not result in IP₃ release (data not shown). A dose response curve of the OTR selective antagonist (L-371,251, K_i= 4.6 nM) was tested to further validate the assay by showing the dependence of OTR activity (fig. 4.9.). The IC₅₀ calculated from a dose response curve for the selective OTR antagonist, L-371,251, was 1.7 μM for this assay. The EC₅₀ calculated for OT and compound 39 were 3.8 nM and 893 nM, respectively. OT was 236x more potent than compound 39 (fig. 4.6.). The efficacy for compound 39 was decreased 40% when compared to OT

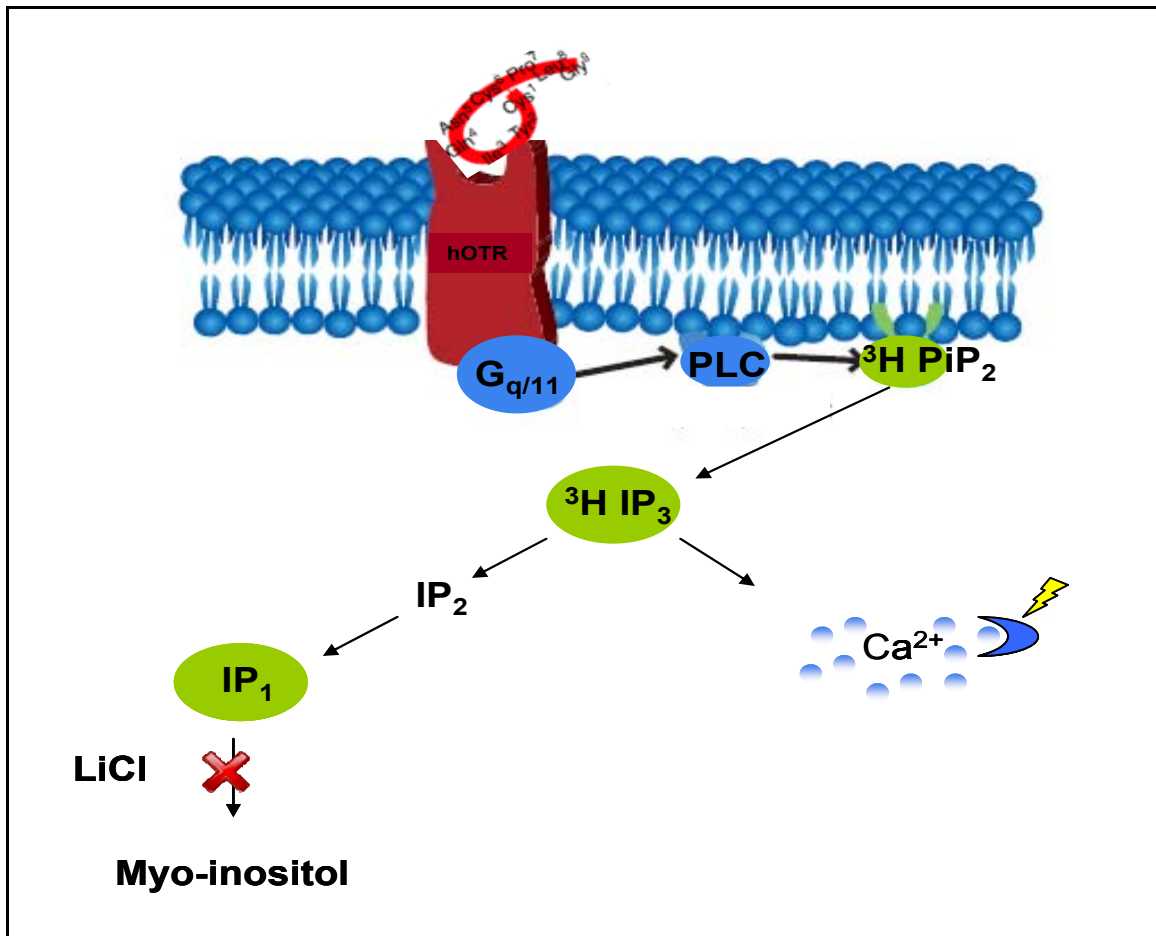


Fig. 4.5. PLC- Catalyzed Hydrolysis of [³H] PIP₂ caused by receptor activation. A scintillation proximity assay (SPA) was used to measure accumulation of [³H] inositol phosphates. LiCl prevented inositol phosphates to further convert into myo-inositol. Figure was obtained from [275].

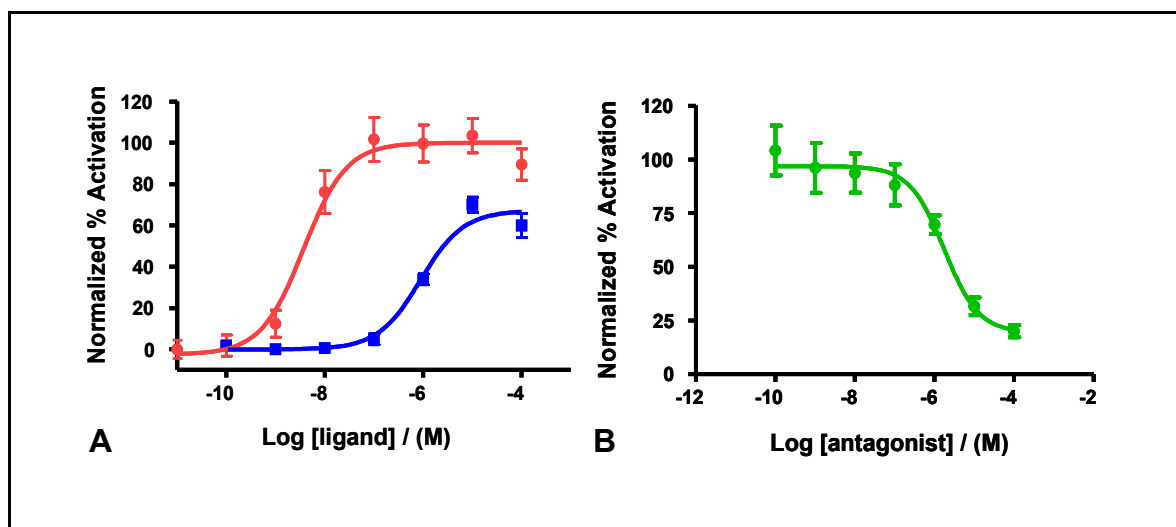


Fig. 4.6. Monitoring of IP₃ release to confirm activation of the hOTR. An inositol phosphate scintillation proximity assay (SPA) was used to validate the activation of the hOTR. A. OT (red) and Compound 39 (blue) dose response curves. The values are expressed as normalized % activation of the hOTR. The EC₅₀ calculated were 3.8 nM and 893 nM, respectively. Each data point was mean \pm SD (n=3). B. Dose response curve for L-371,251, a selective OTR antagonist (green). [OT] was 100 nM. The IC₅₀ calculated was 1.700 μ M. Each data point was mean \pm SD (n=4).

activation. This could be due to the pharmacology involved in activation of the hOTR by compound 39 which caused a smaller amplification of the signal at least in the time frame of this experiment. The OTR selective antagonist used above abrogated the activation of the OTR by compound 39 (data not shown). The results shown here confirmed that compound 39 activated the hOTR and coupled to the G_q pathway.

Cytotoxicity evaluation of actives

In order to move forward it was necessary to assess the in vitro drug-induced cytotoxicity of compound 39 before starting any animal testing [276]. A cytotoxicity colorimetric assay was used to assess inhibition of cell growth after exposure to various concentrations of the active molecules. This assay is used by the NCI disease oriented in vitro anticancer-drug discovery screen [277]. The sulforhodamine B (SRB) method has been optimized for the toxicity screening of compounds to adherent cells in a 96-well format. This assay is used for cell density determination, based on the measurement of cellular protein content [276, 277]. The HEK-293 cell line was chosen as a representative human cell line that is easily grown and readily available. Human hepatocytes are more commonly used for this experiment, but they were not available at the time of the experiment. This cell line is commercially available only at specific times of the year.

HEK 293 cells were exposed to compound 39 for 3 days at various concentrations. A dose response curve of the ellipticine was used as a positive control. Cell growth inhibition was reported and the threshold implemented to consider a compound toxic was 50% or above. Compound 39 presented a cell growth inhibition of less than

30% even at 100 μ M. The positive control ellipticine presented an IC_{50} of 73nM that was calculated from its dose response curve (fig 4.7.). We concluded that compound 39 was not cytotoxic and could be implemented in animal studies.

Our validation pipeline has demonstrated that compound 39 is an excellent OTR agonist (see fig. 4.8.). It presents 23 x selectivity for the OTR versus the VR family; it activates the receptor specifically as demonstrated through the IP quantification experiment, and it is not toxic in vitro. This compound is an excellent candidate to be tested in animals to evaluate receptor activation and its consequent behavior modifications. Also, compound 39 did not show significant activation of a battery of receptors screened at the PDSP. The smallest affinity calculated was for the muscarinic M2, M3, M4, and M5 subtype receptors (high nM range in binding assays). Further investigation showed that compound 39 did not activate these receptors significantly in a functional assay. More over, there was no significant activation of the h-ERG receptor (data not shown).

The outcome of our medium-throughput campaign has not been as successful as anticipated. The only compound considered active enough to enter animal studies is one that was previously reported as a OTR agonist. . This result is not discouraging as we had expected a low number of candidates given that false positives are inherent to any HTS. In addition, the high homology of the OTR and the VR family represents an important obstacle to overcome. The lack of reproducibility during the efficacy screen suggests that a larger library needs to be screened to cover a large structural diversity space. We have submitted all our data to the

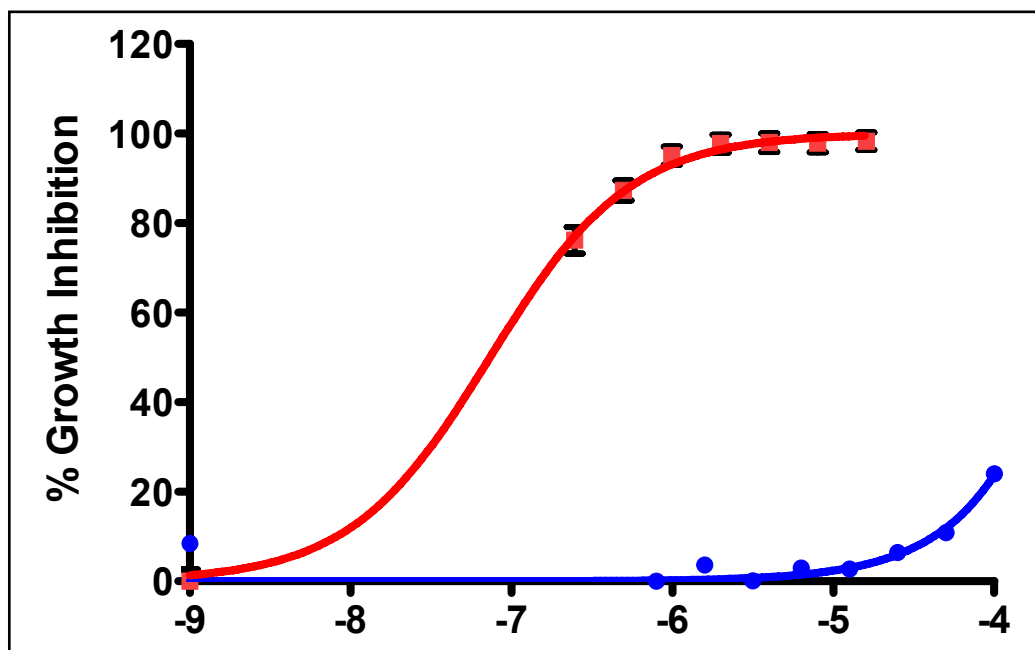


Fig. 4.7. Cell toxicity assessment of compound 39 in a SRB assay using HEK-293 cells. Cell growth inhibition was evaluated as a marker for cytotoxicity. The positive control ellipticine (red) showed an IC_{50} of 73nM. Compound 39 (blue) did not inhibit cell growth significantly. Each data point was mean \pm SD (n=4).

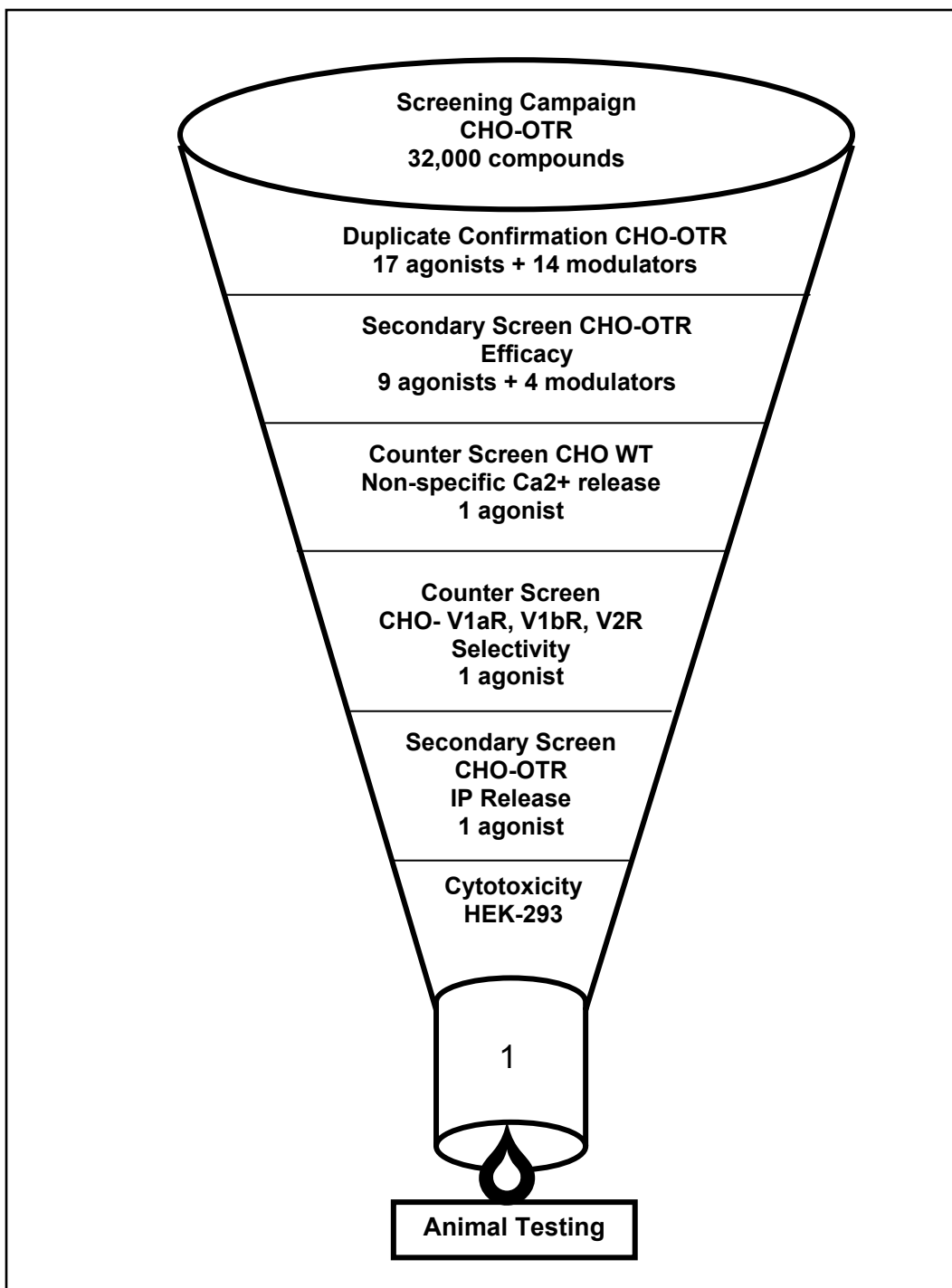


Fig. 4.8. Pipeline flowchart. Tests run are in chronological order. The cell line used is displayed, together with the number of compounds that presented a successful outcome at each stage.

Scripp's HTS center directed by Dr. Peter Hodder. We are waiting for our screen to be implemented at this facility. We expect to have results within 6 months.

Another caveat that has been foreseen for compounds being considered for animal testing stage is the selectivity between the hOTR and the mOTR. Figure 4.9. shows the aligned sequences for the human, mouse, and rat OTR (BLAST was used to investigate homology of these receptors, www.blast.ncbi.nlm.nih.gov). The % identity for the different OTRs is shown in table 4.3. To investigate this matter further, the sequences that form the oxytocin natural binding pocket were aligned [17]. These sequences include the 1-37 and 92-116 sequences that bind to the linear part of oxytocin, and the 173-201 sequence that interacts with the circular section of oxytocin. Table 4.4. shows the homology of these segments. These receptors share a high sequence identity, including the orthosteric binding pocket, therefore we anticipate that the small molecules that are active at the human receptor in our cell models, will activate the receptors in a similar fashion in our animal models.

h 1	MEGALAANWS AEAANASAAP PGAEGNRTAG PPRNEALAR VEVAVLCLIL LLALSGNACV
m 1	MEGTPAANWS IELDLGSGVP PGAEGNLTAG PPRNEALAR VEVAVLCLIL FLALSGNACV
r 1	MEGTPAANWS VELDLGSGVP PGEEGNRTAG PPQRNEALAR VEVAVLCLIL FLALSGNACV
h 61	LLALRTRRQK HSRLFFFMKH LSIADLVVAV FQVLPQLLWD ITFRFYGPD L CRLVKYLQV
m 61	LLALRTRRQK HSRLFFFMKH LSIADLVVAV FQVLPQLLWD ITFRFYGPD L CRLVKYLQV
r 61	LLALRTRRHK HSRLFFFMKH LSIADLVVAV FQVLPQLLWD ITFRFYGPD L CRLVKYLQV
h 121	VGMFASTYLL LLMSLDRCLA ICQPLRSLRR RTDRLAVLAT WLGCLVASAP QVHIFSLREV
m 121	VGMFASTYLL LLMSLDRCLA ICQPLRSLRR RTDRLAVLAT WLGCLVASAP QVHIFSLREV
r 121	VGMFASTYLL LLMSLDRCLA ICQPLRSLRR RTDRLAVLAT WLGCLVASAP QVHIFSLREV
h 181	ADGVFDCWAV FIQPWGP KAY ITWITLAVYI VPVIVLAACY GLISFKIWQN LRLKTA AAAAA
m 181	ADGVFDCWAV FIQPWGP KAY VTWITLAVYI VPVIVLAACY GLISFKIWQN LRLKTA AAAAA
r 181	ADGVFDCWAV FIQPWGP KAY VTWITLAVYI VPVIVLAACY GLISFKIWQN LRLKTA AAAAA
h 241	AEAPEGAAAAG DG GRVALARV SSVKLISKAK I RTVKMTFII V LAFIVCWTP F FVQMWSVW D
m 241	AAEGSDAAAAG A GRVALARV SSVKLISKAK I RTVKMTFII V LAFIVCWTP F FVQMWSVW D
r 241	AAEGNDAAAAG A GRVALARV SSVKLISKAK I RTVKMTFII V LAFIVCWTP F FVQMWSVW D
h 301	ANAPKEASA F IVMLLASL N SCCNPWIYM L FTGHLFHEL V QRFLCCSAS Y LKGRRLGET S
m 301	VNAPKEASA F IVMLLASL N SCCNPWIYM L FTGHLFHEL V QRFLCCSAS Y LKGRRLGET S
r 301	VNAPKEASA F IVMLLASL N SCCNPWIYM L FTGHLFHEL V QRFLCCSAS Y LKGRRLGET S
h 361	ASKKSNSS S F VLSHRSSSQ R SCSQPSTA
m 361	ISKKSNSS T F VLSHRSSSQ R SCSQPSTA
r 361	VSKKSNSS T F VLSRRSSSQ R SCSQPSSA

Fig. 4.9. Primary sequence alignments of the OTR for human (h), mouse (m), and rat (r). The conserved residues are outlined in black. Sequences were obtained from NCBI protein database. NCBI reference sequences: human: NP_000907; mouse: NP_001074616; and rat: NP_037003. BLAST was used to investigate homology of these receptors (www.blast.ncbi.nlm.nih.gov). The % identity for the different OTRs is shown in table 4.3.

Organism	NCBI Reference Sequence	Number of aminoacids	% identity
Homo Sapiens	NP_000907.2	389	---
Mus musculus	NP_001074616.1	388	92
Rattus norvegicus	NP_037003.2	388	91

Table 4.3. Similarity among the OTR in human, mouse, and rat. The protein sequences were aligned using the tool BLAST. The similarities were expressed in percent identity compared to the human sequence. The NCBI reference protein sequence and the total number of aminoacids are shown.

Organism	Sequence		
	1-37	92-116	173-201
Mus musculus	75	100	97
Rattus norvegicus	72	100	97

Table 4.4. Similarity between the human, the mouse, and rat OTR protein sequences. The protein sequences were aligned using the tool BLAST. The similarities were expressed in percent identity compared to the human sequence.

FUTURE PLANS

New hits will be found and tested when the ultrahigh-throughput screen is finished. We confirmed that compound 39 is a useful tool that will help elucidate how complex behavior works and the involvement of oxytocin in regulation of these behaviors and it is ready to be tested in animals. It also serves as a new potential lead for a drug discovery campaign in the treatment of specific neuropsychiatric disorders. The strong pharmacological profile of this compound will help us evaluate the hypothesis that small-molecule activation of the OTR can influence complex behaviors in animal models.

The cell-based assay was transferred to the MLPCN and it is waiting in queue for assay implementation. The primary uHTS campaign will begin immediately following the completion of the assay implementation. The confirmed actives will undergo efficacy screening in this center. The compounds that arise from this stage will be transferred to our laboratory where the remaining validation process will be done. After prioritizing the actives, a hit to lead stage will begin. Mainly, this stage will focus in structure-activity relationship analysis and setting the objectives for the chemistry plan to synthesize analogs of the most promising compounds.

In the case that the small molecules that activate the human OTR do not show similar affinity for the mouse receptor, stable CHO-mOTR cell lines could be developed to test activation of this receptor during the cell-based assays. Rat receptor could be also transfected into CHO cells in the future in the event that it is recommended to perform animal testing in this species as well.

CHAPTER 5

MOUSE MODELS OF COMPLEX BEHAVIOR AFFECTED BY THE OXYTOCIN PATHWAY

INTRODUCTION

This chapter's aim was to determine clinically-relevant behavioral effects of OT and the small-molecule OTR agonists and positive allosteric modulators evaluated and validated in Chapters 4 and 5. OT's effects were investigated in specific animal models that were considered relevant to several neuropsychiatric diseases, such as schizophrenia, autism spectrum disorders, anxiety, and depression. These robust mouse models provide translational tools for developing effective treatments [278].

As a first step, we assessed the effects of OT in relevant mouse models to obtain a baseline response. In addition, we tested the efficacy of cmpd39 (cmpd 39) as the first OTR agonist in the regulation of complex behaviors. In the future, validated OTR agonists and modulators will be used in the behavioral tests established here to determine their ability to augment activity of the OT pathway. The key to assessing the effects of OT and cmpd39 relied on the selection of established animal models for the different paradigms that we were investigating.

The tests used included: toxicity test, self-grooming, hot plate nociception test, elevated plus and zero mazes, social memory duration test, acoustic startle response (ASR) and prepulse inhibition (PPI) test, and open field locomotion test. These tests are validated indicators of clinically relevant behaviors.

Our first approach was to reproduce the published regulation of self-grooming behavior elicited by OT. Injection of OT induces self-grooming of the facial, truncal, and genital areas of the body in male and female rats and mice. This characteristic behavior is an indicator of activation of central OTR [124, 125, 279-281], and allows a simple assessment of drug administration, blood-brain-barrier crossing, and specific activation of the OTR.

The oxytocinergic system has been reported to have a modulatory function on nociception [129, 282, 283]. The hot plate nociception test is a well-established animal model to evaluate analgesic effects of drugs. Analgesia testing in this model allows quantification of pain threshold, showing a correlation between the efficacy of a compound and the latency to react to a painful stimulus [284-286].

Anxiety-like behaviors are present in many psychiatric diseases; therefore, including a battery of tests that could evaluate anxiolytic-like effects of drugs tested would provide valuable information. The elevated plus maze (EPM) is a test based in the natural tendency of mice to actively explore a new environment versus the innate fear of open spaces [287]. As a result of the aversive properties of the open quadrants, animals spend a greater proportion of time in the closed quadrants. Compounds that increase the percentage time an animal spends in the open quadrants of the maze are considered to exhibit anxiolytic-like activity. The elevated

zero maze (EZM) is a modification of the EPM that consists of a circular platform that lacks the central area. The EZM has been pharmacologically validated for mice, demonstrating the ability to detect anxiolytic-like activity of reference anxiolytic compounds [108].

The mouse phenotype for autism is defined by behavioral criteria relevant to its three diagnostic symptoms: aberrant reciprocal social interactions, deficits in social communication, and stereotyped, ritualistic, repetitive behaviors with narrow, restricted interests [144]. The challenge is to design mouse behavioral tasks with sufficient analogies to the three diagnostic symptoms. Behavioral neuroscientists are generating useful assays for autism-like social and communication deficits, motor stereotypies, repetitive behaviors, and perseverative habits [278]. Modeling the behavioral symptoms of autism in mice has shed light on the genetic mechanisms underlying social deficits. The first diagnostic symptom, social deficits, is perhaps the most straightforward to model in mice. Most strains of mice show high levels of social interaction. The development of social familiarity in rodents depends predominantly on olfactory cues and can critically influence reproductive success. Researchers have operationally defined this memory by a reliable decrease in olfactory investigation in repeated or prolonged encounters with a conspecific [62, 63].

Acoustic startle is the reflex response to a sudden, loud noise. Prepulse inhibition (PPI) is the suppression of the normal response to a startling stimulus when a stimulus is immediately preceded by a weak prestimulus or prepulse [288]. A number of studies have shown that schizophrenic and autistic patients have an

impaired prepulse inhibition response [138, 185, 188, 189, 191, 192]. The impairment observed in schizophrenic is thought to reflect an underlying problem with inhibitory mechanisms similar to those used for sensorimotor gating [288, 289]. Rats and mice show schizophrenic-like reductions in prepulse inhibition when treated with dopaminergic agonists [191]. The prepulse inhibition paradigm is an ideal animal model to study the mechanisms underlying the sensorimotor gating deficits observed in schizophrenia and for screening new antipsychotic therapeutics [138, 188, 189, 288, 290-293].

The open field test is one of the oldest, most extensively used, and simplest measures of mouse and rat emotional behavior. Motor activity underlies almost every mouse behavioral paradigm. Behavioral measures of the open field locomotion have been proposed as indices of anxiety. Some additional measures most commonly assessed are: rearing behavior, which decreases in an anxiogenic environment, and thigmotaxis, the proportion of time the animal remains close to the walls of the open field. Increasing the stress of the animal, results in decreased activity [288]. In addition, overall activity tends to decrease over time allowing quantification of habituation to the novelty of the open field [294].

Our goal was to obtain new small molecules that influence complex behavior. By assessing the efficacy of cmpd39 in these well established behavioral tests we have provided evidence to show that a small molecule can modify complex behavior in mice. The results obtained for cmpd39 show that small molecules can serve as tools to investigate the role of OT in complex behavior and provide new leads in the treatment of neuropsychiatric disorders.

METHODS AND MATERIALS

Materials. All reagents were ACS reagent grade and used without further purification unless otherwise noted. Oxytocin (Bachem), d-amphetamine sulfate (Sigma), and (+) MK-801 hydrogen maleate (Sigma) were purchased in the powder form. Sterile normal saline solution (0.9% NaCl) and isoflurane were purchased as a liquid. Cmpd39 was synthesized by the Center for Integrative Chemical Biology and Drug Discovery at UNC-CH.

Animals. Intracerebro-ventricular (ICV) cannulated and non-cannulated male mice from two inbred strains, C57BL/6J and BALB/C, and ovariectomized C57BL/6J females were purchased from The Jackson Laboratory (Bar Harbor, ME). Mice were 5-8 weeks of age at the time of testing. All ICV cannulated animals were housed individually and all the non-cannulated ones were housed in group cages, separated by gender, four to five per plastic cage, and provided with food and water ad libitum. The housing room was maintained at 23 °C on a 12-h light/dark cycle (lights off at 7 PM). All procedures were conducted in strict compliance with the policies on animal welfare of the National Institutes of Health and the University of North Carolina (stated in the "Guide for the Care and Use of Laboratory Animals," Institute of Laboratory Animal Resources, National Research Council, 1996 edition) and approved by the University of North Carolina Institutional Animal Care and Use Committee.

Drug stock solutions. OT was dissolved to 5 mg/ml in a 5% acetic acid and 0.9% NaCl solution (normal saline, NS). Doses tested were diluted with NS. Cmpd39 was dissolved to 5 mg/ml in 15% DMSO, 0.5% Tween-20, and NS solution. MK-801 and amphetamine were dissolved with NS.

OT and cmpd39 testing. Doses tested were expressed in mg/kg based on the weight of the animals. The injection volume was 10 ml/kg body weight. Normal saline was used as a vehicle (negative) control.

Behavior tests

Toxicity test. Male C57BL/6J mice were injected with highly concentrated solutions of the compounds to be tested. The concentration of these solutions was chosen according to available data from the HTS and from the literature when possible. The animals were injected intraperitoneally with OT at 10 mg/kg or cmpd39 at 75 mg/kg and housed individually. They were observed periodically for five consecutive days and evaluated for general health, including body weight, appearance of the fur and whiskers, body posture, and normality of gait [287]. Signs of distress or sickness were particularly looked for like locomotor function, dehydration, neurological damage, etc. If after this period of time, there were no obvious signs of toxicity, the compounds were considered safe to be tested at those concentrations in the animals.

Self-grooming behavior test. Animals that were infused ICV were previously anesthetized with isoflurane. OT was injected at a 0.5 µg/µl dose in a 2 µl volume during a 40 second period and an additional 40 seconds before removing the cannula to allow pressure stabilization after injection. Control animals received normal saline vehicle alone. Behavioral testing started 10 min after ICV injection. In a separate group of animals, OT was injected intraperitoneally (i.p.) and behavioral testing started after 10 min.

Behavioral observations were made blind to treatment. Grooming activity was scored as follows: the mice were placed individually into transparent plastic cages (24 × 12 × 24 cm) in a low-noise room. The behavior of each mouse was observed every minute for 10 sec beginning 10 min after animals were placed in the boxes. The occurrence of the following behavioral elements of grooming was recorded: vibration of the forepaws, face washing, body grooming, scratching, paw licking, head shaking, body shaking, and genital grooming. Behavioral observations lasted 90 min.

The data was collected in Microsoft Excel 5 and analyzed by adding the grooming occurrences in a 5 min period. A positive grooming behavior represented 1 and the absence of this behavior was scored as 0. The maximum possible score per 5 min interval was 5.

Hot plate nociception (HPN) test. We performed this test with three groups of C57BL/6J male mice: non-cannulated, ICV cannulated awake (no anesthesia), and ICV slightly anesthetized. We initially obtained a baseline of pain threshold. We

tested OT dose (0.5 and 1 µg/µl, ICV) and injection pretreatment time ((25, 30, and 35 min prior to the HPN test). Saline injected mice were used as controls.

Mice were confined to a horizontal hotplate surface at 55°C and observed for responses including licking of paws, jumping, or vocalizing. Animals were removed immediately after showing a response, or after 40 sec of being placed on the hotplate. During each test, a plastic cylinder was used to confine the animal on the hotplate surface. The latency to exhibit an aversive response to the heated surface was recorded by using a hot-plate analgesia meter (IITC, Life Science, Model 39, Woodlands Hills, CA) (see fig.5.1.A.). Data was collected and analyzed using GraphPad Prism 5. Analysis of variance (ANOVA) was used to evaluate the statistical significance of the results.

Elevated Plus Maze (EPM) test. ICV cannulated Balb/C and C57BL/6J individually housed male mice were tested. The EPM, which was elevated 50 cm from the floor, consisted of two opposite facing open arms (30 x 5 cm) and two closed arms (30 x 5 cm with 15-cm-high walls) with a central area (8 x 8 cm) (fig.5.1.B.). Mice were placed on the central platform, facing an open arm and they were allowed to freely explore the maze. The mice were observed and scored for 5 min. An arm entry was defined by two paws entering an arm of the EPM [295]. The surface and walls of the EPM were thoroughly cleaned with fresh wet towels after each animal was tested. OT or saline were administered ICV to slightly anesthetized or awake animals 20 or 30 min before starting the test. Various pretreatment times were used to assess optimal drug effect.

The number and duration of entries into open or closed arms were simultaneously scored by a treatment-blind observer. Percent open arm time was calculated as $100 \times (\text{time spent on the open arms} / (\text{time in the open arms} + \text{time in the closed arms}))$. Percent open arm entries was calculated using the same formula [296]. Data was collected and analyzed using GraphPad Prism 5. Analysis of variance (ANOVA) was used to evaluate the statistical significance of the results.

Elevated zero maze (EZM) test. ICV cannulated Balb/C and C57BL/6J individually housed male mice were tested. The EZM is a circular platform (outer diameter = 60 cm, width = 5 cm) made of metal that is elevated on legs 55 cm above the floor. The EZM is composed of 4 quadrants, 2 open and 2 closed, each of equal length (fig.5.1.C.). The 2 closed quadrants, which are located opposite each other and separated by open quadrants, have metal Plexiglas walls that rise 30 cm above the surface of the maze. The outer edges of the open quadrants have perpendicular lips of metal that are 3 cm high. Each test began with placement of the subject in the middle of one of the closed quadrants and they were allowed to freely explore the maze. Mice were observed and scored for 5 min. An arm entry was defined by two paws entering an arm of the EZM. OT or saline were administered ICV to slightly anesthetized or awake animals 20 or 30 min before starting the test, and the surface and walls of the EZM were thoroughly cleaned with fresh wet towels after each animal was tested. Various pretreatment times were used to assess optimal drug effect.

The number and duration of entries into open or closed arms were simultaneously scored by a treatment-blind observer. Percent open arm time was calculated as $100 \times (\text{time spent on the open arms} / (\text{time in the open arms} + \text{time in the closed arms}))$. Percent open arm entries was calculated using the same formula [296]. Data was collected and analyzed using GraphPad Prism 5. ANOVA was used to evaluate the statistical significance of the results.

Social memory duration test. ICV cannulated C57BL/6J males: the male mouse was introduced to a stranger female for 5 min during four consecutive days in his own cage to allow habituation to a stranger and avoid future aggressive behavior. Cages and bedding were changed daily after encounters. Animals that showed more mounting activity or aggression toward the female were not tested further. The test was held in the male's cage to permit establishment of a home-cage territory. After habituation, mice were separated into two groups: one was tested with the same female and the other with a different female in every encounter. All the male mice were exposed to a novel female (F1) for 5 min ($t=0$ min). After this first encounter period, the female was removed from the cage and placed in a new cage to avoid acquiring odors from the grouped house cage. The same female was reintroduced in the cage after 10 min for 5 min ($t=15$ min), after which they were returned to the same holding cage. The same female was reintroduced for another 5 min after 60 min ($t=80$ min). The different female group males were introduced to a novel female (F2) for 5 min after 60 min ($t=65$ min) and placed in a new holding cage after this encounter. After another 10 min the same female (F2) was placed in the cage with

the male for 5 min ($t=75$ min). To investigate longer inter-trial intervals (2 h), male mice were divided into the same two groups to be exposed to the same or different female. All the male mice were exposed to a novel female (F1) for 5 min ($t=0$ min). After a 2 h separation interval, during which the females were kept in individual cages, either the same (F1) or a different (F2) female was placed in the male's cage to allow investigation for 5 min a third and shorter inter-trial interval was tested (30 min). The same procedure as the 2 h interval was followed with a 30 min inter-trial interval ($t=35$ min). Trials were recorded and coded by an operator blind to the treatment (same vs. different female). Animals were considered investigating if they were proximally oriented towards the female or in direct contact with it, sniffing (specially the anogenital area), close following, grooming, generally inspecting any body surface of the female, nosing, and pawing [297]. The total investigation time was scored.

ICV cannulated Balb/C: the test was performed in a special cage dedicated to social investigation. A three chambered Plexiglass box with wire containers was used for this test (see fig.5.1.E.). The chambers doors were removed to allow free movement of the subject. On the test day, the cages of the subject mice were brought from the vivarium to a holding area outside of the test room, 1 h before the start of behavioral testing. C57BL/6J mice were used as stranger subjects. Balb/C male mice were injected a $1 \mu\text{g}/\mu\text{l}$ OT solution ICV. The subject mouse was placed into the center chamber after 10 min and allowed to investigate the new environment for 10 min (habituation). An empty round wire cage was placed in the center of one of the side chambers. The wire holding cage was a stainless steel inverted pencil

cup, 11 cm high, composed of a solid 10.5 cm diameter bottom and stainless steel bars spaced at 1 cm intervals. A stranger mouse was placed in another identical round wire cage in the center of the other side chamber (see fig.5.1.F.) A plastic cup containing a heavy lead weight was placed on top of each wire cage, to prevent the stranger from moving the cage around the floor, and to prevent the subject from climbing onto the flat top of the wire cage. Exploration of the three chambers by the subject mouse was recorded for 30 min. A second stranger was introduced into the empty wire cage and recording resumed for another 30 min to evaluate preference for social novelty. The cages were cleaned between subjects [144, 287, 298]. Time spent in direct sniffing of the strangers by the subject mouse and direct sniffing of the empty wire cage by the subject mouse were scored. The total investigation time for each stranger was scored. Data are expressed as mean \pm s.e.m. Data was analyzed by overall analysis of variance. When the ANOVA indicated significant difference among treatments, individual groups were compared using the Bonferroni post hoc test for multiple comparisons.

Acoustic Startle Response (ASR) and prepulse inhibition (PPI) test. Animals were tested with a San Diego Instruments SR-Lab system (see fig 5.1.G.). Male C57BL/6J mice were placed in a small Plexiglas cylinder within a larger, sound-attenuating chamber (San Diego Instruments). The cylinder was seated upon a piezoelectric transducer, which allowed vibrations to be quantified and displayed on a computer (see fig 5.1.H.). The chamber included a house light, fan, and a loudspeaker for the acoustic stimuli (bursts of white noise). Background sound levels

(70 dB) and calibration of the acoustic stimuli were confirmed with a digital sound level meter.

Drug, OT or cmpd39, were administered i.p. 50 min before tests were conducted. The psychoto-mimetics MK-801 or d-amphetamine were administered s.c. 5 and 15 min before the start of the test, respectively. Each mouse was tested only once as MK-801 showed an accumulative effect. OT was administered i.p. at 1, 2, and 3 mg/kg. Cmpd39 was administered i.p. at 10, 30, 50, 75, and 100 mg/kg. The doses used for MK-801 and amphetamine were 0.5 and 1 mg/kg and 9, 10, 14, and 15 mg/kg, respectively. All the dilutions were made using 0.9% NaCl (normal saline). Injection volume was 1 ml/100 g body weight.

Each test session consisted of 42 trials following a five-minute habituation period. The seven different types of trials were: no-stimulus trials, trials with the acoustic startle stimulus (40 ms; 120 dB) alone, and trials in which a prepulse stimulus (20 ms; 74, 78, 82, 86, or 90 dB) had onset 100 ms before the onset of the startle stimulus. The different trial types were organized in blocks of 7, in randomized order within each block, with an average inter-trial interval of 15 s (range: 10 to 20 s). Measures were taken of the startle amplitude for each trial, defined as the peak response during a 65-ms sampling window that began with the onset of the startle stimulus. An overall analysis was performed for each subject's data for levels of startle response and prepulse inhibition at each prepulse sound level. The prepulse inhibition was calculated as $100 - [(response\ amplitude\ for\ prepulse\ stimulus\ and\ startle\ stimulus\ together / response\ amplitude\ for\ startle\ stimulus\ alone) \times 100]$ [299].

Data was analyzed using GraphPad Prism 5. For acoustic startle PPI studies, overall repeated measures ANOVAs were used for each drug dose and intensity level of the acoustic stimulus for startle response and prepulse inhibition. Post-hoc repeated measures ANOVAs were used to determine drug effects at each dB level only when the within-group ANOVA indicated a significant effect of drug treatment. For all comparisons, significance was set at $p < 0.05$.

Open field locomotion test. Locomotor activity, including horizontal activity, ambulation (total distance traveled), fine movements (repeated breaking of the same set of photobeams), rearing movements, and time spent in the center region of the chamber, was assessed in a photocell-equipped automated open field (40 cm × 40 cm × 30 cm; Versamax system, Accuscan Instruments). Testing was conducted in the morning or early afternoon, during the light phase of the mouse light/dark cycle. Activity chambers were contained inside sound-attenuating boxes, equipped with houselights and fans (see fig 5.1.D.) [287]. Mice were tested immediately after the acoustic startle test. Doses evaluated for OT, cmpd39, MK-801, and d-amphetamine were explained above (see ASR test).

Activity data were collected for each mouse over a 90 or 120 min time course, beginning when the mouse was first placed in the testing chamber. Data were collected in five-minute intervals. Locomotion was analyzed by calculating horizontal and vertical beam breaks, distance travelled, and time spent in the center. The distance traveled in each five-minute interval was measured as the total of all vectored X–Y coordinate changes. For each group of mice, the mean ± SEM was

calculated for each five-minute time interval. Data from each drug dose were first tested by repeated measures ANOVA. A separate analysis of the locomotor data was performed in order to more clearly present overall drug effects. In this case, data from each drug dose were summed for each 30 min of the 90 or 120 min sessions, and were tested by repeated measures ANOVAS. Post-hoc comparisons were performed using Bonferroni tests.

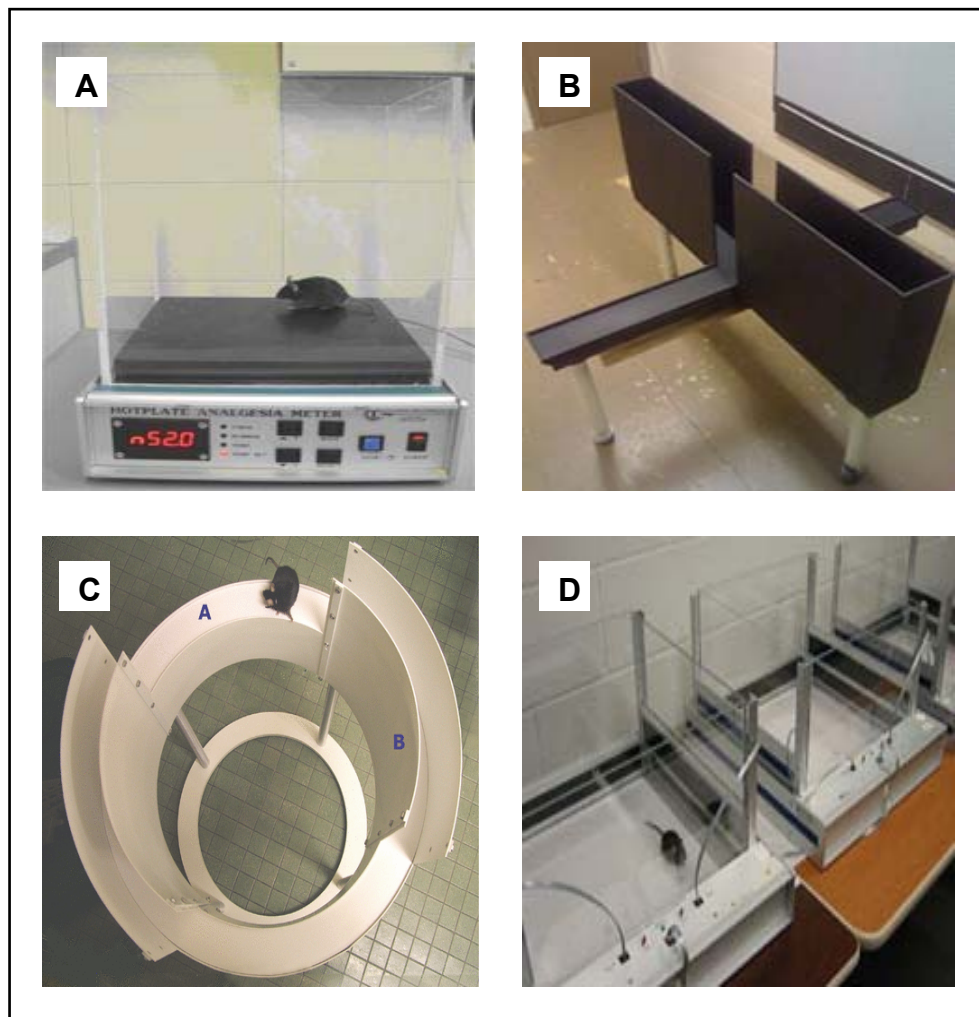


Fig 5.1. Apparatus used for animal neurophysiological and behavioral testing. A. Hot plate for nociception. The latency to exhibit a reaction to the heated surface was used to evaluate analgesic efficacy. B. Elevated plus maze and C. Elevated zero maze. Mice were given a choice between staying within the safety of two walled arms (the closed arms); versus exploring two open arms to calculate anxiety related behavior and anxiolytic effects of drugs. D. System to evaluate locomotor activity. Levels of locomotion and rearing are measured and used to calculate hyper- or hypo- activity in experimental groups, and to detect aberrant exploration and habituation in a novel environment. Pictures from [300].

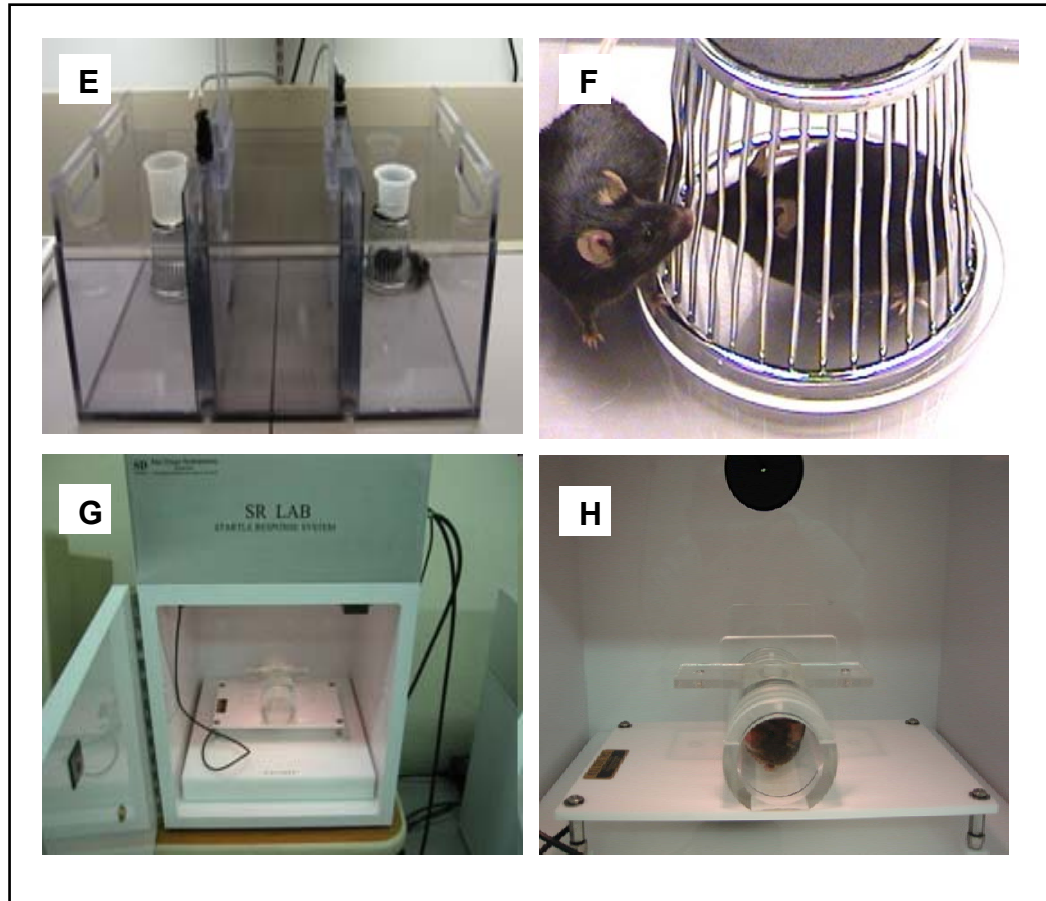


Fig. 5.1. Apparatus used for animal neurophysiological and behavioral testing (continued). E. Three chambered plexiglass box for social memory. For this test the inner doors were removed to allow the mouse to move freely. F. Wired cage to hold stranger mouse for the social memory test. Proximity to the cage was scored as social investigation behavior. G. Acoustic startle response chamber for assessment of prepulse inhibition effect of a drug and its antipsychotic effects. H. Tube used to hold mouse during test. Pictures from [300].

RESULTS AND DISCUSSION

A variety of behavioral tests were conducted to evaluate the ability of OT and the small-molecules compounds to influence complex behaviors such as anxiety, pain threshold, social memory duration, and prepulse inhibition of the acoustic startle response. The tests performed were chosen as they are well-established animal models for OT activity. As an example, social memory has been considered analogous to the social deficits present in pervasive developmental disorders like autism, and attenuation of prepulse inhibition is a core sign of schizophrenia.

The first step was to assess a baseline for each experiment, followed by evaluation of the dose dependent effect of OT. The next step was to test the ability of cmpd39, the small-molecule OTR agonist validated previously, to affect complex behaviors and to compare its efficacy to OT's. Mouse behavioral experiments require 10 to 20 mice per treatment group for proper statistical analyses. Different ages can be combined, under the general guidelines that 3 to 10 month old mice are adults and share similar behaviors. Positive findings from the first batch of mice require replication in a second batch of mice to ensure reproducibility of the findings [300].

Toxicity test. Before embarking into in animal tests, toxicity of test compounds was determined. This information helped assess the highest possible safe doses . OT was reported to cause motor disturbances at higher doses [301]. OT at a 10 mg/kg concentration was injected i.p. to five C57BL/6J mice and observed for 1 hour after injection and five consecutive days for signs of distress or neurological and

physiological damage. Any distress or damage was apparent during the observation period. Cmpd39 was tested initially at 10 mg/kg and 40 mg/kg and later at 70 mg/kg. Two mice per dose were injected i.p. and observed for 2 hs immediately after injection and for the following five days for signs of distress. No signs of neurological damage or motor disturbances were seen during the week of observation. Only signs of sedation and grooming were observed during the first hours after injection, which correlated with acute OT effects (see next section). In fact, mice recuperated from the acute treatment overnight and showed normal behavior on the second day. Therefore, both compounds were considered safe for further studies.

Self-grooming behavior test. Central OT plays a physiologically relevant role in the activation of grooming behavior through the selective activation of the CNS OTR system [124, 279]. Our previous data and literature reports showed that administration of ICV OT elicited OTR-mediated self-grooming of wild-type Sprague-Dawley rats [280]. The enhanced grooming was selective to OTR as indicated by the results that showed that the administration of the selective oxytocin antagonist reduced self-grooming significantly [124, 125, 281].

First, the OT effect on self-grooming was tested for ICV and i.p. administration. Intraperitoneal administration is very easy, but we decided to test ICV as well because some actives would not cross the blood-brain barrier from the blood stream in such an effective concentration that would cause any CNS effects. OT-treated C57BL/6J mice showed an increase in self-grooming episodes per 5 min intervals in a dose dependent manner when 1 and 2 μ g were administered ICV.

There was a significant difference between mice that were treated with OT in comparison with the saline group, especially between 1 and 15 min after injection (fig. 5.2.A). These results showed that OT had its maximal effect on the OTR in the CNS at around 5-15 min. Fig 5.2.B. shows the self-grooming effect elicited by OT at 10 mg/kg when administered i.p. The maximal effect appeared between 45 and 65 min. The administration route delayed the OT effect, but this test showed that OT can penetrate the BBB in an effective dose. With the results obtained from these two experiments, it was concluded that in order to obtain OT maximal effects to assess changes in behavior, the most favorable latency times would be 10-15 min for ICV administration and 45-60 min for the i.p. route.

The effects of cmpd39 on self-grooming were only evaluated in the intraperitoneal route. The high doses of 10 and 50 mg/kg of cmpd39 were investigated in conjunction with toxicity assessment. Both concentrations caused non-stop self-grooming behavior at around 60 and 90 min for 5 min. The mice recuperated from the injections rapidly and there were no obvious behavioral changes. Given these results, we concluded that cmpd39 crossed the BBB and it elicited grooming behavior through the selective activation of the CNS OTR system (fig. 5.3.).

The Balb/C mouse strain was used in the anxiety-related tests. The OT effect on self-grooming in these mice was investigated to assess accurate ICV administration of OT. Each mouse received 2 µg of OT in a 2 µl injection volume. They were placed in their home cage for continuous observation for 1 hr. None (n=5) showed any grooming episodes that could attributed to the effect of OT. These mice

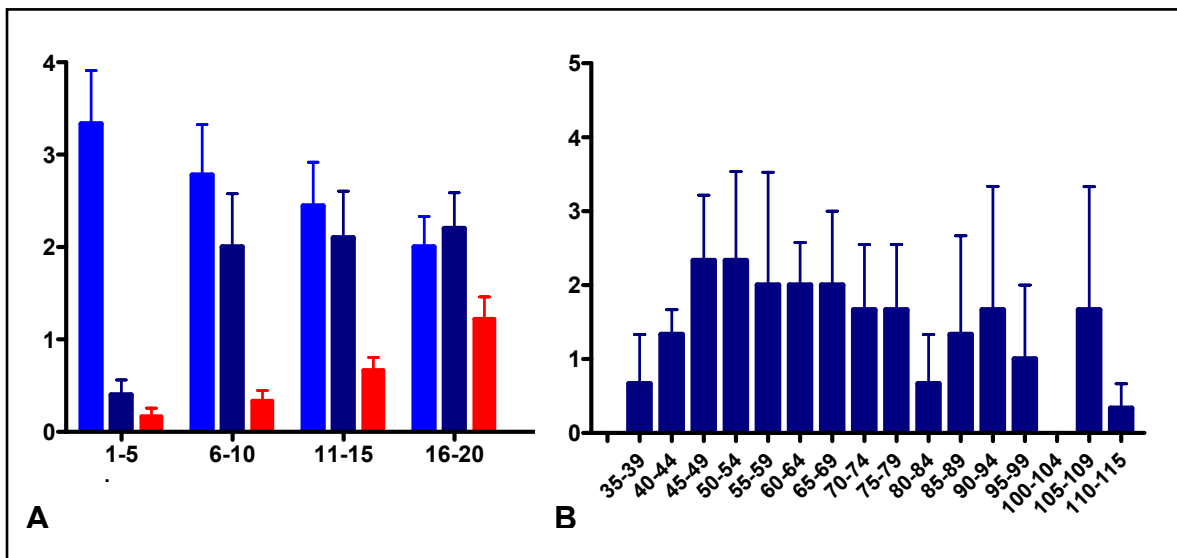


Fig 5.2. OT self-grooming effect. Self-grooming behavior was tested in mice treated with OT by ICV or i.p administration. Positive behavior was given a value of 1 and negative behavior a value of 0. The results are reported as self-grooming bouts (0-5) in a five min interval. The x axis represents the 5 min intervals tested. A. OT effect in ICV cannulated mice. OT at 1 μ g (light blue, n=10), OT at 2 μ g (dark blue, n=10), and saline (red, n=18) treatments are shown. Each ICV cannulated mouse was infused with 2 μ l of solution over a 1min period. B. OT effect in i.p. injected mice (n=3). OT dose was 10 mg/kg and the injection volume was 1 ml/100 g body weight. All the results were reported as average \pm S.E.M.

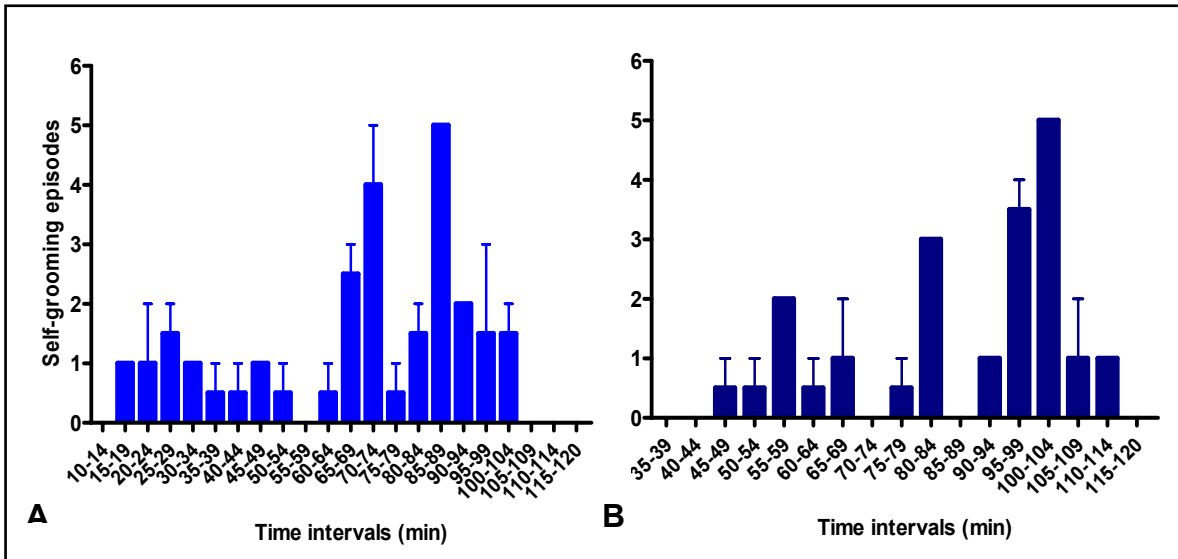


Fig 5.3. Cmpd39 self-grooming effect via intraperitoneal administration. Self-grooming behavior was tested in mice treated with OT by i.p. administration. Self-grooming behavior was scored every min for 10 sec. Positive behavior was given a value of 1 and negative behavior a value of 0. The results are reported as self-grooming bouts (0-5) in a five min interval. The x axis represents the 5 min intervals tested. A. Cmpd39 effect at 10 mg/kg (n=2). B. Cmpd39 at 50 mg/kg (n=2). All the results were reported as average \pm S.E.M. Injection volume was 1 ml/100 g body weight.

remained in a corner of their cage without moving for the entire time. We concluded that Balb/C is not a strain that could be used for quantification of the self-grooming effect caused by OT. There was no literature available for this strain that reported grooming behavior.

Hot plate nociception (HPN) test. We assessed pain perception and analgesic efficacy of OT using the hot plate nociception (HPN) test [127, 130]. Male ICV cannulated C57BL6/J mice were tested to evaluate the latency they show to an aversive response to the hot plate. The responses observed included licking of paws, jumping, or vocalizing. A baseline was first investigated to assess the effects of isoflurane on latency after 15 min of administration to respond to the hot plate. This anesthetic was used to facilitate ICV infusion on the mice (fig. 5.4. A.). A comparison between treatments did not show any significant differences ($p < 0.05$), validating this method of anesthesia. The next step was to investigate the optimal waiting interval by comparing 15, 25, 30, and 35 mins between injection and HPN test. The OT dose of 2 μg was chosen according to the literature to mimic the results reported in the past [128, 129, 282, 302]. Investigation of OT effects at 15, 25, 30, and 35 min did not show significant differences with the saline control; therefore we could not show any effects of OT in analgesia (fig. 5.4.B.). At this point, we decided to focus our efforts in other behavioral tests that were showing positive results and were more germane to complex behaviors present in some neuropsychiatric disorders.

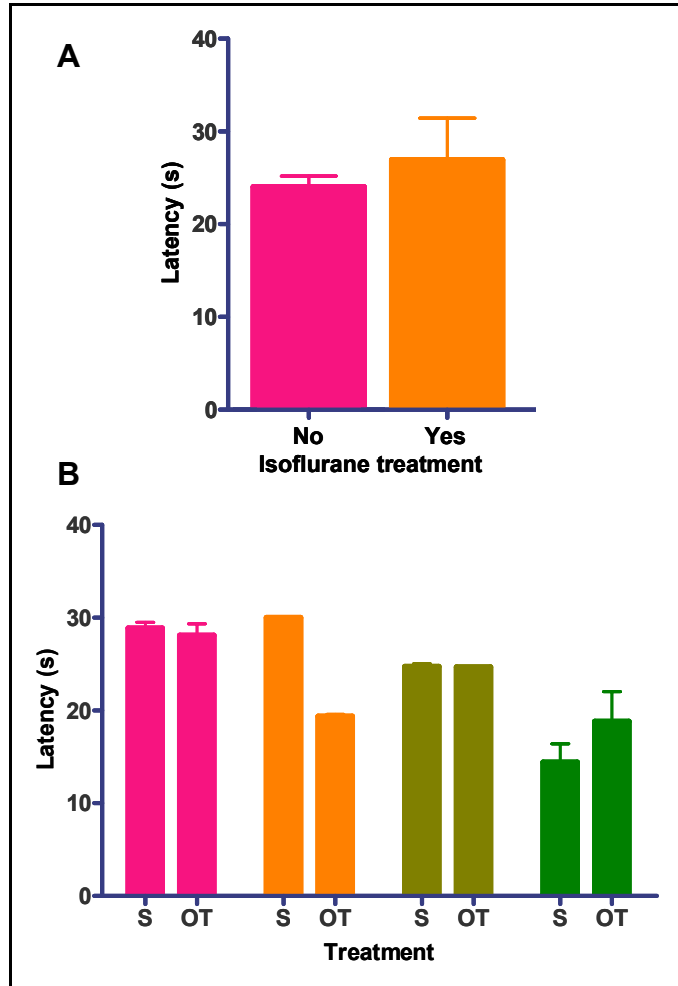


Fig. 5.4. OT effects on latency to respond to the hot plate nociception test.

Mice were placed on the hot plate (55°C) and timed until they showed any sign of discomfort or after 40 s of being placed on it. A. Isoflurane effect on nociception. No isoflurane (pink) and isoflurane (orange) treatments. Means are not significantly different. N=8. B. Maximal effect of 2 ug of OT was investigated for various latency times in min: 15 (pink, n=5), 25 (orange, n=3), 30 (soft green, n=3), and 35 (green, n=10). A statistical comparison of OT (2 ug) vs. Saline showed no significant differences ($p < 0.05$). All results are expressed as mean \pm S.E.M.

Elevated Plus Maze (EPM) test. The elevated plus maze test is a well established behavioral test used to assess anxiety-related behavior [109, 110, 303, 304]. It has been reported that OT promotes anxiolytic-like behavior in male mice in a dose dependent manner [108]. Our goal was to reproduce these findings so we could compare the anxiolytic effects of the OTR active compounds. The first step was to set up a baseline of unanesthetized mice in order to compare this group to historical data [287]. Baseline activity was first investigated using C57BL6/J ICV cannulated awake mice (fig. 5.5.).

Since the C57BL6/J mice were ICV cannulated and there was a need to slightly to anesthetize them to administer drugs, the isoflurane affect on the mouse performance in EPM tests was tested. Briefly, mice were anesthetized with isoflurane for 2 min and were placed in the EPM after 30 min for a 5 min test. Fig. 5.6. shows that isoflurane has no effect on the open arm time and entries percentages ($p < 0.05$) indicating no anxiolytic activity.

The mice used in the previous experiment were tested on the elevated plus maze 30 minutes following the end of the ICV injection (vehicle or oxytocin). Data from mice that did not show any increase in grooming behavior after OT ICV administration was discarded because OT-mediated self-grooming was used as an indicator of accurate central administration. Overall, there were no significant differences in percent open arm time or entries between the vehicle and OT groups (fig. 5.7.). There was a non-significant trend for higher numbers of entries in the OT mice ($p = 0.0716$). A repeated measures analysis of time spent on the open and closed arms revealed a significant interaction between treatment and arm

($p=0.0389$). Post-hoc tests indicated that the mice given OT spent significantly less time in the closed arms (211 ± 14 sec), in comparison to the vehicle mice (251 ± 11 sec). Mice were allowed at least two weeks to recuperate from the stress of the test and to avoid anxiety decrease because of repeated exposure to the maze and handling.

The Balb/C mice strain was previously shown to display increased anxiety-like behavior compared to other strains; they spent less than 5% of the test time in the open arms of an elevated plus maze [287]. These findings made this strain very attractive to be tested with OT. Consequently, it has been reported that the Balb/C strain showed decreased anxiety behavior in the elevated zero maze when they were administered 1 μg of OT ICV [108]. Molecules that elicit anxiolytic effects would be easily identified using this strain in the maze test. Our efforts shifted to try to reproduce these findings in our laboratory using the elevated plus maze to later be able to test the anxiolytic effects of the validated OTR agonists and allosteric modulators.

In the EPM, centrally administered OT (2 μg), did not produce a significant change in the percent entries to the closed arms and the percent time spent in the closed arms of the EPM in Balb/C male mice ($p<0.05$, $n=10$) (fig. 5.8.). All the mice, including the ones that received the OT treatment, stayed in the closed arms for the entire test. The effects reported in the literature could not be reproduced.

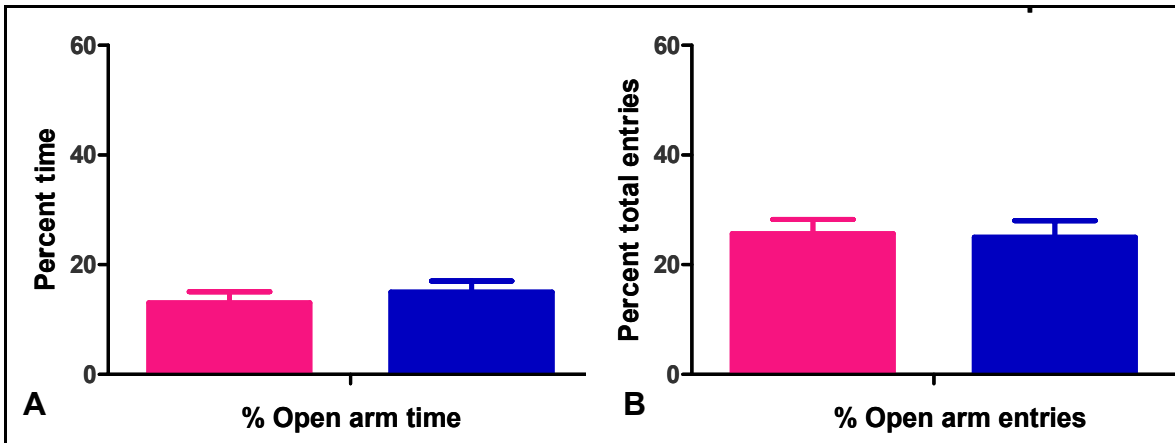


Fig 5.5. Comparison between untreated C57BL/6J mice and literature data of the elevated plus maze. Percent time (A) for the open arm and (B) percent entries of the elevated plus maze. Our data (pink). Literature data (blue). Data are mean \pm S.E.M. and n= 20 for each group.

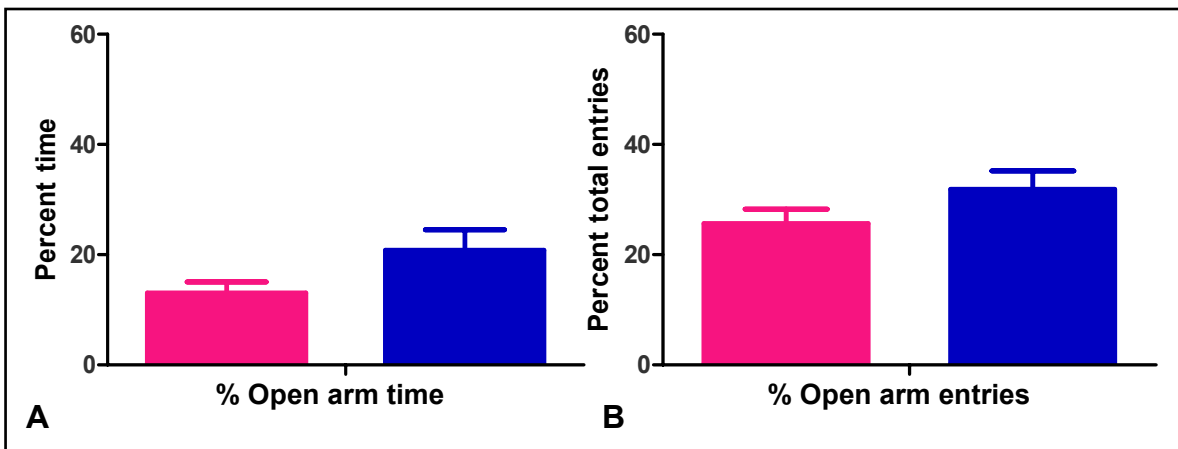


Fig. 5.6. Isoflurane effect as an anesthetic to be used in the elevated plus maze with ICV cannulated C57BL/6J mice. Percent time (A) for the open arm and (B) percent entries of the elevated plus maze. No isoflurane (pink). Isoflurane (blue). Data are mean \pm S.E.M. and n= 20 for each group.

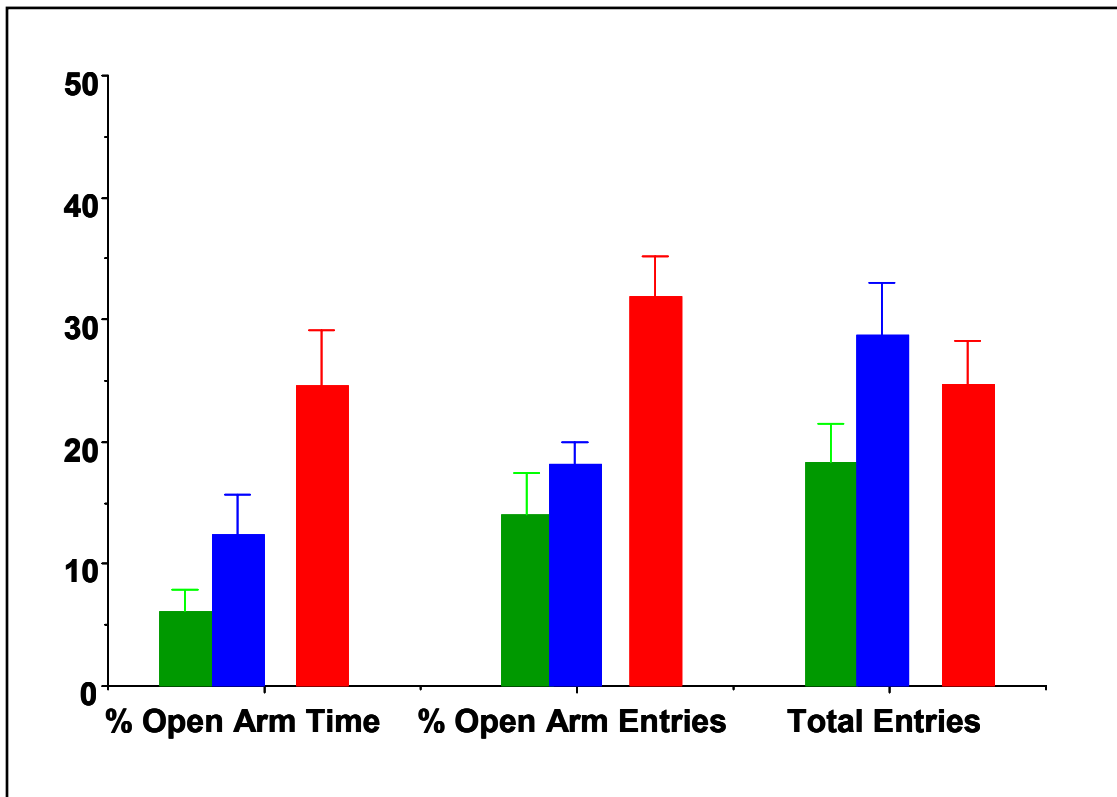


Fig. 5.7. OT anxiolytic effects in the elevated plus maze in ICV cannulated mice. Anxiolytic effects were tested in mice using 1 μg of OT administered ICV. Percent time and percent entries for the open arms of the elevated plus maze, and total number of entries are shown. Treatments shown are: saline (green, n=18), OT (blue, n=18), and control (red, n=5). Percent open arm time = time spent in open arms / (time in open arms + time in closed arms) x 100. Percent open arm entries = entries into open arms / (entries into open arms + entries into closed arms) x 100. Data are mean \pm S.E.M. for each group. Overall, there were no significant differences in percent open arm time or entries between the vehicle and OT groups. Post-hoc tests indicated that the mice given OT spent significantly less time in the closed arms (211 ± 14 sec), in comparison to the vehicle mice (251 ± 11 sec).

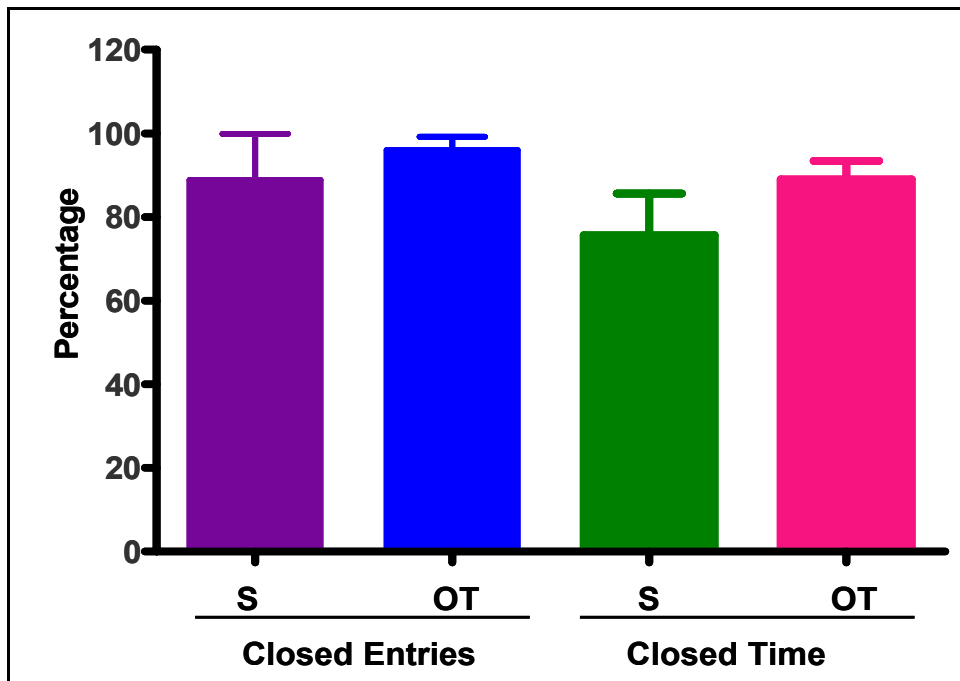


Fig. 5.8. Anxiolytic-like effects of OT in Balb/C mouse strain in EPM. Central administration of OT (2 μ g) did not produce a significant change in the percent entries to the closed arms and the percent time spent in the closed arms of the EPM in Balb/C male mice ($p < 0.05$, $n = 10$).

Elevated zero maze (EZM) test. The elevated zero maze (EZM) test is a well established behavioral test used to assess anxiety-related behavior. It is similar in concept to the elevated plus maze, but it presents the advantage of not having the central area that can cause inconsistencies in scoring. Mice were allowed at least two weeks to recuperate from the stress of the test and to avoid anxiety decrease because of repeated exposure to the maze and handling. The OT effects seen in the EPM were also reported for the EZM; therefore, our goal was to investigate this modified paradigm to use it in the identification of small molecules that produce anxiolytic-like effects. Two strains of mice were used: C57BL6/J and Balb/C male mice. These experiments were conducted on awake mice to avoid anesthetic effects (isoflurane). Central administration of drugs did not show any significant differences between OT (2 µg) and saline treatments ($p < 0.05$) (fig. 5.9.). Since the results published previously were not reproduced, we decided to stop anxiety testing and focus our efforts on other mouse tests expected to be sensitive to OTR agonists.

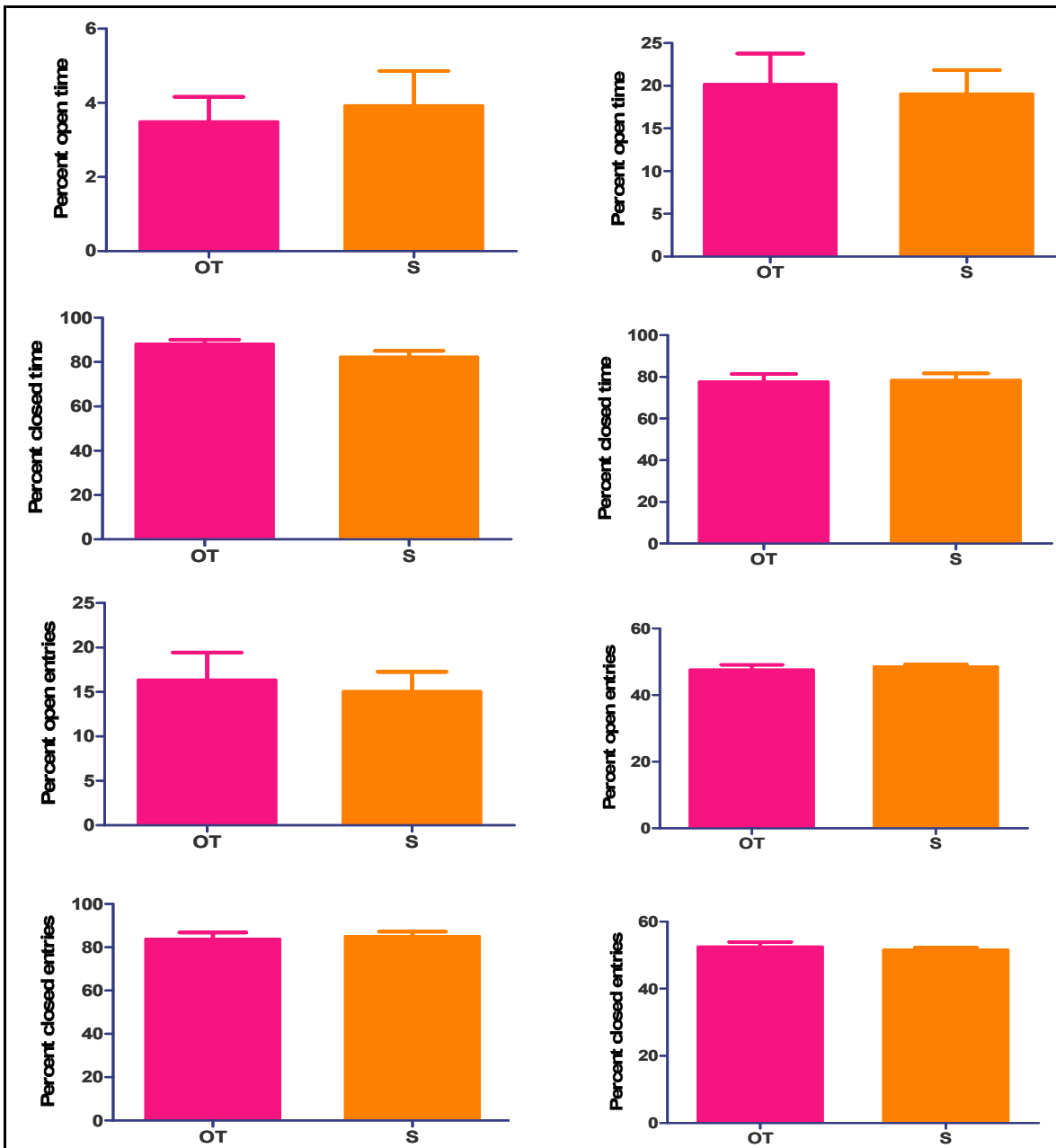


Fig. 5.9. Anxiolytic-like effects of OT in C57BL6/J (left) and Balb/C (right) male mouse strains in EZM. Central administration of OT (2 μ g) did not produce a significant change in the percent entries and the percent time spent in the open and closed arms of the EZM ($p < 0.05$). OT treatment is shown in pink and saline treatment in orange. N= 18 for C57BL/6J and n=10 for Balb/C strains.

Social memory duration test. A social memory test was designed to measure social approach initiated by the subject mouse toward an unfamiliar conspecific as compared to social approach initiated by the subject mouse toward a more familiar conspecific, defining preference for social novelty, as well as confirming the ability of the subject to distinguish between two different mice [144]. Given that impairments in social interaction and communication are the primary diagnostic indicators in ASDs, the assessment of social behavior was considered an essential component of our studies in mouse models [298]. Initial work with this test for social approach has shown that most inbred mouse strains choose to spend more time near unfamiliar strangers. This preference for social proximity can be observed in juvenile and adult mice and in males and females [305-307]. The development of social memory is defined as a decrease in olfactory investigation in repeated encounters with a conspecific [308, 309]. Our goal was to assess the effects of centrally administered OT to prolong social memory in male mice. The first approach was to determine the inter-exposure time interval that maintained a social memory of a subject repeatedly introduced in opposition to an unfamiliar subject in the C57BL6/J mouse strain.

The social investigation task was conducted in the males' home cages to avoid dominance behavior. Mice were allowed to move freely in the cage. The male subjects were habituated to the presence of a female stranger five days prior to testing to avoid aggressive behavior. During this habituation period, mice that showed aggressive or sexual behaviors were not tested further. Measures were taken of the amount of time spent in proximity to the ovariectomized female, as well as sniffing and allo-grooming behavior towards the stranger.

The first stage of this test consisted of introducing the male to a novel ovariectomized female for a 5 min exposure time to start forming a social memory. The second exposure interval was at 10 min and it was included to allow consolidation of social memory of a familiar stranger. After different inter-exposure intervals (30, 60, and 120 min), either the same female or another stimulus animal was introduced to the male for another 5 min. This stage was designed to assess social novelty memory as well as duration of memory regarding a familiar stranger. This phase of the social preference test provided information on the ability of the mice to distinguish between two conspecifics. The expected outcome emphasized the decrease in time the male would spend investigating the reintroduced female as opposed to the time spent investigating a novel stranger [58, 62].

Our results showed that male mice could not distinguish between familiar and unfamiliar conspecifics in three different time intervals (fig. 5.10.). A proper baseline that showed differences between time and / or subject introduced could not be established; therefore, this social memory prolongation paradigm was not pursued further to evaluate OT effects.

A short pilot test (n=5) was also done using ICV Balb/C male mice. This strain did not show any interest in investigating strangers (data not shown). In fact, these mice did not move at all when placed in the cage and observed for 1 hr. This particular strain did not seem to be a suitable strain to be used in social behavior paradigms.

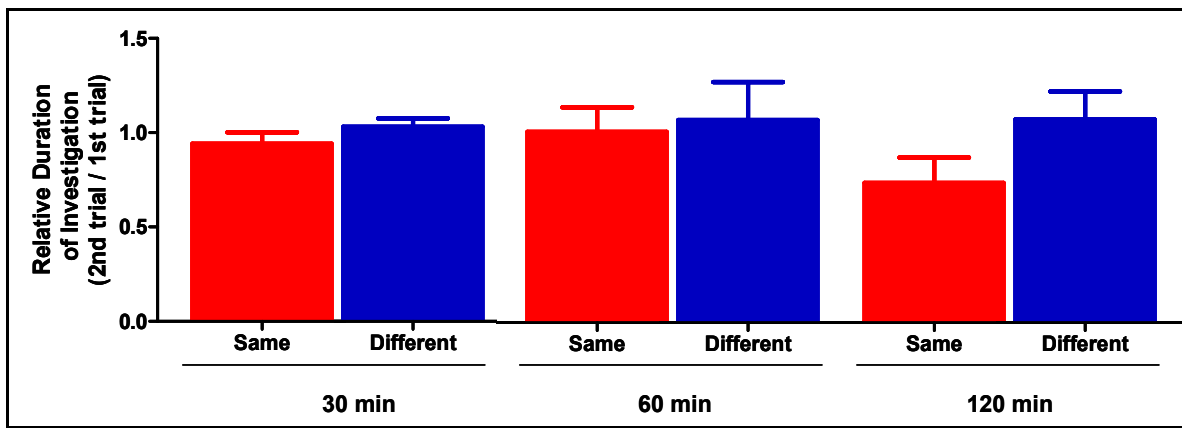


Fig. 5.10. Social memory duration of male C57BL/J mice after exposure to different female strangers. We tested different inter-exposure intervals to calculate the amount of time a male mouse would “remember” a familiar subject (30, 60, and 120 min). Males were introduced to familiar (same = red, n=10) or unfamiliar (different = blue, n=10) females for 5 min intervals to allow social investigation. The relative duration of investigation between the first and second exposures did not any significant changes at 30, 60, or 120 min and between same and different female groups.

Acoustic Startle Response (ASR) and prepulse inhibition (PPI) test. Prepulse inhibition of the startle reflex is an operational measure of sensorimotor gating and refers to the normal suppression of startle the startle reflex when the intense startling stimulus (“pulse”) is immediately preceded by a weaker stimulus (“prepulse”). The PPI paradigm has been widely applied in studies of information processing in normal animals and humans [139]. The acoustic startle measure was based on the reflexive whole-body flinch, or startle response, following exposure to a sudden noise. Decreased PPI has been reported for patients with schizophrenia and autism spectrum disorders [185, 192, 310]. In rats, PPI is decreased in a manner homologous to that seen in schizophrenia by administration of certain psychotomimetic drugs, including the direct and indirect dopamine agonists, apomorphine and amphetamine, and the non-competitive NMDA antagonists, PCP and dizocilpine (MK-801) [311-314]. Antagonism of psychotomimetic-induced disruption of PPI has been proposed as a strong predictor of antipsychotic activity [315]. It has been reported that OT plays a role in the modulation of regulation of PPI in rats, and that it may act as a novel endogenous antipsychotic [139]. Our goal was to reproduce those findings in a mouse PPI behavioral model and to later test OTR agonists to assess their antipsychotic-like activity in this paradigm.

The first step was to optimize the psychotomimetic drug (MK-801) dosage to obtain the most significant differences when compared to saline treated animals. Fig. 5.11. shows a dose-dependent effect of MK-801 in the startle amplitude and the percent prepulse inhibition when administered subcutaneously. MK-801 at 1 mg/kg showed a main treatment effect on startle response [$F(2,322) = 58.95, p < 0.0001$]

and a significant overall interaction effect [$F(12,322) = 1.90, p < 0.0001$]. MK-801 at 1 mg/kg showed a main treatment effect on prepulse inhibition [$F(2,225) = 28.94, p < 0.0001$]. The MK-801 dose chosen to evaluate OT and OTR agonists effect on PPI disruption was 1 mg/kg since this dose showed the most significant effect through out all the prepulses ($p < 0.01$).

OT effects on startle amplitude and PPI disruption were investigated next on ICV cannulated mice. A dose response curve was tested (1 and 3 μ g of OT given centrally) followed by a subcutaneous MK-801 (1 mg/kg) injection. The data shown on figure 5.12. show no apparent effects of s.c. MK-801 on the cannulated mice. This data did not reproduce the results obtained previously. We argued that the cannula implanted in the mice may have caused some negative effect on this test or on the normal functioning of the mice.

Our efforts then shifted to evaluate the effects of OT administered systemically (intraperitoneal). We investigated the dose-dependent response of OT (1, 2, and 3 mg/kg) on startle amplitude and PPI, specifically, the ability of OT to rescue the disruption of PPI caused by MK-801 (1 mg/kg) in mice.

Repeated measures ANOVA and multiple group comparisons using the Bonferroni post-hoc test were calculated to identify significant differences among treatment and prepulse groups. Treatment with OT showed a main treatment effect on startle response [$F(5, 1393) = 69.42, p < 0.0001$] and a significant overall interaction effect [$F(30, 1393) = 2.322, p < 0.0001$]. Fig. 5.13. shows that OT (3 mg/kg) significantly blocked MK-801 effect on startle response at all the prepulse levels by reducing the increased startle response caused by administration of MK-

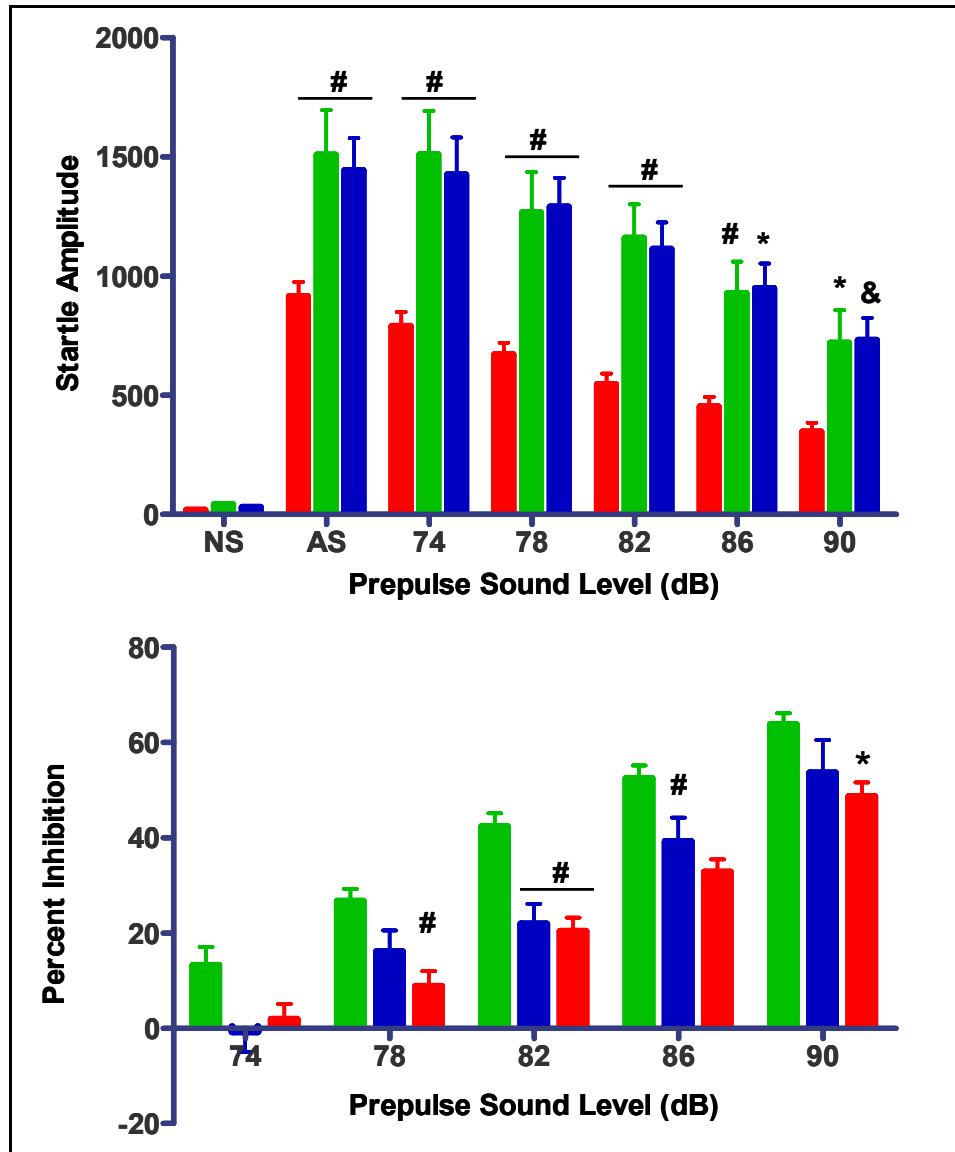


Fig. 5.11. Dose-dependent effect of subcutaneous MK-801 on acoustic startle response (top) and prepulse inhibition (bottom) in male C57BL/6J mice. The acoustic startle measure was based on the reflexive whole-body flinch, or startle response, following exposure to a sudden noise. Prepulse inhibition of the startle reflex refers to the normal suppression of startle the startle reflex when the pulse is immediately preceded by a prepulse. Saline (green, n=25), MK-801 at 0.5 mg/kg (blue, n=9), and MK-801 at 1 mg/kg (red, n=14). All treatments were administered 5 min before start of test. The results were expressed as mean \pm S.E.M. for all prepulses. Significantly different to saline group: # ($p < 0.001$), * ($p < 0.01$), and & ($p < 0.05$).

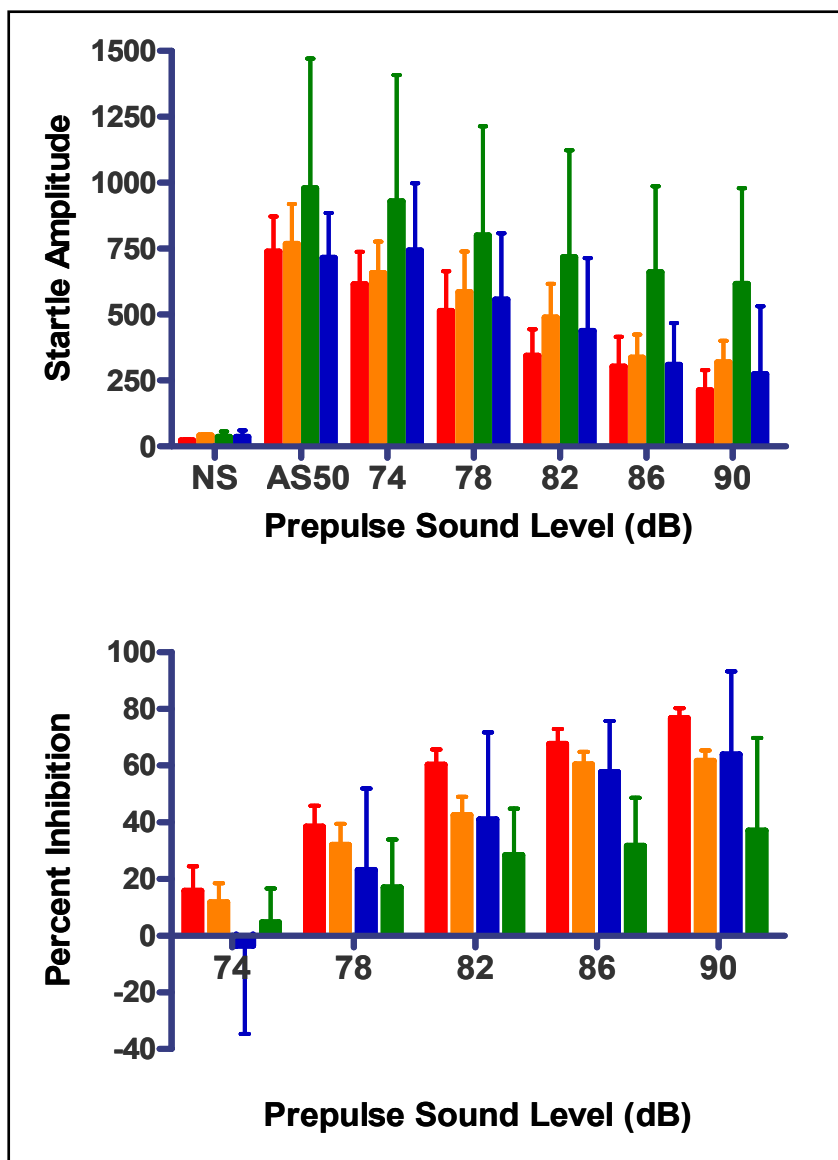


Fig. 5.12. Dose-dependent effect of ICV OT on acoustic startle response (top) and PPI (bottom) in mice treated with MK-801 (1 mg/kg) subcutaneously. The acoustic startle measure was based on the reflexive whole-body flinch following exposure to a sudden noise. Prepulse inhibition of the startle reflex is the suppression of this reflex when the pulse is immediately preceded by a prepulse. OT (ICV) and MK-801 (s.c.) were administered 50 and 5 min before test, respectively. Treatments: saline/saline (red, n= 11), saline/MK (orange, n= 11), OT 1 µg/ MK (blue, n= 7), and OT 3 µg/ MK (green, n= 8). MK-801 did not produce a significant change in startle amplitude nor in disruption of PPI.

801 at 1 mg/kg. OT by itself did not modify the baseline startle response per comparison with the saline/saline control group ($p>0.05$).

Treatment with OT showed a main treatment effect on prepulse inhibition [$F(5, 985) = 33.22, p<0.0001$]. OT significantly blocked the MK-801-elicited disruption of PPI at 86 and 90 dB prepulse level at 2 mg/kg and at 90 dB at 3 mg/kg (see fig 5.14.). This data suggested that OT could modulate glutaminergic modulation of PPI. The control group that was administered OT at 1 mg/kg with saline (OT/S group) did not show any significant differences with the baseline group (saline/saline, $p>0.05$).

Restoration of MK-801 disruption of PPI has been strongly associated with antipsychotic drugs, and it is considered a predictive marker for potential antipsychotic activity. The ability to restore NMDA antagonist-disrupted PPI is more selectively associated with members of the “atypical” antipsychotic family [142, 316-318]. Based upon its ability to restore MK-801 reduced PPI, oxytocin demonstrates a potent “atypical”-like antipsychotic profile [139]. In order to expand the therapeutic profile of OT, psychotomimetic-induced PPI disruption needed to be investigated with the dopamine agonist amphetamine. Administration of amphetamine at different concentrations (9-15 mg/kg) did not result in disruption of PPI or even startle amplitude increase as reported in the literature when compared to saline control groups (data not shown) [139, 206]. Amphetamine is one of the classical psychotomimetic drugs of choice to evaluate potential antipsychotic value of new drugs; therefore, our data did not seem correct. Further testing of amphetamine effects need to be done with newly-purchased drug to avoid any kind of degradation (our batch dated from 2001).

Since this study employed systemic injections of oxytocin, it is not possible to conclude whether the observed effects were mediated by central and/or peripheral sites. The highly selective nature of the effects produced by oxytocin in this study argues against a peripheral action, since startle amplitude and baseline PPI were not significantly affected. In fact, the only significant actions produced by oxytocin in this study amounted to a normalization of a centrally regulated process (PPI), which had been disrupted by centrally acting psychotomimetics. Since a small proportion of oxytocin, administered systemically, crosses the blood-brain barrier, a central site of action for the observed effects on PPI is quite feasible [139]. Other studies have also reported that systemic injections of oxytocin produce significant effects on centrally mediated behaviors [319-321] and evidence supports a central site of action for these effects. It was reported that nanogram-range doses of oxytocin administered intracerebroventricularly produced locomotor effects similar to milligram-range doses of the same peptide administered systemically [320].

Given the ability of OT to rescue MK-801 psychotomimetic effects in PPI, the next logical step was to investigate the effects of cmpd39, as there were no reports on mouse tests for it. Our pharmacological work demonstrated that cmpd39 selectively activated the OTR system in a similarly to the natural ligand OT. Therefore it was anticipated that this compound would elicit similar effects on PPI. This battery of tests would also be used for in the future to assess efficacy of selective activators of the OTR identified from high throughput screening. As explained previously, OTR agonists and allosteric modulators must cross the BBB to

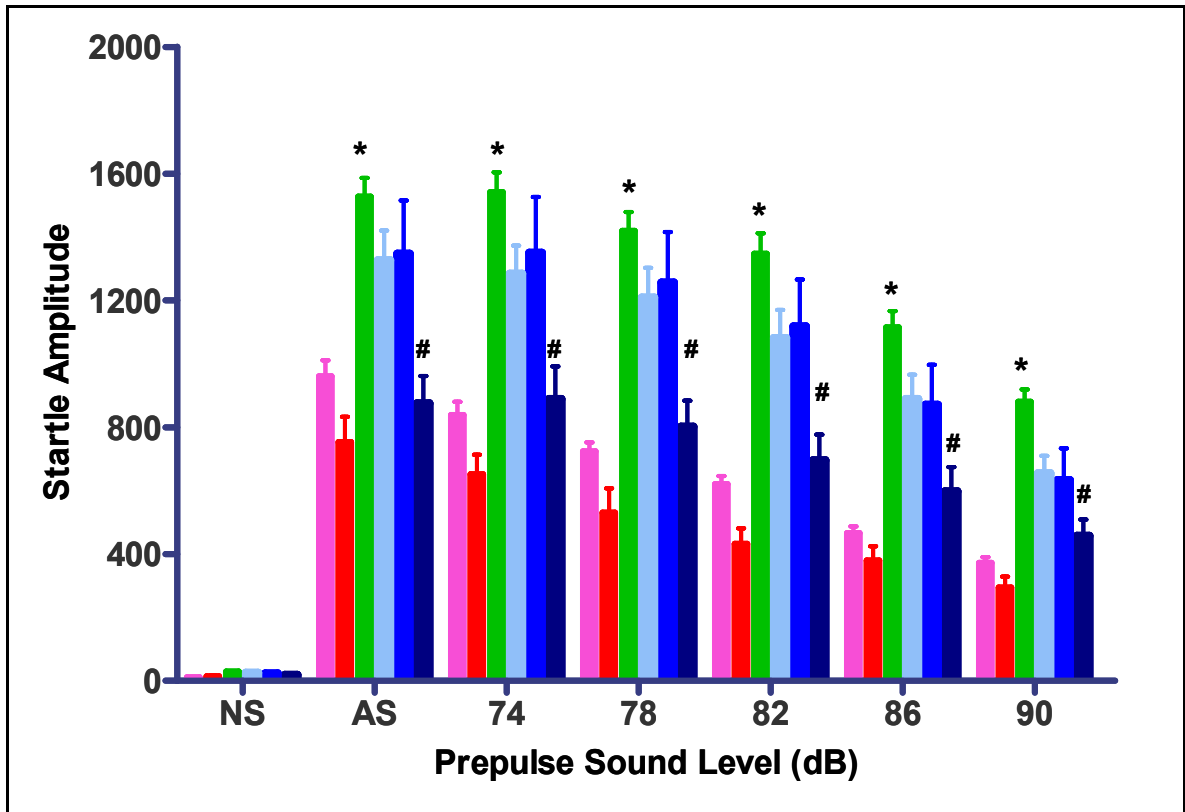


Fig. 5.13. Dose-dependent effects of i.p. OT on acoustic startle response in mice treated with s.c. injections of MK-801. The acoustic startle measure was based on the reflexive whole-body flinch following exposure to a sudden noise. Prepulse inhibition of the startle reflex is the suppression of the startle reflex when the pulse is immediately preceded by a prepulse. First injection was OT (1, 2, and 3 mg/kg) or saline (i.p.) 50 min before test. Second injection was saline or MK-801 (1 mg/kg, s.c.) 5 min before test. Treatment groups were: saline/saline (pink, n=47), OT/saline (red, 1 mg/kg, n= 12), saline/ MK-801 (green, 1 mg/kg, n= 75), OT/ MK-801 (light blue, 1 mg/kg, n= 38), OT/ MK-801 (blue, 2 mg/kg, n= 14), and OT/ MK-801 (dark blue, 3 mg/kg, n= 19). # No significant differences between the saline/saline and the OT 3 mg/kg /MK-801 groups ($p>0.05$). * Significant differences between the saline/saline and saline/MK-801 groups ($p<0.001$). The control groups saline/saline and OT 1 mg/kg/saline did not show significant differences. The data was analyzed using repeated measures ANOVA and Bonferroni post-hoc test.

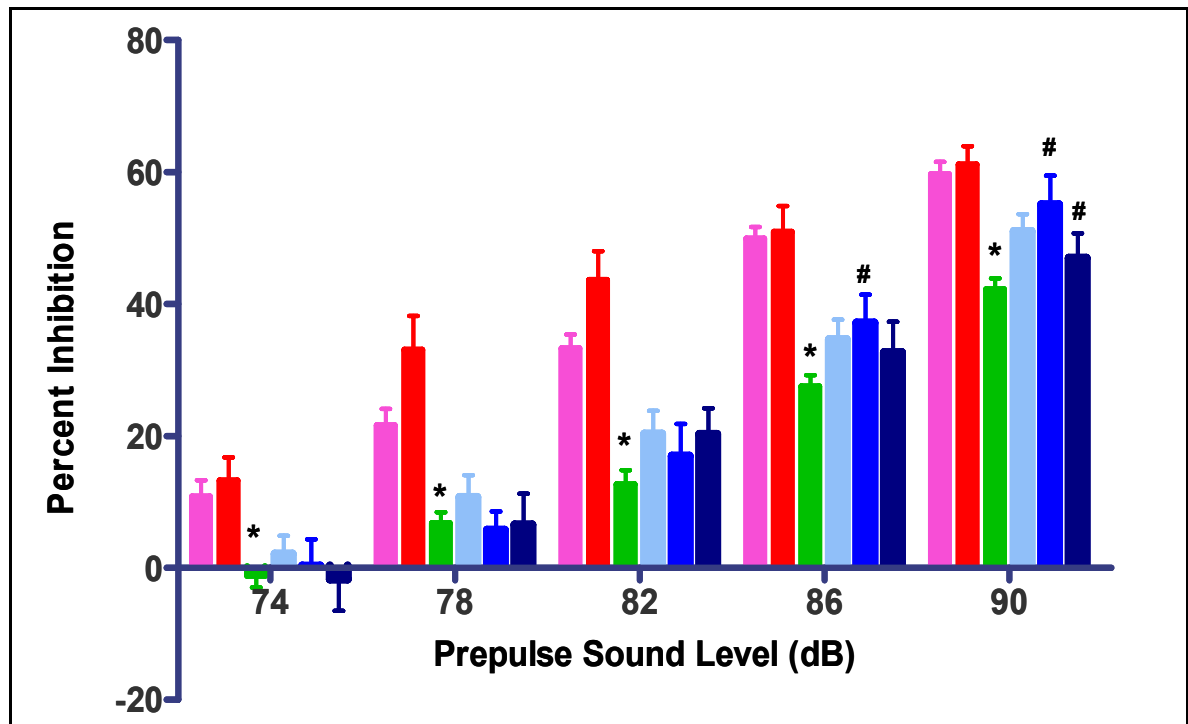


Fig. 5.14. Dose-dependent effects of i.p. OT on prepulse inhibition in mice treated with s.c. injections of MK-801. The acoustic startle measure was based on the reflexive whole-body flinch following exposure to a sudden noise. Prepulse inhibition of the startle reflex is the suppression of the startle reflex when the pulse is immediately preceded by a prepulse. First injection was OT (1, 2, and 3 mg/kg) or saline (i.p.) 50 min before test. Second injection was saline or MK-801 (1 mg/kg, s.c.) 5 min before test. Treatment groups were: saline/saline (pink, n=47), OT/saline (red, 1 mg/kg, n= 12), saline/ MK-801 (green, 1 mg/kg, n= 75), OT/ MK-801 (light blue, 1 mg/kg, n= 38), OT/MK-801 (blue, 2 mg/kg, n= 14), and OT/MK-801 (dark blue, 3 mg/kg, n= 19). # No significant differences between the saline/saline and the OT/MK groups ($p>0.05$). * Significant differences between the saline/saline and saline/MK-801 groups ($p<0.001$). The control groups saline/saline and OT 1 mg/kg/saline did not show significant differences. The prepulse inhibition was calculated as $100 - [(response\ amplitude\ for\ prepulse\ stimulus\ and\ startle\ stimulus\ together / response\ amplitude\ for\ startle\ stimulus\ alone) \times 100]$. The data was analyzed using repeated measures ANOVA and Bonferroni post-hoc test.

be successful. We anticipated that small molecules would cross the BBB more efficiently than OT as this peptide is larger in size.

We studied the effects of cmpd39 (10-100 mg/kg, i.p. 50 min prior to test) on reversal of PPI disruption produced by MK-801 (1 mg/kg, s.c., 5 min prior to test). Cmpd39 significantly attenuated MK-801 induced deficits in PPI at 75 mg/kg ($p < 0.0001$) (fig. 5.15.). For comparison, treatment with OT showed a main treatment effect on prepulse inhibition [$F(8, 835) = 24.96, p < 0.0001$]. In addition, cmpd39 showed startle amplitude values comparable to the saline control groups (fig. 5.16.). Treatment with cmpd39 showed a main treatment effect on startle response [$F(8, 1204) = 56.12, p < 0.0001$] and a significant overall interaction effect [$F(48, 1204) = 1.828, p = 0.0006$]. The administration of cmpd39 with a subsequent saline injection (cmpd39 control group) resulted in slightly lower startle amplitude values and a slight increase in PPI inhibition than saline control. This effect is suggestive that cmpd39 has antipsychotic properties. Lower doses of cmpd39 (10, 30, and 50 mg/kg) resulted in no significant effect on either startle amplitude or PPI. Notably, the highest dose administered (100 mg/kg) caused the mice to be very lethargic (maybe cataleptic?). Further observation (1 day) showed that this dose was not lethal. We hypothesize that the lethargy observed in these mice could be comparable to high doses of the commonly used, antipsychotic drug, haloperidol [322, 323].

In summary, our investigation of cmpd39 revealed a dose dependent profile of therapeutically relevant effects of antipsychotic-like activity in the PPI paradigm. It could be suggested that cmpd39 acts as an atypical antipsychotic as the psychotomimetic MK-801 induced deregulated glutaminergic neurotransmission

[189, 206]. Future investigation should include testing cmpd39 in PPI experiments by inducing psychosis with amphetamine, which has been historically used to identify typical antipsychotic drugs (see future plans).

Open field locomotion test. Motor activity underlies almost every mouse behavioral paradigm. Simple, automated tests of spontaneous locomotion are routinely performed. Photocell beam measurements of open field locomotion, in standard photocell-equipped automated open field equipment, can evaluate total amount of movement, rate of movement, and type of spontaneous activity. The open field test is also one of the oldest, most extensively used, and simplest measures of mouse and rat emotional behavior. Over 20 additional behavioral measures have been proposed as indices of emotionality/anxiety in the open field. Of these additional measures, rearing behavior, which decreases in an anxiogenic environment, and thigmotaxis, the proportion of time the animal remains close to the walls of the open field, are the additional behaviors most commonly assessed. High levels of ambulation and rearing are positively correlated with each other. Increasing the stressful properties of the open field, by increasing illumination level or background noise, generally results in decreased activity. Environmental conditions and prior treatments, such as handling, stress, surgery, and drug treatments, will affect performance in open field testing. In general, the C57 inbred strains of mice, including C57BL/6, consistently show high levels of open field locomotion, and low levels of anxiety-related measures in the open field. Strains typically exhibiting low

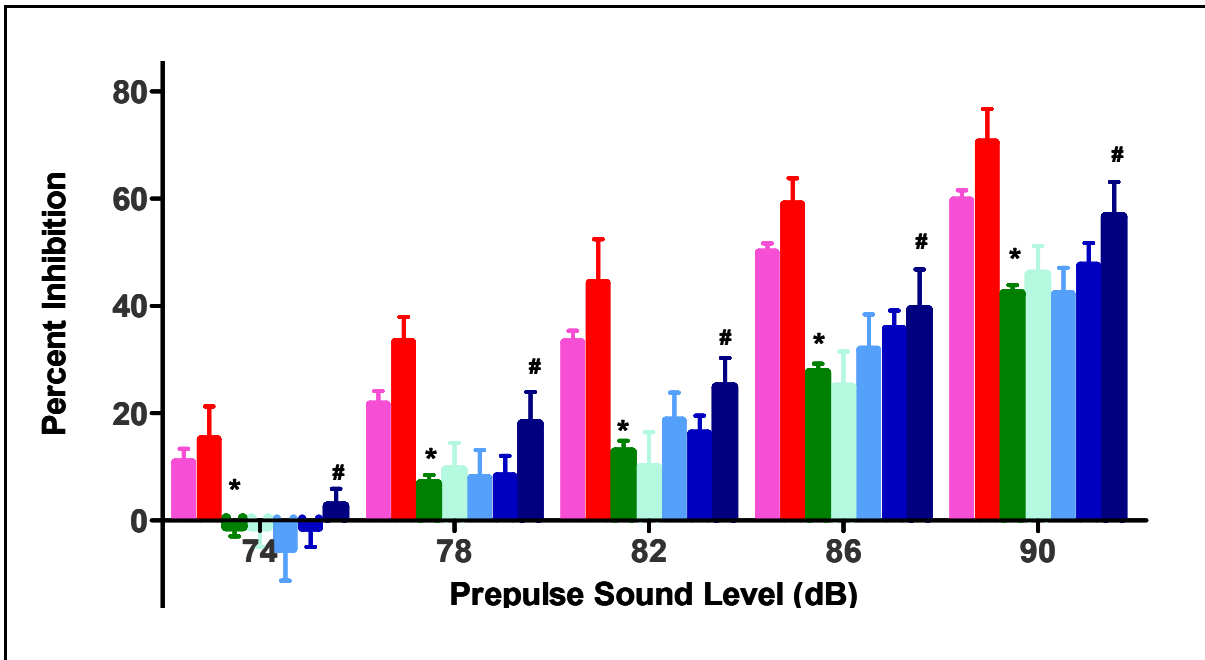


Fig. 5.15. Dose-dependent effects of i.p. cmpd39 on prepulse inhibition in mice treated with s.c. injections of MK-801. The acoustic startle measure was based on the reflexive whole-body flinch following exposure to a sudden noise. Prepulse inhibition of the startle reflex is the suppression of the startle reflex when the pulse is immediately preceded by a prepulse. First injection was cmpd39 (10, 30, 50, 75, or 100 mg/kg) or saline (i.p.) 50 min before test. Second injection was saline or MK-801 (1 mg/kg, s.c.) 5 min before test. Treatment groups were: saline/saline (pink, n=47), cmpd39/saline (red, 75 mg/kg, n= 14), saline/ MK-801 (green, 1 mg/kg, n= 73), cmpd39/ MK-801 (light blue, 10 mg/kg, n= 10), cmpd39/MK-801 (blue, 30 mg/kg, n= 10), cmpd39/MK-801 (darker blue, 50 mg/kg, n= 11), and cmpd39/MK-801 (darkest blue, 75 mg/kg, n= 14). Data not shown for cmpd39 at 100 mg/kg, see text. # No significant differences between the saline/saline and the cmpd39/MK groups ($p > 0.05$). * Significant differences between the saline/saline and saline/MK-801 groups ($p < 0.001$). The control groups saline/saline and cmpd39 75 mg/kg/saline did not show significant differences. The prepulse inhibition was calculated as $100 - [(response\ amplitude\ for\ prepulse\ stimulus\ and\ startle\ stimulus\ together / response\ amplitude\ for\ startle\ stimulus\ alone) \times 100]$. The data was analyzed using repeated measures ANOVA and Bonferroni post-hoc test.

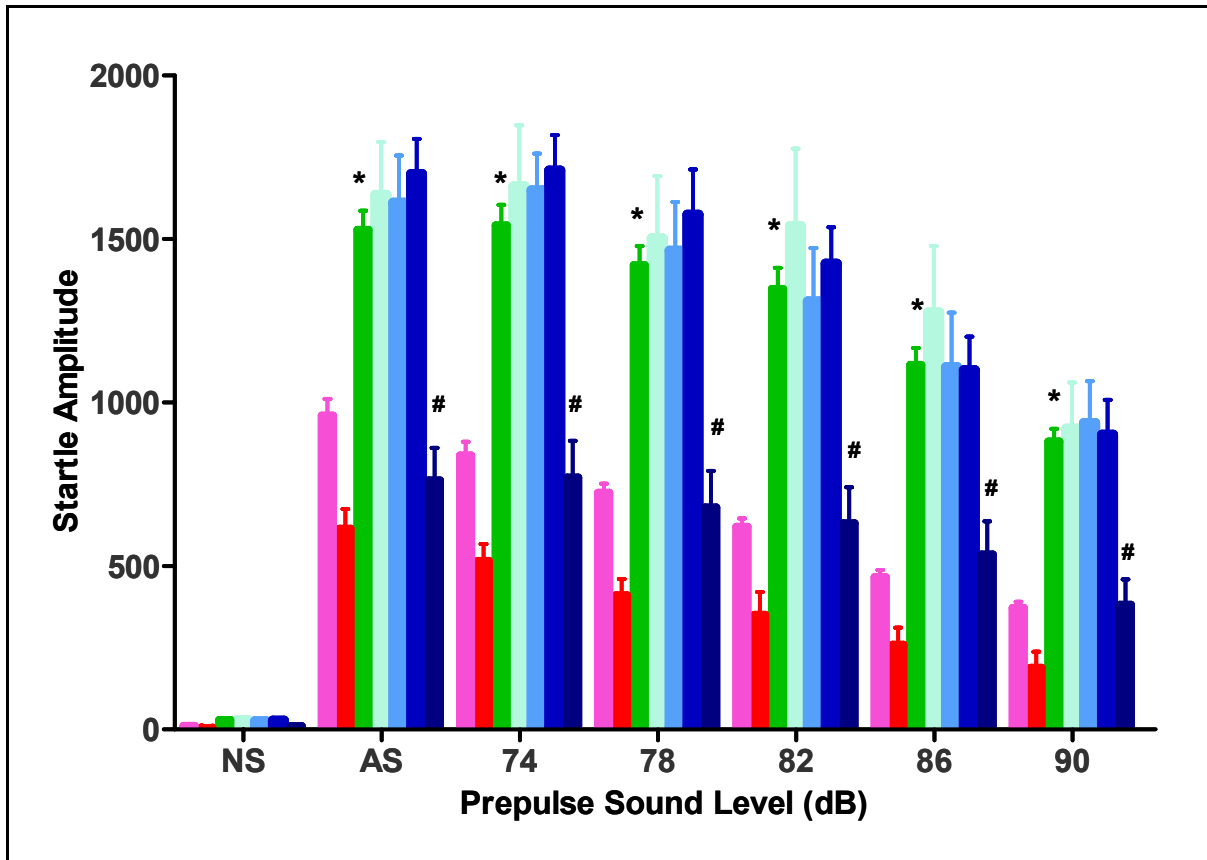


Fig. 5.16. Dose-dependent effects of i.p. cmpd39 on acoustic startle response in mice treated with s.c. injections of MK-801. The acoustic startle measure was based on the reflexive whole-body flinch following exposure to a sudden noise. Prepulse inhibition of the startle reflex is the suppression of the startle reflex when the pulse is immediately preceded by a prepulse. First injection was cmpd39 (10, 30, 50, or 75 mg/kg) or saline (i.p.) 50 min before test. Second injection was saline or MK-801 (1 mg/kg, s.c.) 5 min before test. Treatment groups were: saline/saline (pink, n=47), cmpd39/saline (red, 75 mg/kg, n= 8), saline/ MK-801 (green, 1 mg/kg, n= 75), cmpd39/ MK-801 (light blue, 10 mg/kg, n= 10), cmpd39/MK-801 (blue, 30 mg/kg, n= 10), cmpd39/MK-801 (darker blue, 50 mg/kg, n= 14) and cmpd39 /MK-801 (darkest blue, 75 mg/kg, n= 13). # No significant differences between the saline/saline and the cmpd39/MK groups ($p>0.05$). * Significant differences between the saline/saline and saline/MK-801 groups ($p<0.001$). The control groups saline/saline and cmpd39 75 mg/kg/saline did not show significant differences. The data was analyzed using repeated measures ANOVA and Bonferroni post-hoc test.

locomotor activity and high levels of emotional reactivity include DBA/1, BALB/c and A/J [288].

Immediately following the elevated plus maze test, mice were given a 15-min test in a novel open field. Measures were taken of ambulation (distance traveled), fine movements (the repeated breaking of the same set of photo-beams), rearing movements, and time spent in the center region, an index of anxiety-like behavior (fig. 5.17.). Untreated and non-cannulated male C57BL/6J mice were tested to assess any differences caused by the ICV cannulation. Treatment with OT led to higher locomotor activity [treatment main effect on distance traveled, $F(1, 14) = 5.36$, $p = 0.0363$]. Significant differences were not observed for the other measures.

Male C57BL/6J non-cannulated mice were tested to compare saline, OT (1 mg/kg, i.p.), and MK-801 (1 mg/kg, s.c.) for future reference as control groups (single injection test). Mice first underwent the acoustic startle test before being immediately placed into the open field boxes to assess activity for a period of 3 h. In all, the mice were introduced into the activity chambers 75 min after the first injection for a total time of 3 h. Treatment with OT and MK-801 showed main effect differences and an overall interaction effect in every parameter measured (see fig. 5.18.). Higher levels of activity in mice treated with MK-801 were observed. Specifically, mice that received a MK-801 treatment showed increased horizontal activity, fine movements, distance traveled and time spent in center region, and rearing movements (vertical activity) after 130 min. These results show that the maximal efficacy of i.p. administered drugs was obtained during this time frame. Interestingly, the rearing movements were decreased compared to the saline group

from the beginning of the test for 40 min. Treatment of OT (1 mg/kg) resulted in a notable decrease of total activity as shown by decreased horizontal activity, total distance traveled, rearing and fine movements (fig. 5.18.). Time spent in the center region, which is used as an index of anxiety-like behavior was decreased for the first 30 min. The statistical results are shown in table 5.1. Together, these data are consistent with an anxiolytic-like effect of OT on treated mice.

Further analysis of the data obtained for this single injection test showed that the main treatment differences were observed in the 75-105 min and 135-255 min intervals. The most significant differences in the initial interval (75-105 min) were present in the OT group. This could suggest OT's maximal efficacy window. On the contrary, the differences found in the final time frame (135-255 min) could represent the degradation of OT and the persistence of the MK-801. Fig. 5.19. represents the overall differences observed in those specific time intervals and their statistical significance.

We then investigated the effect of OT dose on open field locomotion in mice treated with MK-801 (1 mg/kg). Non-cannulated C57BL/6J mice tested in the acoustic startle paradigm were immediately placed in the activity chamber to assess differences among treatments. In particular, we anticipated that OT could rescue the MK-801 effect. The effects observed corresponded to treatment effects in the 75 to 190 min interval (2 hs test). Treatment with several OT concentrations showed main effect differences and an overall interaction effect in every parameter measured (see table 5.2.). In the horizontal and total distance traveled (fig. 5.20.), MK-801 showed a marked difference ($p < 0.001$) compared to the saline/saline group, especially after

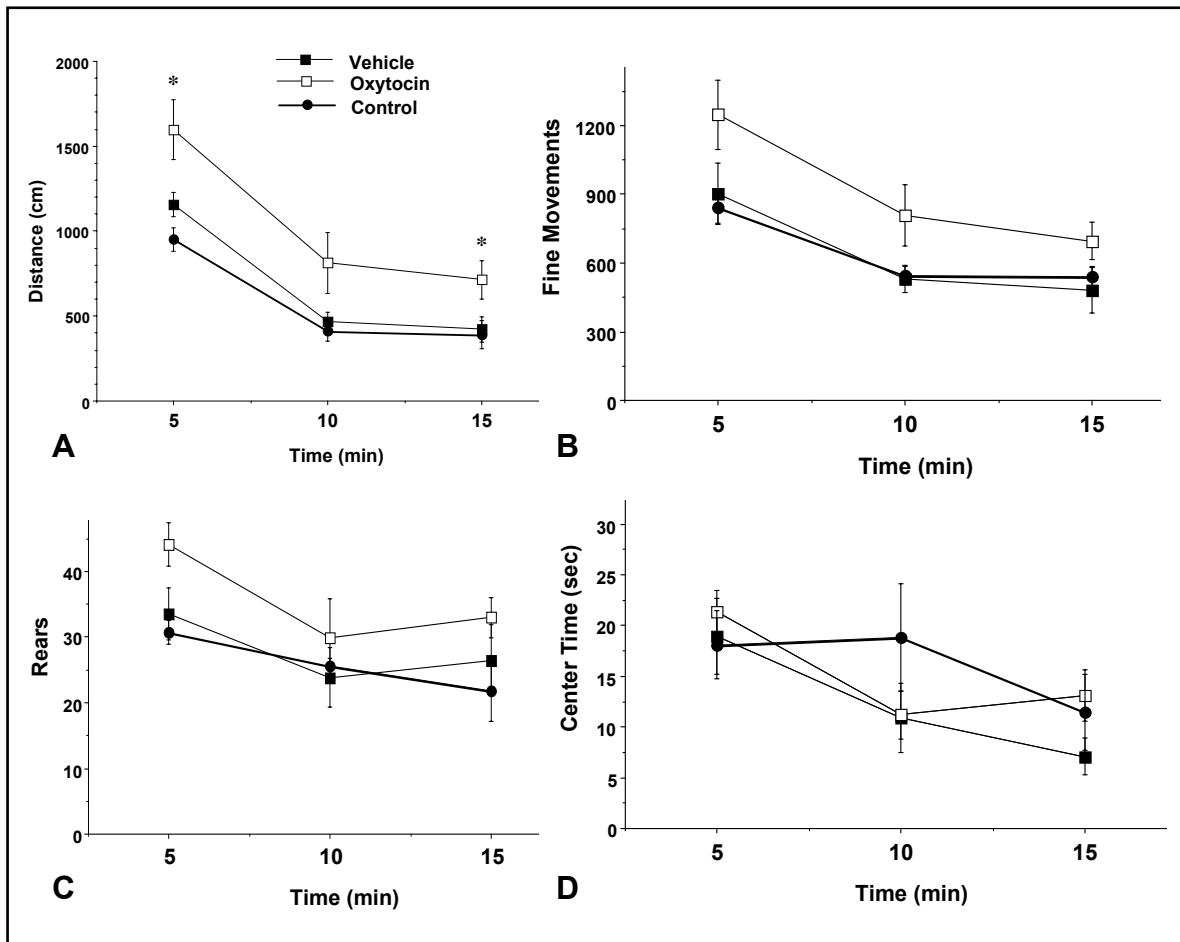


Fig. 5.17. OT effect in the open field test for ICV cannulated male mice (15 min). Untreated and non-cannulated male C57BL/6J mice were tested to assess any differences caused by the ICV cannulation. Vehicle group (n= 8), and oxytocin group (n=8) received saline or OT (1 μ g) ICV injection, respectively. Control group (n=5) was non-injected non-cannulated male mice. A. Distance traveled and B. fine movements showed significant differences ($p < 0.05$). C. Rearing movements and D. time spent in the center region did not show significant differences.

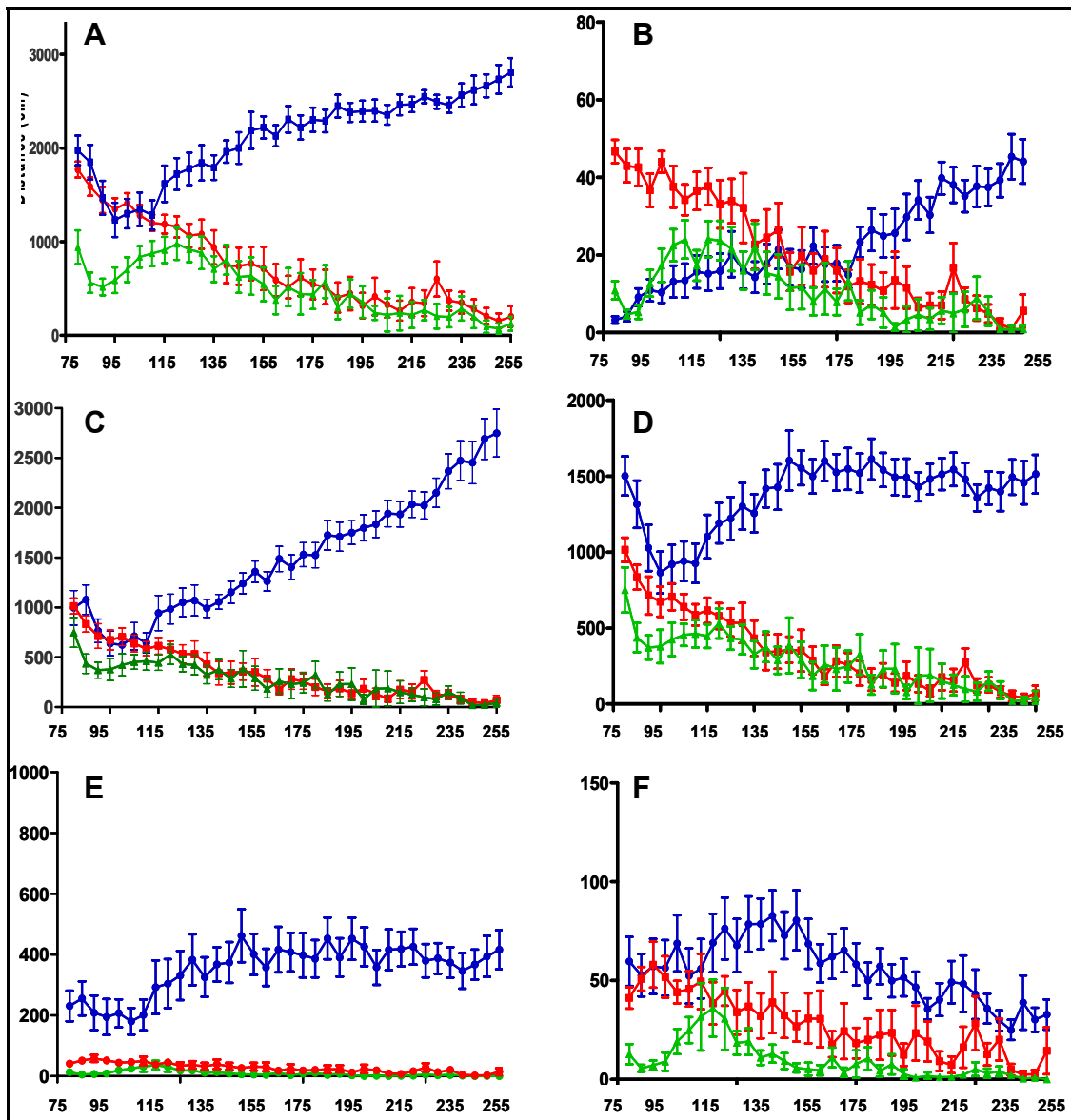


Fig 5.18. OT and MK-801 intraperitoneal effect in a 3 hs open field test for non-cannulated male mice. Male C57BL/6J non-cannulated mice were tested to compare saline (red, n= 10), OT (1 mg/kg, green, n=10), and MK-801 (1 mg/kg, blue, n=10) for future reference as control groups (single injection test). Y-axis on the right represents distance (cm). X-axis represents time (min). A. Distance traveled horizontally. C. Total distance traveled. E. Distance traveled in center region. B. Upright rearing movements, Y-axis represents rear movements. D. Repetitive fine movements, Y-axis represent repeated breaking of the same set of photobeams). F. Time spent in center region (s).

Parameter	Effect	F value (df ₁ ,df ₂)	p value
HACT	main treatment	F (2, 1332) = 1080	<0.0001
	overall interaction	F (70, 1332) = 8,243	<0.0001
TOTDIST	main treatment	F (2, 972) = 532.5	<0.0001
	overall interaction	F (70, 972) = 7.894	<0.0001
FINE MOVEMENTS	main treatment	F (70, 720) = 758.2	<0.0001
	overall interaction	F (70, 720) = 2.809	<0.0001
CTRDIST	main treatment	F (2, 1332) = 378.8	<0.0001
	overall interaction	---	---
CTRTIME	main treatment	F (2, 1332) = 136.2	<0.0001
	overall interaction	---	---
REAR MOVEMENTS	main treatment	F (2, 1332) = 58.68	<0.0001
	overall interaction	F (70, 1332) = 6.131	<0.0001

Table 5.1. Statistical data obtained for OT, saline, and MK-801 intraperitoneal effect in a 3 hs open field test for non-cannulated male mice. Male C57BL/6J non-cannulated mice were tested to compare saline, OT, and MK-801 for future reference as control groups (single injection test). HACT: Horizontal distance traveled. TOTDIST: Total distance traveled. FINE MOVEMENTS: Repetitive fine movements. CTRDIST: Distance traveled in the center region. CTRTIME: Time spent in the center region. REAR MOVEMENTS: Upright rearing movements. Df: degrees of freedom.

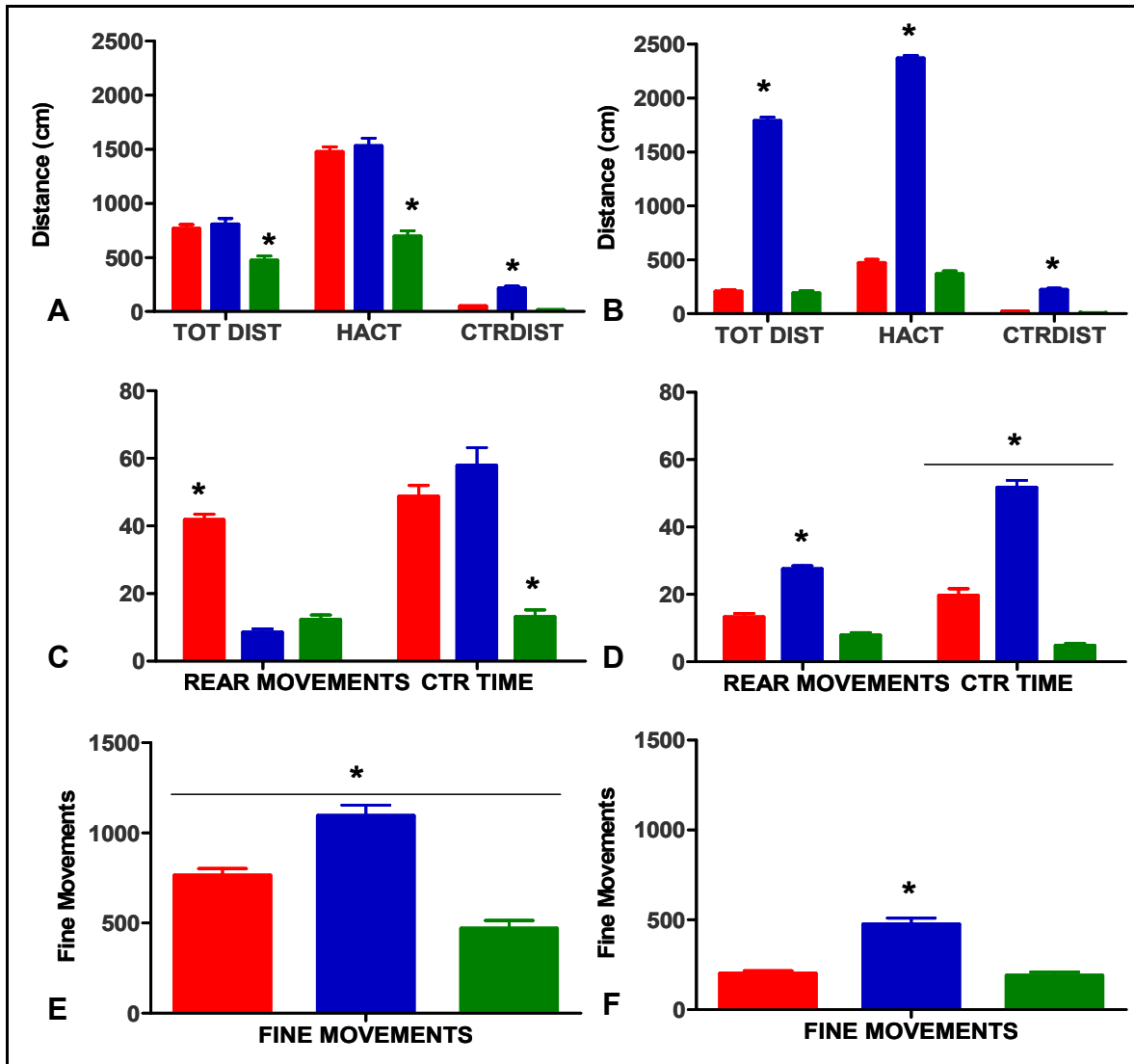


Fig 5.19. OT and MK-801 intraperitoneal effect in an open field test: 75-105 and 135-255 min intervals. The values for each 5 min interval had been added to provide a better understanding of the drug effects in each time period. Saline (red, n= 60), OT (1 mg/kg, green, n=60), and MK-801 (1 mg/kg, blue, n=120) control groups. A, C, and E. represent the data for the 75-105 min interval. A and B. Total (TOT DIST), horizontal (HACT), and center (CTRDIST) distances traveled. C and D. Rearing movements (y-axis= rear #) and time spent in center region (y-axis= time in s). E and F. Repetitive fine movements. Data are expressed as mean \pm S.E.M. * Significant differences between groups ($p < 0.001$). The data was analyzed using repeated measures ANOVA and Bonferroni post-hoc test.

Parameter	Effect	F value (df ₁ ,df ₂)	p value
HACT	main treatment	F (4, 1152) = 237.3	<0.0001
	overall interaction	F (92, 1152) = 6.051	<0.0001
TOTDIST	main treatment	F (4, 1152) = 66.61	<0.0001
	overall interaction	F (92, 1152) = 8.129	<0.0001
FINE MOVEMENTS	main treatment	F (4, 1152) = 273.6	<0.0001
	overall interaction	F (92, 1152) = 7.760	<0.0001
CTRDIST	main treatment	F (4, 1152) = 71.97	<0.0001
	overall interaction	F (92, 1152) = 2.468	---
CTRTIME	main treatment	F (4, 1152) = 168.7	<0.0001
	overall interaction	---	---
REAR MOVEMENTS	main treatment	F (4, 1152) = 23.43	<0.0001
	overall interaction	---	<0.0001

Table 5.2. Statistical data obtained for OT dose dependent effect in the open field locomotion test (2 h) for non-cannulated male mice. Male C57BL/6J non-cannulated mice were tested for effects of MK-801 in locomotion and the properties of OT to block these effects. Mice were investigated immediately after finishing ASR test. Male C57BL/6J non-cannulated mice were tested. HACT: Horizontal distance traveled. TOTDIST: Total distance traveled. FINE MOVEMENTS: Repetitive fine movements. CTRDIST: Distance traveled in the center region. CTRTIME: Time spent in the center region. REAR MOVEMENTS: Upright rearing movements. Df: degrees of freedom.

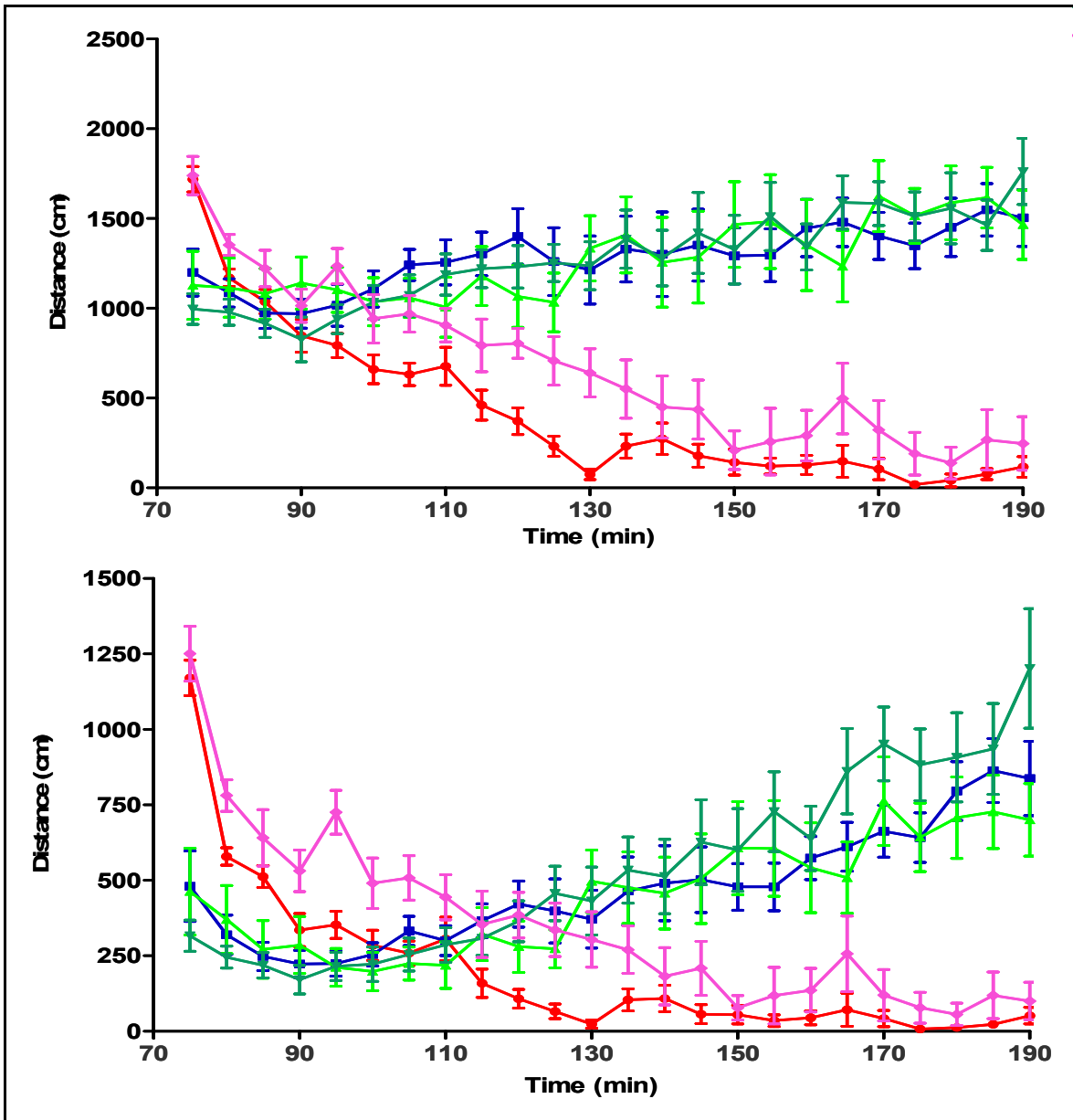


Fig. 5.20. OT dose dependent effect in the horizontal (top) and total (bottom) distance traveled for the open field locomotion test (2 hs). Male C57BL/6J non-cannulated mice were tested for effects of MK-801 in locomotion and the properties of OT to block these effects. Mice were investigated immediately after finishing ASR test. OT and MK-801 were administered i.p. 50 min and s.c. 5 min before ASR test, respectively. Saline/ saline (red, n= 14), OT/saline (1 mg/kg, pink, n=7), saline/MK-801 (1 mg/kg, blue, n=12), OT/MK-801 (2 mg/kg, light green, n=10), and OT/MK-801 (3 mg/kg, dark green, n=10). Data are expressed as mean \pm S.E.M.

45 min of starting this test. This can be attributed at the long lasting effect of this psychotomimetic drug, and it can be also concluded that the MK-801 effect lasts for more than 3 hs. OT did not elicit any effects by itself. OT did not attenuate the effect of preadministered MK-801 at any dose tested.

Mice that were injected with S/MK-801 spent more time in this region in the 80 to 170 min interval (see fig. 5.21., top). This effect was certainly not caused by anxiolytic-type effects as the total distance traveled in this interval is lower; most likely the mice could not move properly as there is an observable motor dysfunction elicited by the MK-801. This same effect was observed with the OT/MK-801 treatment which suggested that OT did not attenuate the MK-801 effect. OT alone did not show any significant effects by itself.

The saline/MK-801 and the OT/saline groups did not show any differences in distance traveled in the center region ($p > 0.05$) when compared with the saline/saline group (see fig. 5.21., bottom). It was of interest to note that both OT/MK-801 doses were significantly different than the saline/saline control for the last 40 min of the test. This result suggests an additive effect of MK-801 combined with OT.

The S/MK-801 group showed an increase in repetitive fine movements ($p < 0.001$) for the last 90 min of the test when compared to the saline/saline group (see fig. 5.22., top), and OT did not overcome this effect. OT itself did not affect fine movements when compared to the saline/saline control group ($p > 0.05$). Finally, none of the groups presented any differences in upright rearing movements ($p > 0.05$). The statistical parameters are shown in table 5.2.

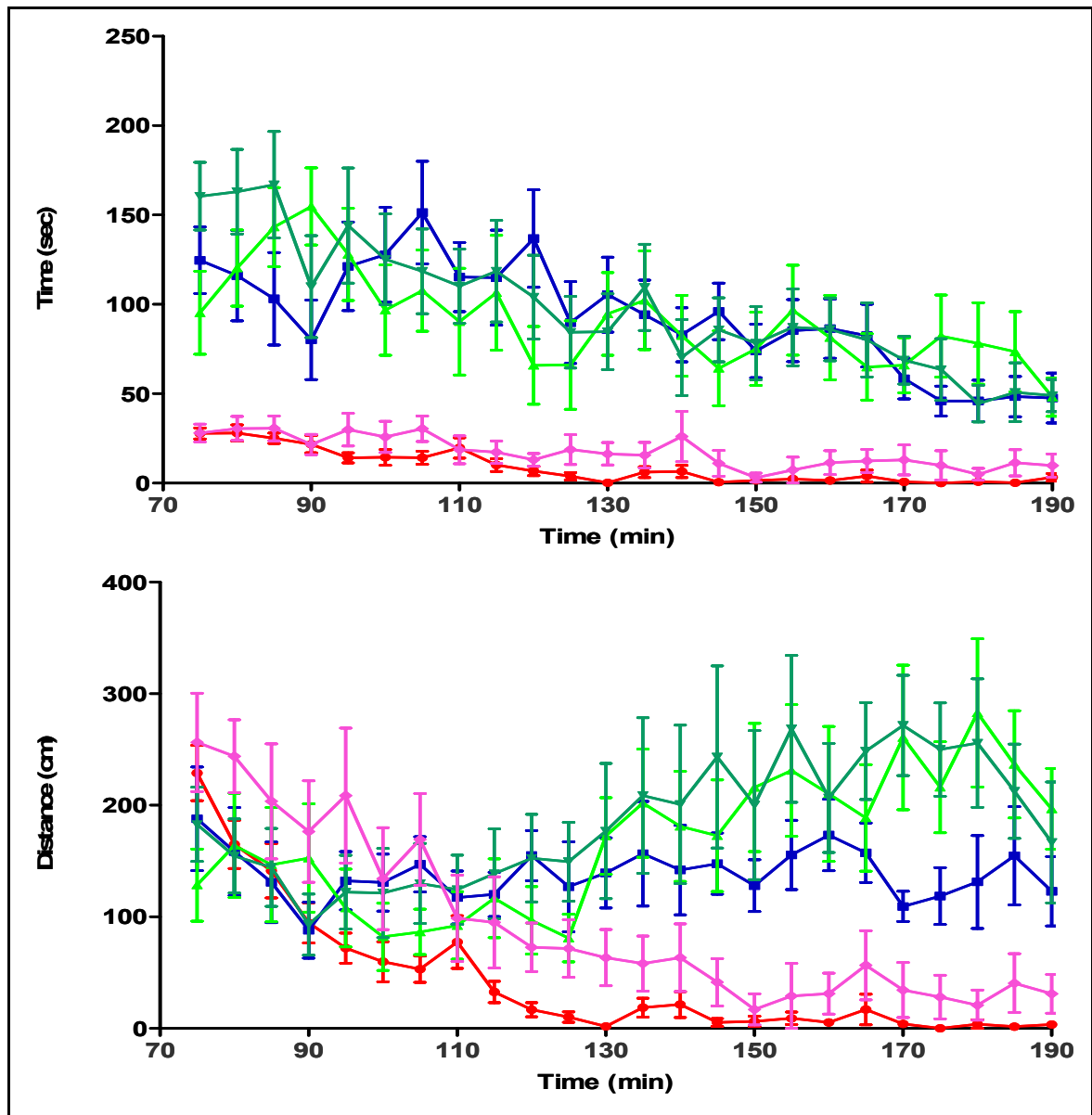


Fig. 5.21. OT dose dependent effect in time spent (top) and distance traveled (bottom) in the center region for the open field locomotion test (2 hs). Male C57BL/6J non-cannulated mice were tested for effects of MK-801 in locomotion and the properties of OT to block these effects. Mice were investigated immediately after finishing ASR test. OT and MK-801 were administered i.p. 50 min and s.c. 5 min before ASR test, respectively. Saline/ saline (red, n= 14), OT/saline (1 mg/kg, pink, n=7), saline/MK-801 (1 mg/kg, blue, n=12), OT/MK-801 (2 mg/kg, light green, n=10), and OT/MK-801 (3 mg/kg, dark green, n=10). Data are expressed as mean \pm S.E.M.

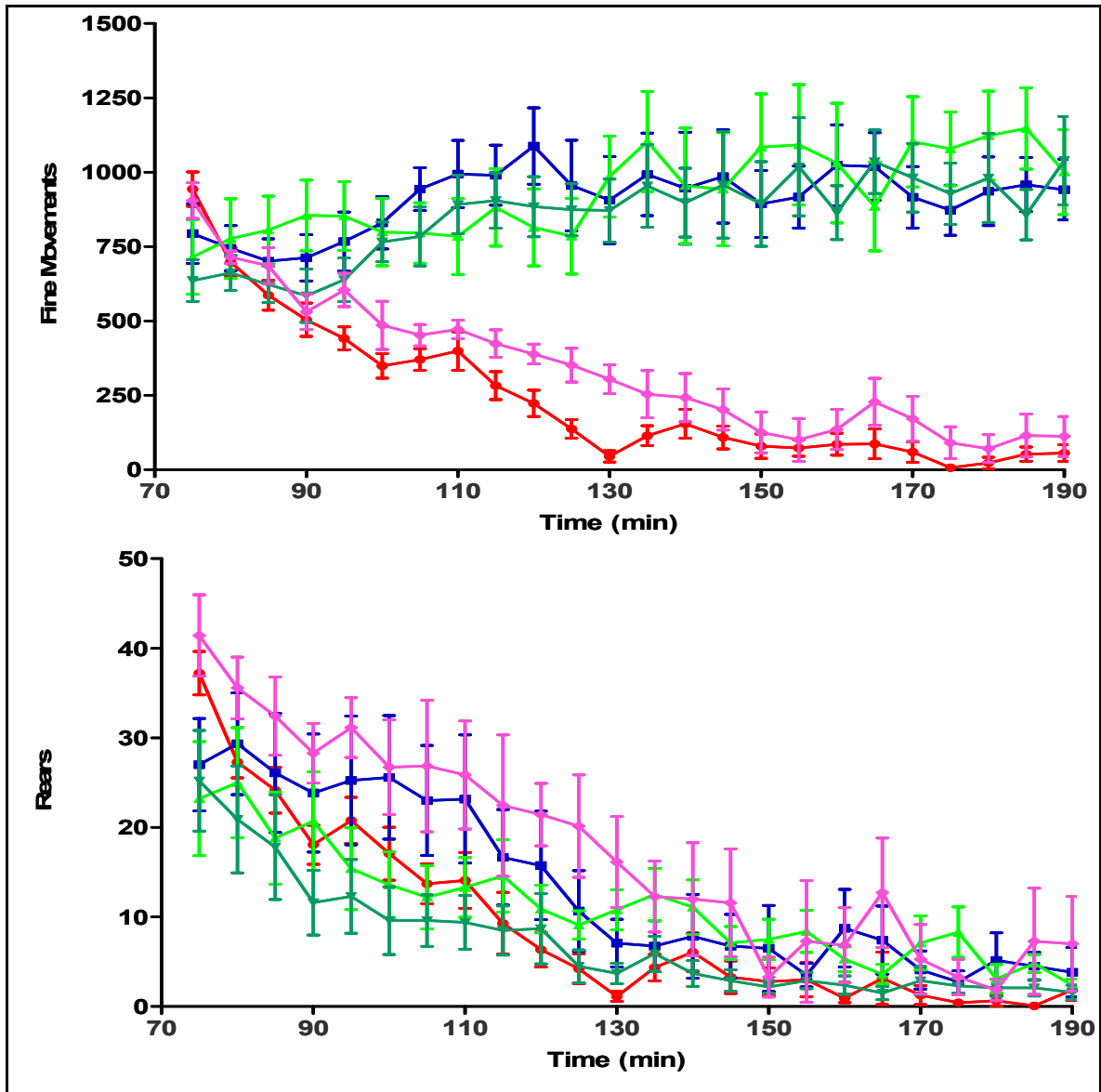


Fig 5.22. OT dose dependent effect in repetitive fine movements (top) and upright rearing movements (bottom) of the open field locomotion test (2 h).

Male C57BL/6J non-cannulated mice were tested for effects of MK-801 in locomotion and the properties of OT to block these effects. Mice were investigated immediately after finishing ASR test. OT and MK-801 were administered i.p. 50 min and s.c. 5 min before ASR test, respectively. Saline/ saline (red, n= 14), OT/saline (1 mg/kg, pink, n=7), saline/MK-801 (1 mg/kg, blue, n=12), OT/MK-801 (2 mg/kg, light green, n=10), and OT/MK-801 (3 mg/kg, dark green, n=10). Data are expressed as mean \pm S.E.M.

This open field activity test did not show any dose dependent OT effects to mitigate the MK-801 properties, at least during the time frame investigated. This could be due to the fact that administered OT could be degraded before the mice entered the open field locomotion test (see future plans).

Our focus then shifted to the evaluation of the effects elicited by cmpd39 in the open field locomotion test. We supposed that the synthetic compound may enjoy a longer half-life in vivo. Mice that underwent the acoustic startle response test were immediately placed in activity chambers to evaluate drug effects for 2 hs. The effects of cmpd39 were tested at 50 and 75 mg/kg (i.p.). Subjects were placed in the chamber exactly 75 min after administration of the first drug (saline or cmpd39) and their movements were recorder for 120 min in intervals of 5 min each.

Compound 39 affected overall performance of the mice in the open field test, mainly at 75 mg/kg. Treatment with several cmpd39 concentrations showed main effect differences and an overall interaction effect in every parameter measured (see fig. 5.23., 5.24., and 5.25.). The group that received the saline/MK-801 treatment showed differences in the distance traveled horizontally and in the center region. This group also spent more time in the center region and showed an increase in fine repetitive movements, replicating the results obtained in the single injection test explained above. Cmpd39 at 75 mg/kg seemed to have some effect on distance travelled horizontally with defined effects at different time frames; less investigation was observed at the beginning of the test and an increase later on when compared to the saline/saline control group. Similar time dependent effects were observed for this group in the fine and upright rearing movements. The control group that

received cmpd39/ saline as a treatment did not show important differences with the saline/saline control group; therefore, cmpd39 did not elicit any effect by itself. The statistical parameters are shown in table 5.3.

In order to better understand the effects of cmpd39 in the open field locomotion test and since time-dependent effects were seen on the different treatment groups; the results when broken down into two time frames: 75-110 and 115-145 min after first injection. Treatment with cmpd39 concentrations showed main effect differences in every parameter measured for both intervals investigated (see table 5.4.).

In the earliest interval, cmpd39 showed lower horizontal, total, and center region distances traveled (fig. 5.26. A, C, and E) and upright rearing movements (fig. 5.27.C) compared to the saline/saline control, while it did not show any changes in the time spent in the center region (fig. 5.27. E). Regarding fine movements, cmpd39 seemed to have overcome the effects of MK-801 (fig. 5.27.A). At the latest time point, mice treated with cmpd39 exhibited appreciable differences compared with the saline/MK-801 group. Treatment with S/MK or cmpd39/MK showed significant differences with the saline/saline group ($p < 0.001$) as well (fig. 5.26 and 5.27). Overall, the results demonstrated that cmpd39 attenuated MK-801 induced deficits in PPI at 75 mg/kg.

Our investigation of OT and cmpd39 revealed a profile of therapeutically relevant effects of antipsychotic-like activity in the PPI paradigm. These results provide new insights into the role of OTR as a site of action for OT effects on CNS function, and the significance of these findings to future development of OTR

agonists as neuropsychiatric therapeutics [206]. Our results support the use of compd39 as a probe to discern the intricacy of the OTR system and its involvement in complex behaviors and neuropsychiatric diseases.

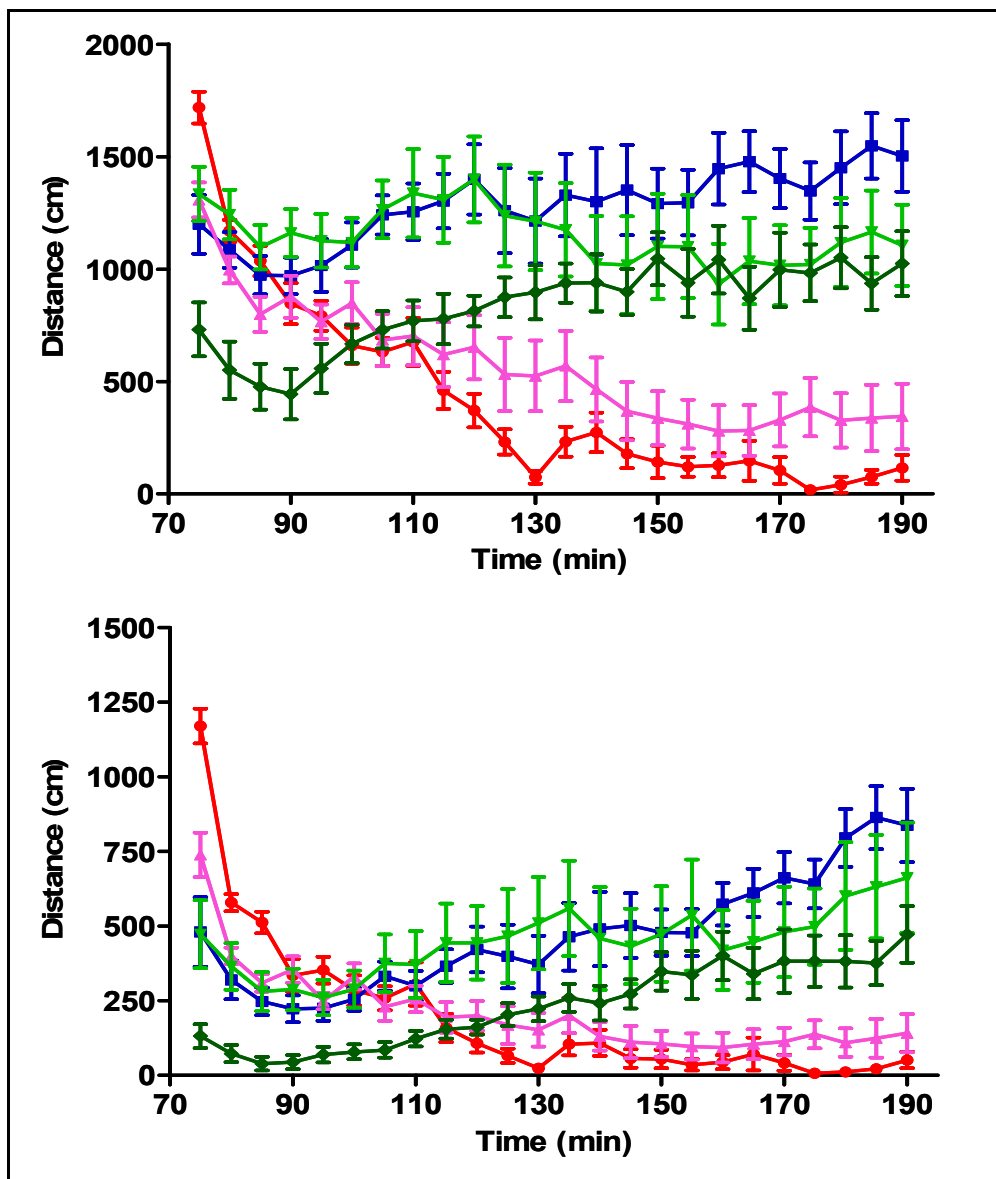


Fig. 5.23. Cmpd39 dose dependent effect in the horizontal (top) and total (bottom) distance traveled for the open field locomotion test (2 h). Male C57BL/6J non-cannulated mice were tested for effects of MK-801 in locomotion and the properties of OT to block these effects. Mice were investigated immediately after finishing ASR test. Cmpd39 and MK-801 were administered i.p. 50 min and s.c. 5 min before ASR test, respectively. Saline/ saline (red, n= 14), cmpd39 /saline (75 mg/kg, pink, n=14), saline/MK-801 (1 mg/kg, blue, n=12), cmpd39/MK-801 (50 mg/kg, light green, n=10), and cmpd39/MK-801 (75 mg/kg, dark green, n=10). Data are expressed as mean \pm S.E.M.

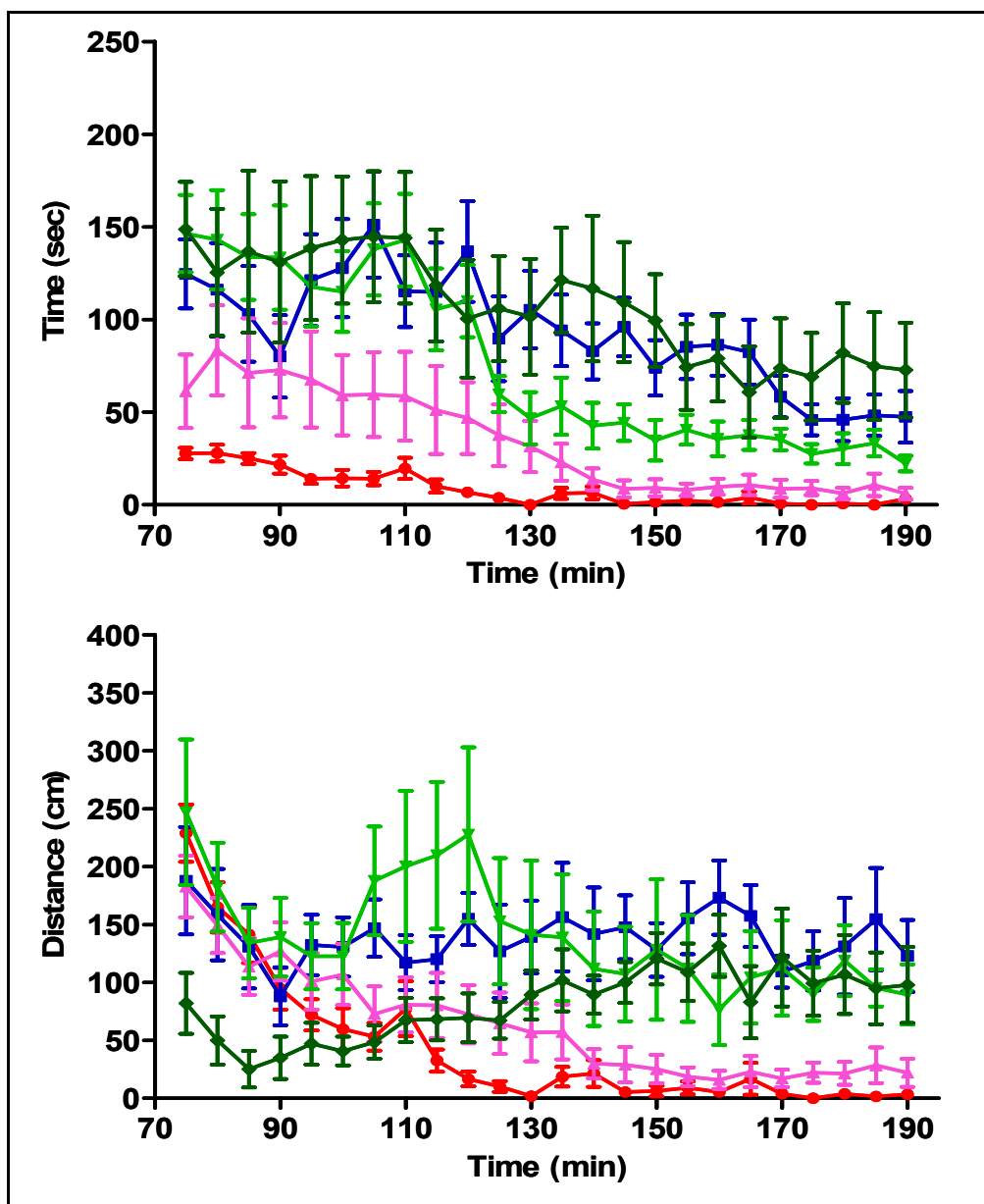


Fig. 5.24. Cmpd39 dose dependent effect in time spent (top) and distance traveled (bottom) in the center region for the open field locomotion test (2 h). Male C57BL/6J non-cannulated mice were tested for effects of MK-801 in locomotion and the properties of OT to block these effects. Mice were investigated immediately after finishing ASR test. OT and MK-801 were administered i.p. 50 min and s.c. 5 min before ASR test, respectively. Saline/ saline (red, n= 14), cmpd39 /saline (75 mg/kg, pink, n=14), saline/MK-801 (1 mg/kg, blue, n=12), cmpd39/MK-801 (50 mg/kg, light green, n=10), and cmpd39/MK-801 (75 mg/kg, dark green, n=10). Data are expressed as mean \pm S.E.M.

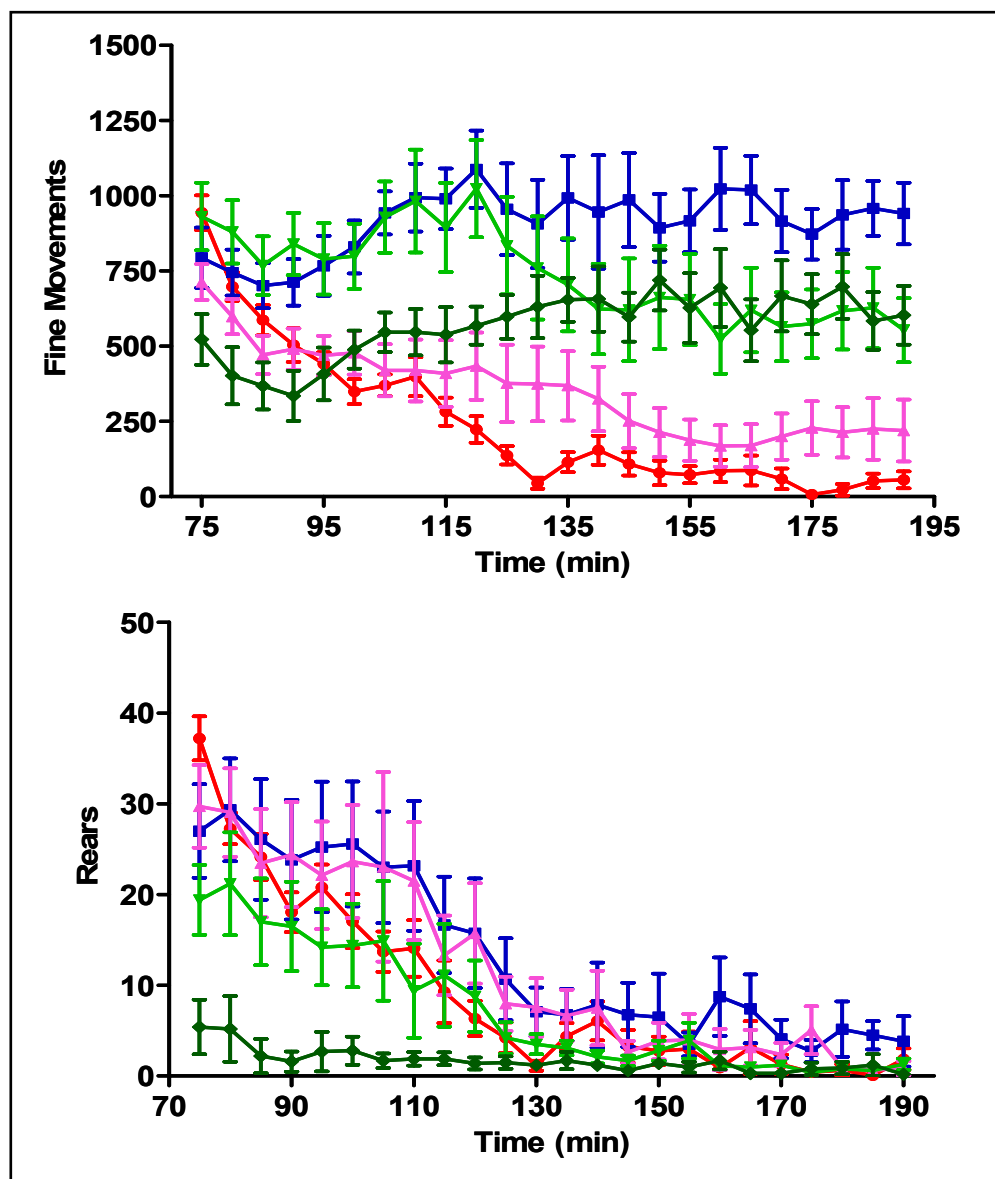


Fig. 5.25. Cmpd39 dose dependent effect in repetitive fine movements (top) and upright rearing movements (bottom) of the open field locomotion test (2 h). Male C57BL/6J non-cannulated mice were tested for effects of MK-801 in locomotion and the properties of OT to block these effects. Mice were investigated immediately after finishing ASR test. OT and MK-801 were administered i.p. 50 min and s.c. 5 min before ASR test, respectively. Saline/ saline (red, n= 14), cmpd39/saline (75 mg/kg, pink, n=14), saline/MK-801 (1 mg/kg, blue, n=12), cmpd39/MK-801 (50 mg/kg, light green, n=10), and cmpd39/MK-801 (75 mg/kg, dark green, n=10). Data are expressed as mean \pm S.E.M.

Parameter	Effect	F value (df ₁ ,df ₂)	p value
HACT	main treatment	F (4, 1320) = 209.2	<0.0001
	overall interaction	F (92, 1320) = 4.378	<0.0001
TOTDIST	main treatment	F (4, 1152) = 66.61	<0.0001
	overall interaction	F (92, 1152) = 8.129	<0.0001
FINE MOVEMENTS	main treatment	F(4, 1152) = 273.6	<0.0001
	overall interaction	F (92, 1152) = 3.652	<0.0001
CTRDIST	main treatment	F (4, 1320) = 63.69	<0.0001
	overall interaction	F (92, 1320) = 1.929	---
CTRTIME	main treatment	F (4, 1320) = 126.5	<0.0001
	overall interaction	---	---
REAR MOVEMENTS	main treatment	F (4, 1320) = 35.17	<0.0001
	overall interaction	F (92, 1320) = 1.275	<0.0001

Table 5.3. Statistical data obtained for cmpd39 dose dependent effect in the open field locomotion test (2 h) for non-cannulated male mice. Male C57BL/6J non-cannulated mice were tested for effects of MK-801 in locomotion and the properties of cmpd39 to block these effects. Mice were investigated immediately after finishing ASR test. Male C57BL/6J non-cannulated mice were tested. HACT: Horizontal distance traveled. TOTDIST: Total distance traveled. FINE MOVEMENTS: Repetitive fine movements. CTRDIST: Distance traveled in the center region. CTRTIME: Time spent in the center region. REAR MOVEMENTS: Upright rearing movements. Df: degrees of freedom.

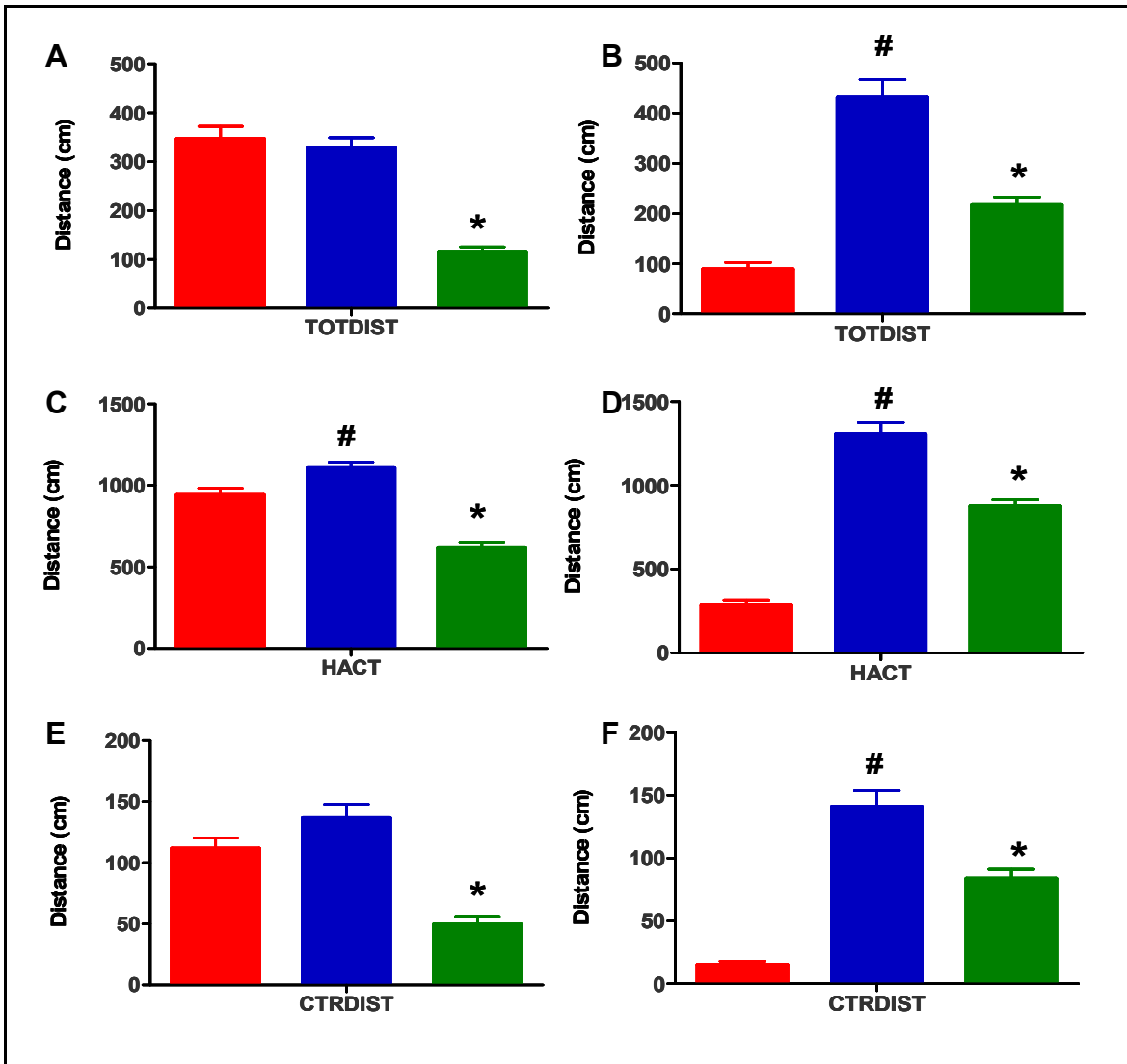


Fig. 5.26. Cmpd39 and MK-801 effect in an open field test (TOTDIST, HACT, and CTRDIST): 75-110 (left) and 115-145 (right) min intervals. Male C57BL/6J non-cannulated mice were tested for effects of MK-801 in locomotion and the properties of cmpd39 to block these effects. Saline/saline (red, n= 60), cmpd39/MK (75 mg/kg/ 1 mg/kg, green, n=60), and saline/MK-801 (1 mg/kg, blue, n=120). A and B. Total distance traveled (TOT DIST). C and D. Horizontal distance traveled (HACT). E and F. Center distance traveled (CTRDIST). Data are expressed as mean \pm S.E.M. * Significant differences between cmpd39/MK and saline/saline control group ($p < 0.001$). # Significant differences between saline/MK and saline/saline control group ($p < 0.01$).

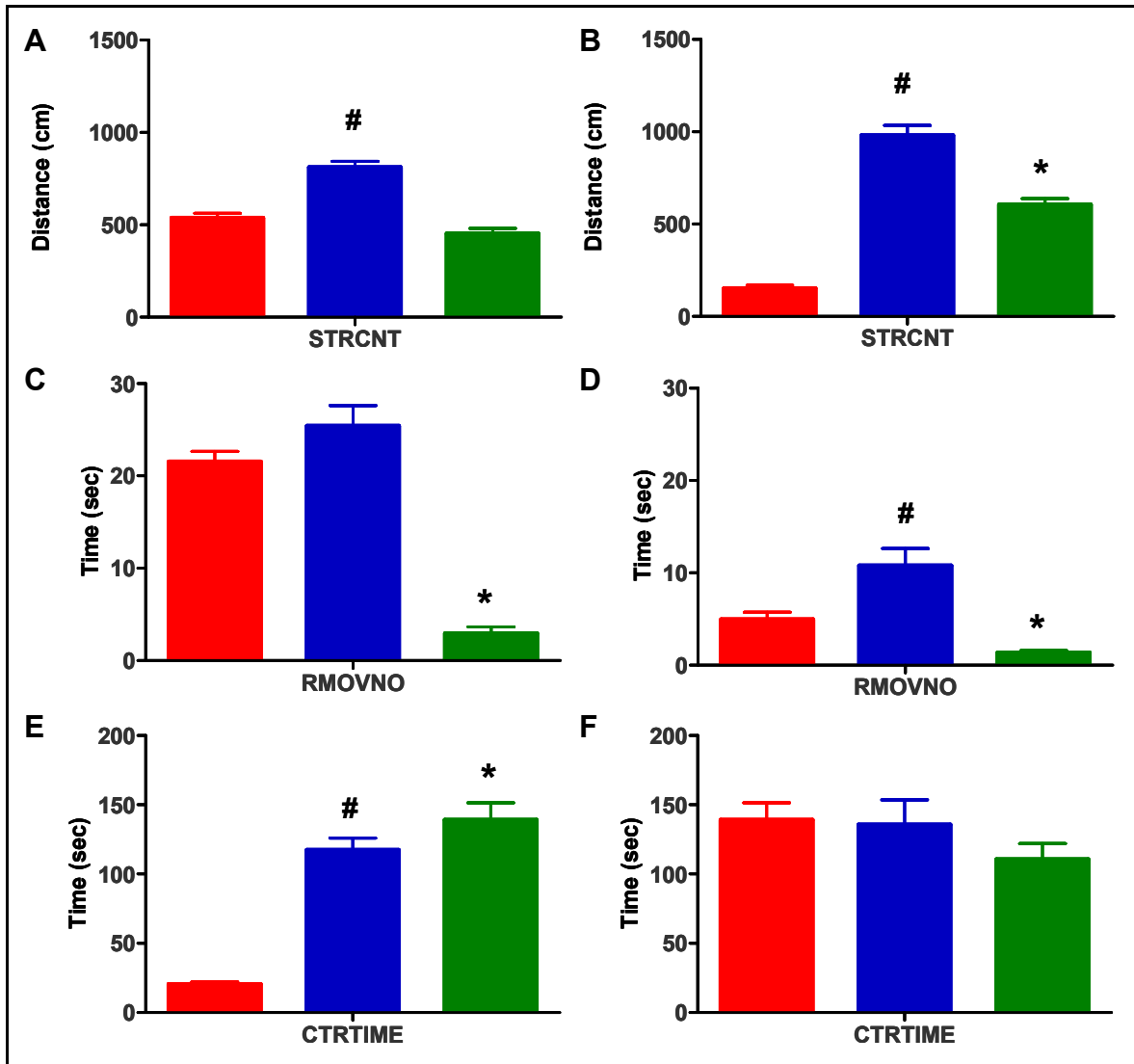


Fig. 5.27. Cmpd39 and MK-801 effect in an open field test (STRCNT, RMOVNO, and CTRTIME): 75-110 (left) and 115-145 (right) min intervals. Male C57BL/6J non-cannulated mice were tested for effects of MK-801 in locomotion and the properties of cmpd39 to block these effects. Saline/saline (red, n= 60), cmpd39/MK (75 mg/kg/ 1 mg/kg, green, n=60), and saline/MK-801 (1 mg/kg, blue, n=120). A and B. Repetitive fine movements (STRCNT). C and D. Upright rearing movements (RMOVNO). E and F. Time spent in center region (CTRTIME). Data are expressed as mean \pm S.E.M. * Significant differences between cmpd39/MK and saline/saline control group ($p < 0.001$). # Significant differences between saline/MK and saline/saline control group ($p < 0.01$).

Parameter	Interval (min)	F value (df ₁ ,df ₂)	p value
HACT	75-110	F (2, 285) = 35.61	<0.0001
	115-145	F (2, 249) = 130.1	<0.0001
TOTDIST	75-110	F (2, 429) = 31.7	<0.0001
	115-145	F (2, 249) = 53.70	<0.0001
FINE MOVEMENTS	75-110	F (2, 285) = 41.85	<0.0001
	115-145	F (2, 249) = 142.6,	<0.0001
CTRDIST	75-110	F (2, 285) = 20.69	<0.0001
	115-145	F (2, 249) = 63.25	---
CTRTIME	75-110	F (2, 285) = 68.75	<0.0001
	115-145	F (2, 187) = 1.464	0.2340
REAR MOVEMENTS	75-110	F (2, 285) = 55.99	<0.0001
	115-145	F (2, 237) = 16.39	<0.0001

Table 5.4. Statistical data obtained for cmpd39 dose dependent effect in the open field locomotion test (2 h) for non-cannulated male mice during the two intervals investigated (75-110 and 115-145). Male C57BL/6J non-cannulated mice were tested for effects of MK-801 in locomotion and the properties of cmpd39 to block these effects. Mice were investigated immediately after finishing ASR test. Male C57BL/6J non-cannulated mice were tested. HACT: Horizontal distance traveled. TOTDIST: Total distance traveled. FINE MOVEMENTS: Repetitive fine movements. CTRDIST: Distance traveled in the center region. CTRTIME: Time spent in the center region. REAR MOVEMENTS: Upright rearing movements. Df: degrees of freedom.

FUTURE PLANS

Immediate future investigation should include testing OT and cmpd39 in the startle response model using amphetamine. This psychotomimetic has been historically used to identify typical antipsychotic drugs through the dopaminergic system [189]. An amphetamine PPI disruption effect should be demonstrated first with a subsequent investigation of the potential OT and cmpd39 to regulate dopaminergic neurotransmission in schizophrenia.

The locomotion activity tests showed promising effects for cmpd39 to overcome MK-801 hyperactivity. On the contrary, MK-801-dependent hyperactivity could not be mitigated by OT at any dose tested. Thorough investigation of these effects should include repeating the open field locomotion test administering either OT or cmpd39 at t=0 min and immediately placing the mice in the activity chambers. After 30 min the mice should be removed from the chambers to receive an MK-801 dose and returned to the boxes to assess activity for at least another 90 min. This scheme should provide information on the effects of the test drug alone from the first 30 min, and also it will offer valuable data about the half life of OT and cmpd39.

An interesting approach would be to test these compounds in a mouse line that expresses low levels of the NMDA R1 subunit (NR1) of the NMDA receptor that has been generated to model endogenous NMDA hypofunction. These mutant mice showed increased locomotor activity, increased acoustic startle reactivity, and deficits in prepulse inhibition (PPI) of acoustic startle [299]

One of the main mouse behavioral assays that are relevant to the symptoms of autism is sociability. Acquiring a social memory as opposed to remembering an

object is key to normal human functioning, and impairments in social interaction are a defining feature of autism [324]. Revisiting the social memory test should provide important data to assess drug efficacy to recuperate this type of memory. In order to investigate this behavior, there is a need to obtain OT-KO mouse as there is compelling evidence that shows the social memory deficits that these mice have [62, 64]. This model should be used to reproduce the reported findings that showed that OT regulates social memory and to assess the efficacy of cmpd39 to mimic the OT effects. We have recently established communications with Dr. W. Scott Young from the Laboratory of Cellular and Molecular Regulation at the NIMH and he has agreed to kindly provide us with a breeding pair of this mouse line. His group has also developed a Cre-loxP conditional knockout mouse line of the oxytocin receptor. This mice line could be useful to allow inactivation of the receptor in specific sites at defined times to better understand the roles of the OTR [325].

The Mouse Behavioral Phenotyping Laboratory, directed by Dr. Sheryl Moy, has been developing a mouse test for repetitive, restricted behaviors which are a core symptom of autism. Their results show that the mouse strain NR1neo/neo present more repetitive nose poke responses than wildtype mice [326]. This lab has also reported low social preference, abnormal overt motoric stereotypy, and resistance to changes in a learned pattern of behavior for the inbred mouse strain C58/J [327]. It would be interesting to investigate the effects of OT and cmpd39 to assess if these molecules can modify these behaviors.

Finally, the validated selective molecules that will be obtained through the HTS at the NIH screening center (see chapter 3) will undergo testing to evaluate

their effects on OT-regulated complex behaviors. Initially, these compounds will be tested in the acoustic startle response and open field locomotion tests to calculate their influence in regulation of these behaviors in comparison to the natural ligand OT.

CHAPTER 6

FUTURE PLANS

The oxytocin pathway is a very intriguing and exciting system that promises interesting advances in deciphering the mystery of how complex behavior is regulated (see fig.6.1.). We could take that knowledge and use it to our advantage to treat some neuropsychiatry disorders that thus far have only been addressed and treated to cope with symptoms rather than addressing the underlying causes. Many options and routes are available to provide new information on this system, from molecular pharmacology to provide insight on how prospective agonists and allosteric modulators activate the OT pathway to human studies that could, in the future, be used as therapeutical tools to improve the quality of life of patients who have been diagnosed with complex neuropsychiatric disorders, such as schizophrenia, autism spectrum disorders, depression, compulsive-obsessive disorders. This chapter intends to cover some of the possibilities that the investigation of the OT pathway can provide to the advancing of the understanding of the neuropharmacological control of social behavior. Short-term future plans have been already discussed at the end of each individual chapter.

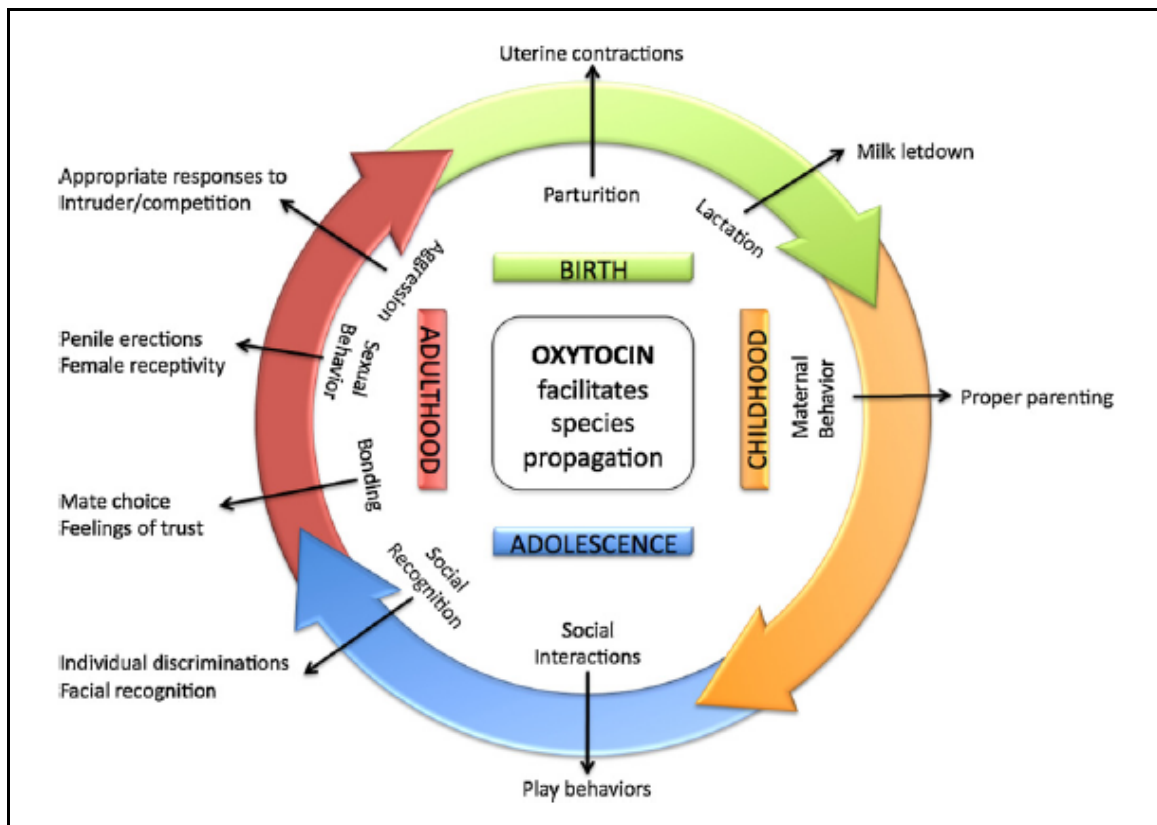


Fig.6.1. A simple cycle of life illustrates numerous points at which OT may affect behaviors and physiology to facilitate the propagation of the species. Picture borrowed from [102].

High-throughput screening campaign

The main goal of this dissertation work was to identify small molecules probes of the OT pathway. Significant progress has been made; however, we determined that screening a larger library is necessary to make greater progress. The ultra-highthroughput screen campaign is being done at the Scripps High Throughput Screening Core in Florida. The initial hits from that campaign will be selected by statistical analysis and cluster sampling. Confirmation of these hits will include EC₅₀ calculations, structure and purity assessment of the original sample and resynthesis, purification and/or purchase of the compounds for further investigation. The successful actives will be prioritized according to selectivity against vasopressin receptors, developability of the molecules, mechanism of action, synthetic tractability, and novelty of the structures. The hit-to-lead plan will include activity-structure relationship assays (SAR), and the chemistry plan will cover the definition of the key hurdles for each series and the definition of a lead compound.

The optimization of the lead compounds will be focused on *in vivo* assays, drug metabolism and pharmacokinetics (DMPK) studies, solubility, permeability, and toxicity assessment. The *in vivo* assays will focus in mechanism of action confirmation by pharmacokinetic/ pharmacodynamic (pk/pd) and efficacy evaluations. The DMPK studies should include *in vivo* and *in vitro* (CYP450). Finally, toxicity should be evaluated at least *in vitro*, through obtaining a consensus value (CV) for the ion channel h-erg and the evaluation in hepatocytes, and *in vivo*, by acute and chronic exposure of the compound for 7 days in rats.

Molecular pharmacology of the OTR system

One possible approach that could be followed in the future would be to investigate the molecular pharmacology of the validated small molecules. In the near future, it would be interesting to set up a research project to investigate how and where compound 39 binds to the receptor. Mutagenesis studies should answer these questions and provide data for concise SAR studies.

The discovery and validation of positive allosteric modulators of the OTR would open new scenery that has never been reported. Interesting research topics would include molecular pharmacology that will investigate binding site, allosteric activity (how does the molecule enhance receptor activation from a distance), and receptor active conformations.

Mouse models for regulation of complex behavior

Since we have confirmed that OT and compound 39 reverse prepulse inhibition deficits in MK-801-treated mice [328], it would be interesting to pursue the investigation of the mechanism that underlies this regulation. An initial step should include distinction, if any, between regulation of this phenomenon through the dopaminergic or glutaminergic pathways. The results would support the use of compound 39 as a probe to discern the intricacy of the OTR system and its involvement in complex behaviors and neuropsychiatric diseases.

One of the main mouse behavioral assays that are relevant to the symptoms of autism is sociability. Acquiring a social memory as opposed to remembering an object is key to normal human functioning, and impairments in social interaction are

a defining feature of autism [324]. Revisiting the social memory test described in Chapter 5 should provide important data to assess drug efficacy to recuperate this type of memory. These experiments would benefit from the use of OT-KO mouse as there is compelling evidence that these mice display deficits in social memory [62, 64]. Dr. W. Scott Young from the Laboratory of Cellular and Molecular Regulation at the NIMH has agreed to provide us with a breeding pair of OT-KO mice. Further investigation of social memory using conditional OT and OTR knockouts [325, 329] and tissue-specific knockout will allow also more detailed analyses of the role of the OT pathway in social memory [102].

The Mouse Behavioral Phenotyping Laboratory, directed by Dr. Sheryl Moy, has been developing a mouse test for repetitive, restricted behaviors which are a core symptom of autism. Their results show that the mouse strain NR1neo/neo presents more repetitive nose poke responses than wildtype mice [326]. This lab has also reported low social preference, abnormal overt motoric stereotypy, and resistance to changes in a learned pattern of behavior for the inbred mouse strain C58/J [327]. It would be interesting to investigate the effects of OT and compound 39 to assess if these molecules can modify these behaviors.

Use of OT and agonists as therapeutic tools for the treatment of complex behavior

The involvement of OT in these stages of human behavior promises a variety of therapeutic benefits that need to be explored. OT, OTR selective agonists, and positive allosteric modulators will enrich the current knowledge on the OT system

and will help elucidate the roles of OT in establishing and regulating complex behaviors at the CNS level. They will also serve as new chemical tools to elucidate the complex roles for OT in these behaviors, and they will provide new potential leads for a drug discovery campaign in the treatment of specific neuropsychiatric disorders.

Sexual behavior

Since OT is involved in both men and women's sexual behavior, could OT and OTR agonists be the ecstasy (MDMA) of the future? Certainly, OT and any molecule that activates the OTR receptor could be evaluated for treatment of anorgasmia or other sexual dysfunctions.

Generosity

Similar to the trust game, intranasal OT increases generosity (Subject 1 gives money to Subject 2 while taking into consideration the amount Subject 2 finds acceptable), but not overall altruism (Subject 1 gives to Subject 2 with no feedback from Subject 2 [67]). Therefore, OT seems to particularly affect the ability to understand others' emotions, i.e., affects empathy. Intranasal OT increases the amount of time spent gazing at the eye region of human faces [70] as well as the likelihood of recalling a happy face [330]. Intranasal OT also improves the ability to infer the mental state of others from social cues in the eye region [68]. Similarly, intranasal OT attenuates feelings of negativity towards faces conditioned with negative affective ratings, particularly in faces with direct gaze [331]. OT may thus increase feelings of trust and empathy by increasing eye gaze and subsequent

understanding of social cues. Overall, this line of research should investigate further the findings that OT enhances feelings of generosity, trust, and may aid in detection and understanding of others' feelings (empathy) [102]. Using allosteric modulators in human trust and generosity tests, specifically using the intranasal route, would allow testing the effects of the endogenous hormone avoiding use of large doses of OT.

Depression, anxiety, and mood disorders

OT imbalances have been associated with both anxiety and depression, though direct evidence for OT's role as a therapeutic agent is still awaited. Given the presence of OT receptors in the hypothalamus and extended amygdala and its link to HPA function and mood, there is potential for therapeutic use of OT in mood disorders [89, 102, 332-334].

Autism

Autism spectrum disorders (ASD) are labeled as pervasive developmental disorders, and can include other medical disorders, such as retardation and seizures, and psychological problems, such as heightened anxiety [335]. Recently, much effort has gone into determining the underlying causes of autism and related disorders. The positive relationship between OT and formation of social bonds in animal studies [336] has led many to believe that OT abnormalities may play a part in autism. Intravenous infusion of OT into adults with autism and Asperger's disorder significantly reduces both number and severity of repetitive behaviors (such as repeating, self-injury, and touching) and increases ability to comprehend and

remember the affective component of spoken words (happy, indifferent, angry, or sad) [158, 159]. There is strong evidence of the possible link between OT and autism, as well as other neuropsychiatric disorders [25, 102]. Investigation of the effects of OTR agonists and allosteric modulators in core symptoms tests would provide the benefits of OT as a therapeutic tool without the side effects.

Schizophrenia

Prepulse inhibition (PPI) of the startle reflex is displayed across a variety of species in which the reflexive reaction to a sudden, intense sensory stimulus is reduced by a preceding, weaker sensory stimulus. This gating process is an attentional mechanism that filters potentially distracting stimuli so that attention can be focused on relevant information. Deficits in sensorimotor gating are a feature of many psychiatric and neurological disorders including schizophrenia [102, 186, 187, 337, 338]. OT levels may be elevated in patients with psychiatric disorders such as schizophrenia [160] and OCD [174, 177], although not all studies find such a difference [339]. Using animal models, PPI has been disrupted in a manner similar to that seen in schizophrenics by the administration of psychotomimetic drugs [290, 311, 340], particularly those that affect the dopamine and glutamate/NMDA receptors [341]. A recent study reports lower levels of OT in hyponatremic schizophrenics who display altered HPA activity [161]. However, use of antipsychotics such as amperozide (serotonin antagonist) and clozapine (dopamine and partial serotonin agonist) significantly increases plasma OT levels [193], indicating that OT may act as a natural antipsychotic. Indeed, OT restores PPI that is

disrupted in animal models by dizocilpine (non-competitive NMDA antagonist) and amphetamine (indirect dopamine agonist) [139, 328]. Furthermore, OT KO mice exhibit greater PPI deficits with treatment of phencyclidine (PCP, an NMDA antagonist) than do WT mice [138], indicating that OT in particular affects the glutaminergic component of PPI, and likely underlies disruptions in sensory gating observed in schizophrenic patients [342]. Interestingly, levels of plasma OT in schizophrenics positively predicts their ability to identify facial emotions [161], further implicating OT in the social aspects of schizophrenia [102]. Preliminary results support the hypothesis that OT has therapeutic effects on the negative symptoms of schizophrenia and that intranasal oxytocin may be an effective method of augmenting established antipsychotic medication [194, 195]. Further investigation should be pursued to assess the antipsychotic effects of OT. Using small-molecule OTR agonists should provide information minimizing the side effects. In addition, the use of positive allosteric modulators should take advantage of the endogenous presence of OT and enhance its natural antipsychotic effects.

Addiction

OT within the CNS has been shown to inhibit the development of tolerance to morphine, to attenuate various symptoms of morphine withdrawal, to decrease intravenous self-administration of heroin, and to facilitate behavioral sensitization to cocaine. Tolerance to ethanol was inhibited by OT [137, 180, 343]. Because adaptation and learning are likely to be involved in the neural events leading to drug tolerance and dependence, OT is demonstrated to influence the development of

tolerance of and dependence on abused drugs, like opiates and heroin [344]. It is surprising that clinical studies of OT and addiction have not been conducted.

Positive results in this field are almost warranted.

Atypical antipsychotics: prospective drugs for autism and OCD?

Risperidone, an atypical antipsychotic, is the only FDA approved treatment for autism [345, 346]. Specifically, it is approved for children with autism that is accompanied by irritability, including aggression, self-injury, tantrums, and mood swings [347, 348]. Risperidone reduced interfering repetitive behavior as well as aggression, but it did not lead to improvement in social relatedness or language [349, 350]. Risperidone significantly improved sensory motor behaviors, affectual reactions, and sensory responses. However, there was no significant change on the social relationship to people or language [351]. Risperidone was also used in a randomized control trial for the treatment of fluvoxamine- refractory OCD [352]. Treatment of pervasive developmental disorder patients with olanzapine, another atypical antipsychotic, improved core social and language impairments in addition to other disruptive behaviors and irritability [347, 353-356]. Quetiapine, ziprasidone, and aripiprazole have also been examined in patients with ASD, but none reported significant improvements in core social and language impairments. Larger trials are underway for olanzapine and aripiprazole [347, 357].

These studies suggest efficacy for use of atypical antipsychotics in treating interfering repetitive behaviors in ASD [345]. It is interesting to note that compd 39 and OT show antipsychotic like effects in our animal model of PPI. Further

investigation needs to address whether this compound acts as an atypical drug. Promising results from these experiments would suggest that compounds that activate the OT pathway would be valid treatment strategies for schizophrenia, because of their antipsychotic effects, as well as some of the core symptoms of autism and even OCD.

REFERENCES

1. Kenakin, T., *Predicting therapeutic value in the lead optimization phase of drug discovery*. Nat Rev Drug Discov, 2003. **2**(6): p. 429-38.
2. Drews, J., *Drug discovery: a historical perspective*. Science, 2000. **287**(5460): p. 1960-4.
3. Pandit, N.K., *Introduction to the pharmaceutical Sciences*. 2007: Lippincott, Williams & Wilkins.
4. Inglese, J., et al., *Quantitative high-throughput screening: a titration-based approach that efficiently identifies biological activities in large chemical libraries*. Proc Natl Acad Sci U S A, 2006. **103**(31): p. 11473-8.
5. Inglese, J., C.E. Shamu, and R.K. Guy, *Reporting data from high-throughput screening of small-molecule libraries*. Nat Chem Biol, 2007. **3**(8): p. 438-41.
6. Malo, N., et al., *Statistical practice in high-throughput screening data analysis*. Nat Biotechnol, 2006. **24**(2): p. 167-75.
7. Fu, Y.T., et al., *BRACO19 analog dimers with improved inhibition of telomerase and hPot 1*. Bioorg Med Chem, 2009. **17**(5): p. 2030-7.
8. Chaires, J.B., *Drug--DNA interactions*. Curr Opin Struct Biol, 1998. **8**(3): p. 314-20.
9. Blasco, M.A., *Telomeres and human disease: ageing, cancer and beyond*. Nat Rev Genet, 2005. **6**(8): p. 611-22.
10. Harley, C.B., A.B. Futcher, and C.W. Greider, *Telomeres shorten during ageing of human fibroblasts*. Nature, 1990. **345**(6274): p. 458-60.
11. Autexier, C. and N.F. Lue, *The structure and function of telomerase reverse transcriptase*. Annu Rev Biochem, 2006. **75**: p. 493-517.
12. Cuenca, F., et al., *Tri- and tetra-substituted naphthalene diimides as potent G-quadruplex ligands*. Bioorg Med Chem Lett, 2008. **18**(5): p. 1668-73.
13. Kelland, L.R., *Overcoming the immortality of tumour cells by telomere and telomerase based cancer therapeutics--current status and future prospects*. Eur J Cancer, 2005. **41**(7): p. 971-9.
14. Ren, J. and J.B. Chaires, *Sequence and structural selectivity of nucleic acid binding ligands*. Biochemistry, 1999. **38**(49): p. 16067-75.

15. Burge, S., et al., *Quadruplex DNA: sequence, topology and structure*. Nucleic Acids Res, 2006. **34**(19): p. 5402-15.
16. De Cian, A., et al., *Reevaluation of telomerase inhibition by quadruplex ligands and their mechanisms of action*. Proc Natl Acad Sci U S A, 2007. **104**(44): p. 17347-52.
17. Gimpl, G. and F. Fahrenholz, *The oxytocin receptor system: structure, function, and regulation*. Physiol Rev, 2001. **81**(2): p. 629-83.
18. Barberis, C., B. Mouillac, and T. Durroux, *Structural bases of vasopressin/oxytocin receptor function*. J Endocrinol, 1998. **156**(2): p. 223-9.
19. Gimpl, G., et al., *Oxytocin receptors: ligand binding, signalling and cholesterol dependence*. Prog Brain Res, 2008. **170**: p. 193-204.
20. Rose, J.P., et al., *Crystal structure of the neurophysin-oxytocin complex*. Nat Struct Biol, 1996. **3**(2): p. 163-9.
21. Richard, S. and H.H. Zingg, *The human oxytocin gene promoter is regulated by estrogens*. J Biol Chem, 1990. **265**(11): p. 6098-103.
22. Richard, S. and H.H. Zingg, *Identification of a retinoic acid response element in the human oxytocin promoter*. J Biol Chem, 1991. **266**(32): p. 21428-33.
23. Brownstein, M.J., J.T. Russell, and H. Gainer, *Synthesis, transport, and release of posterior pituitary hormones*. Science, 1980. **207**(4429): p. 373-8.
24. Poulain, D.A. and J.B. Wakerley, *Electrophysiology of hypothalamic magnocellular neurones secreting oxytocin and vasopressin*. Neuroscience, 1982. **7**(4): p. 773-808.
25. Marazziti, D. and M. Catena Dell'osso, *The role of oxytocin in neuropsychiatric disorders*. Curr Med Chem, 2008. **15**(7): p. 698-704.
26. Pittman, Q.J., et al., *Neurohypophysial peptides as retrograde transmitters in the supraoptic nucleus of the rat*. Exp Physiol, 2000. **85 Spec No**: p. 139S-143S.
27. Neumann, I., et al., *Oxytocin released within the supraoptic nucleus of the rat brain by positive feedback action is involved in parturition-related events*. J Neuroendocrinol, 1996. **8**(3): p. 227-33.
28. Amico, J.A., S.M. Challinor, and J.L. Cameron, *Pattern of oxytocin concentrations in the plasma and cerebrospinal fluid of lactating rhesus monkeys (Macaca mulatta): evidence for functionally independent oxytocinergic pathways in primates*. J Clin Endocrinol Metab, 1990. **71**(6): p. 1531-5.

29. Breton, C., et al., *Oxytocin receptor messenger ribonucleic acid: characterization, regulation, and cellular localization in the rat pituitary gland*. *Endocrinology*, 1995. **136**(7): p. 2928-36.
30. Boyle, L.L., et al., *Intensive venous sampling of adrenocorticotrophic hormone in rats with sham or paraventricular nucleus lesions*. *J Endocrinol*, 1997. **153**(1): p. 159-67.
31. Hull, M.L., et al., *Pre-ovulatory oxytocin administration promotes the onset of the luteinizing hormone surge in human females*. *Hum Reprod*, 1995. **10**(9): p. 2266-9.
32. Leng, G., C.H. Brown, and J.A. Russell, *Physiological pathways regulating the activity of magnocellular neurosecretory cells*. *Prog Neurobiol*, 1999. **57**(6): p. 625-55.
33. Landgraf, R., et al., *Push-pull perfusion and microdialysis studies of central oxytocin and vasopressin release in freely moving rats during pregnancy, parturition, and lactation*. *Ann N Y Acad Sci*, 1992. **652**: p. 326-39.
34. Jones, P.M., I.C. Robinson, and M.C. Harris, *Release of oxytocin into blood and cerebrospinal fluid by electrical stimulation of the hypothalamus or neural lobe in the rat*. *Neuroendocrinology*, 1983. **37**(6): p. 454-8.
35. Jones, P.M. and I.C. Robinson, *Differential clearance of neurophysin and neurohypophysial peptides from the cerebrospinal fluid in conscious guinea pigs*. *Neuroendocrinology*, 1982. **34**(4): p. 297-302.
36. Amico, J.A., et al., *A time-dependent peak of oxytocin exists in cerebrospinal fluid but not in plasma of humans*. *J Clin Endocrinol Metab*, 1983. **57**(5): p. 947-51.
37. de Wied, D., M. Diamant, and M. Fodor, *Central nervous system effects of the neurohypophyseal hormones and related peptides*. *Front Neuroendocrinol*, 1993. **14**(4): p. 251-302.
38. Neumann, I., J.A. Russell, and R. Landgraf, *Oxytocin and vasopressin release within the supraoptic and paraventricular nuclei of pregnant, parturient and lactating rats: a microdialysis study*. *Neuroscience*, 1993. **53**(1): p. 65-75.
39. Moos, F., et al., *Release of oxytocin within the supraoptic nucleus during the milk ejection reflex in rats*. *Exp Brain Res*, 1989. **76**(3): p. 593-602.
40. Foord, S.M., et al., *International Union of Pharmacology. XLVI. G protein-coupled receptor list*. *Pharmacol Rev*, 2005. **57**(2): p. 279-88.

41. Zingg, H.H. and S.A. Laporte, *The oxytocin receptor*. Trends Endocrinol Metab, 2003. **14**(5): p. 222-7.
42. Gimpl, G., et al., *Cholesterol and steroid hormones: modulators of oxytocin receptor function*. Prog Brain Res, 2002. **139**: p. 43-55.
43. Pliska, V. and H. Kohlhauf Albertin, *Effect of Mg²⁺ on the binding of oxytocin to sheep myometrial cells*. Biochem J, 1991. **277 (Pt 1)**: p. 97-101.
44. Gimpl, G., K. Burger, and F. Fahrenholz, *Cholesterol as modulator of receptor function*. Biochemistry, 1997. **36**(36): p. 10959-74.
45. Grazzini, E., et al., *Inhibition of oxytocin receptor function by direct binding of progesterone*. Nature, 1998. **392**(6675): p. 509-12.
46. Ivell, R., et al., *The molecular basis of oxytocin and oxytocin receptor gene expression in reproductive tissues*. Adv Exp Med Biol, 1998. **449**: p. 297-306.
47. Ludwig, M., *Dendritic release of vasopressin and oxytocin*. J Neuroendocrinol, 1998. **10**(12): p. 881-95.
48. Leng, G., C. Caquineau, and N. Sabatier, *Regulation of oxytocin secretion*. Vitam Horm, 2005. **71**: p. 27-58.
49. Fuchs, A.R., et al., *Oxytocin secretion and human parturition: pulse frequency and duration increase during spontaneous labor in women*. Am J Obstet Gynecol, 1991. **165**(5 Pt 1): p. 1515-23.
50. Gimpl, G. and F. Fahrenholz, *Cholesterol as stabilizer of the oxytocin receptor*. Biochim Biophys Acta, 2002. **1564**(2): p. 384-92.
51. Insel, T.R. and R.D. Fernald, *How the brain processes social information: searching for the social brain*. Annu Rev Neurosci, 2004. **27**: p. 697-722.
52. Popik, P. and J. Vetulani, *Opposite action of oxytocin and its peptide antagonists on social memory in rats*. Neuropeptides, 1991. **18**(1): p. 23-7.
53. Popik, P., et al., *Recognition cue in the rat's social memory paradigm*. J Basic Clin Physiol Pharmacol, 1991. **2**(4): p. 315-27.
54. Popik, P., J. Vetulani, and J.M. van Ree, *Low doses of oxytocin facilitate social recognition in rats*. Psychopharmacology (Berl), 1992. **106**(1): p. 71-4.
55. Benelli, A., et al., *Polymodal dose-response curve for oxytocin in the social recognition test*. Neuropeptides, 1995. **28**(4): p. 251-5.
56. Bielsky, I.F. and L.J. Young, *Oxytocin, vasopressin, and social recognition in mammals*. Peptides, 2004. **25**(9): p. 1565-74.

57. Lee, P.R., et al., *Social interaction deficits caused by chronic phencyclidine administration are reversed by oxytocin*. *Neuropsychopharmacology*, 2005. **30**(10): p. 1883-94.
58. Ferguson, J.N., et al., *Oxytocin in the medial amygdala is essential for social recognition in the mouse*. *J Neurosci*, 2001. **21**(20): p. 8278-85.
59. Choleris, E., et al., *An estrogen-dependent four-gene micronet regulating social recognition: a study with oxytocin and estrogen receptor-alpha and -beta knockout mice*. *Proc Natl Acad Sci U S A*, 2003. **100**(10): p. 6192-7.
60. Kavaliers, M., et al., *Impaired discrimination of and aversion to parasitized male odors by female oxytocin knockout mice*. *Genes Brain Behav*, 2003. **2**(4): p. 220-30.
61. Temple, J.L., Young, W.S., Wersinger, S.R., *Disruption of the genes for either oxytocin or the vasopressin 1B receptor alters male-induced pregnancy block (the Bruce effect)*. in *Society for Neuroscience*. 2003: New Orleans.
62. Ferguson, J.N., et al., *Social amnesia in mice lacking the oxytocin gene*. *Nat Genet*, 2000. **25**(3): p. 284-8.
63. Winslow, J.T. and T.R. Insel, *The social deficits of the oxytocin knockout mouse*. *Neuropeptides*, 2002. **36**(2-3): p. 221-9.
64. Jin, D., et al., *CD38 is critical for social behaviour by regulating oxytocin secretion*. *Nature*, 2007. **446**(7131): p. 41-5.
65. Kosfeld, M., et al., *Oxytocin increases trust in humans*. *Nature*, 2005. **435**(7042): p. 673-6.
66. Baumgartner, T., et al., *Oxytocin shapes the neural circuitry of trust and trust adaptation in humans*. *Neuron*, 2008. **58**(4): p. 639-50.
67. Zak, P.J., A.A. Stanton, and S. Ahmadi, *Oxytocin increases generosity in humans*. *PLoS One*, 2007. **2**(11): p. e1128.
68. Domes, G., et al., *Oxytocin improves "mind-reading" in humans*. *Biol Psychiatry*, 2007. **61**(6): p. 731-3.
69. Guastella, A.J., et al., *Does oxytocin influence the early detection of angry and happy faces?* *Psychoneuroendocrinology*, 2009. **34**(2): p. 220-5.
70. Guastella, A.J., P.B. Mitchell, and M.R. Dadds, *Oxytocin increases gaze to the eye region of human faces*. *Biol Psychiatry*, 2008. **63**(1): p. 3-5.
71. Insel, T.R., L. Young, and Z. Wang, *Central oxytocin and reproductive behaviours*. *Rev Reprod*, 1997. **2**(1): p. 28-37.

72. Pedersen, C.A., et al., *Oxytocin induces maternal behavior in virgin female rats*. Science, 1982. **216**(4546): p. 648-50.
73. Pedersen, C.A. and M.L. Boccia, *Oxytocin links mothering received, mothering bestowed and adult stress responses*. Stress, 2002. **5**(4): p. 259-67.
74. Tomizawa, K., et al., *Oxytocin improves long-lasting spatial memory during motherhood through MAP kinase cascade*. Nat Neurosci, 2003. **6**(4): p. 384-90.
75. Engelmann, M., et al., *Endogenous oxytocin is involved in short-term olfactory memory in female rats*. Behav Brain Res, 1998. **90**(1): p. 89-94.
76. Takayanagi, Y., et al., *Pervasive social deficits, but normal parturition, in oxytocin receptor-deficient mice*. Proc Natl Acad Sci U S A, 2005. **102**(44): p. 16096-101.
77. Boccia, M.L., et al., *Peripherally administered non-peptide oxytocin antagonist, L368,899, accumulates in limbic brain areas: a new pharmacological tool for the study of social motivation in non-human primates*. Horm Behav, 2007. **52**(3): p. 344-51.
78. Meinlschmidt, G. and C. Heim, *Sensitivity to intranasal oxytocin in adult men with early parental separation*. Biol Psychiatry, 2007. **61**(9): p. 1109-11.
79. Levine, A., et al., *Oxytocin during pregnancy and early postpartum: individual patterns and maternal-fetal attachment*. Peptides, 2007. **28**(6): p. 1162-9.
80. Feldman, R., et al., *Evidence for a neuroendocrinological foundation of human affiliation: plasma oxytocin levels across pregnancy and the postpartum period predict mother-infant bonding*. Psychol Sci, 2007. **18**(11): p. 965-70.
81. Bartels, A. and S. Zeki, *The neural correlates of maternal and romantic love*. Neuroimage, 2004. **21**(3): p. 1155-66.
82. Bakermans-Kranenburg, M.J. and M.H. van Ijzendoorn, *Oxytocin receptor (OXTR) and serotonin transporter (5-HTT) genes associated with observed parenting*. Soc Cogn Affect Neurosci, 2008. **3**(2): p. 128-34.
83. Witt, D.M., *Oxytocin and rodent sociosexual responses: from behavior to gene expression*. Neurosci Biobehav Rev, 1995. **19**(2): p. 315-24.
84. Insel, T.R. and L.J. Young, *The neurobiology of attachment*. Nat Rev Neurosci, 2001. **2**(2): p. 129-36.

85. Young, L.J., et al., *Cellular mechanisms of social attachment*. Horm Behav, 2001. **40**(2): p. 133-8.
86. Young, L.J., Z. Wang, and T.R. Insel, *Neuroendocrine bases of monogamy*. Trends Neurosci, 1998. **21**(2): p. 71-5.
87. Insel, T.R., et al., *Oxytocin, vasopressin, and the neuroendocrine basis of pair bond formation*. Adv Exp Med Biol, 1998. **449**: p. 215-24.
88. Ditzen, B., et al., *Intranasal oxytocin increases positive communication and reduces cortisol levels during couple conflict*. Biol Psychiatry, 2009. **65**(9): p. 728-31.
89. Heinrichs, M., et al., *Social support and oxytocin interact to suppress cortisol and subjective responses to psychosocial stress*. Biol Psychiatry, 2003. **54**(12): p. 1389-98.
90. Tops, M., et al., *Anxiety, cortisol, and attachment predict plasma oxytocin*. Psychophysiology, 2007. **44**(3): p. 444-9.
91. Fisher, H., A. Aron, and L.L. Brown, *Romantic love: an fMRI study of a neural mechanism for mate choice*. J Comp Neurol, 2005. **493**(1): p. 58-62.
92. Fisher, H.E., A. Aron, and L.L. Brown, *Romantic love: a mammalian brain system for mate choice*. Philos Trans R Soc Lond B Biol Sci, 2006. **361**(1476): p. 2173-86.
93. Campbell, A., *Attachment, aggression and affiliation: the role of oxytocin in female social behavior*. Biol Psychol, 2008. **77**(1): p. 1-10.
94. Pedersen, C.A. and M.L. Boccia, *Oxytocin maintains as well as initiates female sexual behavior: effects of a highly selective oxytocin antagonist*. Horm Behav, 2002. **41**(2): p. 170-7.
95. Pedersen, C.A. and M.L. Boccia, *Vasopressin interactions with oxytocin in the control of female sexual behavior*. Neuroscience, 2006. **139**(3): p. 843-51.
96. Vignozzi, L., et al., *Oxytocin receptor is expressed in the penis and mediates an estrogen-dependent smooth muscle contractility*. Endocrinology, 2004. **145**(4): p. 1823-34.
97. Vignozzi, L., et al., *Identification, characterization and biological activity of oxytocin receptor in the developing human penis*. Mol Hum Reprod, 2005. **11**(2): p. 99-106.
98. Filippi, S., et al., *Role of oxytocin in the ejaculatory process*. J Endocrinol Invest, 2003. **26**(3 Suppl): p. 82-6.

99. Carmichael, M.S., et al., *Plasma oxytocin increases in the human sexual response*. J Clin Endocrinol Metab, 1987. **64**(1): p. 27-31.
100. Burri, A., et al., *The acute effects of intranasal oxytocin administration on endocrine and sexual function in males*. Psychoneuroendocrinology, 2008. **33**(5): p. 591-600.
101. Ishak, W.W., D.S. Berman, and A. Peters, *Male anorgasmia treated with oxytocin*. J Sex Med, 2008. **5**(4): p. 1022-4.
102. Lee, H.J., et al., *Oxytocin: the great facilitator of life*. Prog Neurobiol, 2009. **88**(2): p. 127-51.
103. Carter, C.S., *Developmental consequences of oxytocin*. Physiol Behav, 2003. **79**(3): p. 383-97.
104. Anderson, P.O. and V. Valdes, *A critical review of pharmaceutical galactagogues*. Breastfeed Med, 2007. **2**(4): p. 229-42.
105. Anderson-Hunt, M. and L. Dennerstein, *Increased female sexual response after oxytocin*. BMJ, 1994. **309**(6959): p. 929.
106. Salonia, A., et al., *Menstrual cycle-related changes in plasma oxytocin are relevant to normal sexual function in healthy women*. Horm Behav, 2005. **47**(2): p. 164-9.
107. Blaicher, W., et al., *The role of oxytocin in relation to female sexual arousal*. Gynecol Obstet Invest, 1999. **47**(2): p. 125-6.
108. Ring, R.H., et al., *Anxiolytic-like activity of oxytocin in male mice: behavioral and autonomic evidence, therapeutic implications*. Psychopharmacology (Berl), 2006. **185**(2): p. 218-25.
109. Amico, J.A., et al., *Anxiety and stress responses in female oxytocin deficient mice*. J Neuroendocrinol, 2004. **16**(4): p. 319-24.
110. Amico, J.A., et al., *Oxytocin knockout mice: a model for studying stress-related and ingestive behaviours*. Prog Brain Res, 2008. **170**: p. 53-64.
111. Kirsch, P., et al., *Oxytocin modulates neural circuitry for social cognition and fear in humans*. J Neurosci, 2005. **25**(49): p. 11489-93.
112. Fetissov, S.O., et al., *Aggressive behavior linked to corticotropin-reactive autoantibodies*. Biol Psychiatry, 2006. **60**(8): p. 799-802.
113. Bosch, O.J., et al., *Brain oxytocin correlates with maternal aggression: link to anxiety*. J Neurosci, 2005. **25**(29): p. 6807-15.

114. Bosch, O.J., et al., *Extracellular amino acid levels in the paraventricular nucleus and the central amygdala in high- and low-anxiety dams rats during maternal aggression: regulation by oxytocin*. *Stress*, 2007. **10**(3): p. 261-70.
115. Winslow, J.T., et al., *Infant vocalization, adult aggression, and fear behavior of an oxytocin null mutant mouse*. *Horm Behav*, 2000. **37**(2): p. 145-55.
116. Savaskan, E., et al., *Post-learning intranasal oxytocin modulates human memory for facial identity*. *Psychoneuroendocrinology*, 2008. **33**(3): p. 368-74.
117. Fehm-Wolfsdorf, G. and J. Born, *Behavioral effects of neurohypophyseal peptides in healthy volunteers: 10 years of research*. *Peptides*, 1991. **12**(6): p. 1399-406.
118. Engelmann, M., et al., *Behavioral consequences of intracerebral vasopressin and oxytocin: focus on learning and memory*. *Neurosci Biobehav Rev*, 1996. **20**(3): p. 341-58.
119. Bruins, J., R. Hijman, and J.M. Van Ree, *Effect of a single dose of des-glycinamide-[Arg8]vasopressin or oxytocin on cognitive processes in young healthy subjects*. *Peptides*, 1992. **13**(3): p. 461-8.
120. Ferrier, B.M., D.J. Kennett, and M.C. Devlin, *Influence of oxytocin on human memory processes*. *Life Sci*, 1980. **27**(24): p. 2311-7.
121. Geenen, V., et al., *Inhibitory influence of oxytocin infusion on contingent negative variation and some memory tasks in normal men*. *Psychoneuroendocrinology*, 1988. **13**(5): p. 367-75.
122. Heinrichs, M., et al., *Selective amnesic effects of oxytocin on human memory*. *Physiol Behav*, 2004. **83**(1): p. 31-8.
123. Fehm-Wolfsdorf, G., et al., *Human memory and neurohypophyseal hormones: opposite effects of vasopressin and oxytocin*. *Psychoneuroendocrinology*, 1984. **9**(3): p. 285-92.
124. Pedersen, C.A., et al., *Grooming behavioral effects of oxytocin. Pharmacology, ontogeny, and comparisons with other nonapeptides*. *Ann N Y Acad Sci*, 1988. **525**: p. 245-56.
125. Amico, J.A., et al., *Centrally administered oxytocin elicits exaggerated grooming in oxytocin null mice*. *Pharmacol Biochem Behav*, 2004. **78**(2): p. 333-9.
126. Yang, J., et al., *Effect of oxytocin on acupuncture analgesia in the rat*. *Neuropeptides*, 2007. **41**(5): p. 285-92.

127. Yang, J., et al., *Central oxytocin enhances antinociception in the rat*. Peptides, 2007. **28**(5): p. 1113-9.
128. Arletti, R., A. Benelli, and A. Bertolini, *Influence of oxytocin on nociception and morphine antinociception*. Neuropeptides, 1993. **24**(3): p. 125-9.
129. Lundeberg, T., et al., *Anti-nociceptive effects of oxytocin in rats and mice*. Neurosci Lett, 1994. **170**(1): p. 153-7.
130. Robinson, D.A., et al., *Oxytocin mediates stress-induced analgesia in adult mice*. J Physiol, 2002. **540**(Pt 2): p. 593-606.
131. Breton, J.D., et al., *Oxytocin-induced antinociception in the spinal cord is mediated by a subpopulation of glutamatergic neurons in lamina I-II which amplify GABAergic inhibition*. Mol Pain, 2008. **4**: p. 19.
132. Grewen, K.M., et al., *Ethnicity is associated with alterations in oxytocin relationships to pain sensitivity in women*. Ethn Health, 2008. **13**(3): p. 219-41.
133. Kovacs, G.L. and G. Telegdy, *Beta-endorphin tolerance is inhibited by oxytocin*. Pharmacol Biochem Behav, 1987. **26**(1): p. 57-60.
134. Kovacs, C.L. and J.M. Van Ree, *Behaviorally active oxytocin fragments simultaneously attenuate heroin self-administration and tolerance in rats*. Life Sci, 1985. **37**(20): p. 1895-900.
135. Sarnyai, Z., *Oxytocin and neuroadaptation to cocaine*. Prog Brain Res, 1998. **119**: p. 449-66.
136. Szabo, G., G.L. Kovacs, and G. Telegdy, *Effects of neurohypophyseal peptide hormones on alcohol dependence and withdrawal*. Alcohol Alcohol, 1987. **22**(1): p. 71-4.
137. Kovacs, G.L., Z. Sarnyai, and G. Szabo, *Oxytocin and addiction: a review*. Psychoneuroendocrinology, 1998. **23**(8): p. 945-62.
138. Caldwell, H.K., S.L. Stephens, and W.S. Young, 3rd, *Oxytocin as a natural antipsychotic: a study using oxytocin knockout mice*. Mol Psychiatry, 2009. **14**(2): p. 190-6.
139. Feifel, D. and T. Reza, *Oxytocin modulates psychotomimetic-induced deficits in sensorimotor gating*. Psychopharmacology (Berl), 1999. **141**(1): p. 93-8.
140. Swerdlow, N.R., et al., *Assessing the validity of an animal model of deficient sensorimotor gating in schizophrenic patients*. Arch Gen Psychiatry, 1994. **51**(2): p. 139-54.

141. Varty, G.B. and G.A. Higgins, *Examination of drug-induced and isolation-induced disruptions of prepulse inhibition as models to screen antipsychotic drugs*. *Psychopharmacology (Berl)*, 1995. **122**(1): p. 15-26.
142. Swerdlow, N.R. and M.A. Geyer, *Clozapine and haloperidol in an animal model of sensorimotor gating deficits in schizophrenia*. *Pharmacol Biochem Behav*, 1993. **44**(3): p. 741-4.
143. Varty, G.B. and G.A. Higgins, *Reversal of dizocilpine-induced disruption of prepulse inhibition of an acoustic startle response by the 5-HT₂ receptor antagonist ketanserin*. *Eur J Pharmacol*, 1995. **287**(2): p. 201-5.
144. Crawley, J.N., et al., *Social approach behaviors in oxytocin knockout mice: comparison of two independent lines tested in different laboratory environments*. *Neuropeptides*, 2007. **41**(3): p. 145-63.
145. Marazziti, D. and M.C. Dell'osso, *The role of oxytocin in neuropsychiatric disorders*. *Curr Med Chem*, 2008. **15**(7): p. 698-704.
146. Insel, T.R., D.J. O'Brien, and J.F. Leckman, *Oxytocin, vasopressin, and autism: is there a connection?* *Biol Psychiatry*, 1999. **45**(2): p. 145-57.
147. Modahl, C., et al., *Plasma oxytocin levels in autistic children*. *Biol Psychiatry*, 1998. **43**(4): p. 270-7.
148. Green, L., et al., *Oxytocin and autistic disorder: alterations in peptide forms*. *Biol Psychiatry*, 2001. **50**(8): p. 609-13.
149. Yrigollen, C.M., et al., *Genes controlling affiliative behavior as candidate genes for autism*. *Biol Psychiatry*, 2008. **63**(10): p. 911-6.
150. Jacob, S., et al., *Association of the oxytocin receptor gene (OXTR) in Caucasian children and adolescents with autism*. *Neurosci Lett*, 2007. **417**(1): p. 6-9.
151. Lerer, E., et al., *Association between the oxytocin receptor (OXTR) gene and autism: relationship to Vineland Adaptive Behavior Scales and cognition*. *Mol Psychiatry*, 2008. **13**(10): p. 980-8.
152. Wu, S., et al., *Positive association of the oxytocin receptor gene (OXTR) with autism in the Chinese Han population*. *Biol Psychiatry*, 2005. **58**(1): p. 74-7.
153. Lerer, E., et al., *Association between the oxytocin receptor (OXTR) gene and autism: relationship to Vineland Adaptive Behavior Scales and cognition*. *Mol Psychiatry*, 2007.

154. Ylisaukko-oja, T., et al., *Search for autism loci by combined analysis of Autism Genetic Resource Exchange and Finnish families*. *Ann Neurol*, 2006. **59**(1): p. 145-55.
155. Levy, S.E. and S.L. Hyman, *Novel treatments for autistic spectrum disorders*. *Ment Retard Dev Disabil Res Rev*, 2005. **11**(2): p. 131-42.
156. Langworthy-Lam, K.S., M.G. Aman, and M.E. Van Bourgondien, *Prevalence and patterns of use of psychoactive medicines in individuals with autism in the Autism Society of North Carolina*. *J Child Adolesc Psychopharmacol*, 2002. **12**(4): p. 311-21.
157. Myers, S.M., *The status of pharmacotherapy for autism spectrum disorders*. *Expert Opin Pharmacother*, 2007. **8**(11): p. 1579-603.
158. Hollander, E., et al., *Oxytocin increases retention of social cognition in autism*. *Biol Psychiatry*, 2007. **61**(4): p. 498-503.
159. Hollander, E., et al., *Oxytocin infusion reduces repetitive behaviors in adults with autistic and Asperger's disorders*. *Neuropsychopharmacology*, 2003. **28**(1): p. 193-8.
160. Beckmann, H., R.E. Lang, and W.F. Gattaz, *Vasopressin--oxytocin in cerebrospinal fluid of schizophrenic patients and normal controls*. *Psychoneuroendocrinology*, 1985. **10**(2): p. 187-91.
161. Goldman, M., et al., *Diminished plasma oxytocin in schizophrenic patients with neuroendocrine dysfunction and emotional deficits*. *Schizophr Res*, 2008. **98**(1-3): p. 247-55.
162. Mai, J.K., K. Berger, and M.V. Sofroniew, *Morphometric evaluation of neurophysin-immunoreactivity in the human brain: pronounced inter-individual variability and evidence for altered staining patterns in schizophrenia*. *J Hirnforsch*, 1993. **34**(2): p. 133-54.
163. Onitsuka, T., et al., *Fusiform gyrus volume reduction and facial recognition in chronic schizophrenia*. *Arch Gen Psychiatry*, 2003. **60**(4): p. 349-55.
164. Pariante, C.M. and A.H. Miller, *Glucocorticoid receptors in major depression: relevance to pathophysiology and treatment*. *Biol Psychiatry*, 2001. **49**(5): p. 391-404.
165. Bell, C.J., et al., *Plasma oxytocin levels in depression and their correlation with the temperament dimension of reward dependence*. *J Psychopharmacol*, 2006. **20**(5): p. 656-60.

166. Purba, J.S., et al., *Increased number of vasopressin- and oxytocin-expressing neurons in the paraventricular nucleus of the hypothalamus in depression.* Arch Gen Psychiatry, 1996. **53**(2): p. 137-43.
167. Scantamburlo, G., et al., *Plasma oxytocin levels and anxiety in patients with major depression.* Psychoneuroendocrinology, 2007. **32**(4): p. 407-10.
168. Frasch, A., et al., *Reduction of plasma oxytocin levels in patients suffering from major depression.* Adv Exp Med Biol, 1995. **395**: p. 257-8.
169. Cyranowski, J.M., et al., *Evidence of dysregulated peripheral oxytocin release among depressed women.* Psychosom Med, 2008. **70**(9): p. 967-75.
170. Gordon, I., et al., *Oxytocin and cortisol in romantically unattached young adults: associations with bonding and psychological distress.* Psychophysiology, 2008. **45**(3): p. 349-52.
171. Mezzacappa, E.S. and E.S. Katlin, *Breast-feeding is associated with reduced perceived stress and negative mood in mothers.* Health Psychol, 2002. **21**(2): p. 187-93.
172. Jonas, W., et al., *Influence of oxytocin or epidural analgesia on personality profile in breastfeeding women: a comparative study.* Arch Womens Ment Health, 2008. **11**(5-6): p. 335-45.
173. Insel, T.R. and J.T. Winslow, *Neurobiology of obsessive compulsive disorder.* Psychiatr Clin North Am, 1992. **15**(4): p. 813-24.
174. Leckman, J.F., et al., *The role of central oxytocin in obsessive compulsive disorder and related normal behavior.* Psychoneuroendocrinology, 1994. **19**(8): p. 723-49.
175. Neziroglu, F., R. Anemone, and J.A. Yaryura-Tobias, *Onset of obsessive-compulsive disorder in pregnancy.* Am J Psychiatry, 1992. **149**(7): p. 947-50.
176. Sichel, D.A., et al., *Postpartum onset of obsessive-compulsive disorder.* Psychosomatics, 1993. **34**(3): p. 277-9.
177. Leckman, J.F., et al., *Elevated cerebrospinal fluid levels of oxytocin in obsessive-compulsive disorder. Comparison with Tourette's syndrome and healthy controls.* Arch Gen Psychiatry, 1994. **51**(10): p. 782-92.
178. Ansseau, M., et al., *Intranasal oxytocin in obsessive-compulsive disorder.* Psychoneuroendocrinology, 1987. **12**(3): p. 231-6.
179. Salzberg, A.D. and S.E. Swedo, *Oxytocin and vasopressin in obsessive-compulsive disorder.* Am J Psychiatry, 1992. **149**(5): p. 713-4.

180. Light, K.C., et al., *Deficits in plasma oxytocin responses and increased negative affect, stress, and blood pressure in mothers with cocaine exposure during pregnancy*. *Addict Behav*, 2004. **29**(8): p. 1541-64.
181. Marchesi, C., et al., *Abnormal plasma oxytocin and beta-endorphin levels in alcoholics after short and long term abstinence*. *Prog Neuropsychopharmacol Biol Psychiatry*, 1997. **21**(5): p. 797-807.
182. Holden, K.L., et al., *Accelerated mental aging in alcoholic patients*. *J Clin Psychol*, 1988. **44**(2): p. 286-92.
183. Bohus, B., G.L. Kovacs, and D. de Wied, *Oxytocin, vasopressin and memory: opposite effects on consolidation and retrieval processes*. *Brain Res*, 1978. **157**(2): p. 414-7.
184. Maes, M., et al., *Higher serum prollyl endopeptidase activity in patients with post-traumatic stress disorder*. *J Affect Disord*, 1999. **53**(1): p. 27-34.
185. McAlonan, G.M., et al., *Brain anatomy and sensorimotor gating in Asperger's syndrome*. *Brain*, 2002. **125**(Pt 7): p. 1594-606.
186. Braff, D.L., et al., *Impact of prepulse characteristics on the detection of sensorimotor gating deficits in schizophrenia*. *Schizophr Res*, 2001. **49**(1-2): p. 171-8.
187. Braff, D.L., C. Grillon, and M.A. Geyer, *Gating and habituation of the startle reflex in schizophrenic patients*. *Arch Gen Psychiatry*, 1992. **49**(3): p. 206-15.
188. Geyer, M.A. and D.L. Braff, *Startle habituation and sensorimotor gating in schizophrenia and related animal models*. *Schizophr Bull*, 1987. **13**(4): p. 643-68.
189. Geyer, M.A., et al., *Pharmacological studies of prepulse inhibition models of sensorimotor gating deficits in schizophrenia: a decade in review*. *Psychopharmacology (Berl)*, 2001. **156**(2-3): p. 117-54.
190. Geyer, M.A. and N.R. Swerdlow, *Measurement of startle response, prepulse inhibition, and habituation*. *Curr Protoc Neurosci*, 2001. **Chapter 8**: p. Unit 8 7.
191. Geyer, M.A., et al., *Startle response models of sensorimotor gating and habituation deficits in schizophrenia*. *Brain Res Bull*, 1990. **25**(3): p. 485-98.
192. Perry, W., et al., *Sensorimotor gating deficits in adults with autism*. *Biol Psychiatry*, 2007. **61**(4): p. 482-6.

193. Uvnas-Moberg, K., P. Alster, and T.H. Svensson, *Amperozide and clozapine but not haloperidol or raclopride increase the secretion of oxytocin in rats*. *Psychopharmacology (Berl)*, 1992. **109**(4): p. 473-6.
194. D. Feifel, K.M., A. Nguyen, H. Warlan, B. Galangue, P. Cobb, A. Minassian, O. Becker, J. Cooper, W. Perry, M. Lefebvre, J. Gonzalez, A. Hadley. *Intranasal oxytocin augmentation of antipsychotic medication in schizophrenia patients*. in *Society for Neuroscience*. 2009. Chicago, IL: Neuroscience Meeting Planner.
195. Pedersen, C., *Oxytocin treatment of schizophrenia symptoms*. 2009: Chapel Hill, NC.
196. Borthwick, A.D., *Oxytocin antagonists and agonists*. *Annual Reports in Medicinal Chemistry*, ed. A. Wood. Vol. 41. 2006, New York: Elsevier. 409-421.
197. Pardridge, W.M., *Neuropeptides and the blood-brain barrier*. *Annu Rev Physiol*, 1983. **45**: p. 73-82.
198. Borthwick, A.D., et al., *2,5-diketopiperazines as potent, selective, and orally bioavailable oxytocin antagonists. 3. Synthesis, pharmacokinetics, and in vivo potency*. *J Med Chem*, 2006. **49**(14): p. 4159-70.
199. Schwarz, M.K. and P. Page, *Preterm labour: an overview of current and emerging therapeutics*. *Curr Med Chem*, 2003. **10**(15): p. 1441-68.
200. Patka, J.H., A.E. Lodolce, and A.K. Johnston, *High- versus low-dose oxytocin for augmentation or induction of labor*. *Ann Pharmacother*, 2005. **39**(1): p. 95-101.
201. Jouppila, P., *Postpartum haemorrhage*. *Curr Opin Obstet Gynecol*, 1995. **7**(6): p. 446-50.
202. Chini, B. and M. Manning, *Agonist selectivity in the oxytocin/vasopressin receptor family: new insights and challenges*. *Biochem Soc Trans*, 2007. **35**(Pt 4): p. 737-41.
203. Chini, B., M. Manning, and G. Guillon, *Affinity and efficacy of selective agonists and antagonists for vasopressin and oxytocin receptors: an "easy guide" to receptor pharmacology*. *Prog Brain Res*, 2008. **170**: p. 513-7.
204. Pitt, G.R., et al., *Non-peptide oxytocin agonists*. *Bioorg Med Chem Lett*, 2004. **14**(17): p. 4585-9.
205. Reversi, A., et al., *The oxytocin receptor antagonist atosiban inhibits cell growth via a "biased agonist" mechanism*. *J Biol Chem*, 2005. **280**(16): p. 16311-8.

206. Ring, R.H., et al., *Receptor and behavioral pharmacology of WAY-267464, a non-peptide oxytocin receptor agonist*. Neuropharmacology, 2009.
207. Gorbulev, V., et al., *Molecular cloning and functional characterization of V2 [8-lysine] vasopressin and oxytocin receptors from a pig kidney cell line*. Eur J Biochem, 1993. **215**(1): p. 1-7.
208. May, L.T. and A. Christopoulos, *Allosteric modulators of G-protein-coupled receptors*. Curr Opin Pharmacol, 2003. **3**(5): p. 551-6.
209. Christopoulos, A., *Allosteric binding sites on cell-surface receptors: novel targets for drug discovery*. Nat Rev Drug Discov, 2002. **1**(3): p. 198-210.
210. May, L.T., et al., *Allosteric modulation of G protein-coupled receptors*. Curr Pharm Des, 2004. **10**(17): p. 2003-13.
211. Leach, K., P.M. Sexton, and A. Christopoulos, *Allosteric GPCR modulators: taking advantage of permissive receptor pharmacology*. Trends Pharmacol Sci, 2007. **28**(8): p. 382-9.
212. May, L.T., et al., *Allosteric modulation of G protein-coupled receptors*. Annu Rev Pharmacol Toxicol, 2007. **47**: p. 1-51.
213. Benneyworth, M.A., et al., *A selective positive allosteric modulator of metabotropic glutamate receptor subtype 2 blocks a hallucinogenic drug model of psychosis*. Mol Pharmacol, 2007. **72**(2): p. 477-84.
214. Marino, M.J., et al., *Allosteric modulation of group III metabotropic glutamate receptor 4: a potential approach to Parkinson's disease treatment*. Proc Natl Acad Sci U S A, 2003. **100**(23): p. 13668-73.
215. O'Brien, J.A., et al., *A family of highly selective allosteric modulators of the metabotropic glutamate receptor subtype 5*. Mol Pharmacol, 2003. **64**(3): p. 731-40.
216. Lindsley, C.W., et al., *Discovery of positive allosteric modulators for the metabotropic glutamate receptor subtype 5 from a series of N-(1,3-diphenyl-1H-pyrazol-5-yl)benzamides that potentiate receptor function in vivo*. J Med Chem, 2004. **47**(24): p. 5825-8.
217. Kinney, G.G., et al., *A novel selective positive allosteric modulator of metabotropic glutamate receptor subtype 5 has in vivo activity and antipsychotic-like effects in rat behavioral models*. J Pharmacol Exp Ther, 2005. **313**(1): p. 199-206.
218. Zhao, Z., et al., *Challenges in the development of mGluR5 positive allosteric modulators: the discovery of CPPHA*. Bioorg Med Chem Lett, 2007. **17**(5): p. 1386-91.

219. Shirey, J.K., et al., *An allosteric potentiator of M4 mAChR modulates hippocampal synaptic transmission*. Nat Chem Biol, 2008. **4**(1): p. 42-50.
220. Lewis, L.M., et al., *Synthesis and SAR of selective muscarinic acetylcholine receptor subtype 1 (M1 mAChR) antagonists*. Bioorg Med Chem Lett, 2008. **18**(3): p. 885-90.
221. Hurst, R.S., et al., *A novel positive allosteric modulator of the alpha7 neuronal nicotinic acetylcholine receptor: in vitro and in vivo characterization*. J Neurosci, 2005. **25**(17): p. 4396-405.
222. Brauner-Osborne, H., P. Wellendorph, and A.A. Jensen, *Structure, pharmacology and therapeutic prospects of family C G-protein coupled receptors*. Curr Drug Targets, 2007. **8**(1): p. 169-84.
223. Neidle, S. and G.N. Parkinson, *The structure of telomeric DNA*. Curr Opin Struct Biol, 2003. **13**(3): p. 275-83.
224. Bryan, T.M. and T.R. Cech, *Telomerase and the maintenance of chromosome ends*. Curr Opin Cell Biol, 1999. **11**(3): p. 318-24.
225. Cech, T.R. and J. Lingner, *Telomerase and the chromosome end replication problem*. Ciba Found Symp, 1997. **211**: p. 20-8; discussion 28-34.
226. Cech, T.R., *Life at the End of the Chromosome: Telomeres and Telomerase*. Angew Chem Int Ed Engl, 2000. **39**(1): p. 34-43.
227. Hanahan, D. and R.A. Weinberg, *The hallmarks of cancer*. Cell, 2000. **100**(1): p. 57-70.
228. Rezler, E.M., D.J. Bearss, and L.H. Hurley, *Telomere inhibition and telomere disruption as processes for drug targeting*. Annu Rev Pharmacol Toxicol, 2003. **43**: p. 359-79.
229. Neidle, S. and G. Parkinson, *Telomere maintenance as a target for anticancer drug discovery*. Nat Rev Drug Discov, 2002. **1**(5): p. 383-93.
230. Monchaud, D. and M.P. Teulade-Fichou, *A hitchhiker's guide to G-quadruplex ligands*. Org Biomol Chem, 2008. **6**(4): p. 627-36.
231. Todd, A.K., M. Johnston, and S. Neidle, *Highly prevalent putative quadruplex sequence motifs in human DNA*. Nucleic Acids Res, 2005. **33**(9): p. 2901-7.
232. Huppert, J.L. and S. Balasubramanian, *G-quadruplexes in promoters throughout the human genome*. Nucleic Acids Res, 2007. **35**(2): p. 406-13.

233. Oganessian, L. and T.M. Bryan, *Physiological relevance of telomeric G-quadruplex formation: a potential drug target*. *Bioessays*, 2007. **29**(2): p. 155-65.
234. Pagano, B. and C. Giancola, *Energetics of quadruplex-drug recognition in anticancer therapy*. *Curr Cancer Drug Targets*, 2007. **7**(6): p. 520-40.
235. Keppler, B.R. and M.B. Jarstfer, *Inhibition of telomerase activity by preventing proper assemblage*. *Biochemistry*, 2004. **43**(2): p. 334-43.
236. Cristofari, G., et al., *Low- to high-throughput analysis of telomerase modulators with Telospot*. *Nat Methods*, 2007. **4**(10): p. 851-3.
237. Burger, A.M., et al., *The G-quadruplex-interactive molecule BRACO-19 inhibits tumor growth, consistent with telomere targeting and interference with telomerase function*. *Cancer Res*, 2005. **65**(4): p. 1489-96.
238. Pitts, A.E. and D.R. Corey, *Inhibition of human telomerase by 2'-O-methyl-RNA*. *Proc Natl Acad Sci U S A*, 1998. **95**(20): p. 11549-54.
239. Rezler, E.M., et al., *Telomestatin and diseleno saphyrin bind selectively to two different forms of the human telomeric G-quadruplex structure*. *J Am Chem Soc*, 2005. **127**(26): p. 9439-47.
240. Han, H., L.H. Hurley, and M. Salazar, *A DNA polymerase stop assay for G-quadruplex-interactive compounds*. *Nucleic Acids Res*, 1999. **27**(2): p. 537-42.
241. White, E.W., et al., *Structure-specific recognition of quadruplex DNA by organic cations: influence of shape, substituents and charge*. *Biophys Chem*, 2007. **126**(1-3): p. 140-53.
242. Garbett, N.C., P.A. Ragazzon, and J.B. Chaires, *Circular dichroism to determine binding mode and affinity of ligand-DNA interactions*. *Nat Protoc*, 2007. **2**(12): p. 3166-72.
243. Keniry, M.A., *Quadruplex structures in nucleic acids*. *Biopolymers*, 2000. **56**(3): p. 123-46.
244. Balagurumoorthy, P., et al., *Hairpin and parallel quartet structures for telomeric sequences*. *Nucleic Acids Res*, 1992. **20**(15): p. 4061-7.
245. Bryan, T.M. and M.B. Jarstfer, *Interrogation of G-quadruplex-protein interactions*. *Methods*, 2007. **43**(4): p. 332-9.
246. Moon, I.K. and M.B. Jarstfer, *The human telomere and its relationship to human disease, therapy, and tissue engineering*. *Front Biosci*, 2007. **12**: p. 4595-620.

247. Garbett, N.C. and D.E. Graves, *Extending nature's leads: the anticancer agent ellipticine*. *Curr Med Chem Anticancer Agents*, 2004. **4**(2): p. 149-72.
248. Armbruster, B.N. and B.L. Roth, *Mining the receptorome*. *J Biol Chem*, 2005. **280**(7): p. 5129-32.
249. Kroeze, W.K. and B.L. Roth, *Screening the receptorome*. *J Psychopharmacol*, 2006. **20**(4 Suppl): p. 41-6.
250. Hodder, P., et al., *Miniaturization of intracellular calcium functional assays to 1536-well plate format using a fluorometric imaging plate reader*. *J Biomol Screen*, 2004. **9**(5): p. 417-26.
251. Sullivan, E., E.M. Tucker, and I.L. Dale, *Measurement of [Ca²⁺] using the Fluorometric Imaging Plate Reader (FLIPR)*. *Methods Mol Biol*, 1999. **114**: p. 125-33.
252. Coward, P., et al., *Chimeric G proteins allow a high-throughput signaling assay of Gi-coupled receptors*. *Anal Biochem*, 1999. **270**(2): p. 242-8.
253. Offermanns, S. and M.I. Simon, *G alpha 15 and G alpha 16 couple a wide variety of receptors to phospholipase C*. *J Biol Chem*, 1995. **270**(25): p. 15175-80.
254. Lawler, C.P., et al., *Interactions of the novel antipsychotic aripiprazole (OPC-14597) with dopamine and serotonin receptor subtypes*. *Neuropsychopharmacology*, 1999. **20**(6): p. 612-27.
255. Shapiro, D.A., et al., *Aripiprazole, a novel atypical antipsychotic drug with a unique and robust pharmacology*. *Neuropsychopharmacology*, 2003. **28**(8): p. 1400-11.
256. Kenakin, T., *Agonist-receptor efficacy. II. Agonist trafficking of receptor signals*. *Trends Pharmacol Sci*, 1995. **16**(7): p. 232-8.
257. Kristiansen, K., *Molecular mechanisms of ligand binding, signaling, and regulation within the superfamily of G-protein-coupled receptors: molecular modeling and mutagenesis approaches to receptor structure and function*. *Pharmacol Ther*, 2004. **103**(1): p. 21-80.
258. Eglén, R.M., R. Bosse, and T. Reisine, *Emerging concepts of guanine nucleotide-binding protein-coupled receptor (GPCR) function and implications for high throughput screening*. *Assay Drug Dev Technol*, 2007. **5**(3): p. 425-51.
259. www.probes.invitrogen.com/media/pis/mp36205.pdf.
260. www.moleculardevices.com/pages/reagents/cal4_kit.html.

261. www.abdbioquest.com/CGI-BIN/dispresults.pl?Cid=36316.
262. Lefkowitz, R.J., *G protein-coupled receptors. III. New roles for receptor kinases and beta-arrestins in receptor signaling and desensitization*. J Biol Chem, 1998. **273**(30): p. 18677-80.
263. www.discoverx.com/gpcrs/arrestin.php.
264. Burger, K., G. Gimpl, and F. Fahrenholz, *Regulation of receptor function by cholesterol*. Cell Mol Life Sci, 2000. **57**(11): p. 1577-92.
265. Gimpl, G., et al., *Oxytocin receptors and cholesterol: interaction and regulation*. Exp Physiol, 2000. **85 Spec No**: p. 41S-49S.
266. Williams, P.D., et al., *1-(1-[4-[(N-acetyl-4-piperidinyloxy]-2-methoxybenzoyl]piperidin-4-yl)-4H-3,1-benzoxazin-2(1H)-one (L-371,257): a new, orally bioavailable, non-peptide oxytocin antagonist*. J Med Chem, 1995. **38**(23): p. 4634-6.
267. Zhang, J.H., T.D. Chung, and K.R. Oldenburg, *A Simple Statistical Parameter for Use in Evaluation and Validation of High Throughput Screening Assays*. J Biomol Screen, 1999. **4**(2): p. 67-73.
268. www.ncgc.nih.gov/guidance/.
269. Strunecka, A., S. Hynie, and V. Klenerova, *Role of oxytocin/oxytocin receptor system in regulation of cell growth and neoplastic processes*. Folia Biol (Praha), 2009. **55**(5): p. 159-65.
270. Cattaneo, M.G., G. Lucci, and L.M. Vicentini, *Oxytocin stimulates in vitro angiogenesis via a Pyk-2/Src-dependent mechanism*. Exp Cell Res, 2009. **315**(18): p. 3210-9.
271. Kenakin, T., *Functional selectivity in GPCR modulator screening*. Comb Chem High Throughput Screen, 2008. **11**(5): p. 337-43.
272. Mailman, R.B., *GPCR functional selectivity has therapeutic impact*. Trends Pharmacol Sci, 2007. **28**(8): p. 390-6.
273. Acher, R., *Neurohypophysial peptide systems: processing machinery, hydroosmotic regulation, adaptation and evolution*. Regul Pept, 1993. **45**(1-2): p. 1-13.
274. Bourdon, D.M., et al., *Quantification of isozyme-specific activation of phospholipase C-beta2 by Rac GTPases and phospholipase C-epsilon by Rho GTPases in an intact cell assay system*. Methods Enzymol, 2006. **406**: p. 489-99.

275. www.biocompare.com/images/bc/006/ArticleImages/HTRF_Appl_No_2.jpg.
276. Vichai, V. and K. Kirtikara, *Sulforhodamine B colorimetric assay for cytotoxicity screening*. Nat Protoc, 2006. **1**(3): p. 1112-6.
277. Skehan, P., et al., *New colorimetric cytotoxicity assay for anticancer-drug screening*. J Natl Cancer Inst, 1990. **82**(13): p. 1107-12.
278. Crawley, J.N., *Medicine. Testing hypotheses about autism*. Science, 2007. **318**(5847): p. 56-7.
279. Caldwell, J.D., et al., *A comparison of grooming behavior potencies of neurohypophyseal nonapeptides*. Regul Pept, 1986. **14**(3): p. 261-71.
280. Drago, F., et al., *Oxytocin potently enhances novelty-induced grooming behavior in the rat*. Brain Res, 1986. **368**(2): p. 287-95.
281. Drago, F., Z. Sarnyai, and V. D'Agata, *The inhibition of oxytocin-induced grooming by a specific receptor antagonist*. Physiol Behav, 1991. **50**(3): p. 533-6.
282. Kang, Y.S. and J.H. Park, *Brain uptake and the analgesic effect of oxytocin--its usefulness as an analgesic agent*. Arch Pharm Res, 2000. **23**(4): p. 391-5.
283. Han, Y. and L.C. Yu, *Involvement of oxytocin and its receptor in nociceptive modulation in the central nucleus of amygdala of rats*. Neurosci Lett, 2009. **454**(1): p. 101-4.
284. Rubinstein, M., et al., *Absence of opioid stress-induced analgesia in mice lacking beta-endorphin by site-directed mutagenesis*. Proc Natl Acad Sci U S A, 1996. **93**(9): p. 3995-4000.
285. Fields, H.L., M.M. Heinricher, and P. Mason, *Neurotransmitters in nociceptive modulatory circuits*. Annu Rev Neurosci, 1991. **14**: p. 219-45.
286. Wiesenfeld-Hallin, Z., et al., *PD134308, a selective antagonist of cholecystinin type B receptor, enhances the analgesic effect of morphine and synergistically interacts with intrathecal galanin to depress spinal nociceptive reflexes*. Proc Natl Acad Sci U S A, 1990. **87**(18): p. 7105-9.
287. Moy, S.S., et al., *Mouse behavioral tasks relevant to autism: phenotypes of 10 inbred strains*. Behav Brain Res, 2007. **176**(1): p. 4-20.
288. Crawley, J.N., et al., *Behavioral phenotypes of inbred mouse strains: implications and recommendations for molecular studies*. Psychopharmacology (Berl), 1997. **132**(2): p. 107-24.

289. Braff, D., et al., *Prestimulus effects on human startle reflex in normals and schizophrenics*. *Psychophysiology*, 1978. **15**(4): p. 339-43.
290. Davis, M., et al., *Apomorphine disrupts the inhibition of acoustic startle induced by weak prepulses in rats*. *Psychopharmacology (Berl)*, 1990. **102**(1): p. 1-4.
291. Gray, L., et al., *Clozapine reverses schizophrenia-related behaviours in the metabotropic glutamate receptor 5 knockout mouse: association with N-methyl-D-aspartic acid receptor up-regulation*. *Int J Neuropsychopharmacol*, 2009. **12**(1): p. 45-60.
292. Powell, S.B., X. Zhou, and M.A. Geyer, *Prepulse inhibition and genetic mouse models of schizophrenia*. *Behav Brain Res*, 2009. **204**(2): p. 282-94.
293. Braff, D.L., M.A. Geyer, and N.R. Swerdlow, *Human studies of prepulse inhibition of startle: normal subjects, patient groups, and pharmacological studies*. *Psychopharmacology (Berl)*, 2001. **156**(2-3): p. 234-58.
294. Crawley, J.N. and R. Paylor, *A proposed test battery and constellations of specific behavioral paradigms to investigate the behavioral phenotypes of transgenic and knockout mice*. *Horm Behav*, 1997. **31**(3): p. 197-211.
295. Mantella, R.C., et al., *Female oxytocin-deficient mice display enhanced anxiety-related behavior*. *Endocrinology*, 2003. **144**(6): p. 2291-6.
296. Moy, S.S., et al., *Impaired sociability and cognitive function in Nrcam-null mice*. *Behav Brain Res*, 2009.
297. Arletti, R., et al., *Aged rats are still responsive to the antidepressant and memory-improving effects of oxytocin*. *Neuropeptides*, 1995. **29**(3): p. 177-82.
298. Moy, S.S., et al., *Mouse models of autism spectrum disorders: the challenge for behavioral genetics*. *Am J Med Genet C Semin Med Genet*, 2006. **142C**(1): p. 40-51.
299. Duncan, G.E., et al., *Typical and atypical antipsychotic drug effects on locomotor hyperactivity and deficits in sensorimotor gating in a genetic model of NMDA receptor hypofunction*. *Pharmacol Biochem Behav*, 2006. **85**(3): p. 481-91.
300. www.fpg.unc.edu/~ndrc/core_services/mouse_behavioral_laboratory.cfm.
301. Melis, M.R., et al., *Oxytocin-induced motor disturbances: relationship with penile erection and yawning*. *Pharmacol Biochem Behav*, 1989. **34**(3): p. 673-5.

302. Caldwell, J.D., et al., *Effects of nonapeptide antagonists on oxytocin- and arginine-vasopressin-induced analgesia in mice*. Regul Pept, 1987. **18**(3-4): p. 233-41.
303. Landgraf, R., et al., *Hyper-reactive hypothalamo-pituitary-adrenocortical axis in rats bred for high anxiety-related behaviour*. J Neuroendocrinol, 1999. **11**(6): p. 405-7.
304. McNamara, I.M., et al., *Further studies in the developmental hyperserotonemia model (DHS) of autism: social, behavioral and peptide changes*. Brain Res, 2008. **1189**: p. 203-14.
305. Brodtkin, E.S., et al., *Social approach-avoidance behavior of inbred mouse strains towards DBA/2 mice*. Brain Res, 2004. **1002**(1-2): p. 151-7.
306. Moy, S.S., et al., *Sociability and preference for social novelty in five inbred strains: an approach to assess autistic-like behavior in mice*. Genes Brain Behav, 2004. **3**(5): p. 287-302.
307. Nadler, J.J., et al., *Automated apparatus for quantitation of social approach behaviors in mice*. Genes Brain Behav, 2004. **3**(5): p. 303-14.
308. Thor, D.H. and W.R. Holloway, Jr., *Social play in juvenile rats: a decade of methodological and experimental research*. Neurosci Biobehav Rev, 1984. **8**(4): p. 455-64.
309. Winslow, J.T. and F. Camacho, *Cholinergic modulation of a decrement in social investigation following repeated contacts between mice*. Psychopharmacology (Berl), 1995. **121**(2): p. 164-72.
310. Braff, D.L. and M.A. Geyer, *Sensorimotor gating and schizophrenia. Human and animal model studies*. Arch Gen Psychiatry, 1990. **47**(2): p. 181-8.
311. Mansbach, R.S., M.A. Geyer, and D.L. Braff, *Dopaminergic stimulation disrupts sensorimotor gating in the rat*. Psychopharmacology (Berl), 1988. **94**(4): p. 507-14.
312. Mansbach, R.S., et al., *Behavioral studies with anxiolytic drugs. V. Behavioral and in vivo neurochemical analyses in pigeons of drugs that increase punished responding*. J Pharmacol Exp Ther, 1988. **246**(1): p. 114-20.
313. Mansbach, R.S. and M.A. Geyer, *Effects of phencyclidine and phencyclidine biologs on sensorimotor gating in the rat*. Neuropsychopharmacology, 1989. **2**(4): p. 299-308.
314. Varty, G.B., et al., *Comparison of apomorphine, amphetamine and dizocilpine disruptions of prepulse inhibition in inbred and outbred mice strains*. Eur J Pharmacol, 2001. **424**(1): p. 27-36.

315. Swerdlow, N.R., D. Zisook, and N. Taaid, *Seroquel (ICI 204,636) restores prepulse inhibition of acoustic startle in apomorphine-treated rats: Similarities to clozapine*. *Psychopharmacology (Berl)*, 1994. **114**(4): p. 675-8.
316. Bakshi, V.P. and M.A. Geyer, *Antagonism of phencyclidine-induced deficits in prepulse inhibition by the putative atypical antipsychotic olanzapine*. *Psychopharmacology (Berl)*, 1995. **122**(2): p. 198-201.
317. Keith, V.A., R.S. Mansbach, and M.A. Geyer, *Failure of haloperidol to block the effects of phencyclidine and dizocilpine on prepulse inhibition of startle*. *Biol Psychiatry*, 1991. **30**(6): p. 557-66.
318. Swerdlow, N.R., et al., *Seroquel, clozapine and chlorpromazine restore sensorimotor gating in ketamine-treated rats*. *Psychopharmacology (Berl)*, 1998. **140**(1): p. 75-80.
319. Kovacs, G.L., et al., *The role of oxytocin-dopamine interactions in cocaine-induced locomotor hyperactivity*. *Neuropharmacology*, 1990. **29**(4): p. 365-8.
320. Uvnas-Moberg, K., et al., *Oxytocin reduces exploratory motor behaviour and shifts the activity towards the centre of the arena in male rats*. *Acta Physiol Scand*, 1992. **145**(4): p. 429-30.
321. McCarthy, M.M., et al., *An anxiolytic action of oxytocin is enhanced by estrogen in the mouse*. *Physiol Behav*, 1996. **60**(5): p. 1209-15.
322. Arenas, M.C., et al., *Dose dependency of sex differences in the effects of repeated haloperidol administration in avoidance conditioning in mice*. *Pharmacol Biochem Behav*, 1999. **62**(4): p. 703-9.
323. Zharkovskii, A.M. and A.V. Beliakov, *[Effect of varying the dose of haloperidol during its prolonged administration on the development of tolerance and hypersensitivity in dopamine receptors]*. *Farmakol Toksikol*, 1983. **46**(5): p. 22-4.
324. Association, A.P., *Diagnostic and Statistical Manual of Mental Disorders (DMS-IV)*, ed. A.P. Association. 1994.
325. Lee, H.J., et al., *A conditional knockout mouse line of the oxytocin receptor*. *Endocrinology*, 2008. **149**(7): p. 3256-63.
326. Moy, S.S., et al., *Development of a mouse test for repetitive, restricted behaviors: relevance to autism*. *Behav Brain Res*, 2008. **188**(1): p. 178-94.
327. Moy, S.S., et al., *Social approach and repetitive behavior in eleven inbred mouse strains*. *Behav Brain Res*, 2008. **191**(1): p. 118-29.

328. Sassano, M.F., et al. *Oxytocin reverses prepulse inhibition deficits in MK-801-treated mice*. in *Neuroscience*. 2009. Chicago, IL.
329. Lee, H.J., et al., *Behavioural studies using temporal and spatial inactivation of the oxytocin receptor*. *Prog Brain Res*, 2008. **170**: p. 73-7.
330. Guastella, A.J., P.B. Mitchell, and F. Mathews, *Oxytocin enhances the encoding of positive social memories in humans*. *Biol Psychiatry*, 2008. **64**(3): p. 256-8.
331. Petrovic, P., et al., *Oxytocin attenuates affective evaluations of conditioned faces and amygdala activity*. *J Neurosci*, 2008. **28**(26): p. 6607-15.
332. Di Simplicio, M., et al., *Oxytocin enhances processing of positive versus negative emotional information in healthy male volunteers*. *J Psychopharmacol*, 2009. **23**(3): p. 241-8.
333. Landry, M., et al., *Fluoxetine treatment of prepubescent rats produces a selective functional reduction in the 5-HT_{2A} receptor-mediated stimulation of oxytocin*. *Synapse*, 2005. **58**(2): p. 102-9.
334. Pietrowsky, R., et al., *Vasopressin and oxytocin do not influence early sensory processing but affect mood and activation in man*. *Peptides*, 1991. **12**(6): p. 1385-91.
335. Fombonne, E., *Epidemiology of autistic disorder and other pervasive developmental disorders*. *J Clin Psychiatry*, 2005. **66 Suppl 10**: p. 3-8.
336. Hammock, E.A. and L.J. Young, *Oxytocin, vasopressin and pair bonding: implications for autism*. *Philos Trans R Soc Lond B Biol Sci*, 2006. **361**(1476): p. 2187-98.
337. Grillon, C., et al., *Startle gating deficits occur across prepulse intensities in schizophrenic patients*. *Biol Psychiatry*, 1992. **32**(10): p. 939-43.
338. Light, G.A. and D.L. Braff, *Human and animal studies of schizophrenia-related gating deficits*. *Curr Psychiatry Rep*, 1999. **1**(1): p. 31-40.
339. Glovinsky, D., et al., *Cerebrospinal fluid oxytocin concentration in schizophrenic patients does not differ from control subjects and is not changed by neuroleptic medication*. *Schizophr Res*, 1994. **11**(3): p. 273-6.
340. Mansbach, R.S., D.L. Braff, and M.A. Geyer, *Prepulse inhibition of the acoustic startle response is disrupted by N-ethyl-3,4-methylenedioxyamphetamine (MDEA) in the rat*. *Eur J Pharmacol*, 1989. **167**(1): p. 49-55.

341. Martinez, Z.A., et al., *Ontogeny of phencyclidine and apomorphine-induced startle gating deficits in rats*. *Pharmacol Biochem Behav*, 2000. **65**(3): p. 449-57.
342. Swerdlow, N.R., et al., *Convergence and divergence in the neurochemical regulation of prepulse inhibition of startle and N40 suppression in rats*. *Neuropsychopharmacology*, 2006. **31**(3): p. 506-15.
343. McGregor, I.S., P.D. Callaghan, and G.E. Hunt, *From ultrasocial to antisocial: a role for oxytocin in the acute reinforcing effects and long-term adverse consequences of drug use?* *Br J Pharmacol*, 2008. **154**(2): p. 358-68.
344. Sarnyai, Z. and G.L. Kovacs, *Role of oxytocin in the neuroadaptation to drugs of abuse*. *Psychoneuroendocrinology*, 1994. **19**(1): p. 85-117.
345. Soorya, L., J. Kiarashi, and E. Hollander, *Psychopharmacologic interventions for repetitive behaviors in autism spectrum disorders*. *Child Adolesc Psychiatr Clin N Am*, 2008. **17**(4): p. 753-71, viii.
346. Witwer, A. and L. Lecavalier, *Treatment incidence and patterns in children and adolescents with autism spectrum disorders*. *J Child Adolesc Psychopharmacol*, 2005. **15**(4): p. 671-81.
347. Posey, D.J., C.A. Erickson, and C.J. McDougle, *Developing drugs for core social and communication impairment in autism*. *Child Adolesc Psychiatr Clin N Am*, 2008. **17**(4): p. 787-801, viii-ix.
348. McDougle, C.J., et al., *A double-blind, placebo-controlled study of risperidone in adults with autistic disorder and other pervasive developmental disorders*. *Arch Gen Psychiatry*, 1998. **55**(7): p. 633-41.
349. Erickson, C.A., et al., *Risperidone in pervasive developmental disorders*. *Expert Rev Neurother*, 2005. **5**(6): p. 713-9.
350. McDougle, C.J., et al., *Risperidone for the core symptom domains of autism: results from the study by the autism network of the research units on pediatric psychopharmacology*. *Am J Psychiatry*, 2005. **162**(6): p. 1142-8.
351. Network, R.U.o.P.P.A., *Risperidone in children with autism and serious behavioral problems*. *New England Journal of Medicine*, 2002. **347**(5): p. 314-21.
352. McDougle, C.J., et al., *Risperidone addition in fluvoxamine-refractory obsessive-compulsive disorder: three cases*. *J Clin Psychiatry*, 1995. **56**(11): p. 526-8.

353. Potenza, M.N., et al., *Olanzapine treatment of children, adolescents, and adults with pervasive developmental disorders: an open-label pilot study*. J Clin Psychopharmacol, 1999. **19**(1): p. 37-44.
354. Malone, R.P., et al., *Olanzapine versus haloperidol in children with autistic disorder: an open pilot study*. J Am Acad Child Adolesc Psychiatry, 2001. **40**(8): p. 887-94.
355. Kemner, C., et al., *Open-label study of olanzapine in children with pervasive developmental disorder*. J Clin Psychopharmacol, 2002. **22**(5): p. 455-60.
356. Hollander, E., et al., *A double-blind placebo-controlled pilot study of olanzapine in childhood/adolescent pervasive developmental disorder*. J Child Adolesc Psychopharmacol, 2006. **16**(5): p. 541-8.
357. ClinicalTrials.gov. <http://www.clinicaltrials.gov>.